ITRI-144
NOVEMBER 1994
CATEGORY: UC-408

# INHALATION TOXICOLOGY RESEARCH INSTITUTE ANNUAL REPORT

## 1993 - 1994

by the Staff of the
Inhalation Toxicology Research Institute


INHALATION TOXICOLOGY RESEARCH INSTITUTE
LOVELACE BIOMEDICAL & ENVIRONMENTAL RESEARCH INSTITUTE
P.O. Box 5890 Albuquerque, NM 87185

PREPARED FOR THE OFFICE OF HEALTH
AND ENVIRONMENTAL RESEARCH
OF THE U.S. DEPARTMENT OF ENERGY
UNDER CONTRACT NUMBER DE-AC04-76EV01013

## DISCLAIMER

The research described in this report involved animals maintained in animal care facilities fully accredited by the American Association for Accreditation of Laboratory Animal Care. The research described in this report that involved humans was conducted in compliance with government regulations protecting human subjects.

Printed in the United States of America

Available to DOE and DOE contractors from the Office of Scientific and Technical Information, P. O. Box 62, Oak Ridge, TN 37831: prices available from (615) 576-8401.

Available to the public from the National Technical Information Service, U.S. Department of Commerce, 5285 Port Royal Rd., Springfield, VA 22161.

ITRI-144
November 1994
Category: UC-408

# Annual Report of the Inhalation Toxicology Research Institute Operated for the United States Department of Energy by the Lovelace Biomedical and Environmental Research Institute

## October 1, 1993 through September 30, 1994

by the Staff of the
Inhalation Toxicology Research Institute
Joe L. Mauderly, D.V.M., Director

Steven A. Belinsky, Ph.D., Senior Editor
Mark D. Hoover, Ph.D., Associate Editor
Paula L. Bradley, M.A., Technical Editor



November 1994

Prepared for the Office of Health and Environmental Research of the U.S. Department of Energy Under Contract Number DE-AC04-76EV01013

# TABLE OF CONTENTS

## VIII. THE APPLICATION OF MATHEMATICAL MODELING TO RISK ESTIMATES



## IX. APPENDICES

# INTRODUCTION

## The Institute

The Inhalation Toxicology Research Institute (ITRI) is a Federally Funded Research and Development Center operated for the U. S. Department of Energy (DOE) by The Lovelace Biomedical and Environmental Research Institute, a nonprofit subsidiary of The Lovelace Institutes. ITRI is designated as a "Specific Mission Laboratory" within the DOE Office of Health and Environmental Research, Office of Energy Research. Approximately 80% of the Institute's research is funded by DOE; the remainder is funded by a variety of governmental, trade association, and industry sources.

The mission of ITRI is to conduct basic and applied research to improve our understanding of the nature and magnitude of the human health impacts of inhaling airborne materials in the home, workplace, and general environment. Institute research programs have a strong basic science orientation with emphasis on the nature and behavior of airborne materials, the fundamental biology of the respiratory tract, the fate of inhaled materials and the mechanisms by which they cause disease, and the means by which data produced in the laboratory can be used to estimate risks to human health. Disorders of the respiratory tract continue to be a major health concern, and inhaled toxicants are thought to contribute substantially to respiratory morbidity. As the largest laboratory dedicated to the study of basic inhalation toxicology, ITRI provides a national resource of specialized facilities, personnel, and educational activities serving the needs of government, academia, and industry.

The Institute's multidisciplinary staff works in specialized facilities and takes a collaborative research approach to resolving scientific issues. ITRI is located on Kirtland Air Force Base East, approximately 10 miles southeast of Albuquerque, New Mexico. The more than 290,000 square feet of laboratory and support facilities include unique facilities and equipment for basic biological research and exposures of animals to all types of airborne toxicants. The staff of approximately 200 includes doctoral-level scientists in physical, chemical, biological, medical, and mathematical disciplines. Working with the scientists are highly trained scientific technicians, laboratory animal technicians, and a full range of support staff. The entire range of biological systems is employed, including macromolecules, cells, tissues, laboratory animals, and humans. The research includes both field and laboratory studies. Strong emphasis is placed on the quality of research and resulting data; the Institute has a Quality Assurance Unit and is fully capable of research in adherence to Good Laboratory Practices guidelines.

The Institute's scientific and support staffs are organized into disciplinary and functional scientific groups and support units (see Appendix B). The research is organized into programs which are administered by the Assistant Directors (see Appendix C). The programs are composed of projects having common research themes, but which typically cut across research disciplines. For example, the Pathogenesis Program contains projects oriented largely toward the development of noncancerous respiratory tract disease, but the projects involve molecular biology, biochemistry, pathology, physiology, and inhalation exposure technology.

## The Report

The papers in this report are organized along topical lines, rather than by research program, so that research within specific disciplines is more readily identified. The papers include summaries of research funded by both DOE and other sources, to represent the full scope of Institute activities. The source of funding is acknowledged for each paper. The appendices summarize the organization of the Institute's staff and research programs, publications and presentations by ITRI Scientists, seminars by visiting scientists, collaborations with scientists in other institutions, and a description of ITRI's educational activities.

A separate series of reports entitled, *Annual Report on Long-Term Dose-Response Studies of Inhaled or Injected Radionuclides*, summarize the design and status of the long-term studies of the health effects of radionuclides in dogs, conducted at ITRI and the University of Utah. This separate report also contains the status of each dog, the detailed tables which were previously included as appendices in the ITRI Annual Report. This report of the Long-Term Dose Response Studies can be obtained from NTIS, and by request from the Institute.

Joe L. Mauderly, D.V.M.
Director

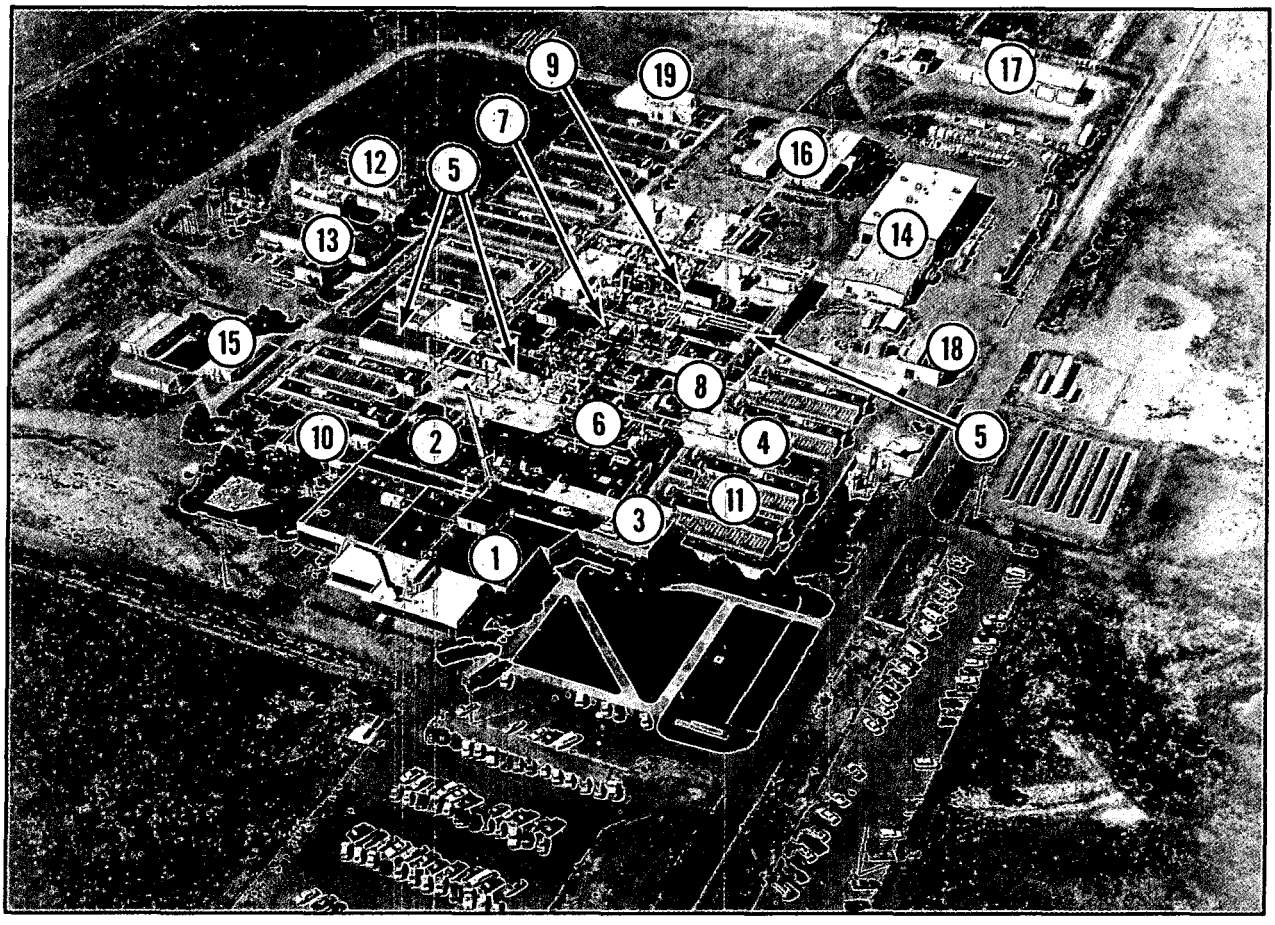


An aerial view of the Inhalation Toxicology Research Institute which was constructed in several increments, starting in June 1962. The Institute's facilities consist of (1) administrative area, including the directorate, personnel, business, purchasing, and editorial offices, a cafeteria, conference rooms, and health protection operations; (2) central laboratory and office area, including aerosol science, radiobiology, pathology, chemistry and toxicology laboratories; (3) cell toxicology laboratories; (4) pathophysiology laboratories; (5) chronic inhalation exposure complex with some laboratories suitable for use with carcinogenic materials; (6) exposure facility for acute inhalation exposures to chemical toxicants and beta- and gamma-radionuclides; (7) exposure facilities for acute inhalation exposures to alpha-emitting radionuclides; (8) veterinary hospital and facilities for detailed clinical observations; (9) small-animal barrier-type housing facilities; (10) library and quality assurance facilities; (11) kennel buildings; (12) analytical chemistry building; (13) engineering and maintenance support building; (14) property management, receiving, and storage building; (15) auxiliary office and classroom complex; (16) auxiliary laboratories; (17) waste storage and treatment facility; (18) standby power facility; and (19) animal quarantine facility.

## LIST OF ANNUAL REPORTS

Selective Summary of Studies in the Fission Product Inhalation Program (July 1964 through June 1966);

LF-28, 1965 LF-33, 1966

Fission Product Inhalation Program Annual Report (1966-1972);

| | | |
|---|---|---|
| LF-38, 1967 | LF-41, 1969 | LF-44, 1971 |
| LF-39, 1968 | LF-43, 1970 | LF-45, 1972 |

Inhalation Toxicology Research Institute Annual Report (1972-1994);

| | | |
|---|---|---|
| LF-46, 1973 | LMF-91, 1981 | LMF-126, 1989 |
| LF-49, 1974 | LMF-102, 1982 | LMF-129, 1990 |
| LF-52, 1975 | LMF-107, 1983 | LMF-134, 1991 |
| LF-56, 1976 | LMF-113, 1984 | LMF-138, 1992 |
| LF-58, 1977 | LMF-114, 1985 | ITRI-140, 1993 |
| LF-60, 1978 | LMF-115, 1986 | ITRI-144, 1994 |
| LF-69, 1979 | LMF-120, 1987 | |
| LMF-84, 1980 | LMF-121, 1988 | |

Long-Term Dose-Response Studies of Inhaled or Injected Radionuclides (1988-1993);

| | | |
|---|---|---|
| LMF-128, 1989 | LMF-130, 1990 | LMF-135, 1991 |
| ITRI-139, 1992-1993 | | |

# I. AEROSOL TECHNOLOGY AND CHARACTERIZATION OF AIRBORNE MATERIALS

# DETERMINATION OF AEROSOL SIZE DISTRIBUTIONS AT URANIUM MILL TAILINGS REMEDIAL ACTION PROJECT SITES

*George J. Newton, Mark D. Hoover, and Ronald H. Reif**

The U.S. Department of Energy (DOE) has an ongoing program, the Uranium Mill Tailings Remedial Action (UMTRA) Project, to stabilize piles of uranium mill tailings in order to reduce the potential radiological hazards to the public. Protection of workers and the general public against airborne radioactivity during remedial action is a top priority at the UMTRA Project. The primary occupational radionuclides of concern are $^{230}Th$, $^{226}Ra$, $^{210}Pb$, $^{210}Po$, and the short-lived decay products of $^{222}Rn$ with $^{230}Th$ causing the majority of the committed effective dose equivalent (CEDE) from inhaling uranium mill tailings (Reif, R. H. *et al. Health Phys. 63*: 398; 1992).

Prior to this study, a default particle size of 1.0 $\mu$m activity median aerodynamic diameter (AMAD) was assumed for airborne radioactive tailings dust. Because of recent changes in DOE requirements (DOE 1993, 10 CFR 835, Final Rule, December 14, 1993), all DOE operations are now required to use the CEDE methodology, instead of the annual effective dose equivalent (AEDE) methodology, to evaluate internal radiation exposures. Under the transition from AEDE to CEDE, with a 1.0 $\mu$m AMAD particle size, lower bioassay action levels would be required for the UMTRA Project. This translates into an expanded internal dosimetry program where significantly more bioassay monitoring would be required at the UMTRA Project sites. However, for situations where the particle size distribution is known to differ significantly from 1.0 $\mu$m AMAD, the DOE allows for corrections to be made to both the estimated dose to workers and the derived air concentration (DAC) values (DOE, 1993). For particle sizes larger than 1.0 $\mu$m AMAD, the calculated CEDE from inhaling tailings would be relatively lower.

The present study was undertaken to determine the actual particle size distribution for mill tailings aerosols, and thereby improve the technical basis for the internal dosimetry program. There were a number of reasons to believe that the assumption of a 1 $\mu$m aerodynamic diameter particle size for airborne uranium mill tailings was overly conservative and that the actual particle size would be much larger. Air sampling data collected between 1988-1989 at the Durango, Colorado, site were provided by the UMTRA program. This information included a number of simultaneous measurements of total airborne particle concentrations and respirable (< 10 $\mu$m aerodynamic diameter) particle concentrations. Evaluation of these data showed that under relatively dusty conditions (> 0.5 mg/m$^3$ total airborne dust) particles larger than 10 $\mu$m aerodynamic diameter make up 93% ± 7% of the total airborne particle mass. Under all dust conditions evaluated, the fraction of airborne particle mass greater than 10 $\mu$m was 77% ± 21%. This was an encouraging indication that the aerodynamic equivalent particle diameter for worker exposures was substantially larger than the default assumption of 1 $\mu$m. This observation was supported by size-selective data from a single cascade impactor sample collected in 1992 during a dusty operation at an UMTRA Project site located at Grand Junction, Colorado. The mass median aerodynamic diameter (MMAD) of this sample indicated that the mean particle size for the sample collected was larger than 10 $\mu$m; in fact, more than 99% of the particle mass was larger than 10 $\mu$m aerodynamic diameter.

The approach developed for characterizing the size of tailings particles involved the following steps:

*CWM Federal Environmental Services, Inc., Albuquerque, New Mexico

(1) Obtain representative, bulk samples of mill tailings from active UMTRA Project sites.

(2) Pass the mill tailings samples through graded sieves to estimate the mass median sieve diameter (MMSD) of the particle size distribution.

(3) Determine the activity median sieve diameter (AMSD) of the tailings samples by measuring the $^{226}Ra$ radioactivity in the sieved fractions.

(4) Determine the density of the mill tailings by standard pycnometry.

(5) Obtain the AMAD of the tailings samples by multiplying the AMSD by the square root of the tailings density.

(6) Extrapolate the sieve-based size distribution into the respirable size range (< 10 $\mu$m AMAD) to obtain an initial estimate of the fraction of uranium mill tailings particles that are respirable.

(7) Use a dry powder disperser to aerosolize the particles which penetrated the smallest sieve (400 mesh, 38 $\mu$m sieve diameter, nominal 60 $\mu$m aerodynamic diameter).

(8) Determine the MMAD of the aerosolized particles by weighing size-fractionated samples collected using a five-stage aerosol cyclone.

(9) Compare the aerosol cyclone measurements for mass distribution with the sieve measurements to confirm the validity of the extrapolation from sieved data to estimate the respirable fraction (< 10 $\mu$m AMAD) of tailings samples.

(10) Determine the AMAD of $^{226}Ra$ in the aerosolized tailings samples by measuring the $^{226}Ra$ radioactivity in the cyclone fractions.

(11) Determine the AMAD of $^{230}Th$ in the aerosolized tailings samples by radiochemical determination of the $^{230}Th$ radioactivity in the cyclone fractions.

(12) Compare the aerosol cyclone measurements for $^{226}Ra$ and $^{230}Th$ radioactivity distributions with the sieve measurements to confirm the validity of the extrapolation from sieved data to estimate the respirable fraction (< 10 $\mu$m AMAD) of tailings samples.

(13) Recommend an effective particle size to be used in adjustment of the annual limits on intake (ALIs) and DACs in the UMTRA Projects internal dosimetry program.

Thirty seven tailings samples were collected from six UMTRA Project sites under remedial action in 1993. The MMSDs of these samples ranged from 40 $\mu$m to 457 $\mu$m. Based on the mean tailings density of 2.6 g/cm$^3$, this corresponds to MMADs of 64 to 737 $\mu$m. The AMSDs for $^{226}Ra$ were smaller than the MMSDs, and typically ranged from as low as 23 $\mu$m to as high as 308 $\mu$m. This range corresponds to an AMAD range of 37 $\mu$m to 497 $\mu$m. The sample with the smallest AMAD (37 $\mu$m), from a site located near Rifle, Colorado (RFL), had a particle size distribution in which about 9% of the total sample radioactivity was distributed in the respirable range (< 10 $\mu$m). Prior to selecting a technically defensible aerodynamic size for material to which workers might be exposed, an aerosol cyclone was used to determine the aerodynamic size distributions of the tailings particles which had penetrated the smallest sieve (< 38 $\mu$m). These aerosol cyclone measurements were made using the four samples with the smallest sizes based on sieved data counted for $^{226}Ra$. The mass distribution, $^{226}Ra$ distribution, and $^{230}Th$ distribution were determined for these samples. Table 1 summarizes the physical size distributions for mass, $^{226}Ra$, and $^{230}Th$ for sieved bulk samples; Table 2 summarizes data for aerodynamic size distributions as determined by aerosolization and cyclone separation of the resuspended particle. Three of the samples had similarly small size distributions; the

fourth sample had a size distribution that was a factor of 2 to 3 larger. To be conservative, for dose estimates, we recommend the use of the mean particle sizes from the three smaller distributions. The MMAD of the aerosolized fractions was 20 $\mu$m ± 6 $\mu$m (mean ± S.D.). The AMAD of the $^{226}$Ra radioactivity was associated with a somewhat smaller particle size of 15 $\mu$m ± 1 $\mu$m. The AMAD of the $^{230}$Th was associated with a still smaller diameter of 11 $\mu$m ± 1 $\mu$m. The solubility of $^{230}$Th causes it to become associated with smaller particles than the bulk material.

Table 1

Physical Size Distributions of Particle Mass, $^{226}$Ra Radioactivity, and $^{230}$Th Radioactivity in Uranium Mill Tailings Determined by Sieving

| | Mass | | $^{226}$Ra | | $^{230}$Th | |
|---|---|---|---|---|---|---|
| Sample ID[a] | MMSD ($\mu$m) | $\sigma_g$ | AMSD ($\mu$m) | $\sigma_g$ | AMSD ($\mu$m) | $\sigma_g$ |
| RFL-1780 | 40 | 2.1 | 23 | 2.6 | 29 | 2.4 |
| AMB-183 | 95 | 2.5 | 40 | 3.2 | 29 | 4.6 |
| FCT-14339 | 84 | 2.4 | 73 | 2.4 | 73 | 2.5 |
| GUN-0697 | 120 | 2.5 | 87 | 3.0 | 100 | 2.3 |
| Mean ± S.D. | 85 ± 33 | 2.4 | 56 ± 30 | 2.8 | 58 ± 35 | 3.0 |
| Conservative[b] Mean ± S.D. | 73 ± 29 | 2.3 | 45 ± 26 | 2.7 | 44 ± 35 | 3.2 |

[a]The four samples were from Rifle, Colorado (RFL), Ambrosia Lake, New Mexico (AMB), Falls City Texas (FCT), and Gunnison, Colorado (GUN).
[b]The conservative values are calculated without the GUN-0697 sample.

Table 2

Aerodynamic Size Distributions of Particle Mass, $^{226}$Ra Radioactivity, and $^{230}$Th Radioactivity in the 38 $\mu$m Sieve Fraction of Uranium Mill Tailings Determined by Aerosolization and Cyclone Separation of the Resuspended Particles

| | Mass | | $^{226}$Ra | | $^{230}$Th | |
|---|---|---|---|---|---|---|
| Sample ID | MMSD ($\mu$m) | $\sigma_g$ | AMSD ($\mu$m) | $\sigma_g$ | AMSD ($\mu$m) | $\sigma_g$ |
| RFL-1780 | 26 | 3.2 | 15 | 3.4 | 12 | 3.1 |
| AMB-183 | 20 | 2.9 | 15 | 2.8 | 10 | 2.5 |
| FCT-14339 | 15 | 3.1 | 17 | 3.0 | 11 | 3.0 |
| GUN-0697 | 37 | 3.1 | 33 | 3.6 | 29 | 3.8 |
| Mean ± S.D. | 25 ± 10 | 3.1 | 20 ± 9 | 3.2 | 16 ± 10 | 3.1 |
| Conservative Mean ± S.D. | 20 ± 6 | 3.1 | 15 ± 1 | 3.1 | 11 ± 1 | 2.9 |

[a]The conservative values are calculated without the GUN-0697 sample.

Based on these findings, single particle sizes of 11 $\mu$m AMAD for the $^{230}$Th and 15 $\mu$m AMAD for the $^{226}$Ra can generally be assumed to represent the particle size distribution to which workers might be exposed at UMTRA Project sites. With the exception of isotopes of thorium and short-lived radon progeny, all other radionuclides in uranium mill tailings can be assumed to be present as a single particle size of 15 $\mu$m AMAD. This is a conservative assumption, because particle sizes at many sites are larger. Using the ICRP-30 (ICRP-30, 19xx) method, increasing the particle size from 1 $\mu$m to 11 $\mu$m for $^{230}$Th and 15 $\mu$m for $^{226}$Ra allows the ALI for $^{230}$Th and $^{226}$Ra to be raised by a factor of approximately 3. This would be the base assumption for a mill tailing site, but even larger particle size distributions might be confirmed by selected air sampling data from the site. This approach will result in a significant reduction in unnecessary bioassay at uranium mill tailings remedial action sites. Of course, limited field sampling at each site is desirable for verification.

(Research sponsored by the Assistant Secretary for Defense Programs, U.S. Department of Energy, under Contract No. DE-AC04-76EV01013.)

# DESIGN OF A RADIOACTIVE GAS SAMPLING SYSTEM FOR NESHAP COMPLIANCE MEASUREMENTS OF $^{41}Ar$

*George J. Newton, Mark D. Hoover, Edward B. Barr, Marion J. McDonald*, and Faraj Ghanbari**

United States Department of Energy facilities are required to comply with the U.S. Environmental Protection Agency, National Emission Standard for Hazardous Air Pollutants (NESHAP) 40 CFR, part 61, subpart H. Compliance generally requires confirmatory measurements of emitted radionuclides. Although a number of standard procedures exist for extractive sampling of particle-associated radionuclides, sampling approaches for radioactive gases are less defined. Real-time, flow-through sampling of radioactive gases can be done when concentrations are high compared to interferences from background radiation. Cold traps can be used to collect and concentrate condensible effluents in applications where cryogenic conditions can be established and maintained. Commercially available gas-sampling cylinders can be used to capture grab samples of contaminated air under ambient or compressed conditions, if suitable sampling and control hardware are added to the cylinders. The purpose of the current study was to develop an efficient and compact set of sampling and control hardware for use with commercially available gas-sampling cylinders, and to demonstrate its use in NESHAP compliance testing of $^{41}Ar$ at two experimental research reactors.

Figure 1 is a schematic diagram of the gas sampling system. In designing the system, we wanted the physical size of the collection cylinder to be small enough to fit into the counting shield of our existing intrinsic germanium gamma spectrometer systems. A cylinder volume of 1 L was convenient for this purpose. A remote-control capability needed for applications in high radiation areas was provided by using normally closed, electrically actuated (110 V) solenoid valves, in addition to standard manual control valves. In addition, an effective sample volume was required that could be increased beyond 1 L, by as much as a factor of 10 if necessary, to achieve a suitable limit of detection. This was accomplished by incorporating a compressor. Commercially available components were used throughout the system to enable easy and cost-effective replacement of damaged, worn, or contaminated parts. Wherever possible, components of type 304 or 316 stainless steel were selected for durability and corrosion resistance. Pressure ratings were 9000 psig for the plumbing components, 1800 psig for the sample cylinder, and 150 psig for the polyethylene tubing. Thus, operation of the system at 100 psig provides an additional margin of safety beyond those already incorporated into the rated operating pressures of the components.

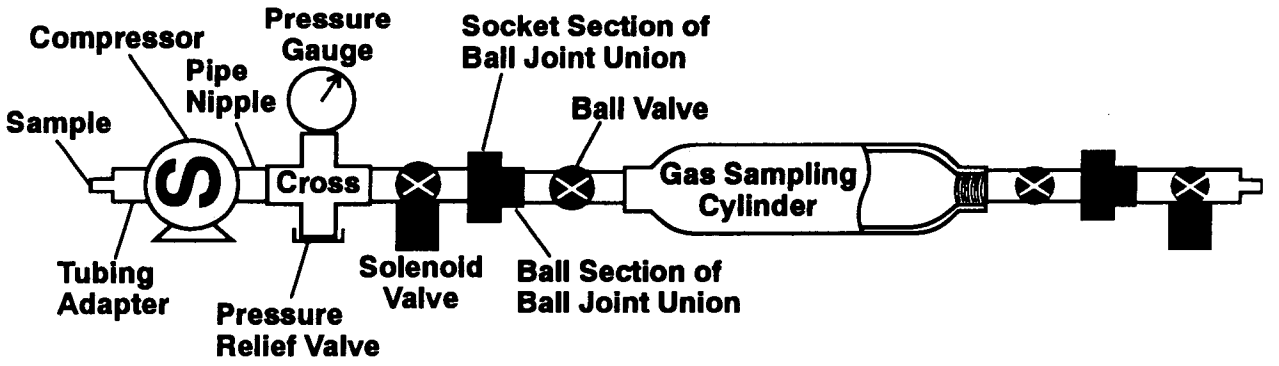


Figure 1. Schematic diagram of the compressed gas sampling system with manual and remote control features. At 100 psig, the compressed volume inside the 1-L sampling cylinder is equivalent to 9.3 L at the ambient pressure in Albuquerque, 109 kPa (625 mm Hg).

*Sandia National Laboratories, Albuquerque, New Mexico

Operation of the system and additional details of the inlet, gas cylinder, and exhaust modules are described here:

(1) A tubing adapter connects the inlet module to the radioactive gas source, usually a stack. Gas enters the compressor and is pumped through the entire gas sampling train to flush out clean air. Flush volumes of about 10 times the internal volume of the sampling train are adequate to achieve total washout of clean air. The 1-L compressed-gas cylinder accounts for most of the internal volume. A flush time of 3 min at the usual compressor flow rate of 5 L/min is typically used. The inlet module includes a pressure gauge and an adjustable pressure relief valve to ensure that the compressed-gas-sampling cylinder is not pressurized over 100 psig during filling. At 100 psig, the 1-L sampling cylinder contains 9.3 L of air at Albuquerque's ambient atmospheric pressure, 109 kPa (625 mm Hg). The electrically actuated solenoid valve in the inlet module, which remains open during flushing and filling operations, is closed by the operator when the cylinder is filled.

(2) The gas cylinder module is connected to the inlet module by a ball joint union. A pair of manual ball valves allows the gas cylinder to be closed after filling and permits the gas cylinder module to be removed for radioactivity counting.

(3) The exhaust module is connected to the gas cylinder module via a ball joint union. The exhaust module contains an electrically actuated solenoid valve which remains open during flushing, and is closed for filling. A tubing adapter at the end of the exhaust module allows the flush gas to be returned to the facility off-gas stack or to be vented to a suitable location.

The gamma spectrometer systems were calibrated using radionuclides with a range of gamma energy. An important consideration was to provide a spatially uniform source of radioactivity within the gas-sampling cylinder. A simulated gas calibration standard was prepared by filling a cylinder with 1/8-in diameter polyurethane beads that had been coated with nine different radionuclides (Analytics Inc., Atlanta, GA). The radionuclides (including their respective gamma energies and half-lives) were $^{109}$Cd (88 keV, 462.6 d), $^{57}$Co (122 keV, 271.7 d), $^{139}$Ce (166 keV, 137.6 d), $^{203}$Hg (279 keV, 46.6 d), $^{113}$Sn (392 keV, 115.1 d), $^{85}$Sr (514 keV, 64.9 d), $^{137}$Cs (662 keV, 30.0 y), $^{88}$Y (898 and 1836 keV, 106.6 d), and $^{60}$Co (1173 and 1332 keV, 5.27 y). The higher energy gamma from $^{60}$Co (1.332 MeV) is an excellent surrogate for the 1.290 MeV gamma from $^{41}$Ar. (Note that a reliable, long-lived counting surrogate for $^{41}$Ar is needed because the half-life of $^{41}$Ar is only 1.83 h.)

Performance of the gas-sampling system was demonstrated by measurements of $^{41}$Ar at the Annular Core Research Reactor (ACRR) and the Sandia Pulsed Reactor III (SPR III), two small reactors at Sandia National Laboratories/New Mexico. The ACRR and the SPR III produce the radioactive gas $^{41}$Ar by neutron activation of stable, naturally occurring $^{40}$Ar, a normal constituent of air. Because the maximum steady-state power level is 2 MW for the ACRR, but only 10 kW for the SPR III, it was important that the gas-sampling system be capable of quantifying a range of $^{41}$Ar radioactivity. Remote operating capability for the sampling system was required because the sampling port for SPR III is located in an area where personnel are not permitted during reactor operation.

Samples were obtained during operation of the ACRR at three steady-state power levels: 0.5, 1.0, and 2.0 MW. A sample of the exhaust gas was also obtained when the ACRR was not operating. The $^{41}$Ar concentration background (reactor shutdown) was less than the minimum detectable activity for the counting system ($< 1.1 \times 10^{-15}$ $\mu$Ci/mL). The measured mean concentrations of $^{41}$Ar in the ACRR exhaust duct during reactor operations were $1.67 \pm 0.03 \times 10^{-4}$ $\mu$Ci/mL, $3.26 \pm 0.12 \times 10^{-4}$ $\mu$Ci/mL, and $6.32 \pm 0.07 \times 10^{-4}$ $\mu$Ci/mL, for power levels of 0.5, 1.0, and 2.0 MW, respectively. These data indicate that the production rate of $^{41}$Ar for the ACRR was $1.092 \times 10^{-4}$ Ci/MJ. Because the neutron spectra and the amounts of air being irradiated are different at the two reactors, it is not

appropriate to extrapolate $^{41}Ar$ production from the ACRR to the SPR III. Steady-state operation of SPR III was 10 kW, and the production rate of $^{41}Ar$ was $1.26 \times 10^{-3}$ Ci/MJ.

An additional purpose for sampling in the ACRR exhaust duct was to provide a defensible calibration of the inline radioactive stack monitor (NMC Model RAK-33 ABIF-P stack monitor, NMC Corporation, Indianapolis, IN). One channel of the NMC monitors radioactive gases and is used to continuously measure any $^{41}Ar$ released from the ACRR. Results of the gas cylinder measurements showed that the actual $^{41}Ar$ concentrations were $0.70 \pm 0.02$ of the NMC values reported under the previous calibration. In addition, when the ACRR was not operating, the NMC reported a nonzero background value of approximately $3.22 \pm 0.35 \times 10^{-6}$ $\mu$Ci/mL, indicating that its NaI(Tl) detector is sensitive to normally encountered gamma radiation background. During reactor operations, the ambient levels of gamma radiation are known to increase and will cause a further over-reporting of the $^{41}Ar$ concentration. The background level response of the NMC was determined during reactor operations by introducing $^{41}Ar$-free air into the NMC sampler. This background was $6.2 \times 10^{-6}$ $\mu$Ci/L, $1.4 \times 10^{-5}$ $\mu$Ci/L, and $2.5 \times 10^{-5}$ $\mu$Ci/L for power levels of 0.5, 1.0, and 2.0 MW, respectively. Thus, if no corrections for background are made, the NMC provides a modestly conservative (about 5%) overestimate of the actual $^{41}Ar$ concentration. However, these results can be used to make background corrections to the reported $^{41}Ar$ concentrations of the NMC monitor.

The gas-sampling system was also used to sample for background levels of radioactive gases at the Sandia Hot Cell Facility (HCF). The HCF is used to disassemble neutron-irradiated packages containing fissile materials, thereby releasing radioactive gases, principally $^{85}Kr$. At the time of background sampling in the HCF, no irradiated packages were being disassembled, and the background concentrations of $^{85}Kr$ were found to be below the limit of detection for the sampling and counting system ($< 1.0 \times 10^{-15}$ $\mu$Ci/mL).

The compressed-gas-sampling system worked flawlessly and was very simple to use. The simulated radioactive gas sample from Analytics, Inc. provided a reliable, long-term calibration source for the intrinsic germanium-counting systems. Results of these tests can be used to confirm the NESHAP compliance status of the ACRR, SPR III, and the HCF. This gas sampling system is a flexible and efficient method to measure the concentration of $^{41}Ar$, $^{85}Kr$, and other gamma-emitting radioactive gases.

(This research was supported by Sandia National Laboratories under Purchase Order No. AB-5225, with the U.S. Department of Energy, under Contract No. DE-AC04-76EV01013.)

# AIR QUALITY IN THE CARLSBAD CAVERN

*Tou-Rong Chen*, Yung-Sung Cheng, and Piotr T. Wasiolek***

The air quality in the Carlsbad Cavern has been investigated (Wilkening, M. H. and D. E. Watkins. *Health Phys. 31*: 139, 1976), but there are no reports on radon progeny and aerosols. The purpose of this experiment was to determine the activity size distribution of radon progeny and the air exchange rate inside the Cavern. Teams from ITRI and New Mexico Institute of Mining and Technology (NMT) conducted the field study in July 1994.

The ITRI graded diffusion battery (GDB) was used to determine the activity size distribution, progeny concentration, equilibrium factor, and unattached fraction of the radon progeny. The design, calibration, and performance of the GDB have been described (Cheng, Y. S. *et al. J. Aerosol Sci. 23*: 361, 1992; *Health Phys. 66*: 72, 1994). For this study, each stage of the GDB contained one stainless steel screen, with the mesh sizes arranged in a series of 30, 50, 145, 200, and 635 mesh (Tetko Inc., Briarcliff, NY) from the air inlet to the outlet. A 47-mm type A/E glass fiber filter (Gelman Co., Ann Arbor, MI) was used to collect all particles that penetrated the screens. The flow rate was 5 L/min.

After a 10-min sampling period, screens and filter were simultaneously counted for gross alpha activity using six scintillation detectors (Model 43-10, Ludlum Measurements, Sweet Water, TX) and six scalers (Model SRM-200, Eberline Inc., Santa Fe, NM). Each system was calibrated separately, and the calibrated efficiency of the six counting systems ranged from 0.313 to 0.452. The activity size distribution was calculated from the corrected penetration data using an expectation-maximization method (Maher, E. F. and N. M. Laird *J. Aerosol Sci. 16*: 557, 1985). A size range of 0.5-200 nm was divided into 40 size intervals. The serial diffusion battery (SDB) program (Cheng, Y. S. *et al.*, 1994), which includes an automatic front-to-total correction, was used to analyze the size distribution of the particles in this study. The NMT GDB was also used to determine the activity size distribution. Five stainless steel screens, 8.9 cm in diameter, with 30, 50, 200, 400, and 635 mesh, were used. The sampling time, sampling place, and analysis computer code were the same as the ITRI GDB; the flow rate was set at 25 L/min.

A radon gas monitor (Model RGM-3, Eberline Inc., Santa Fe, NM) was used to determine the radon gas concentration. From the analysis of the SDB program, the total activity and potential alpha energy concentration (PAEC) of the radon progeny could be obtained. With the radon activity concentration as measured by the RGM-3, the equilibrium factor at a corresponding time could be calculated.

A tracer gas monitor (Model 101 Autotrac, Lagus Applied Technology Inc., San Diego, CA) was used with sulfur hexafluoride ($SF_6$) to measure air ventilation inside the Cavern. AUTOTRAC is a microprocessor-controlled, electron-capture gas chromatograph designed to automatically analyze the $SF_6$ tracer gas. The presence of $SF_6$ will capture electrons from an ionized gas stream in proportion to the concentration of the gas present in the gas sample. The ventilation rate in this study can be given by,

$$C_t = C_o e^{-It},$$

*Institute of Nuclear Science, Tsing-Hua University, Taiwan

**Department of Physics, New Mexico Institute of Mining and Technology, Socorro, New Mexico

where t is the time, $C_o$ and $C_t$ are the initial and final tracer concentrations, respectively, and I is the cavern air change rate. The ventilation rate Q is equal to I*V where V is the volume of the cavern. After collecting several $SF_6$ concentrations, we used the equation to fit these experimental data.

An Ultrafine Condensation Particle Counter (UCPC, Model 3025, TSI Inc., St. Paul, MN) was used to measure the number concentration of submicrometer-sized airborne particles. An external computer was connected to the UCPC and collected data continuously at 2-min intervals. The surrounding temperature was also measured and recorded by the computer.

Five sets of GDB data were analyzed to determine the size distribution of radon progeny in the air. The number particle concentration ranged from 240 particles/$cm^3$ to 360 particles/$cm^3$. The unattached PAEC fraction ranged from 0.28 to 0.45. The PAEC size distributions of radon progeny as measured by the ITRI and NMT GDBs were compared. Most of the size distributions present a bimodal shape except one set of the ITRI GDB data that showed a small second peak (Fig. 1). Good agreement was obtained between the ITRI and NMT data. The unattached fractions ranged from 0.29 to 0.52 with higher values for the NMT GDB data; the equilibrium factor ranged from 0.37 to 0.48.

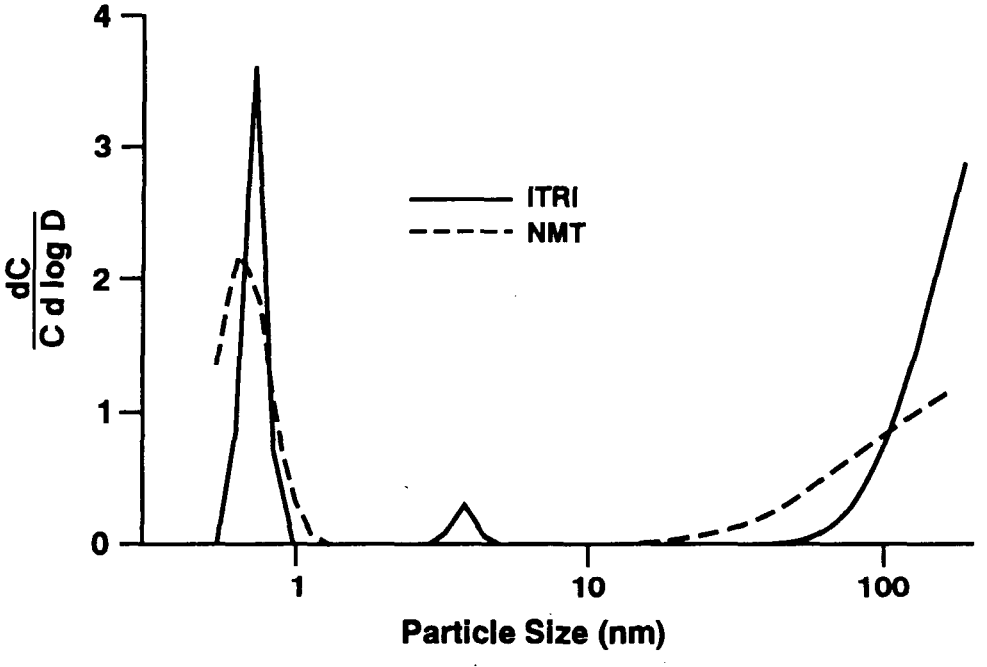


Figure 1. The PAEC of radon progeny as measured by the ITRI and NMT GDBs on July 28, 1994.

The radon concentration was monitored by the RGM-3 from the evening of July 25 to the morning of July 29, 1994. It was nearly constant during the experimental period. The average radon activity concentration was 1806 Bq/$m^3$ (48.4 pCi/l). This value was much higher than the radon concentration level of 0.64 Bq/$m^3$ which was measured at the Visitor Center. The Visitor Center is on the ground level and connected by elevator with the Main Cavern which is on average 228 m below the surface.

The average ventilation rate in the cavern is 0.0026 V/hr, as calculated by our equation. Our results showed that the Cavern atmosphere may be quite different from other underground environments. The atmosphere in the summer is stable and relatively free of airborne particles, partly due to the extremely slow air exchange rate.

(Research sponsored by the Office of Health and Environmental Research, U.S. Department of Energy, under Contract No. DE-AC04-76EV01013.)

# EVALUATION OF THE PERFORMANCE OF ANNULAR DIFFUSION DENUDERS

*Bijian Fan*, Yung-Sung Cheng, and Hsu-Chi Yeh*

An annular diffusion denuder (ADD) is used to trap gases from an air sample stream and to minimize sampling artifacts. An ADD consists of two coaxial cylinders with inner seals at both ends; its internal wall is coated with material suitable for collecting the gas. As the air sample stream is drawn through the annular space, the gas molecules diffuse rapidly and adsorb onto the coated wall. Comprehensive information on the diffusion technique and diffusion denuder has been presented (Cheng, Y. S. In *Air Sampling Instruments for Evaluation of Atmospheric Contaminants* [S. V. Herring, ed.], ACGIH, Cincinnati, OH, p. 46, 1989).

The purpose of this study was to determine the collection efficiency, E, of an ADD. To this end, a fractional loss of mass of the gas inside the denuder was calculated, given as:

$$E = \frac{m_{in} - m_{out}}{m_{in}} = 1 - \frac{\int_{\kappa}^{1} c_{out}\, u_{out}\, r\, dr}{\int_{\kappa}^{1} c_{in}\, u_{in}\, r\, dr} . \qquad (1)$$

In the calculation, the gas concentration was determined, $c$, inside an annulus by numerically solving its governing equation, which is given by:

$$u\frac{\partial c}{\partial x} = \frac{1}{Pe}\nabla^2 c , \qquad (2)$$

where the velocity (u) is assumed to have a fully developed flow laminar profile (Bird, R. B. *et al. Transport Phenomena*, John Wiley & Sons, Inc., New York, NY, 1960). The numerical solution was obtained using a software package for computational fluid dynamics (Fluid Dynamics International. *FIDAP User Manual 7.0*, Evanston, IL, 1994).

An earlier study (Possanzini, M. *et al. Atmos. Environ. 17*: 2605, 1983) characterized the gas collection efficiency of an ADD by a single deposition parameter, $\Delta = DL/(\nu Re_{\delta}\delta)$. Here $\delta$ denotes the annulus gap, L the ADD length, $D$ the gas diffusivity, $\nu$ the flow kinematic viscosity, and $Re$ the flow Reynolds number. An inefficiency of the single-parameter characterization showed that the gas collection efficiency depends on two parameters: the Peclet number ($Pe = R_o U_m/D$) which characterizes the diffusion behavior of gas, and the annulus radii ratio ($\kappa = R_i/R_o$) which characterizes the shape of an annulus. Here, $R_i$ and $R_o$ are the inner and outer radii of the ADD, and $U_m$ is the mean flow velocity. To confirm the model, the calculated collection efficiency was compared with the experimental data of Possanzini *et al.* and found a coefficient of variance of 0.61%. This comparison validated the computational fluid dynamics approach as a useful method for determining the collection efficiency of the annular denuder.

---

*Postdoctoral Participant

After the validation, a parametric calculation for a broad range of *Pe* and κ was developed by regressing the calculated collection efficiency for a one-equation model:

$$E = 100 \exp(a(1-\kappa)^b \, Pe^c) , \tag{3}$$

where the regression coefficients were: a = –0.0766, b = 3.3, and c = 1.385. The coefficient of variance between the calculation and the model was 4.57%.

To confirm the accuracy of equation (1) for predicting collection efficiency, its prediction was compared with a set of experimental data (Possanzini *et al.*, 1983), which covers collection efficiencies for three annular denuders with various flow rates. Introducing a dimensionless deposition factor, $D_f = (1-\kappa)^{3.3} Pe^{1.385}$ showed the comparison in a two-dimensional mode (Fig. 1). The difference between the present model and the experimental data was measured by the coefficient of variance, which was found to be 3.26%. This agreement demonstrates that the model involving the Peclet number and the annulus radii ratio is a dependable tool for predicting the collection efficiency of an annular denuder.

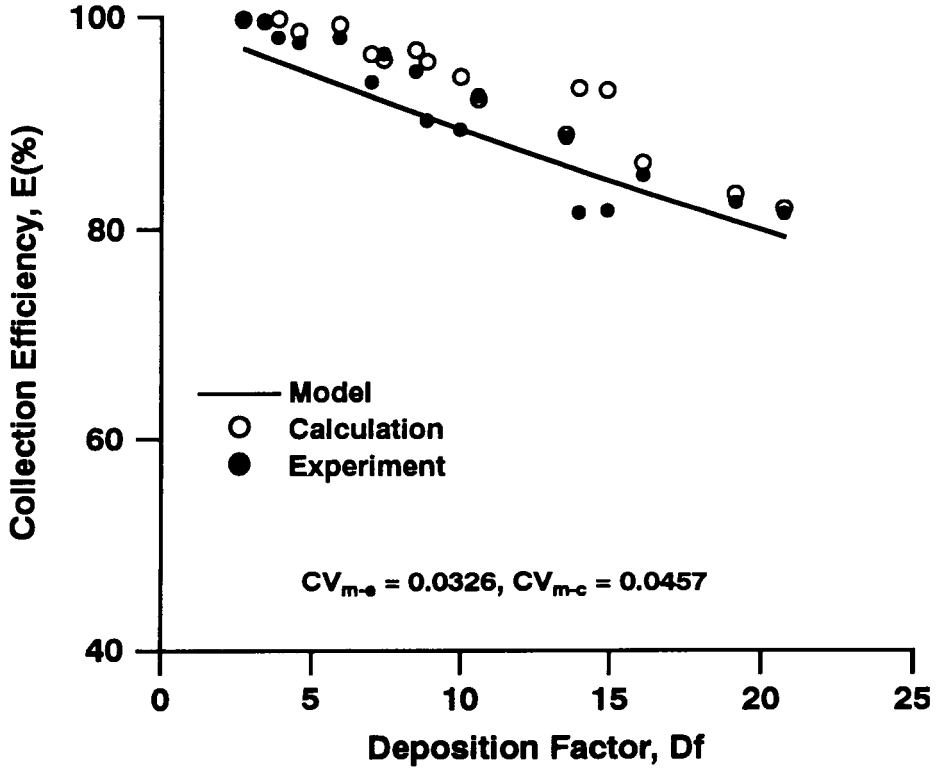


Figure 1. Comparison of the prediction of the ADD efficiency model with the calculations of the computational fluid dynamics program and with the experimental results of Possanzini *et al.* (1983).

(Research supported by the Office of Health and Environmental Research, U.S. Department of Energy, under Contract No. DE-AC04-76EV01013.)

# EVALUATION OF THE TSI SMALL-SCALE POWDER DISPERSER

*Bean T. Chen, Hsu-Chi Yeh, and Bijian Fan**

Several dry powder generators, including the Wright-dust-feed, the fluidized-bed, the venturi tube, and the jet-o-mizer systems, have been used for inhalation toxicity studies involving relatively high concentrations of aerosols (Carpenter, R. L. and K. Yerkes. *Am. Ind. Hyg. Assoc. J. 41*: 888, 1980; Cheng, Y. S. *et al. Am. Ind. Hyg. Assoc. J. 46*: 449, 1985). For fundamental laboratory studies, however, a powder generator that can produce a limited quantity of test aerosol is more practical than a system that generates high concentrations. The TSI small-scale powder disperser (SSPD) (Model 3433, TSI Inc., St Paul, MN) is a low flow rate, low mass output generator that uses venturi aspiration through a capillary tube to remove particles from the surface of a turntable, like a vacuum cleaner. The particles are then deagglomerated in a venturi throat and an expansion cone. The purpose of this study was to evaluate the SSPD by investigating the effects of flow rate, particle size, and particle shape on the generation efficiency and internal losses.

Carbon fibers (Hercules, Inc., Wilmington, DE), talc (commercial grade), alumina (Duke Scientific, Palo Alto, CA), and polystyrene latex (PSL) microspheres (Duke Scientific) were used to study the effects of particle shape (cylindrical, disc, irregular, and spherical shapes, respectively) on the dispersion efficiency of the SSPD. Monodisperse PSL spheres with fluorescent green dye (excitation maximum at 459 nm, emission maximum at 512 nm) and nominal particle diameters of 3, 6, 10, 22, and 97 $\mu$m were used to study the effects of particle size on powder production. Following dispersion, the powder was collected on a fluoropore filter (Millipore Corp., Bedford, MA) placed at the top of the SSPD. After each run, the SSPD was disassembled into six parts: the turntable, capillary tube, two expansion cones, exhaust tube, and sampling probe. The internal surface of each part was rinsed with acetone into a pre-weighed aluminum container. Following evaporation of the acetone in a ventilated hood, each container was reweighed to determine the mass of particles deposited on the corresponding part of the SSPD. The mass on the fluoropore filter was also determined gravimetrically and compared to the mass of the powders before generation to determine generation efficiency and the percentage of internal losses at each disassembled part. For the fluorescence-tagged PSL powders, both the gravimetric and fluorometric methods were used for mass analysis (Chen, B. T. *et al. Am. Ind. Hyg. Assoc. J. 52*: 75, 1991).

Along with the experiments, internal losses were predicted theoretically by considering the forces of drag, gravity, and flow shear-induced lift (Saffman, P. G. *J. Fluid Mech. 22*: 385, 1965). The lift force, generated as a result of the low-velocity particle stream exiting into high-velocity air, is perpendicular to flow direction. The lateral migration distance, $S_{lift}$, is obtained by

$$S_{lift} = 0.0069 d_p^3 \left(\frac{\rho_p}{\rho}\right)\left(\frac{|\kappa|}{\nu^3}\right)^{1/2} W , \qquad (1)$$

where $\rho_p$ and $\rho$ are the particle and air density, respectively; $d_p$ is the particle diameter, $\kappa$ is the flow shear, $\nu$ is the kinematical viscosity, and W is the relative velocity between particles and the flow. From equation (1), it is clear that the lateral migration of a particle is proportional to the relative particle velocity (a function of particle size and inertia), particle density, and particle size. Consequently, internal losses should increase and generation efficiency should decrease with increasing particle velocity, density, and size. Note, however, that the decrease in generation efficiency caused

*Postdoctoral Participant

by higher internal losses at higher flow rates should be offset to some extent by more efficient aspiration of particles from the turntable at higher flow rates.

These theoretical predictions are confirmed by our experimental results. Figure 1 shows that generation efficiency increased when the total flow rate was increased from 5 to 8 L/min and remained relatively constant for flow rates greater than 8 L/min. As predicted, generation efficiency of the higher density talc and alumina particles (densities 3.04 and 3.9 g/cm$^3$, respectively) was lower (only 40% to 60%) as compared to the generation efficiency of the less dense PSL microsphere and carbon fiber materials (densities 1.05 and 1.83 g/cm$^3$, respectively) which was 60% to 80%. Note that no significant effects of particle shape were noted; the carbon fibers behaved similar to the PSL spheres, and the disc-like talc particles behaved similar to the irregularly shaped alumina particles.

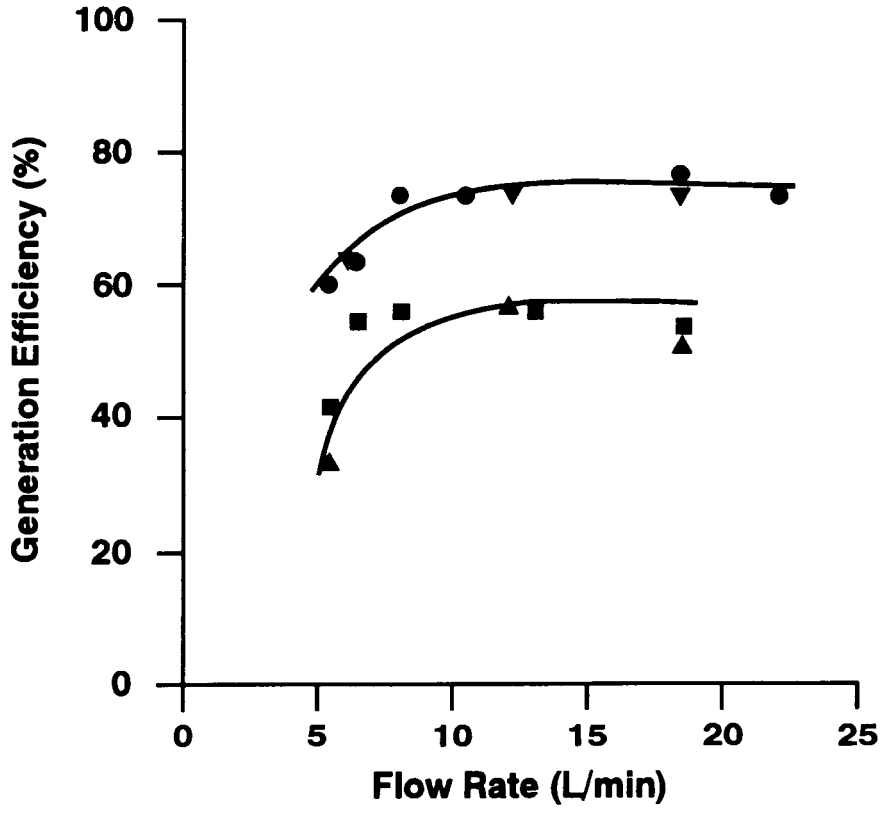


Figure 1. Dispersion efficiency as a function of flow rate in the TSI small-scale powder disperser for carbon fibers (●), 3-$\mu$m diameter polystyrene latex spheres (▼), talc (■), and alumina (▲).

Figure 2 shows the influence of particle size on the generation efficiency of PSL microspheres for flow rates between 5 and 18.5 L/min. As in Figure 1, generation efficiency increased with flow rate for each particle sizes, but the overall efficiency decreased substantially as the particle size increased. For example, at a flow rate of 18.5 L/min, generation efficiency of the PSL aerosol decreased from 74% to 24% as the particle size was increased from 3 to 97 $\mu$m. This is attributed to the fact that larger particles have larger inertia, which makes them more susceptible to impaction on the internal surface of the generator. For particle sizes smaller than 97 $\mu$m, the flow expansion region of the venturi tube was a primary site of internal losses. For the 97-$\mu$m diameter microspheres, impaction losses in the exhaust tube accounted for between 27% and 57% of the aspirated particles, while losses in the exhaust tube were less than 10% for diameters smaller than 97 $\mu$m.

This research shows a good agreement between theoretical predictions and experimental results for performance of the TSI small-scale powder disperser. An understanding of the influence of flow rate, particle density, particle size, and particle shape on generation efficiency can help users apply this device effectively.

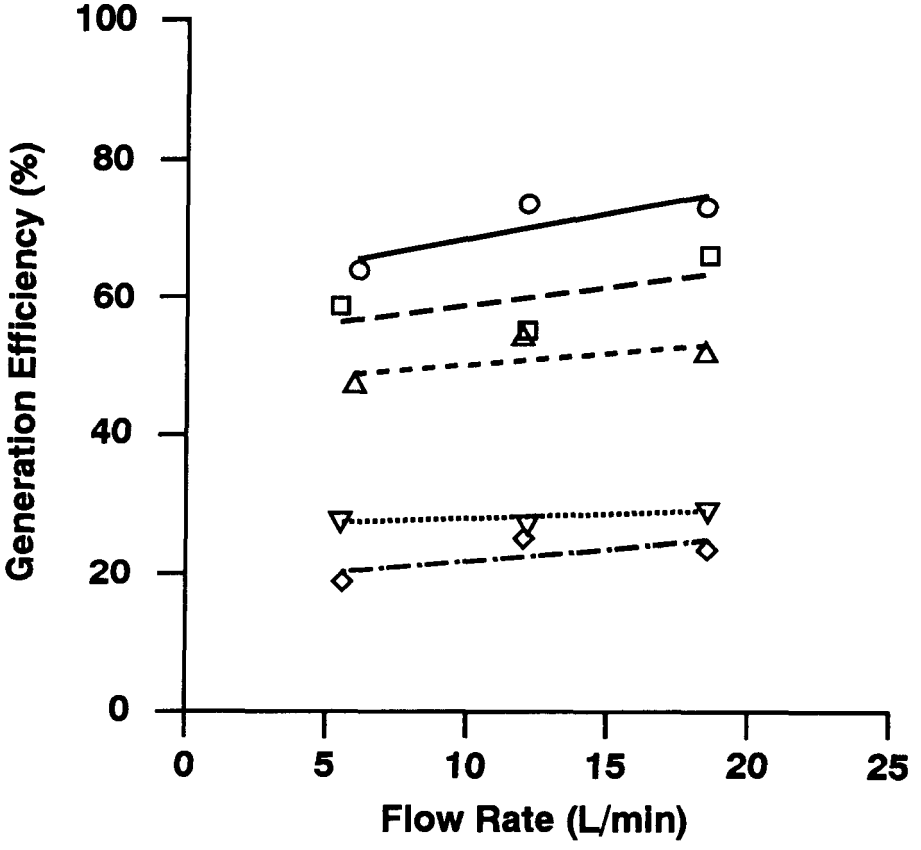


Figure 2. Dispersion efficiency as a function of flow rate in the TSI small-scale powder disperser for monodisperse polystyrene latex spheres with diameters of 3 (○), 6 (□), 10 (△), 22 (▽), and 97 (◇) $\mu$m.

(Research supported by the Office of Health and Environmental Research of the U. S. Department of Energy, under Contract Number DE-AC04-76EV01013.)

# PENETRATION OF ASBESTOS FIBERS IN RESPIRATOR FILTERS

*Yung-Sung Cheng, Sean D. Pearson*, Kevin D. Rohrbacher**, and Hsu-Chi Yeh*

Currently, the health risks associated with asbestos have restricted its use and created a growing asbestos abatement industry with a need for respirator filters that are effective for worker protection. The main purpose of this project is to determine the influence of fiber size, electrostatic charge, and flow rate on the penetration of asbestos fibers in respirator filter cartridges.

The study includes four types of filters each tested at two flow rates: the AO-R57A, a dual cartridge HEPA filter tested at 16 and 42.5 L/min; the MSA-S, a dust and mist filter tested at 16 and 42.5 L/min; the MSA-A power filter tested at 32 and 85 L/min; and the 3M-8710, a low-efficiency disposable face mask filter tested at 32 and 85 L/min. The lower flow rates apply to the dual cartridge type of respirator filters (MSA-S and 3M-8710). The three types of asbestos fibers used (amosite, crocidolite, and chrysotile) ranged in length from 0.04 to 0.5 $\mu$m and in aspect ratio (ratio of length to diameter) from 3 to 60. The fibers were used in both charged and neutralized forms. The results from amosite fibers are reported here.

The fiber aerosols were generated by a small-scale powder disperser, SSPD (Model 3433, TSI Inc., St Paul, MN) (this report, p. 12), which used a venturi feeder to aspire fibers off a small rotating disk. The aerosol was passed into a $^{85}Kr$ discharger tube to neutralize the fibers, through a dilutor to maintain proper concentration, and into the test chamber where a small fan and flow straightener distributed the flow evenly. A fibrous air monitor (FAM-1, MIE Inc., Billerica, MA) served as a real-time monitor for fiber concentration flowing through the chamber. An asbestos filter sampler with conductive material (Millipore Corp., Bedford, MA) was used to confirm the initial concentration of fibers in the test chamber. The filter cartridge to be tested was placed in a test assembly, and fibers that penetrated the cartridge were collected in a filter downstream of the test assembly. Twenty-five and 47 mm membrane filters (mixed cellulose acetate and nitrate, Millipore, Bedford, MA) were used in the upstream and downstream samplers. The pressure in the test chamber and the pressure drop across the test cartridge were monitored to verify that the desired flow rates were maintained.

Filter cartridges were used in an untreated condition directly from the box and in a treated condition which was induced by spraying them with an antistatic fluid (Zero Charge, Tech Spray, Amarillo, TX). The surface charge on the filters before and after the treatment was measured with an electrostatic fieldmeter (Model 245, Monroe Electronics, Lyndonville, NY). The 3M-8710 filter and the MSA-A filter had an initial charge, but the other filters did not.

After fibers were collected in the test filters, the filters were prepared for electron microscopy, then observed and photographed at a magnification of 6000X. The photographs were assembled to produce montages of a small portion of the filter center. The fibers were counted and their length and diameter measured with an electronic digital caliper (MAX-CAL, Cole-Parmer Instrument, Niles, IL). A ratio between the fibers counted in the upstream and downstream samples (with correction for flow rates and areas) was used to determine the average deposition efficiency of the respirator cartridge. Only fibers with aspect ratios greater than 3.0 were considered in the efficiency calculations. Each filter cartridge was tested at both flow rates with both charged and neutralized fibers, then treated with the antistatic spray and retested.

---

*Department of Energy/Associated Western Universities Summer Student Research Participant
**UNM/ITRI Inhalation Toxicology Graduate Student

Figure 1 shows the filtration efficiency for one high-efficiency dual cartridge filter (AO-R57A). Its efficiency was near 100% and was unaffected by either charges on the fibers or the filter itself. Essentially the same results were obtained for the other high-efficiency filter (MSA-A). Figure 2 shows the filtration efficiency of a low efficiency filter (MSA-S) and indicates that the charged fibers were collected more efficiently, especially before the filter was treated with antistatic spray. When electrical charges were removed from either the filter or the fibers, the filtration efficiency decreased.

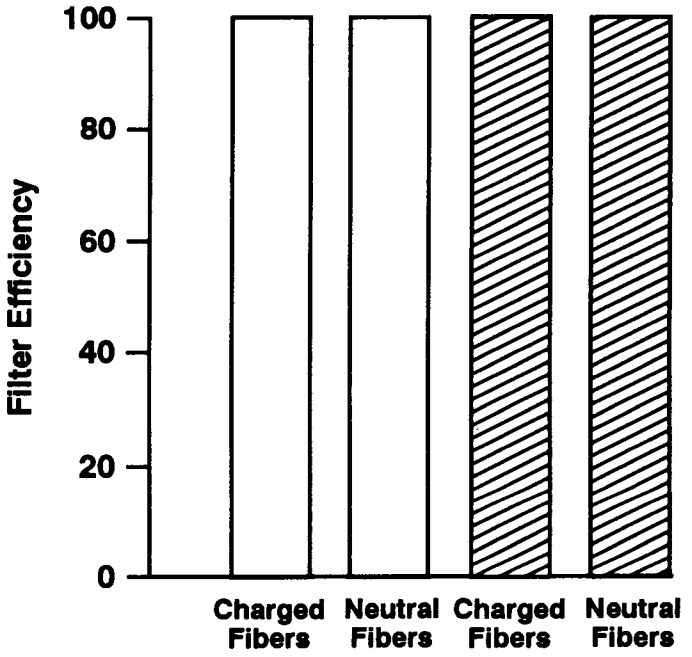


Figure 1. Overall filtration efficiency for amosite fibers in a HEPA respirator filter (AO-R57A) at 16 L/min (n = 1). Open bars are untreated filters and cross-hatched bars are treated filters.

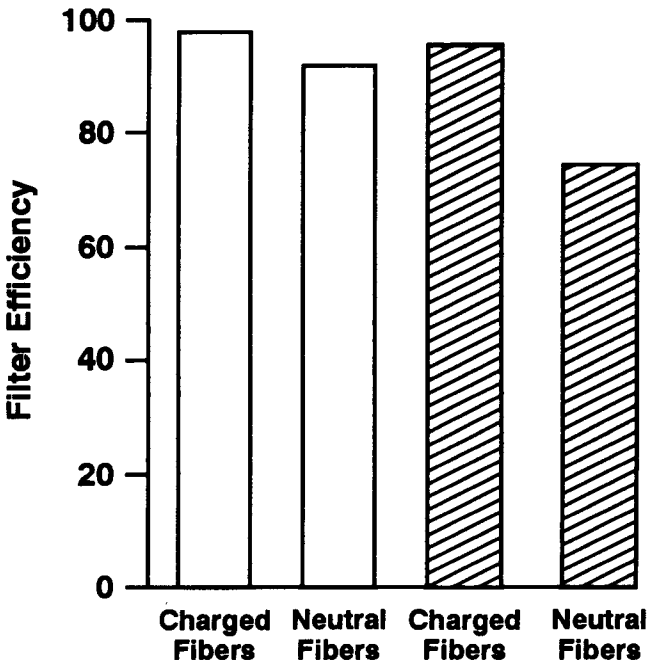


Figure 2. Overall filtration efficiency for amosite fibers in a dust and mist filter (MSA-S) at 16 L/min (n = 1). Open bars are untreated filters and cross-hatched bars are treated filters.

Overall, charge had a measurable effect on the performance of the low-efficiency filters; neutralizing the charge caused the filtration efficiencies to decrease. Flow rate had very little effect on filtration efficiency, but fiber size had some effect because smaller fibers can pass through the filter cartridge more easily. Our results have identified important factors that may need to be considered in testing respirator filters for fiber aerosols. Further studies will evaluate the penetration of two smaller fiber sizes through the same four test filters. Data for these three fiber sizes will enable a thorough evaluation of the relationship between the size of fibers and the overall rate of penetration.

(Research sponsored by the PHS/CDC under Grant R01-OH02922 from the National Institute of Occupational Safety and Health with the U.S. Department of Energy, under Contract No. DE-AC04-76EV01013.)

# MINIMUM DETECTABLE ACTIVITY AND FALSE ALARM RATE RELATIONSHIPS FOR ALPHA CONTINUOUS AIR MONITORS

*Mark D. Hoover and George J. Newton*

The U. S. Department of Energy rule for Occupational Radiation Protection (10 CFR Part 835, December 1993) and the DOE Radiological Control Manual (the RCM) (DOE/EH-0256T, Rev. 1, April 1994) require the use of continuous air monitors (CAMs) in normally occupied areas where an individual is likely to be exposed to a concentration of airborne radioactivity exceeding the derived air concentration (DAC) or where there is a need to alert potentially exposed individuals to unexpected increases in airborne radioactivity levels. The DAC is the airborne concentration that equals the annual limit on intake divided by the volume of air breathed by an average worker for a working year of 2000 h (assuming a breathing volume of 2400 $m^3$). It is equivalent to the airborne concentration to which a worker could be exposed for an entire working year (2000 h) without exceeding the allowable annual limit on intake. The rule and the RCM further require that real-time air monitors have an alarm capability and sufficient sensitivity to alert potentially exposed individuals that immediate action is necessary in order to minimize or terminate inhalation exposures. The RCM also recommends that real-time air monitors should be capable of measuring 1 DAC when averaged over 8 h (8 DAC-h) under laboratory conditions.

The DOE Implementation Guide (IG) for Workplace Air Monitoring (G-10 CFR 835/E2, Rev. 1, September 1994) provides acceptable methodologies for complying with the requirements of 10 CFR 835 and the RCM, including optional program recommendations. The IG clarifies the difference between the recommended sensitivity of CAMs under laboratory conditions and the practical level for alarm set points in the workplace. The IG states that CAMs used for routine monitoring normally should be set at the lowest practical level so as to accurately indicate loss of containment or the need for corrective action without causing a significant number of false alarms. Noting that excessive numbers of false alarms will reduce the CAM's credibility as an early warning device in the eyes of the worker, the IG recommends that false alarms should not exceed one per month per unit. The IG further states that when monitoring for alpha-emitting radionuclides is performed in the presence of high radon and thoron concentrations, an alarm set point of up to 24 DAC-h may be acceptable. In all cases, according to the IG, the actual alarm set point for each unit should be documented. In response to these recommendations, we are developing procedures for determining the basic sensitivity of alpha CAMs under laboratory conditions and for documenting practical alarm set points for routine use of CAMs under a range of radon and thoron concentrations. This work is summarized below.

Table 1 illustrates a realistic statistical situation for monitoring plutonium in the presence of radon and thoron progeny (laboratory conditions involving an effective radon concentration of 0.2 pCi/L). The probability of an alarm during a single measuring period is shown as a function of alarm set point (DAC-h) for a range of integrated plutonium concentrations (DAC-h) on the CAM collection filter. Calculations were done using the probability density functions for normal distributions contained in Microsoft Excel. In an ideal situation, a CAM would operate with no interference from background radiation (radon and thoron progeny), and the uncertainty in counting the signal (plutonium) would be negligible. The CAM would have a 100% probability of alarming if the integrated concentration is greater than the alarm set point, a 0% probability of alarming if the integrated concentration is less than the alarm set point, and a 50% probability of alarming if the integrated concentration is exactly equal to the alarm set point. In the absence of background interference, plutonium could be measured directly by simply counting the alpha emissions in the plutonium region of interest (ROI). Any uncertainty in the reported Pu concentration would only result from the fundamental uncertainty of Poisson counting statistics in which the standard deviation of the reported counts is equal to the square root of the detected counts.

## Table 1

### Probability that a Stated Integrated Concentration of Plutonium (DAC-h) Will Cause a CAM Alarm for a Range of Alarm Set Points (DAC-h) in the Presence of an Effective Radon Concentration of 0.2 pCi/L[a]

| Alarm Set Point (DAC-h) | Probability of an Alarm at the Stated Concentration | | | | | | | | | | | | | |
|---|---|---|---|---|---|---|---|---|---|---|---|---|---|---|
| | 0 DAC-h | 2 DAC-h | 4 DAC-h | 6 DAC-h | 8 DAC-h | 10 DAC-h | 12 DAC-h | 16 DAC-h | 20 DAC-h | 24 DAC-h | 28 DAC-h | 32 DAC-h | 36 DAC-h | 40 DAC-h |
| 0 | 0.5 | 0.87589 | 0.96318 | 0.98833 | 0.99617 | 0.99872 | 0.99956 | 0.99995 | 0.99999 | 1 | 1 | 1 | 1 | 1 |
| 2 | 0.02275 | 0.5 | 0.81445 | 0.93471 | 0.97725 | 0.99207 | 0.99723 | 0.99966 | 0.99996 | 0.99999 | 1 | 1 | 1 | 1 |
| 4 | 3.2e-05 | 0.12411 | 0.5 | 0.77515 | 0.90879 | 0.96478 | 0.98675 | 0.9982 | 0.99976 | 0.99997 | 1 | 1 | 1 | 1 |
| 6 | 9.9e-10 | 0.01046 | 0.18555 | 0.5 | 0.74751 | 0.8861 | 0.95195 | 0.99235 | 0.99887 | 0.99984 | 0.99998 | 1 | 1 | 1 |
| 8 | 6.7e-16 | 0.00027 | 0.03682 | 0.22485 | 0.5 | 0.72675 | 0.86637 | 0.97383 | 0.99559 | 0.99931 | 0.9999 | 0.99999 | 1 | 1 |
| 10 | 0 | 1.9e-06 | 0.00365 | 0.06529 | 0.25249 | 0.5 | 0.71045 | 0.92719 | 0.98545 | 0.99744 | 0.99958 | 0.99994 | 0.99999 | 1 |
| 12 | 0 | 3.9e-09 | 0.00017 | 0.01167 | 0.09121 | 0.27325 | 0.5 | 0.83401 | 0.95957 | 0.9918 | 0.99852 | 0.99975 | 0.99996 | 0.99999 |
| 16 | 0 | 3.3e-16 | 4.00e-08 | 7.9e-05 | 0.00383 | 0.03522 | 0.13363 | 0.5 | 0.80863 | 0.9452 | 0.98707 | 0.99733 | 0.9995 | 0.99991 |
| 20 | 0 | 0 | 4.20e-13 | 6.10e-08 | 3.2e-05 | 0.00128 | 0.01325 | 0.16599 | 0.5 | 0.78814 | 0.9313 | 0.98164 | 0.99574 | 0.99911 |
| 24 | 0 | 0 | 0 | 5.10e-12 | 4.80e-08 | 1.2e-05 | 0.00044 | 0.02617 | 0.19137 | 0.5 | 0.77119 | 0.91813 | 0.97574 | 0.99377 |
| 28 | 0 | 0 | 0 | 0 | 1.30e-11 | 2.90e-08 | 4.60e-06 | 0.0018 | 0.04043 | 0.21186 | 0.5 | 0.75688 | 0.90578 | 0.96954 |
| 32 | 0 | 0 | 0 | 0 | 6.70e-16 | 1.70e-11 | 1.50e-08 | 5.20e-05 | 0.00441 | 0.0548 | 0.22881 | 0.5 | 0.7446 | 0.89424 |
| 36 | 0 | 0 | 0 | 0 | 0 | 2.30e-15 | 1.40e-11 | 6.20e-07 | 0.00024 | 0.0082 | 0.0687 | 0.24312 | 0.5 | 0.73391 |
| 40 | 0 | 0 | 0 | 0 | 0 | 0 | 4.10e-15 | 2.90e-09 | 6.4e-06 | 0.00069 | 0.01293 | 0.08187 | 0.2554 | 0.5 |

[a]The background standard deviation for the CAM at 0.2 pCi/L effective radon concentration is assumed to be 1 DAC-h. The standard deviation of plutonium concentration is estimated from Poisson statistics to equal the square root of the concentration.

In the realistic situation, however, background radioactivity from radon and thoron progeny must be subtracted from the gross reading of a plutonium CAM to provide a net estimate of the true activity of plutonium. The correction algorithm of an alpha CAM estimates this background by counting the activity of radon and thoron progeny in other ROIs and subtracting a fraction of that activity from the plutonium ROI. If the correction algorithm is working properly, a CAM will report zero Pu when no Pu is present. However, even if the mean of the reported counts is zero, the standard deviation of the reported counts will be nonzero and will increase with increasing concentrations of radon and thoron progeny.

The combination of inherent uncertainty in the background correction and the counting of Pu itself yields the total uncertainty in the estimate of the true plutonium radioactivity. When these uncertainties are taken into account, as in Table 1, the basic performance capabilities of a CAM can be assessed. For example, the alarm probabilities in Table 1 illustrate that a CAM with a 1 DAC-h standard deviation for background has a sensitivity of 8 DAC-h. The probability of an 8 DAC-h alarm being triggered is $6.7 \times 10^{-16}$ when the actual Pu accumulation is 0 DAC-h. Note, however, that it would be impractical to set the alarm at 2 DAC-h because there is more than a 2% chance (1 in every 50 measurements) that background alone would activate such an alarm.

Noting that the probabilities in Table 1 are based on a single measuring period (5 min for example, for a CAM operating at 2 cfm flow rate, with a 20% detection efficiency), it is necessary to calculate the false alarm rate when multiple measurements are made over long periods of time, and under any conditions of radon and thoron background. The annual false alarm rate, F, can be calculated as:

$$F = M * P^N , \quad (1)$$

where M is the number of measurements per year, P is the probability of a false positive for a single measurement, and N is the number of sequential positive reports required for activation of the alarm. M is calculated by dividing the number of minutes per year ($5.25 \times 10^5$) by the number of minutes in each measuring period, T. Thus, if T is 5 min, then M is $1.05 \times 10^5$ measuring periods per year. (This approach assumes to a first approximation that the measurements are independent.)

The probability, P, of a false positive report for a single measurement can be determined as a two-step process. The first step is to divide the alarm set point, A, by the standard deviation of the background, STDEV, to calculate how many STDEVs above background the alarm set point is. For example, if the alarm set point is 8 DAC-h and the STDEV of the background is 1 DAC-h, then the set point is 8 STDEVs above the background. (Note that if the radon correction algorithm provides a background correction value greater than zero, then the number of STDEVs above background must be decreased.) Next, consult a standard probability distribution table (or do the calculation explicitly) to obtain the fraction of occurrences greater than the stated number of STDEVs above the mean background. For 8 STDEVs above the background, the probability of a false positive is $6.7 \times 10^{-16}$, as was noted in Table 1. A calculation of greater interest would be for a radon concentration of 1 pCi/L where the standard deviation of the background might be 2.24 DAC-h. In that case, the 8 DAC-h set point is 3.6 STDEVs above the mean, and the probability of a false positive, P = 0.000159 = $1.6 \times 10^{-4}$. Equation (1) can now be used to calculate a value of $7 \times 10^{-7}$/y for the false alarm probability when the background is 0.2 pCi/L radon, and a value of 16.8 false alarms per year when the background concentration is 1 pCi/L radon. (These rates were calculated for a sequential positive report value of N = 1.) This demonstrates that the CAM has an 8 DAC-h sensitivity under laboratory conditions (0.2 pCi/L radon), but that more than one alarm per month will occur if an 8 DAC-h alarm set point is used when the effective radon concentration is 1 pCi/L. At an ambient radon concentration of 4 pCi/L, the number of false alarms per year would be 3770, or more than 10 per day (see Table 2).

Table 2

Calculations of False Alarm Rates as a Function of Alarm Set Point and Alarm Set Points as a Function of False Alarm Rate for a Range of Radon Progeny Concentrations

| Ambient Radon Concentration (pCi/L) | False Alarm Rate per Year as a Function of Alarm Set Point | | Achievable Alarm Set Point as a Function of Desired False Alarm Rate | |
|---|---|---|---|---|
| | 8 DAC-h Alarm Set Point | 24 DAC-h Alarm Set Point | 1/mo False Alarm Rate | 1/y False Alarm Rate |
| 0.2 | $7 \times 10^{-11}$ | negligible | 3.6 | 4.3 |
| 1 | 16.7 | negligible | 8.1 | 9.6 |
| 4 | 3770 | 0.006 | 16.2 | 19.4 |

Noting that some alarm set points will be impractical under actual workplace conditions, a similar calculational approach can be used to select an alarm set point, A, that will provide the desired false alarm rate, F. By rearranging equation (1), we can solve for the required probability, P, of a single false positive:

$$P = (F/M)^{1/N} . \quad (2)$$

For example, if the desired false alarm rate is 1 per month, then F is 12/y. Assuming that a 5-min averaging period is used, then M is still $1.05 \times 10^5$. Assuming that a single positive report will be used, then N = 1. Thus, the required probability of a false positive for a single measurement is $1.14 \times 10^{-4}$. This corresponds to 3.65 STDEVs above background. At 0.2 pCi/L with a background STDEV of 1 DAC-h, the alarm could be set at 3.65 DAC-h. At 1 pCi/L with a background STDEV of 2.24, the alarm could be set at 8.17 DAC-h. However, at 4 pCi/L with a background STDEV of 4.5 DAC-h, the alarm would have to be set at 16.2 DAC-h.

Even alarm rates as infrequent as 1 per month may be intolerable in work areas with multiple CAMs. For example, in a room with 10 or more CAMs, it may be desirable to have false alarm rates as low a 1/y per unit. Table 2 includes examples of the practical alarm set point and false alarm calculations for radon concentrations of 0.2, 1, and 4 pCi/L. Note that at higher concentrations of radon progeny, it may be necessary to increase the duration of the integration period or increase the number of positive reports (N) needed to trigger the alarm, in order to maintain a reasonable alarm set point and false alarm frequency. Note from examination of Table 1 that false alarms can also be triggered by Pu concentrations below the alarm set point. For example, if the accumulated Pu activity is 4 DAC-h, there is nearly a 4% chance that a single measurement will trigger an 8 DAC-h alarm. Thus, one out of every 25 measurements will be a false positive. Such false alarms from measurable activity levels below the alarm set point should be avoided, primarily because they needlessly undermine worker confidence, but also because workplace concentrations below the alarm set point can easily be detected from analyses of retrospective air samples. Where measurable, but tolerable, airborne concentrations are present, the use of multiple positive reports would also reduce the probability of false alarms.

The final consideration in setting appropriate alarm set points is quantification of the probability that an unacceptable air concentration will remain undetected. Inspection of Table 1 provides

information about the rate of false-negative reports. For example, noting that the probability is 0.99931 that a 24 DAC-h release will trigger an 8 DAC-h alarm on a single report, the probability of a false negative under this condition is only $6.9 \times 10^{-4}$. A release of exactly 8 DAC-h will fail to trigger an 8 DAC-h alarm with a probability of 0.5 after one report, 0.25 after two reports, 0.125 after three reports, 0.0625 after four reports, and 0.031 after five reports. Thus, a release at the alarm set point will be detected within a few reporting periods, and the probability of a false-negative condition will decrease rapidly with increasing concentration.

The approaches described here provide a useful method for assessing CAM sensitivity, calculating practical alarm set points, and estimating false alarm rates. The fundamental measurement that must be made for each CAM is the standard deviation of the background under realistic workplace conditions.

(Research sponsored by the Office of Health Physics and Industrial Hygiene Programs of the U.S. Department of Energy, under Contract No. DE-AC04-76EV01013.)

# RESPONSE OF THE SAVANNAH RIVER IMPACTOR-TYPE ALPHA CONTINUOUS AIR MONITOR TO PLUTONIUM AND RADON PROGENY

*Mark D. Hoover, Bean T. Chen, and George J. Newton*

The Savannah River Site (SRS) impactor-type alpha continuous air monitor (CAM) is an innovative, high-volume, real-time alpha air monitoring system. It was developed at SRS (Collins, D. C. *U.S. AEC Report DP-188*, Savannah River Plant, 1956; Tait, G. W. C. *Nucleonics 14*: 53, 1956) and has been routinely used for many years. At the request of the Westinghouse Savannah River Company, we have independently evaluated the ability of this CAM to meet the 8-DAC-h sensitivity recommendation of the U.S. Department of Energy Radiological Control Manual (DOE/EH-0256T). The evaluation included flow calibration and radioactivity counting tests of the impactor CAM, measurements of aerosol collection efficiency and homogeneity, and challenges with plutonium aerosols in the absence and presence of radon progeny. Tests with radioactive aerosols included a direct comparison of the response of the impactor CAM to that of an Eberline Alpha-6A CAM (Eberline Instrument Corporation, Santa Fe, NM) equipped with a remote inline sampling head. Results were confirmed by restrospective analyses of fixed air filters.

Two configurations of the impactor CAM are used at SRS: portable units that operate at 32 cfm using their own vacuum pumps, and installed units that operate under house vacuum at 40 cfm. Both configurations use identical components for the sampling chamber, aerosol impactor, and detector assembly. A portable unit, modified to include a larger vacuum pump when needed, was used for the tests at ITRI at 20 cfm (a lower-than-normal flow rate that might occur during CAM operation), 32 cfm, and 40 cfm.

Particle collection efficiency in the impactor was determined by tests with monodisperse, fluorescent-labeled, polystyrene latex spheres and liquid droplet aerosols (1992–93 Annual Report, p. 15). Delivery efficiency through the inlet dome of the portable unit was greater than 90% for 10-$\mu$m diameter particles at 20, 32, and 40 cfm and increased for smaller particle sizes. Internal delivery efficiencies through the CAM were greater than 95% at 20 and 32 cfm for aerodynamic particle sizes 0.5, 1.1, 2.2, and 3.2 $\mu$m, and greater than 90% and 85% for particle sizes 6.2 $\mu$m and 10 $\mu$m, respectively. The 50% cutoff aerodynamic diameter for the impactor was 3.2 $\mu$m at 20 cfm, which corresponds to values of 2.6 $\mu$m at 32 cfm and 2.3 $\mu$m at 40 cfm. A typical particle size distribution for aerosols from industrial operations can be considered to have an activity median aerodynamic diameter of 5 $\mu$m with a geometric standard deviation of 2.5 (*Human Respiratory Tract Model for Radiological Protection*, Publication 66, Annals of the ICRP 24, No. 1–4, Pergamon Press, Oxford, 1994). That size distribution, which is consistent with measurements at SRS, has 68%, 76%, and 80% of its radioactivity associated with particles larger than cutoff diameters 3.2 $\mu$m, 2.6 $\mu$m, and 2.3 $\mu$m, respectively. Thus, even at the lower-than-normal flow rate, more than two-thirds of the available aerosol mass is expected to be larger than the collection cutoff of the impactor.

No particle bounce off the collection planchet was observed for any particle size when a very thick (15 mg) layer of grease was used. The amount of grease normally used on the particle collection planchets (1.5 mg) was adequate to quantitatively retain all collected particles with diameters of 3.2 $\mu$m or less; for particle sizes of 6.2 and 10 $\mu$m, approximately 85% of the particles entering the CAM were retained on the collection planchet, and 15% penetrated to the backup filter due to particle bounce.

When the SRS CAM was calibrated with no grease layer on the ZnS(Ag)-coated collection substrate, the counting efficiency was essentially 100% of the 2-$\pi$ emissions (50% of the total 4-$\pi$ emissions). Use of a very thick (15 mg) grease layer reduced the counting efficiency to about 50% of the 2-$\pi$ emissions. Use of the typical 1.5-mg grease layer only reduced the counting efficiency by a few percent to about 95% of the 2-$\pi$ emissions.

The efficiencies for all aspects of aerosol sampling can be combined to give overall efficiencies for detection of airborne plutonium as a function of particle size. For 10-$\mu$m aerodynamic diameter particles, the total collection efficiency of the SRS CAM was 62% ([0.90 inlet efficiency] × [0.85 internal delivery efficiency] × [1.0 impactor collection efficiency] × [0.85 impactor retention efficiency due to bounce] × [0.95 counting efficiency through grease] = 0.62). Based on the results for 3.2 $\mu$m particles, the total collection efficiency of the SRS CAM was 55% ([0.90 inlet efficiency] × [0.95 internal delivery efficiency] × [0.70 impactor collection efficiency] × [1.0 impactor retention efficiency] × [0.95 counting efficiency through grease] = 0.55). These values for overall system efficiency compared very favorably with the conservative assumption of 50% efficiency that has been traditionally used at SRS.

Experiments were done with radon progeny and plutonium aerosols to confirm the performance of the SRS CAM. Figure 1 shows the portable SRS CAM with an inline Eberline Alpha-6A CAM installed after the impactor stage for simultaneous, real-time measurements of plutonium and radon progeny aerosols. A final backup filter was included to confirm the concentration of any aerosols that penetrated the impactor stage. Laboratory concentrations of ambient radon progeny aerosols (approximately 0.2 pCi/L radon) were sampled from rooms with normal laboratory ventilation (about six air changes per hour), and elevated concentrations of ambient radon progeny (approximately 4 pCi/L radon) were sampled from a basement area with low ventilation. These aerosols were sampled through the normal inlet of the portable CAM. When plutonium aerosols were sampled, the CAM inlet was connected directly to aerosol generation lines. The radon progeny aerosols for the plutonium tests were generated using a system described previously (1991–92 Annual Report, p. 14).

Figure 2 compares the responses to an 8-DAC-h release of plutonium under laboratory conditions (0.2 pCi/L ambient radon progeny) for the SRS impactor CAM operated at 32 cfm and an inline Eberline Alpha-6A CAM operated at 1 cfm. Prior to the introduction of the plutonium release, both CAMs detected an identical gross concentration of radon progeny aerosol. Because the flow rate of the SRS CAM was 32 times higher than that of the Alpha-6A, it is evident that the impactor design has been effective in allowing approximately 97% of the radon progeny aerosol to pass through the sampling zone without being collected. Note, however, that although the Alpha 6A collected all radon progeny in its sample flow, it uses a correction algorithm that would reduce the net background interference to approximately zero. A limitation of the SRS CAM is that its response to plutonium comes on top of its response to radon progeny. In some cases, this may make it difficult to distinguish a slow release of plutonium aerosol from a gradual increase in radon progeny background. Nevertheless, while the response of the Eberline CAM to the 8-DAC-h release was detectable, the response of the SRS CAM was unmistakable. If elevated radon progeny concentrations present a background interference higher than 8-DAC-h equivalent, then the alarm set point can reasonably be raised without exceeding the recommended 24-DAC-h value noted in the DOE air monitoring implementation guide (this report, p. 18). In the presence of 4 pCi/L radon concentration, the background interference in the SRS CAM ranged as high as 1200 dpm (8 DAC-h equivalent), requiring an increase of the alarm set point, but releases of 8 DAC-h plutonium were easily detected as a departure from that background level.

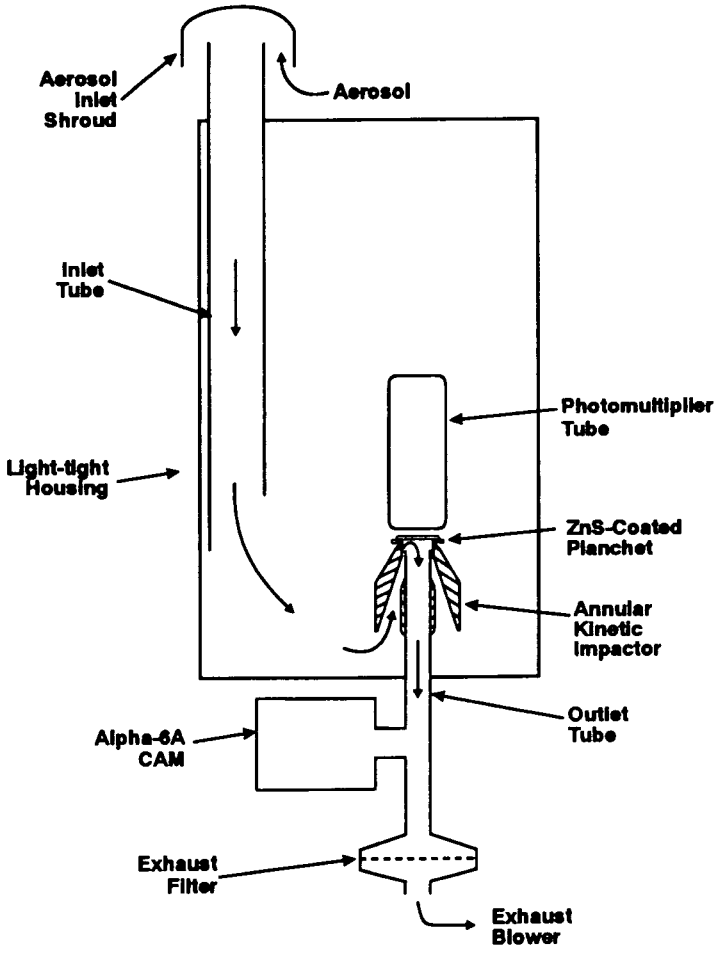


Figure 1. Schematic diagram of the portable Savannah River Impactor CAM with an inline Eberline Alpha-6A CAM and a backup filter for collection of aerosols that penetrate the impactor.

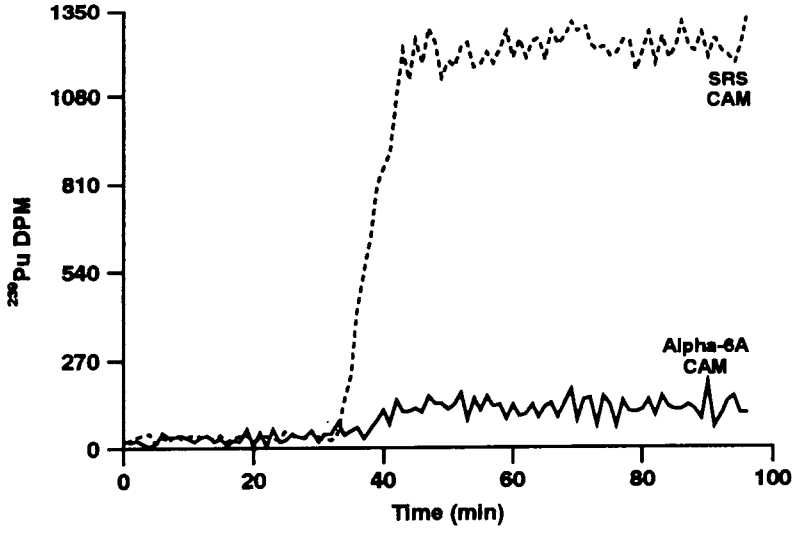


Figure 2. Comparison between responses to an 8-DAC-h release of plutonium under laboratory conditions for the SRS impactor CAM operated at 32 cfm and for an inline Eberline Alpha-6A CAM operated at 1 cfm.

This work has demonstrated that the SRS impactor CAM can meet the 8 DAC-h sensitivity requirement under laboratory conditions and that it also complies with the IG recommendation that an acceptable false alarm rate be achieved with alarm set points at or below 24 DAC-h in the presence of elevated workplace concentrations of radon progeny.

(Research sponsored by the Westinghouse Savannah River Company through Purchase Order No. AA-71928 with the U.S. Department of Energy, under Contract No. DE-AC04-76EV01013.)

# EFFECT OF PRIOR DUST COLLECTION ON DETECTION, COUNTING EFFICIENCY, AND ENERGY RESOLUTION FOR ALPHA CONTINOUS AIR MONITORS

*George J. Newton and Mark D. Hoover*

For the past several years, we have supported the DOE Waste Isolation Pilot Plant (WIPP) project by evaluating the capabilities and performance of the Eberline Alpha 6 (Eberline Instrument Corporation, Santa Fe, NM) continuous air monitor (CAM). This evaluation has focused on the ability of the CAM to correctly report plutonium in the presence of salt dust. Tests involving the simultaneous collection of plutonium and salt have shown that burial by salt can degrade the detection of plutonium, but that this interference is negligible when salt concentrations are below about 0.2 $mg/m^3$ (1989-90 Annual Report, p. 5). It has also been shown that salt concentrations as high as 0.5 $mg/m^3$ can be tolerated by the CAM with minimal interference if the alpha energy region for plutonium detection in the CAM is widened to include detection of alpha radiation that has been degraded by salt (1991-92 Annual Report, p. 11). Throughout the evaluation, it has been assumed that salt burial is a concern for slow, chronic release of plutonium, but that any acute release of plutonium would be collected on the top surface of the filter or salt and would be unattenuated. The spectral quality of alpha radiation detection on membrane filters is observed to improve with filter loading. This is attributed to the probability that accumulations of dust tend to fill in surface irregularities of the collection filter at a faster rate than they create additional surface irregularities. The validity of these assumptions about the improved detection of plutonium on salt-layer surfaces has recently been questioned. Based on electron micrographic examination of salt-laden filters, it has been speculated (Bartlett, W. *et al. An Evaluation of Air Effluent and Workplace Radioactivity Monitoring at the Waste Isolation Pilot Plant,* EEG-52, Environmental Evaluation Group, Albuquerque, NM, 1993) that collection of salt dust on a membrane filter results in formation of pores, fissures, and dendritic shapes of salt on the filter surface. If plutonium were collected, particles could penetrate into the pores and fissures, resulting in a degraded or lost signal from the plutonium. Based on the fact that burial of plutonium by a modest layer of salt results in negligible reduction in detection, it is unlikely that detection of plutonium on the surface of a salt layer could be less efficient than detection on a clean filter. However, because no experimental evidence existed to answer the concern, the purpose of the current study was to quantify any differences between detection of plutonium on clean or salt-laden filters.

Salt-laden Versapor 3000 filters from WIPP Station A were provided for use in the study. Clean filters from the same lot were also provided. Plutonium-239 particles with an activity median aerodynamic diameter less than 1 $\mu$m and a geometric standard deviation of approximately 1.6 were generated with a Lovelace nebulizer and collected in an Eberline Alpha-6 CAM using both types of filters. The target amount of alpha radioactivity during each test was more than 1500 disintegrations per minute (dpm) or 300 counts per minute as detected by the Alpha-6 (20% efficiency, 2.5-cm detector diameter, 2.5-cm diameter filter collection area). After achieving the desired target activity on a filter, alpha energy spectra were collected with the Alpha-6 at 5-min intervals until the total number of counts in the alpha spectrum was greater than 5000. This provided smooth spectra from which to obtain information about the quality of each alpha energy spectrum. The full-width-at-half-maximum-height (FWHM) of the plutonium peak was taken as a measure of the resolution or sharpness of a pulse height energy spectrum. A larger FWHM would indicate poorer resolution as a result of salt attenuation. Following collection of the alpha energy spectra, the filter was removed from the CAM and counted by the ZnS(Ag) method to determine the total plutonium activity on the filter. The efficiency of this method has been shown to be nominally 50%, and to be unaffected by salt layers as thick as several $mg/cm^2$ (1991-92 Annual Report, p. 11). Comparison of the ZnS(Ag) result to the value detected by the CAM confirmed any salt attenuation effects. The Alpha-6 and the

ZnS(Ag) counting efficiencies were calibrated exactly using electroplated $^{239}Pu$ sources traceable to the National Institute of Standards and Technology.

Figure 1 shows the alpha energy spectra when plutonium particles were collected in an Eberline Alpha 6 CAM with a 2.5-cm diameter detector and a 2.5-cm filter collection diameter on a clean filter and on a filter which had accumulated 14.6 mg of salt at WIPP Station A. The total number of Alpha-6 counts accumulated in each spectrum were similar: 5147 counts in the clean filter spectrum and 5297 counts in the salt-laden filter spectrum. As soon as plutonium particles began to accumulate on each filter, the characteristic spectrum shape became evident. Continued detection of the plutonium caused the total number of counts in the spectrum to increase, but did not alter the spectral shape. The FWHMs were 560 keV for plutonium on the clean Versapor filter and 380 kev for plutonium on the salt-laden filter, indicating a greater effective surface roughness on the clean filter. The spectra on the salt-laden filter were sharper and better defined, indicating a more uniform effective surface.

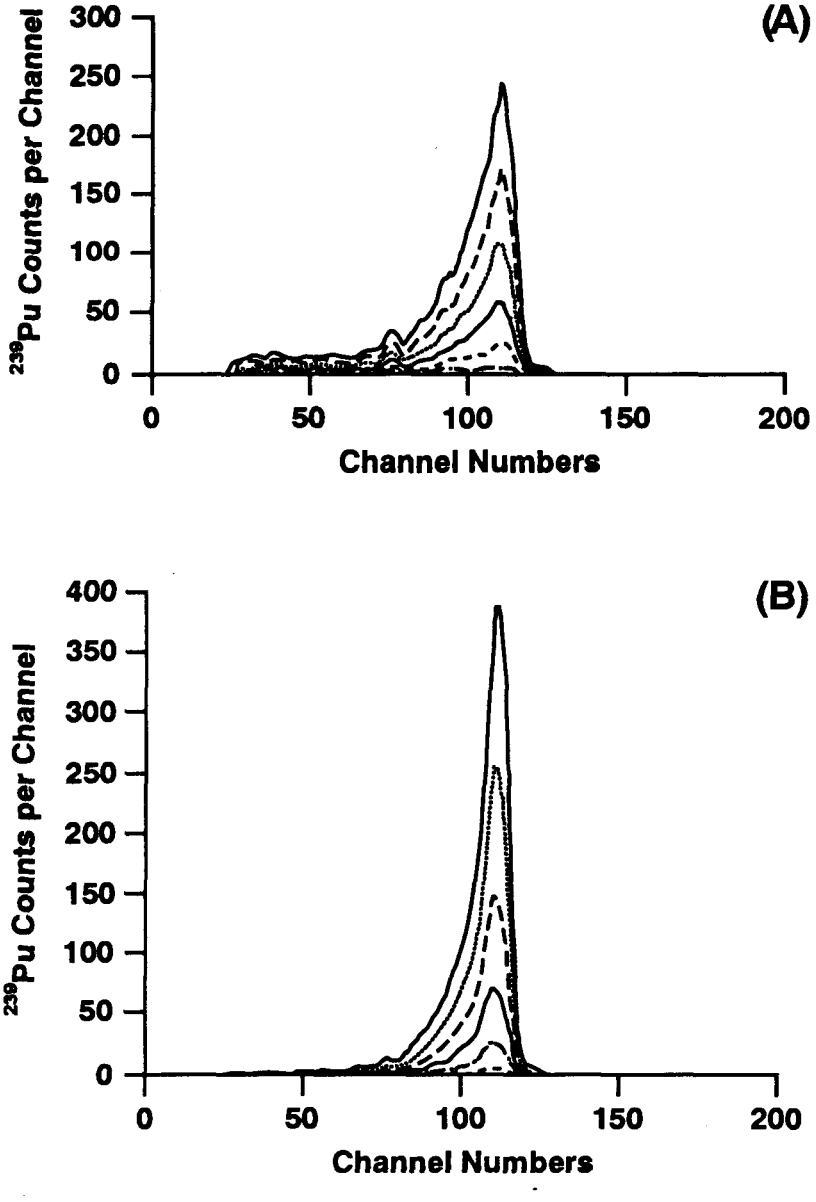


Figure 1. Alpha energy spectra demonstrating that energy resolution is (A) poorer when $^{239}Pu$ is collected on a clean Versapor 3000 filter, than (B) when collected on a salt-laden (14.6 mg) filter from WIPP.

More important than the differences in spectral shape between the clean and salt-laden filters, however, was the similarity of total plutonium detection efficiency in both cases. (Note that the total plutonium radioactivity collected during the each test was not necessarily identical, but was intended to be at least 1500 dpm.) The final activity reported by the Alpha-6 for plutonium collected on the clean filter shown in Figure 1 (1725 dpm) was essentially 100% of the activity measured by the ZnS(Ag) method (1733 dpm). The final count rate reported by the Alpha-6 for plutonium collected on the salt-laden filter (2155) was also essentially 100% of the activity measured by the ZnS(Ag) method (2149 dpm). Thus, there was no loss of detection efficiency when plutonium was collected on salt-laden Versapor 3000 filters, as compared to clean filter surfaces.

This study has shown that the alpha energy resolution for plutonium collected on a salt-laden Versapor 3000 filter is better than the resolution for plutonium collected on a clean filter, and that there is no difference in detection efficiency for plutonium collected under the two different conditions. These results confirm the assumption that attenuation by salt is not a concern for acute releases of plutonium that will deposit material directly on the surface of clean or salt-laden filters.

(Research performed with funding from the DOE Waste Isolation Pilot Plant Program Office under U.S. Department of Energy Contract No. DE-AC04-76EV01013.)

# CHARACTERIZATION OF AEROSOLS PRODUCED BY SURGICAL PROCEDURES: A SUMMARY

*Hsu-Chi Yeh, Bruce A. Muggenburg, David L. Lundgren, Robert S. Turner*, Raymond A. Guilmette, M. Burton Snipes, and Robert K. Jones*

In many types of surgery, especially orthopedic procedures, power tools such as saws and drills are used. These tools can impart considerable energy in disrupting tissue and may produce aerosolized blood and material from bone and other tissues. Surgical lasers and electrocautery tools can also produce aerosols due to vaporization of blood and tissues. A number of studies have been reported concerning production of aerosols during surgery, and some of the aerosols produced may contain infectious materials.

Health care workers have expressed concern and questions pertaining to the occupational transmission of blood-borne pathogens including the human immunodeficiency virus (HIV) and hepatitis B virus (HBV) via blood aerosols during surgery. Little or no data existed characterizing the aerosols produced performing surgical procedures. Because of this lack of data, the National Institute for Occupational Safety and Health funded a project at ITRI to assess the extent of aerosolization of blood and other tissues during surgical procedures in the laboratory and in a hospital surgical suite.

Aerosols generated during 10 surgical procedures were sampled at the Lovelace Medical Center (LMC) (name changed to Lovelace Health System after the conclusion of our site studies). The surgeries included five total hip replacements, one back vertebral fusion, three total knee replacements, and one hip reconstruction. No unusual amount of bleeding was reported during any procedure. No two operations were identical. Surgical activities changed frequently and were not always predictable; different tools were used, and surgeons or nurses changed locations within the room from time to time. Due to the changing nature of the operations, the aerosol mass concentration and the size distribution varied widely from procedure to procedure and from time to time during the same procedure. However, some general observations can be made. The respirable aerosol mass concentration was higher during the total hip replacement procedures than during the total knee replacement procedures. Among the people in the surgical suite wearing the Marple personal cascade (MPC) impactors, the three surgeons had measurable but very low amounts of aerosol (on the order of a few tens of micrograms). Analyses for hemoglobin with Chemstrip 9 (or Hemastix), a product commonly used to detect hemoglobin in urine, consistently indicated that blood-associated aerosol particles were detected (positive results of 3+, 2+, and 1+, corresponding to about 250 ery/$\mu$L, 50 ery/$\mu$L, and 10 ery/$\mu$L, respectively, as specified by the manufacturer) for the first four to five MPC impactor stages which correspond to aerodynamic particle sizes of 3.5 $\mu$m to over 21.3 $\mu$m. During the knee surgery, a tourniquet was applied, and no blood was observed during most of the procedure. Filter samples obtained during the time the tourniquet was applied showed nondetectable or very low blood content as determined by Chemstrip 9 analyses. On the other hand, the Chemstrip 9 analyses on the filter samples obtained after the release of the tourniquet, followed by irrigation/suction to clean the site for suturing, showed a response higher than 1+, similar to observations during the total hip replacement procedure. From these observations, we hypothesized that most of the blood-associated aerosols might be produced during irrigation/suction. Quartz crystal microbalance cascade impactor data indicated that aerosol mass concentration was highest (although the absolute values were still very low) during the earliest stage of surgery, i.e., the opening of the surgical site with a scalpel, the use of electrocautery, and the occasional use of irrigation/suction. The other procedures produced a much lower mass concentration of aerosols. Occasionally, area filter samples and one or two stages of MPC impactor

*Lovelace Health Systems

samples from personnel other than surgeons showed positive responses from Chemstrip 9 (either trace or 1+). This was probably due to splashing during irrigation/suction. Post-surgery room clean-up did not re-suspend any blood-associated aerosols (negative results from Chemstrip 9 analysis).

Note that the aerosols produced from surgical procedures using power tools might contain muscle as well as blood, and that Chemstrip 9 will respond to either the hemoglobin or myoglobin but cannot differentiate between the two. To positively identify the blood-associated aerosols, a laboratory study with $^{51}Cr$ labeled red blood cells was conducted in dogs, using total hip replacement procedures similar to the human procedures. The most important results from the dog study were that: (1) it confirmed that blood-associated aerosols were produced during the orthopedic surgery using power tools, (2) it showed that the degree of Chemstrip 9 response on samples correlated very closely to the $^{51}Cr$ radioactivity measurements indicating that positive responses of the Chemstrip 9 measured from human studies at LMC probably represented blood-associated aerosols, and (3) it provided a basis for quantifying the number of red blood cells (RBCs) associated with each aerosol particle size range; thus, the total inhalable RBCs could be estimated. Under the assumptions that (1) the results of the laboratory studies and the aerosol characterization at the LMC surgical room are similar, and (2) the surgeon's minute volume is 20 L/min (corresponding to moderate activity), we estimated that the total number of RBCs a surgeon might inhale would be $\approx 3 \times 10^5$ (or $\approx 9$ $\mu$g of RBCs). HIV is carried primarily through the lymphocytes, not through the RBCs. The ratio between the RBC and lymphocytes is about 2200:1 for humans (Wintrobe, M. M. *et al.*, *Clinical Hematology, 8th Ed.*, Lea & Febiger, Philadelphia, 1981). Therefore, the estimated number of lymphocytes available for inhalation by a surgeon would be $\approx$ 135 during the course of an orthopedic surgical procedure.

In assessing the potential exposure of surgical personnel to blood-associated aerosols, some consideration must be given to the role of the surgical masks which operating personnel wear to protect the patient and themselves from splashes and droplets. Although surgical masks are not approved as respiratory protection devices, the surgical mask will probably prevent some aerosol particles from reaching the nose or mouth for inhalation. The filter efficiency of a surgical mask, which does not take into account face-seal leakage, has been reported to range from a few percent to 50% for submicrometer-sized particles and from 20% to near 100% for micrometer-sized particles, depending on the type of surgical mask, flow rate, and particle size (Chen, C. C. and K. Willeke. *Am. J. Infect. Control 20*: 177, 1992; Tuomi, T. *Am. Ind. Hyg. Assoc. J. 46*: 308, 1985).

If particles are inhaled, the deposition efficiency within the respiratory tract is dependent on particle size and breathing pattern (flow rate). Our results indicated that about 60% of RBCs are associated with particles larger than 10 $\mu$m and about 8% of RBCs with particles less than 0.5 $\mu$m. The majority of the particles less than 0.5 $\mu$m probably originated from the use of electrocautery. Johnson, G. K. and W. S. Robinson (*J. Med. Virol. 33*: 47, 1991) reported that no infectious HIV-1 was detected in aerosols generated by electrocautery. The probability of a lymphocyte carrying HIV also needs to be taken into account when assessing the potential inhalation hazard. From all of these considerations, the potential inhalation risk from aerosols produced during orthopedic surgery seems very low. One should note that the existing literature does not provide evidence that blood-borne pathogens, such as HIV or HBV, have been transferred by the inhalation route (Tokars, J. I. *et al. JAMA 268*: 489, 1992; Petersen, N. J. *Ann. N. Y. Acad. Science 353*: 157, 1980). A question not addressed by these studies is the viability of HIV in inhaled HIV-associated aerosols produced by surgical procedures. To ascertain the significance of our results, further studies are required to assess the amount and viability of pathogens associated with these blood-associated aerosols.

(Research sponsored by the National Institute of Occupational Safety and Health under Interagency Agreement No. 92-05 with the U.S. Department of Energy, under Contract No. DE-AC04-76EV01013.)

# II. DEPOSITION, TRANSPORT, AND CLEARANCE OF INHALED TOXICANTS

# *IN VITRO* DISSOLUTION OF METAL TRITIDES

*Yung-Sung Cheng, Alan R. Dahl, and Hong-Nian Jow**

Metal tritides including titanium, zirconium, and erbium tritide have been used as components of neutron generators. These compounds can be released to the air as aerosols during fabrication, assembling, and testing of components or in accidental or fugitive releases, and as a result, workers may inhale them. Our understanding of metal tritides and their radiation dosimetry for internal exposure is very limited. Current radiation protection guidelines for metal tritide particles are based on the assumption that their biological behavior is similar to tritiated water which could be easily absorbed into body fluid, and therefore, has a relatively short biological half life (10 d). However, a few papers in the literature suggest that the solubility of metal tritide could be low (Miller, J. M. and S. R. Bokwa. *Leaching Behavior of High Specific Activity Titanium Tritide.* AECL-8870, Chalk River Nuclear Laboratories, Canada, 1985; Miller, J. M. In *Conference Summaries of Radioactive Waste Management*, Winnipeg, Canada, Canada Nuclear Society, CONF-820933 54/NTIS, PC A15/MF A01, p. 192, 1982). If this is true, the biological half-life of metal tritide particles and the dosimetry of inhalation exposure to these particles could be quite different from tritiated water, and this would have significant implications in the current health protection guidelines. The purpose of this study was to investigate the dissolution behavior of metal tritide particles in simulated biological fluids and in rats. Data from these studies will provide information with which to estimate the dosimetry of inhaled metal tritides. A dosimetric model can then be used as the technical basis for setting health protection limits, including annual limits on intake and derived air concentrations for DOE facilities.

For our study, the radioactive titanium tritide was obtained from the Martin Marietta Pinellas Plant, Largo, FL. This material had been a component of a neutron generator and was ground into a coarse powder. Samples of the powder were examined in an optical microscope, and particle size was determined using an image analyzer. A sample of the coarse powder was further ground in a ball mill (U.S. Stoneware, Mahwah, NJ) at ITRI to obtain a fine powder for inclusion in the dissolution studies.

Serum ultrafiltrate was used to determine the dissolution rates of the coarse and fine metal tritides powders (Eidson, A. F. and W. C. Griffith. *Health Phys. 46*: 151, 1984). A static dissolution system (Kanapilly, G. M. *Health Phys. 32*: 89, 1979) was used in the study. About 10 mg of powder was used for each sample. The particles were sandwiched between two, 47-mm membrane filters (Tuffryn HT-100, 0.2 $\mu$m pore size, Millipore Corp., Bedford, MA) and secured in a Teflon filter holder (Free Flow Filter Holder 04-112, In Tox Products, Albuquerque, NM). Duplicate samples were tested. Each filter holder was placed into a 500-mL glass flask containing 100 mL of SUF incubated in a 37°C water bath.

Tritium dissolved in metal tritides can exist as gas or can be exchanged into tritium oxide (Miller and Bokwa, 1985), so the *in vitro* dissolution apparatus used in this study was designed to measure tritium in both states. Figure 1 shows the schematic diagram of the dissolution system. The catalyst columns were used to convert tritium gas released from the powder into tritium oxide, which was subsequently trapped in propylene glycol bubblers. The catalyst column was packed with a precious metal sponge catalyst (GPT, Inc., Manalapan, NJ). The column was placed inside a tube furnace maintained at 550°C. The conversion efficiency of the catalyst column was determined to be 93.3%.

*Sandia National Laboratories, Albuquerque, New Mexico

The size distributions of the coarse and fine titanium tritide powders can be fitted with a lognormal distribution. The coarse powder had a count median diameter (CMD) of 103 $\mu$m, mass median diameter (MMD) of 193 $\mu$m, and a geometric standard deviation ($\sigma_g$ ) of 1.6. The fine powder size had a CMD of 1.0 $\mu$m, MMD of 3.4, and $\sigma_g$ of 1.9.

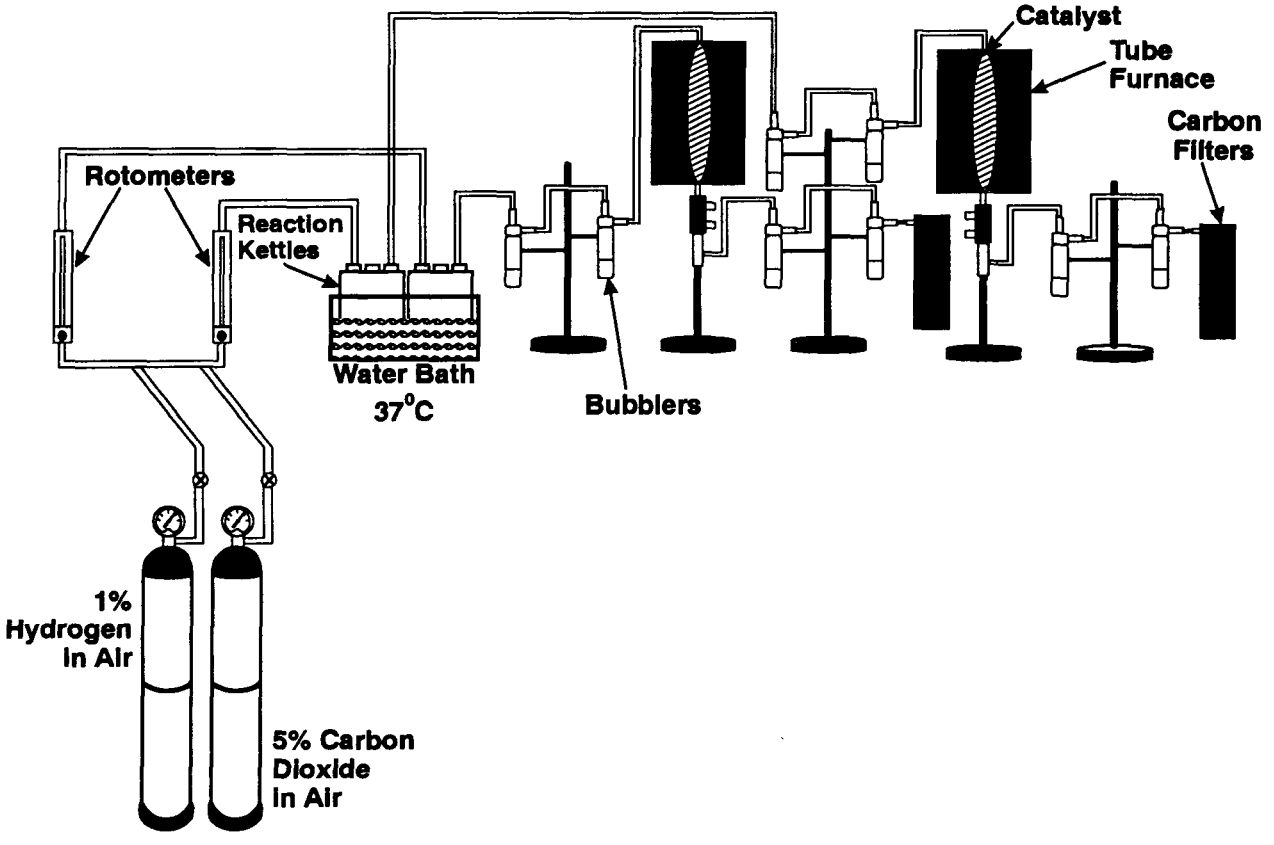


Figure 1. Schematic of the apparatus for measuring the solubility of metal tritide and determining the fraction of tritium released as tritium oxide and tritium gas.

Figure 2 shows the dissolution curves for the coarse and fine titanium tritide powders. The $^3H$ activity retained in the powder can be expressed as a single exponential decay curve (t in days) for the unmilled tritide powder:

$$A = \exp(-1.92 \times 10^{-3}t) .$$

The dissolution half-time, $t_{1/2}$ is 361 d. Milled powder dissolves much faster, and the retention curve can be expressed as a two-component exponential decay curve:

$$A = 0.24 \exp(-0.71t) + 0.76 \exp(-2.09 \times 10^{-2}t).$$

The dissolution half times for $^3H$ are 1.0 and 33 d for the fast and slow phases of the retention curve, respectively.

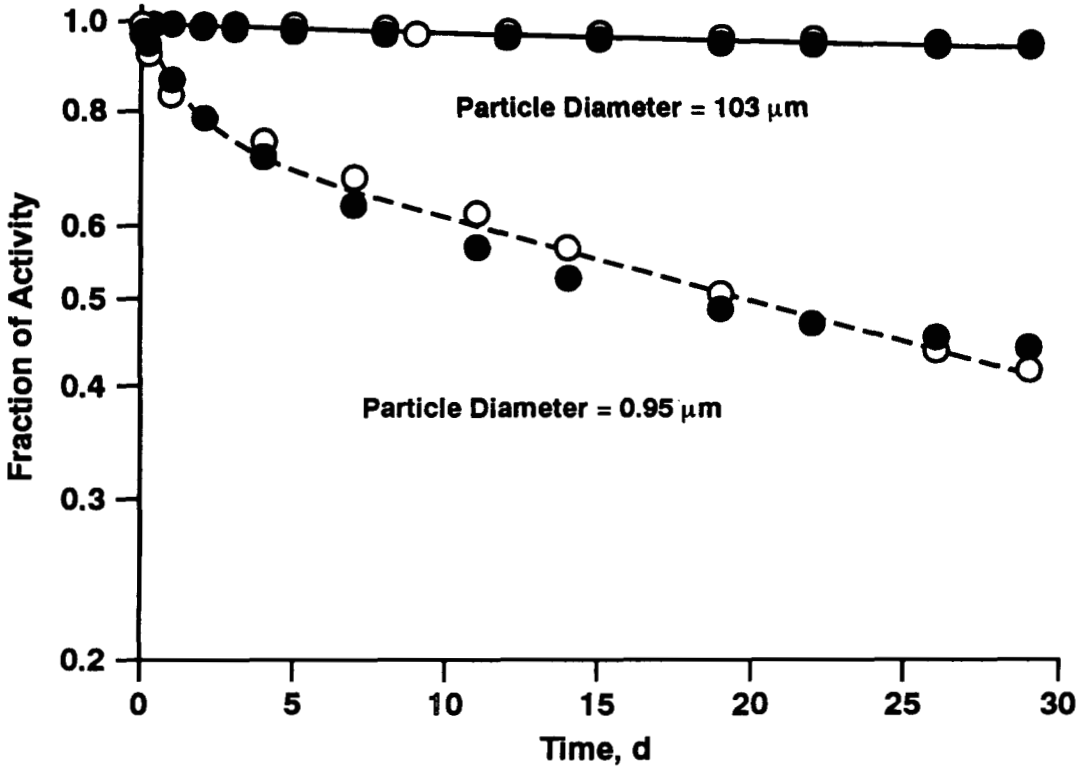


Figure 2. Retention curves of $^{3}H$ in a serum ultrafiltrate solvent for the coarse and fine titanium tritide powders. Open and closed circles represent the results for duplicate samples.

Our results showed a slow dissolution rate with less than 0.2%/d for 100 $\mu$m particles. The rate increased to about 2%/d for the 1 $\mu$m particles. These results are consistent with the theory that the dissolution rate for smaller particles is higher because of the larger specific surface area (Mercer, T. T. *Health Phys. 13*: 1211, 1967). The majority of tritium was released as tritiated water with a small fraction released as tritium gas. If these dissolution and clearance patterns are confirmed in the planned animal study, then the internal dosimetry of this material should be very different from tritiated water which has a biological half-time in the body of 10 d. These results may place metal tritide in the Y- or W-class of materials in terms of dissolution classification instead of the D-class for tritiated water. We plan to continue the *in vitro* dissolution study with erbium tritide using the same solvent and technique, followed by a study in which rats will be injected with metal tritide. These data will be used to develop an internal dosimetry model of metal tritide following inhalation exposure, and the new model should be useful for health protection purposes.

(Research sponsored by Sandia National Laboratory under Purchase Order No. AB-3148 with the U.S. Department of Energy, under Contract No. DE-AC04-76EV01013.)

# CORRELATION OF NASAL GEOMETRY WITH AEROSOL DEPOSITION IN HUMAN VOLUNTEERS

*Yung-Sung Cheng, Hsu-Chi Yeh, Raymond A. Guilmette, Steven Q. Simpson*, Kuo-Hsi Cheng**, and David L. Swift***

The nasal airways act as the first filter in the respiratory tract to remove very large or small particles, that would otherwise penetrate to the lower airways. (Cheng, Y. S. *et al. Radiat. Prot. Dosim. 38*: 41, 1991). Aerosol deposition data obtained with human volunteers vary considerably under comparable experimental conditions ( Yu, C. P. *et al. Am. Ind. Hyg. Assoc. J. 42*: 726, 1981; Cheng *et al.*, 1991). Reasons for the intersubject variations have been frequently attributed to the geometry of the nasal passages. Because there is no direct proof of this hypothesis, nasal deposition of ultrafine particles in human volunteers has been studied in our laboratory. Preliminary results obtained with four adult volunteers also vary considerably between subjects (1992-1993 Annual Report, p. 29). The purpose of this part of the study was to establish a theoretical equation relating diffusional deposition in nasal airways to the geometrical dimensions of the individual nasal airways. This relationship was then applied to the experimental deposition data and measurement of airway morphometry for correlation.

Four healthy, nonsmoking, adult male human volunteers (ages 40 to 57 y) participated in this study. The nasal morphometry of these subjects was measured using the magnetic resonance imaging (MRI) technique as described by Guilmette, R. A. *et al.* (*J. Aerosol Med. 2*: 365, 1989). Images of contiguous 3-mm-thick coronal sections were obtained using a Siemens 1.5 Tesla MRI machine at the Veterans Administration Medical Center, Albuquerque, New Mexico. Images of the entire length of the nasal airway from the external nares to the posterior nasopharynx were taken. Perimeters of the left and right nasal airways, which were digitized from transparency images obtained from the MRI, were analyzed using a sonic digitizer described previously (Guilmette *et al.*, 1989). Both left and right cross-sectional areas and perimeter lengths were calculated from the digitized data.

Each subject underwent nasal deposition experiments at constant flow rates of 4, 10, and 20 L/min. The exposures were conducted in the Human Exposure Laboratory at ITRI as described previously (1991-1992 Annual Report, p. 28). Monodisperse aerosols of silver (5, 8, and 20 nm) and polystyrene latex particles (50 and 100 nm) were used (1992-1993 Annual Report, p. 29). The aerosol entered a nasal mask covering the nose and exited from a tube from the mouth or vice versa. Aerosol concentrations in the inspired and expired air were determined by a TSI condensation particle counter (Model 3025, St. Paul, MN), and the deposition efficiencies were calculated from the ratio of these concentrations, with corrections from particles losses in the transport lines and masks (1992-1993 Annual Report, p. 29).

A theoretical equation for the nasal deposition of ultrafine particles can be derived based on a turbulent diffusion mechanism (Cheng, Y. S. *et al. Aerosol Sci. Technol. 18*: 359, 1993):

$$E = 1 - \exp\left(-a \left(\frac{A_s}{A_c}\right) (\bar{P}_r)^{1/8} D^{1/2} Q^{-1/8}\right), \quad (1)$$

*Department of Medicine, University of New Mexico, Albuquerque, New Mexico
**School of Hygiene and Public Health, Johns Hopkins University, Baltimore, Maryland

where E is the deposition efficiency; D is the diffusion coefficient ($cm^2/s$); Q is the flow rate (L/min); $A_s$ and $\bar{A}_c$ are the total surface area and mean cross-sectional area of the nasal airway, respectively; and $\bar{P}_r$ is the mean perimeter of the nasal airway (equal to the total surface area divided by the airway length). This equation indicates that E is a function of the geometric factor, $A_s/\bar{A}_c(\bar{P}_r)^{1/8}$. Nasal deposition increases when the factor increases; the perimeter has a small effect on deposition.

Table 1 lists the measured total surface area, $A_s$, mean cross-sectional area, $\bar{A}_c$, and mean perimeter, $\bar{P}_r$ for the four subjects. Surface and cross-sectional areas differed substantially. The geometric factor had a range of 76.2 for subject D to 120.7 for subject B. Therefore, we expect to see the highest nasal deposition in subject B and the lowest deposition in subject D. Equation (1) can be rearranged to give

$$-\ln P\, D^{-1/2}Q^{1/8} = a\left(\frac{A_s}{\bar{A}_c}\right)(\bar{P}_r)^{1/8}, \qquad (2)$$

where P is the aerosol penetration defined as (1-E) and is calculated from experimental data. Figure 1 shows the correlation between nasal deposition for inspiratory flow and the geometric factor. A linear relationship between values of $-\ln P\, D^{-1/2}Q^{1/8}$ and the geometric factor indicates that intersubject variation can be explained by the difference of airway dimensions. However, Subject A showed the maximum deposition (Fig. 2) instead of subject B as predicted theoretically. The MRI measurement was performed several months before the deposition study, so it is possible that the airway dimensions, especially the cross-sectional area, may have changed because of the nasal cycle or other reasons. *In situ* measurements of nasal airways at the time of deposition are being conducted in additional subjects to confirm the correlation.

Table 1

Nasal Airway Dimensions and Deposition Parameters for Four Human Volunteers

| Subject | Mean Cross-Sectional Area $\bar{A}_c$ (cm) | Total Surface Area $A_S$ ($cm^2$) | Mean Perimeter $\bar{P}_r$ (cm) | Geometric Factor $(A_S/\bar{A}_c)(\bar{P}_r)^{1/8}$ | Deposition Parameter[a] $-\ln(P)D^{-1/2}Q^{1/8}$ |
|---|---|---|---|---|---|
| A | 2.81 | 213 | 12.9 | 104 | 16.3 ± 6.3 |
| B | 2.03 | 182 | 10.9 | 121 | 16.3 ± 6.4 |
| C | 3.88 | 238 | 14.2 | 85.2 | 11.0 ± 6.1 |
| D | 3.25 | 184 | 11.1 | 76.2 | 11.3 ± 4.5 |

[a]Mean and standard deviation.

In summary, a theoretical frame work has been presented to relate observed intersubject variation in nasal deposition to airway dimensions. The nasal deposition is expected to increase with surface area and decrease with the cross-sectional area. This correlation seems to apply to the experimental data from four adult volunteers. We are augmenting the present results with more subjects and *in situ* measurements of airway dimensions at the time of deposition study. If confirmed, this correlation will provide a useful means to estimate the individual dose.

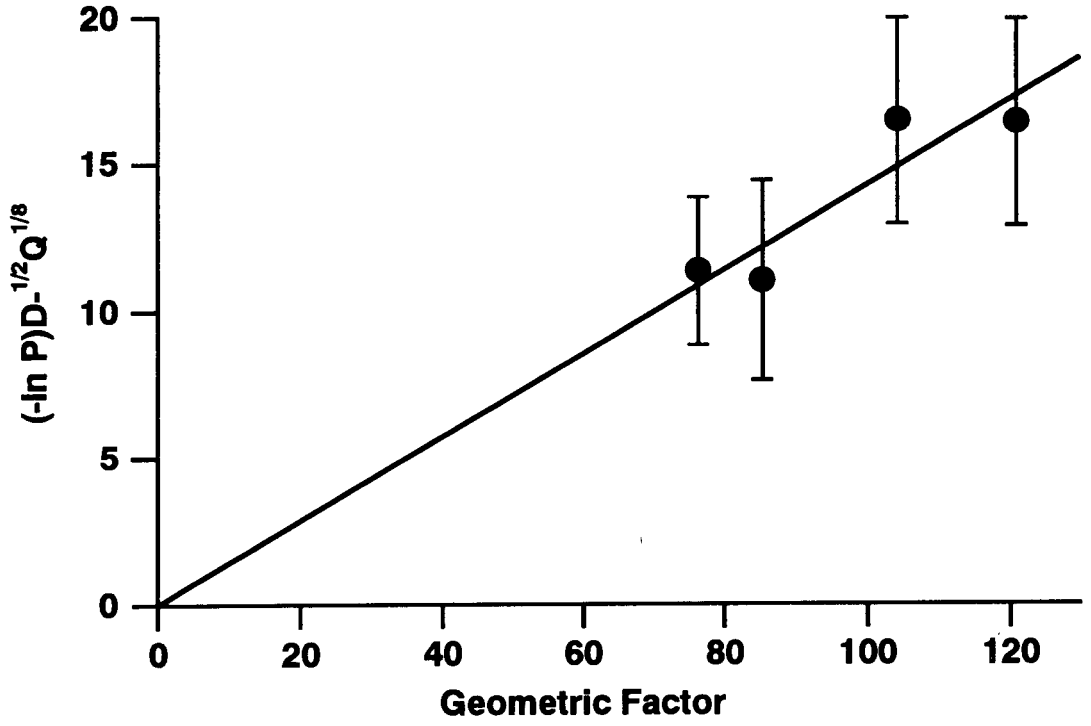


Figure 1. Correlation of the nasal deposition of ultrafine particles with the measured airway geometric factor (Mean ± S.D.).

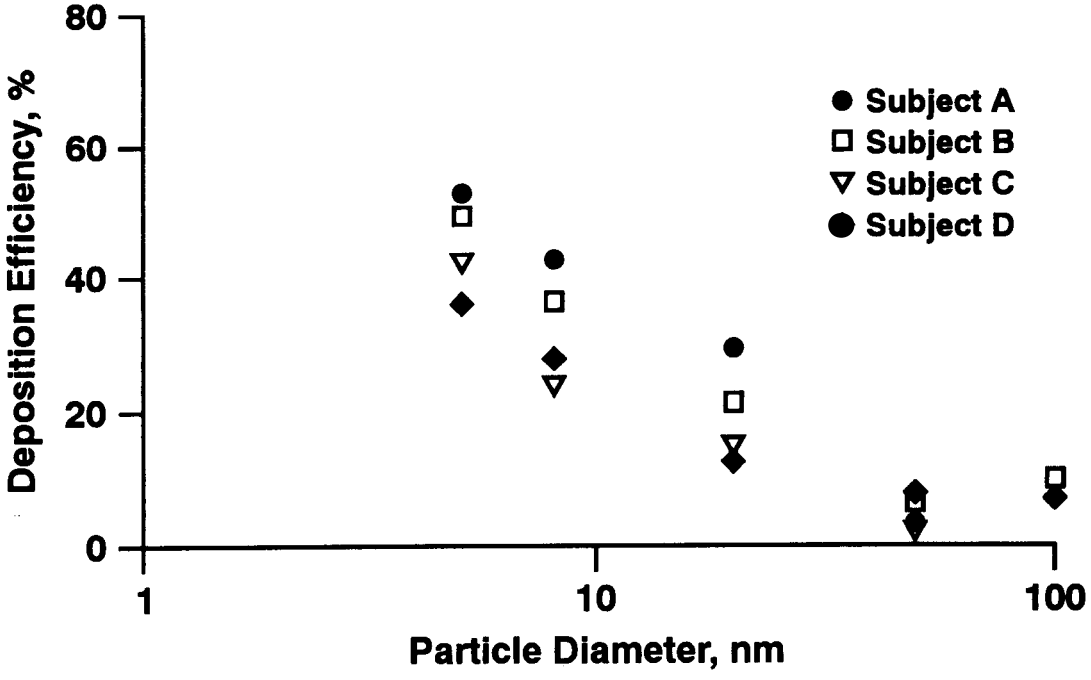


Figure 2. Nasal deposition of monodisperse particles of silica or polystyrene latex particles in four human volunteers at 4 L $min^{-1}$ inspiratory flow.

(Research sponsored by the Office of Health and Environmental Research, U. S. Department of Energy, under Contract No. DE-AC04-76EV01013).

# A COMPARISON OF NATURAL AND PASSIVE METHODS TO MEASURE NASAL DEPOSITION OF ULTRAFINE AEROSOLS USING REPLICATE HUMAN UPPER AIRWAY CASTS

*Kuo-Hsi Cheng*, David L. Swift*, Yung-Sung Cheng, and Hsu-Chi Yeh*

The risk of lung cancer associated with exposure to radon progeny in underground miners has been investigated extensively by epidemiological studies (*National Research Council: Health Risks of Radon and Other Internally Deposited Alpha-emitters*, National Academy Press, Washington DC, 1988). Results indicate that exposure to relatively high concentrations of radon progeny in mines is closely linked to an increased occurrence of lung cancer. Current risk estimates for the general population exposed to indoor radon are primarily based on extrapolations from studies of underground miners. To extend these data to radon exposures of the general population in homes, dosimetric modeling is being used to assess the differences in exposure-dose relationships between the mining and home environments. The human upper airways are the first filter against inhaled particles that would otherwise penetrate into the more distal respiratory tract. Understanding of nasal and oral filtration efficiency is the first step in evaluating dose to the lung from exposure to radon progeny. Of the many factors considered in assessing health effects from exposure to radon progeny, particle size and breathing rate are two important parameters that influence deposition patterns in the respiratory tract.

Natural and passive breathing techniques have been used to measure inspiratory and expiratory nasal deposition of inhaled particles in human subjects. In the natural method, particles are inhaled normally into the respiratory tract. Nasal deposition efficiencies for inspiration and expiration are then calculated from measurements of total particle deposition in the entire respiratory tract using four different breathing maneuvers, including breathing in and out through the nose, breathing in and out through the mouth, breathing in through the nose and out through the mouth, and breathing in through the mouth and out through the nose (Heyder, J. and G. Rudolf In *Inhaled Particles IV* [W. H. Walton, ed.], Pergamon, Great Britain, p.1017, 1977). In the passive method, inhaled particles do not enter the lungs. Instead, an external pump is used to draw test aerosols through the nasal cavity and the oral passage of a breath-holding subject, and the inspiratory or expiratory deposition efficiency is calculated directly from the ratio of inlet and outlet particle concentrations. The direction of aerosol flow can be either in through the nose and out through the mouth, or in through the mouth and out through the nose.

Very little information is available regarding *in vivo* deposition of ultrafine particles in the nasal airway. A systematic study of ultrafine aerosol deposition in the nasal and oral airways of human subjects using the passive method is underway in our laboratories (Cheng, Y. S. *et al. 1992-1993 Annual Report*, p.29). Because the passive exposure method is an artificial maneuver, there is a need to compare nasal deposition resulting from aerosol intake via the nose-mouth path, versus the natural breathing pathway, where aerosols enter into the nose and penetrate through the larynx and trachea. Because of experimental difficulty in direct measurement of particle deposition through the nose-trachea path in human subjects, the purpose of this study was to compare the natural and passive methods in two replicate human upper airway casts.

The hollow replicate upper airway models were constructed to include all the extrathoracic airways extending from the nostrils to the upper trachea, just distal to the larynx. The term Adult-Nasal-Oral-Tracheal (ANOT) is used to describe the sequence of head airway models made from adult casts. Model ANOT1 was constructed entirely from a postmortem cast of a male human head, while model

*School of Hygiene and Public Health, Johns Hopkins University, Baltimore, Maryland

ANOT2 was made from a postmortem nasal cast and an *in vivo* oral cast. Silver wools (99.9+%, Aldrich Chemical Company Inc., Milwaukee, WI) were used to produce aerosols < 20 nm in diameter. For generation of particles > 50 nm, polystyrene latex particles in aqueous suspension (Duke Scientific Corp., Palo Alto, CA) were aerosolized by a Retec X-70 nebulizer. Six particle sizes (3.6, 5, 8, 20, 50, and 100 nm) were studied at five constant flow rates (4, 7.5, 10, 20, and 30 L $min^{-1}$) for model ANOT1. For model ANOT2, six particle sizes (3.6, 5, 8, 20, 100, and 150 nm) were tested at four constant flow rates (7.5, 10, 20, and 30 L $min^{-1}$).

For the inhalation study, the aerosol was drawn into the nasal airway and directed either through the laryngeal-tracheal section or through the oral passage; these flow patterns were reversed for the exhalation study. Each combination of particle size and flow rate was measured four times. The overall penetration fraction in the model and transport lines ($P_{ML}$) was obtained from the ratio of downstream/upstream particle concentration. The penetration fraction of aerosols in the transport lines ($P_L$) as a function of particle size and flow rate was determined using the same length of connecting tubes without the model present. The values of $P_L$ were used as correction factors for taking into account particle losses in the transport lines. The net deposition efficiency in the model was then calculated as $1 - P_{ML}/P_L$.

Based on the assumption that the deposition efficiency of inhaled particles (the response variable in this study) is approximately normally distributed, the method of stratified comparison of two treatments was applied to compare the natural and passive breathing paths (Fleiss, J. L. *The Design and Analysis of Clinical Experiments*, John Wiley & Sons, New York, 1986). The experimental data were stratified according to particle size and flow rate with a total number of strata equal to 54. The test statistic for the average difference between two breathing paths was calculated using one-way analysis of variance. The analysis indicated that the deposition efficiency of ultrafine aerosols was not statistically different at the 95% confidence level between the nose-mouth and nose-trachea paths for both inhalation ($F_{1,324} = 2.77$; $p = 0.10$) and exhalation ($F_{1,324} = 0.96$; $p=0.33$).

Particle deposition during inhalation and exhalation were also compared for the two breathing routes. The combined results showed that nasal deposition of ultrafine aerosols was slightly higher for exhalation compared to inhalation. Although the statistical analysis indicated a significant difference between inspiratory and expiratory deposition, the magnitude of difference was small with expiratory deposition only 0.36% higher than inspiratory deposition for the nose-mouth path and only 0.47% higher for the nose-trachea path. For flow rates < 20 L $min^{-1}$, the overall pressure drop across the nasal airway was indistinguishable between inhalation and exhalation. Pressure drop was about 1.3 to 1.8 mm $H_2O$ higher for exhalation than for inhalation at flow rates > 20 L $min^{-1}$. Comparisons of normal vs. passive and inhalation vs. exhalation breathing routes are summarized in Table 1.

Using two human postmortem casts that are accurate in simulating the shape and configuration of the nasal and oral airways, the results of this study provide a current best estimate of the nasal deposition of particles ranging from 3.6 to 150 nm in diameter. For the range of particle sizes and flow rates studied, the lack of a significant difference between the natural and passive breathing paths suggests that the use of the passive method, where test aerosols are drawn through the nose and mouth during breath holding, is an appropriate approach for determining the inspiratory or expiratory nasal deposition efficiency of ultrafine particles *in vivo*.

Table 1

Comparison of Particle Deposition Efficiencies During Inhalation (INH) and Exhalation (EXH) for Normal (N) and Passive (P) Breathing Paths

| Category | Pooled Mean Comparison | Pooled Mean Difference (%) | $F_{1,324}$ Value | p Value |
|---|---|---|---|---|
| (N vs. P) INH | $INH_{nm} > INH_{nt}$ | 0.28 | 2.77 | 0.10 |
| (N vs. P) EXH | $EXH_{mn} > EXH_{tn}$ | 0.17 | 0.96 | 0.33 |
| (INH vs. EXH) P | $EXH_{mn} > INH_{nm}$ | 0.36 | 4.27 | 0.04 |
| (INH vs. EXH) N | $EXH_{tn} > INH_{nt}$ | 0.47 | 7.33 | 0.01 |

$INH_{nm}$ = Inhalation through nose-in-mouth-out path
$INH_{nt}$ = Inhalation through nose-in-trachea-out path
$EXH_{mn}$ = Exhalation through mouth-in-nose-out path
$EXH_{tn}$ = Exhalation through trachea-in-nose-out path

(Research supported by the Office of Health and Environmental Research, U.S. Department of Energy, under Contract No. DE-FG02-88ER60655 at Johns Hopkins University and Contract No. DE-AC04-76EV01013 at ITRI.)

# DEPOSITION OF FLUORESCENT POLYSTYRENE MICROSPHERES IN SIMULATED HUMAN CASTS OF THE ORAL CAVITY TO THE UPPER BRONCHIAL REGION

*Bean T. Chen, Steven P. Schum*, Kuo-Hsi Cheng**, Hsu-Chi Yeh, and David L. Swift***

Asthmatic patients often use inhalers to deliver medication to their lungs, and many current inhalers contain chlorofluorocarbons (CFCs) as propellant. Due to the damage that CFCs pose to the earth's ozone layer, these inhalers will soon be replaced by alternative methods. One possibility is that drugs in the form of dry powder could be administered by oral inhalation. Numerous studies have been performed on the deposition of aerosol particles in upper respiratory tract casts of humans (Lippmann, M. In *Handbook of Physiology—Reaction to Environmental Agents* [D. H. K. Lee *et al.*, eds.], American Physiological Society, Bethesda, p 212, 1977; Foord, N. A. *et al. J. Aerosol Sci. 9*: 343, 1978; Chan, T. L. and M. Lippmann, *Am. Ind. Hyg. Assoc. J. 41*: 379, 1980; Stahlhofen, W. *et al. Am. Ind. Hyg. Assoc. J. 41*: 385, 1980). These studies and several others has been summarized by Yu, C. P. *et al.* (*Am. Ind. Hyg. Assoc. J.* 42: 726, 1981).

Although mathematical models exist for the tracheobronchial (TB) and pulmonary regions of the lungs (Yeh, H. C. and G. M. Schum. *Bull. Math. Biol. 42*: 461, 1980), the complex anatomy of the oral, oropharyngeal and laryngeal (OPL) region makes it difficult to model the depositions in the complete respiratory tract. The present study provides experimental data on the fractional deposition of monodisperse aerosol particles (ranging from 3 to 22 $\mu$m) in the OPL and TB regions using silicone rubber ("silastic") casts at a constant 30 L/min flow rate through the mouth. The purpose was to determine the deposition "hot spots" of micrometer-size dry powders in different regions of the respiratory tract after a moderate oral puff.

The oral portion of the cast, prepared at Johns Hopkins University, was made using a wax mold, extending from the oral cavity to the upper trachea. From the layered latex cast, numerous wax molds were fabricated. Each mold was carefully sculpted to match the original. Approximately 20 layers of 3145 RTV (Dow Chemical, Midland, MI) silastic dissolved in toluene were poured onto the wax mold to make the cast. After the wax was removed by melting, the cast was boiled in a soap solution and subjected to ultrasonic agitation for several hours to remove the residual wax. Any residual wax was removed by careful scraping. The above process was repeated on the ITRI H.M. #7 wax mold of the middle trachea to just beyond the fourth generation bronchial branches. The lower mold was slightly modified to match the extrathoracic airway cast at the middle trachea, and cuffs were added to the ends of the fourth generation to allow air-tight connections to teflon tubes leading to downstream filters. The lower silastic cast was then joined to the upper cast using silastic to make an air tight seal. Figure 1 shows a schematic diagram of the combined casts.

The cast was checked for leaks, rinsed with ethyl acetate (for later fluorescence analysis), and was attached to a brass tube ten times longer than the oral opening diameter and with a 90° bend at the end. This end was positioned at the exit nozzle of a small-scale powder disperser (SSPD) (Model 3433, TSI, Inc., St. Paul, MN) and the cast was supported with a base template to standardize the orientations of the fourth generation branches in the most natural position possible. Five-cm-long teflon tubes were then inserted into the cuffs at the ends of the fourth generation branches, and plastic zipper clamps were used to make air tight seals. The teflon tubes were attached to 13-mm Swinnex

*U.S. Department of Energy/Associated Western Universities Summer Teacher Participant
**School of Hygiene and Public Health, Johns Hopkins University, Baltimore, Maryland

holders containing 0.5-$\mu$m fluoropore teflon filters. The filters were then attached to eight flow meters connected via manifolds to the house vacuum.

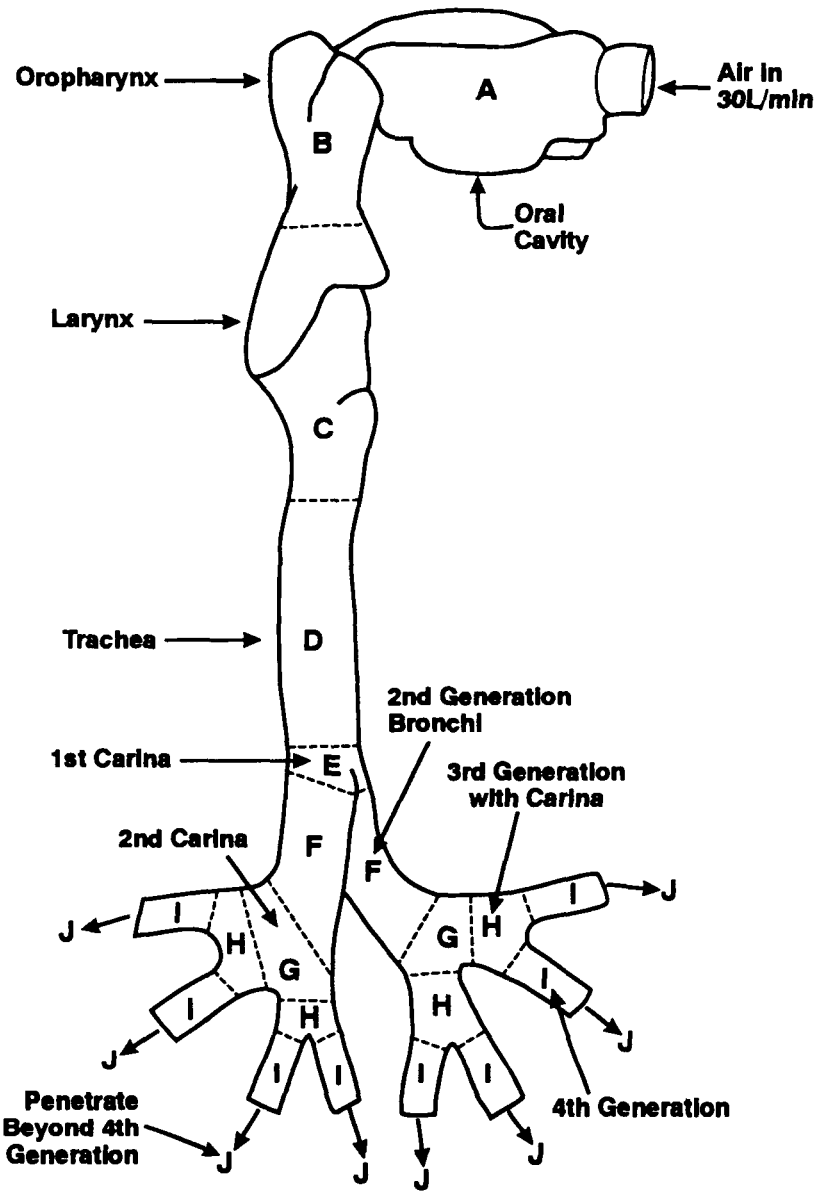


Figure 1. A schematic diagram of the combined casts with the corresponding anatomical regions.

Total flow into the oral cavity included 18.5 L/min from the SSPD plus 11.5 L/min ambient air at the brass tube opening. An anemometer (TSI, Inc.), was used to measure the velocities, and the diameters of the branches in the original lower molds were used to calculate the individual flow rate in each fourth-generation branch. The flow meters attached to these branches were then adjusted to the flow rates determined to simulate continual inhalation. Following verification of individual flow rates and a total oral intake of 30 L/min, the L-bend of the tube to the oral opening was repositioned above the SSPD, and particles were dispersed using 30 mg of 10-$\mu$m green fluorescent monodisperse polystyrene spheres previously treated with polonium-210 to minimize electrostatic charge.

After each run, the cast was removed from the apparatus, cut into 36 segments, and categorized into 10 anatomical regions (oral cavity, oropharyngeal, larynx, trachea, first carina and so on to

downstream from the fourth generation bronchial branches). The fluorescent particles in each segment were extracted with ethyl acetate. Total fluorescence in each segment was determined using a Fluorescence Spectrophotometer (Hitachi, Danbury, CT) scaled to three different concentrations (in $\mu$g/mL) of the original particles dissolved in ethyl acetate. The concentrations of fluorescence were used to determine the total mass of particles collected in the anatomical regions. From this total mass, the fractional deposition in each region was determined. The entire process was repeated for 3-$\mu$m, 6-$\mu$m, and 22-$\mu$m fluorescent spheres. The results are shown in Figure 2.

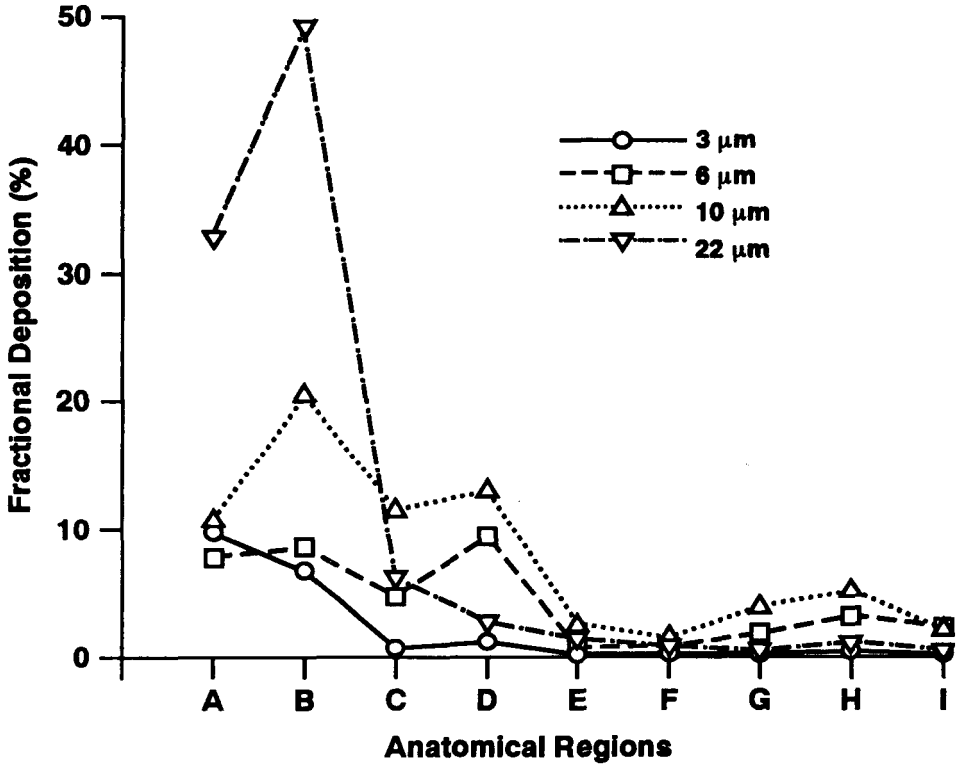


Figure 2. Fractional deposition of fluorescent polystyrene microspheres (ranging from 3-22 $\mu$m) in different regions of the combined casts. (symbols: A = oral cavity, B = oropharynx, C = larynx, D = trachea, E = 1st carina, F = 2nd generation bronchi, G = 2nd carinas, H = 3rd generation with carinas, I = 4th generation.)

Results of this initial phase were in good agreement with similar studies by others, especially those summarized by Yu *et al.* (1981). Ninety percent of the 22 $\mu$m particles were deposited in the head airways (oral cavity, oropharynx, and larynx). The larger surface area of these regions and the 90° bend entering the oropharynx contributed to increased deposition in the head region for all particle sizes. Eighty percent of the 3 $\mu$m particles penetrated beyond the fourth generation branches. Localized "hot spots" of deposition were visually noted at the carina (branch point) between the various generations.

Subsequent phases of this study will vary the flow rates and add other particle sizes. The ultimate outcome of this experiment will be to further clarify the optimal particle sizes for delivery of various therapeutic agents as a dry powder form to specific regions of the respiratory tract.

(Research sponsored by the Office of Health and Environmental Research, U.S. Department of Energy, under Contract No. DE-FG02-88ER60655 at Johns Hopkins University and Contract No. DE-AC04-76EV01013 at ITRI.)

# INVESTIGATIONS OF PARTICLE TRANSPORT IN F344 RAT LUNG USING HOECHST 33342-LABELED MACROPHAGES

*Janet M. Benson, Kristen J. Nikula, and Raymond A. Guilmette*

Particles deposited in the lung are generally phagocytized by alveolar macrophages (AMs) and either cleared via the mucociliary escalator or transported into the interstitium. Once in the interstitium, particles may clear to the lung-associated lymph nodes (LALNs) through the lymphatic system. Species differences exist in the lung clearance rates for relatively insoluble particles that have been attributed to differences in the prevalence of the two pathways. In rodents, clearance via the mucociliary escalator appears to predominate, while in larger species, more particles are preferentially transported into the pulmonary interstitium and to the LALNs.

In order to understand the role of the AMs in determining the fate of particles after they are phagocytized, it is important that the AMs themselves be labeled, independently of their particle labeling. In previous studies investigating AM-mediated transport in lung, the AMs were labeled with fluorescent particles or radiolabeled materials that were rapidly lost from the cells (Harmsen, A. R. *et al. Science 230*: 1277, 1985; Corry, D. *et al. Am. J. Pathol. 115*: 321, 1984). Preliminary studies conducted at this Institute suggest that the nuclear stain, Hoechst 33342, may be useful for evaluating the mechanisms of AM-mediated particle transport in lung (1992-93 Annual Report, p. 45). The purpose of this study was to better define the mechanisms of AM-mediated particle transport within lung using AMs labeled with Hoechst 33342 and fluorescent polystyrene latex microspheres.

The male F344/NHsd rats used for these studies were purchased from Harlan Sprague Dawley, Inc. (Indianapolis, IN). The AMs were obtained from the rats by bronchoalveolar lavage (Benson, J. M. *J. Toxicol. Environ. Health. 19:* 105, 1986). The cells were washed once in RPMI culture medium containing 10% fetal bovine serum and 0.1% gentamicin. After the cell number and viability were determined, the concentration of cells in suspension was adjusted to 1 million cells/mL medium. The cell suspension was divided into three fractions of equal volumes, designated fractions 1 (labeled with Hoechst 33342 only), 2 (double-labeled with Hoechst 33342 and fluorescent microspheres), and 3 (labeled with microspheres only). Fractions 1 and 2 were sedimented by centrifugation, resuspended in saline containing 2.5 $\mu$g Hoechst dye/mL medium, and incubated for 30 min at 37°C. After incubation, the AMs were sedimented and resuspended in RPMI. Fractions 2 and 3 were then transferred to 100 mm plastic petri dishes where the AMs were incubated (37°C, 5% $CO_2$) with polychromatic Fluoresbrite™ microspheres (1 $\mu$m diameter, Polysciences, Inc., Warrington, PA) for 2 h. The microsphere:cell ratio was 15:1. At the end of the incubation period, the cells were recovered from the plates, sedimented by centrifugation, and resuspended in RPMI. Concentrations of AM in fractions 1, 2, and 3 were adjusted to a final density of 2–3 million cells/mL for intratracheal administration into recipient rats. Cytospin preparations for each fraction were used to evaluate the extent of Hoechst staining and/or microsphere uptake by the AMs.

Three groups of 10 male F344/NHsd rats (10 ± 2 wk old) were administered fractions 1, 2, and 3 by intratracheal instillation immediately after the fractions were prepared. Two recipient rats from each dose group were sacrificed at 2, 4, 8, 15, and 32 d later. The lungs were excised, instilled with Tissue Tek:saline (60:40), and frozen in liquid $N_2$; the LALNs were immersed in Tissue-Tek and frozen in liquid $N_2$. Samples were stored at –80°C until processed. The tissue samples were cryosectioned at 5 $\mu$m and neither fixed nor stained prior to evaluation by epifluorescent microscopy.

Because not all tissue sections obtained from each test group at each sacrifice time have been evaluated, only preliminary results are reported. Early evaluations have focused on results obtained

from rats administered Hoechst-stained AMs containing the polychromatic microspheres (fraction 2). In evaluating the numbers and distributions of particles in the lung, entire lung sections were evaluated. The numbers and location of free microspheres, microspheres in Hoechst-stained and unstained AMs, and the numbers of Hoechst AM not containing microspheres were determined.

Microscopic evaluation of cytospin preparations of fraction 2 (Hoechst-stained AMs + microspheres) indicated that the AMs incorporated the Hoechst stain into their nuclei and that the majority of stained cells contained at least one fluorescent microsphere. Two days after administration of the doubly labeled AMs, approximately 5% of the Hoechst-labeled AMs present in lungs also contained microspheres. However, 75–100% of microspheres in the lung sections were contained within unstained AM. Four days after instillation of doubly labeled AM, 10% of the Hoechst AMs contained microspheres, while the majority of the microspheres were present in unstained AMs. At 15 d post instillation, no Hoechst-stained AMs were identified in lung tissue sections; all microspheres were found within unstained AMs. Hoechst-labeled AMs were identified in lungs of rats sacrificed 32 d after instillation, but < 3% of these AMs contained fluorescent microspheres. At this time, > 97% of the microspheres were within unstained AMs.

Over the 32-d period of this study, the AM-containing microspheres redistributed from primarily alveolar regions to interstitial tissue. At 4 d after instillation, 68% of the Hoechst-stained AMs were alveolar, 26% were located on or in alveolar septa, and 6% were in peribronchiolar and perivascular interstitial tissue. By comparison, 60% of the microspheres (generally within unstained AMs) were located in alveoli, 27% were in alveolar septa, and 13% were within the peribronchiolar and perivascular interstitial tissue. At 15 d post instillation, 52% of the microspheres were located in unstained AMs closely adherent to alveolar septa, and 48% of the microspheres were located in alveolar septa. At 32 d after instillation, approximately 30% of the Hoechst AMs were in alveoli, 13% were within alveolar septa, and 53% were within interstitial tissue. The unstained AMs containing microspheres were located within alveoli, within alveolar septa, or within the interstitium surrounding blood vessels and airways.

No polychromatic microspheres were found in LALNs from rats sacrificed 4–32 d after the doubly-stained AM were administered.

The data from lung sections of two rats at each sacrifice point were somewhat variable. However, the results obtained to date suggest the following: (1) Hoechst 33342-stained AMs are detectable in lung tissue up to 32 d after instillation into recipient rats; (2) microspheres in the Hoechst-stained AM appear to be transferred to unstained AMs within 2–4 d after instillation, as suggested by the large proportion of Hoechst-stained AMs without microspheres compared to the number of unstained AMs containing microspheres; (3) Hoechst-stained AMs and microspheres within stained and unstained AMs tend to redistribute to septal and interstitial tissue with increasing time after instillation; and (4) particles were not translocated to lymph nodes during the 32 d after the doubly labeled AMs were administered to rats, possibly because only a few million microspheres, already contained within AMs were instilled.

Particle transfer between AMs has been postulated to occur during particle transport in lung. Our preliminary data suggest that transfer does occur. However, more complete evaluation of the tissue samples is required to confirm these findings.

(Research sponsored by the Office of Health and Environmental Research, U. S. Department of Energy, under Contract No. DE-AC04-76EV01013.)

# DIRECT TRANSPORT OF INHALED XYLENE AND ITS METABOLITES FROM THE OLFACTORY MUCOSA TO THE GLOMERULI OF THE OLFACTORY BULBS

*Johnnye L. Lewis, Alan R. Dahl, and Dean A. Kracko*

The olfactory epithelium is a unique neural tissue in that single receptor neurons have dendrites in contact with the external environment at the nasal airway, and axon terminals that penetrate the cribriform plate and synapse in the olfactory bulb. The Central Nervous System (CNS) is protected from systemically circulating toxicants by a blood-brain barrier primarily composed of tight junctions between endothelial cells in cerebral vessels and a high metabolic capacity within these cells. No such barrier has yet been defined to protect the CNS from inhaled toxicants. Because all inhalants do not seem to access the CNS directly, a nose-brain barrier seems plausible (Lewis, J. L. *et al.* In *The Vulnerable Brain and Environmental Risks, Vol. 3: Toxins in Air and Water* [R. L. Isaacson and K. F. Jenson, eds.], Plenum Press, New York, p. 77, 1994). The purpose of the work described here is to determine whether or not a nose-brain barrier exists and to define its components. Although such a barrier is likely to be multi-faceted, the present work focusses only on the importance of gross histologic and metabolic characteristics of the olfactory epithelium in olfactory transport.

H. I. Ghantous *et al.* (*Pharmacol. Toxicol. 66*: 87, 1990) demonstrated that inhalation of $^{14}$C-xylene results in accumulation of radiolabel in the olfactory bulbs of rats. Although much of the radioactivity observed in that study was associated with nonvolatile metabolites of xylene, the authors could not determine with their methods either the regional localization of those metabolites within the olfactory bulbs or the site of metabolism of the parent compound.

In the present work, F344 rats inhaled $^{14}$C-xylene (435 mg/m$^3$ [TLV concentration], specific activity of 0.7 mCi/mmole) for 1 h. Additional animals inhaled for 6 h either 190 ppm methyl bromide or filtered air 4 d prior to the same $^{14}$C-xylene exposures. Inhalation of methyl bromide under these conditions produces nearly complete destruction of the olfactory epithelium (Hurtt O. O. *et al. Toxicol. Appl. Pharmacol. 94*: 311, 1988). Animals were killed by exsanguination following $CO_2$ anesthesia at 30 min, 4 h, or 18 h post-xylene-exposure. Animals were perfused with saline to remove blood-borne xylene and metabolites. Right and left sagittal brain slices including the olfactory bulbs were cryosectioned. Multiple sets of three serial sections each were processed as follows: (1) the first was kept at -20°C until apposed to Fuji MI-NC, blue base medical imaging film in autoradiography cassettes; (2) the second was evaporated overnight at 25°C to remove volatiles, then placed in cassettes for autoradiography; (3) the third was fixed in formalin and stained with hematoxylin and eosin. Films were exposed at -20°C for 16 wk and examined for localization of exposed silver grains.

The remaining brain tissue was digested in TEAH and counted for radioactivity. Radioactivity in olfactory bulb digests was compared to that in all other brain regions combined. An aliquot of each sample was heated, which eliminates radioactivity associated with the parent xylene and its volatile metabolites. Radioactivity remaining should then be associated with nonvolatile metabolites of xylene.

Only preliminary data are available at this time. At 30 min following exposure to $^{14}$C-xylene alone, the olfactory bulbs contained 25% of the radioactivity found in the remainder of the brain when counting unheated samples containing both volatile and nonvolatile radioactivity. Nonvolatile-associated radioactivity accounted for 93% of the total activity in the olfactory bulbs, but in the rest of the brain only 36% of the total radioactivity was in the nonvolatile fraction. At 4 h post exposure, a nearly identical relationship in the distribution of total radioactivity between the olfactory bulbs and the rest of the brain was observed, but total radioactivity was only 25% of that seen at 30 min post exposure.

All radioactivity in the bulbs was nonvolatile, while 70% of the radioactivity in the rest of the brain was associated with nonvolatiles. By 18 h post exposure, 50% of the detectable radioactivity was in the olfactory bulbs, all in the nonvolatile fraction. The total radioactivity, however, was only about 10% of that seen at 30 min.

At 30 min post $^{14}$C-xylene exposure, autoradiograms showed localization of total and nonvolatile radioactivity in the glomeruli of the olfactory bulbs. Radioactivity was still detectable in the autoradiograms at 4 h post exposure, but not at 18 h. Autoradiograms detected no radioactivity in any other brain region in animals exposed only to $^{14}$C-xylene. Light microscopic examination of hematoxylin and eosin-stained sections from methyl-bromide pre-exposed animals indicated nearly complete atrophy of the olfactory epithelium at the time of the subsequent xylene exposures. Autoradiographic results are not yet available, but preliminary data from scintillation counting of tissue digests indicate that preexposure to methyl bromide results in increased accumulation of volatile-associated radioactivity in the olfactory bulbs.

To determine whether the metabolites of xylene present in the bulb were the result of bulb metabolism after transepithelial transport, or were transported to the bulb following metabolism in the olfactory epithelium, metabolism of xylene was compared in microsomal preparations from either the olfactory bulbs or olfactory mucosa of rats. Preliminary data show no xylene metabolism in olfactory bulb microsomes. In the presence of xylene, microsomes from the olfactory mucosa produced primary metabolites of xylene at the following rates: ~1500 pmoles/mg microsomal protein/min of methyl benzyl alcohol, and ~1700 pmoles/mg microsomal protein/min of dimethyl phenol. Therefore, it is likely that xylene is metabolized within the olfactory mucosa when this mucosa is intact, and the metabolites are subsequently transported to the olfactory bulbs. Preexposure to methyl bromide shifted $^{14}$C-xylene-associated radioactivity in the olfactory bulbs to primarily volatile rather than nonvolatile compounds. This likely reflected the loss of metabolic capacity in the olfactory mucosa due to disruption of the epithelium, and therefore increased accumulation of parent xylene in the olfactory bulbs.

These preliminary results indicate that inhaled xylene is metabolized within the olfactory epithelium, and that nonvolatile metabolites, in addition to a smaller percentage of volatiles representing either parent xylene or volatile metabolites, are transported via the olfactory epithelium to the glomeruli within the olfactory bulbs. The nonvolatile metabolites do not appear to be covalently bound within the bulb and are substantially cleared by 18 h following acute exposure to a TLV concentration of xylene. Disruption of the olfactory epithelium results in accumulation of more volatile compounds in the olfactory bulbs. Whether these volatile compounds show the same glomerular localization or are more diffusely represented within the olfactory bulbs remains to be determined. These results support the conclusion that the metabolic activity of the olfactory mucosa is an important determinant of the form in which an inhalant is transported. Disruption of the anatomical structure of the epithelium will alter at least the form in which metabolizable inhalants enter the brain.

(Research sponsored by the PHS/NIH under Grant R01-DC01714 from the National Institute on Deafness and Other Communication Disorders with the U.S. Department of Energy under Contract No. DE-AC04-76EV01013.)

# A MODEL OF METABOLISM AND CLEARANCE OF ORGANIC COMPOUNDS FROM THE RESPIRATORY TRACT

*Per Gerde* and Alan R. Dahl*

In cases where inhalants induce toxicity in the airway epithelium, the mechanism of absorption is an important determinant of target dose. Absorption of organic solutes in the lungs occurs mainly by two consecutive mechanisms; molecular diffusion drives the chemicals into the tissues, and blood perfusion of the tissues removes the chemicals into the systemic circulation. Solutes having lipophilicities ranging from equally soluble in lipids and water to moderately more lipid-soluble are limited by the perfusion during clearance from the lungs. The perfusion-limited solute enters the blood circulation from all regions of the lungs within minutes and is distributed to other organs via the systemic circulation. In contrast, clearance of highly lipophilic toxicants, such as benzo(a)pyrene, from the lungs is diffusion-limited (Gerde P. *et al. Toxicol. Appl. Pharmacol. 121*: 328, 1993). The limiting process refers to the slowest transport mechanism of either perfusion or diffusion. Because of the short distance from the surface of the alveolar region to the capillary network, diffusion-limited clearance of highly lipophilic solutes occurs within minutes. In the thicker epithelium of the conducting airways, however, clearance may take hours. The purpose of the current modeling effort was to encompass both mechanisms of clearance in a single model in order to explore the influence of toxicant lipophilicity and local metabolism on the dosimetry at the airway portal-of-entry.

The airway mucosa was simulated as a one-dimensional slab with four sub-compartments: the mucous layer, the epithelium, the basement membrane, and the subepithelium (Fig. 1). The transient removal of organic solutes from the airway mucosa following a brief exposure at the air interface could be simulated by introducing into the model a resistance to mass transfer in the tissue from diffusion, in addition to perfusion (Gerde P. and A. R. Dahl. *Toxicol. Appl. Pharmacol. 109*: 276, 1991). Critical input data to the model were morphometry, blood perfusion, metabolism, and distribution of membrane lipids within the cross-section of the mucosa. Systemic compartments, that were assumed to have no internal concentration gradient (well-mixed), allowed for comparison of the local dosimetry of a toxicant with its dosimetry following systemic distribution. Toxicants within the airway mucosa were assumed to be transported through molecular diffusion, partitioning into lipid membranes, membrane trafficking, and perfusion of the subepithelium. Diffusion was introduced as an effective diffusivity, comprised of the parallel phenomena of aqueous-phase diffusion and a lipid-phase diffusion. Effective diffusivity here means the apparent observed diffusivity when more mechanisms than plain molecular diffusion affects transport. Lipid phase diffusion was assumed to be caused both by movements of the lipid membranes (membrane trafficking) and by lateral diffusion within the membrane bilayers. Perfusion was assumed to be distributed over the entire depth of the subepithelium. Between systemic compartments, transport was assumed to occur through blood perfusion as in traditional PBPK models (Bischoff K. B. and R. G. Brown. *Chem. Eng. Prog. Sym. Series. 62*: 33, 1966).

Results showed that absorption of toxicants was virtually completely perfusion-limited when the lipid/aqueous partition coefficient ($PC_{l/a}$) was < 100, giving clearance half-times of minutes depending on the assumed blood flow (Fig. 2). During perfusion-limited clearance, the concentration profile through the mucosa is almost flat, indicating that within a short time period, exposure at the portal-of-entry epithelium will be similar to that of tissues exposed via the systemic circulation. For $PC_{l/a}$s > 100, there was a gradual shift toward diffusion-limited clearance, characterized by a gradual increase in the clearance half-times. A consequence of slower absorption during diffusion-limited

*Also at the National Institute of Occupational Health, S-171 84 Solna, Sweden

clearance would be prolonged exposure of the airway mucosa. Moreover, simulations show that slower diffusion with increasing lipophilicities is accompanied by steeper and steeper concentration profiles through the epithelium (Fig. 1).

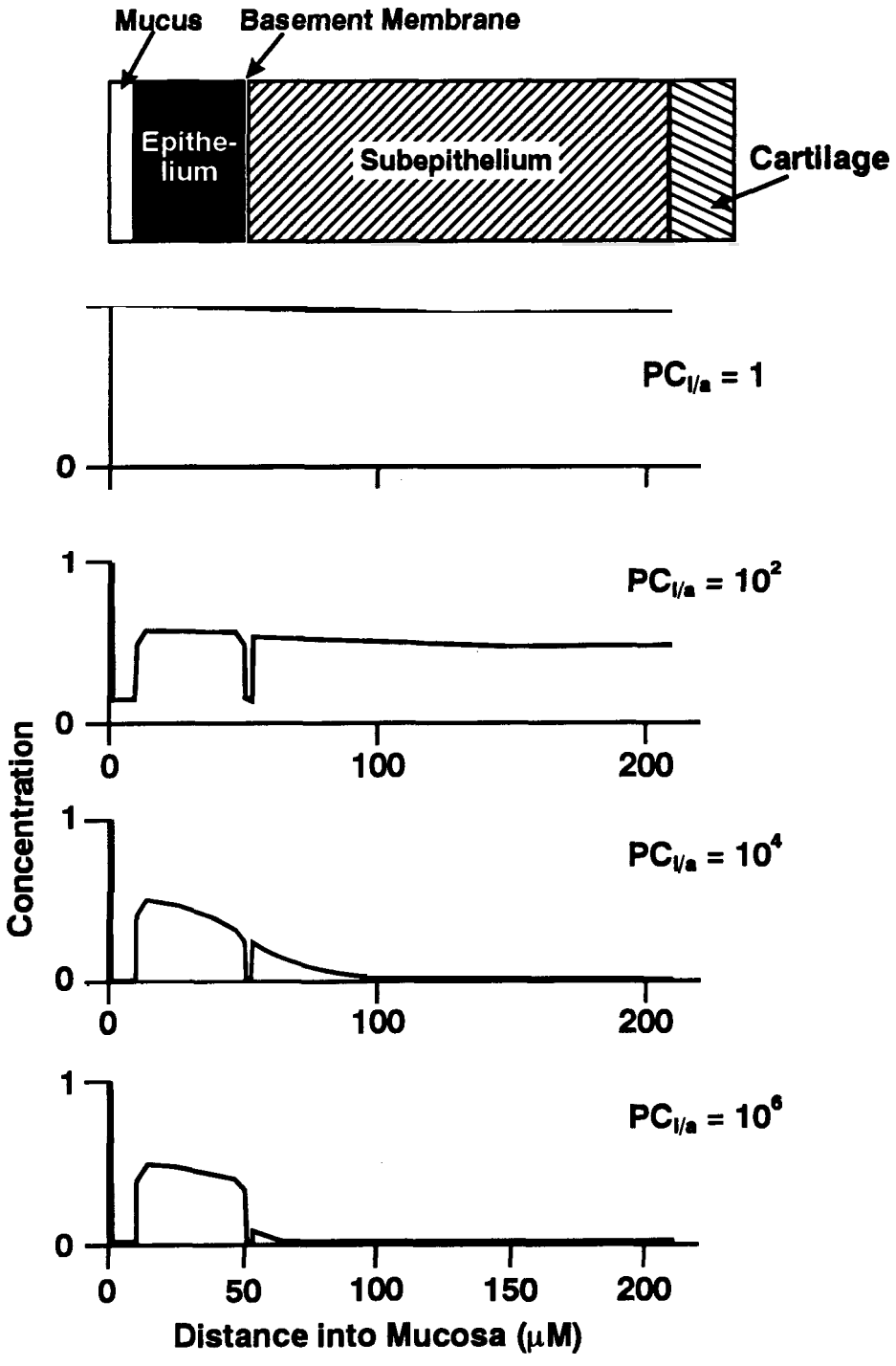


Figure 1. The model of the bronchial mucosa and four simulated concentration profiles of toxicants with different lipophilicities. $PC_{l/a}$ indicates the lipid/aqueous partition coefficient of the toxicants. The concentration profiles are shown at the respective half-times of clearance of the toxicants following a transient exposure.

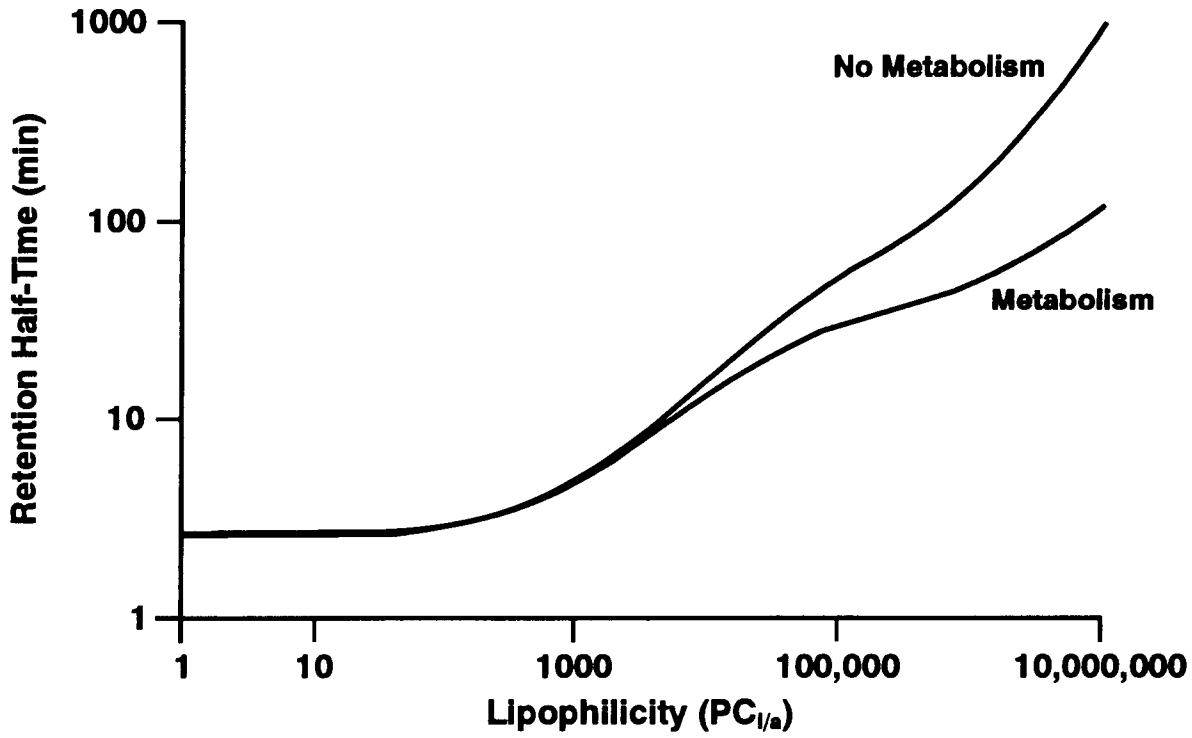


Figure 2. Simulated half-times of absorption of organic solutes in the airway mucosa as a function of their lipid/aqueous partition coefficient, following a transient exposure. Also indicated is the hypothetical influence on airway clearance by a constant activity metabolism within the epithelium.

Two aqueous barriers greatly influence the local disposition of lipophilic solutes in the mucosa. The first barrier is the mucous layer on the ciliated epithelial surface, which slows transport of lipophilic solutes to the epithelium and allows redistribution of dissolved toxicants over the epithelial surface through mucociliary action. The second barrier is the basement membrane which tends to retard passage of lipophilic toxicants into the blood capillaries. Because high epithelial concentrations will result from this retardation, metabolism within the airway epithelium may be a critical factor enhancing diffusion to the capillary bed of the subepithelium by reducing the lipophilicity of a toxic substrate. On the other hand, such metabolites may lead to activation of protoxicants to toxic products. Because of the increased retention of toxicants with increasing lipophilicity, local metabolism is likely to have a greater influence on the portal-of-entry dosimetry of more lipophilic toxicants than of less lipophilic toxicants (Fig. 2). Thus, when tissue damage is induced by reactive metabolites, toxicity to the portal-of-entry is more likely to be induced by highly lipophilic toxicants than by less lipophilic toxicants.

(Research sponsored by the PHS/NIH under Grant R01-ES05910 from the National Institute of Environmental Health Services with the U.S. Department of Energy, under Contract No. DE-AC04-76EV01013, and by the Swedish Environment Fund, Grant 91-0359.)

# CLEARANCE PATTERNS FOR $^{111}$In-OXIDE PARTICLES DEPOSITED IN SPECIFIC AIRWAYS OF BEAGLE DOGS

*M. Burton Snipes, Bruce A. Muggenburg, William C. Griffith, and Raymond A. Guilmette*

The International Commission on Radiological Protection (ICRP) has incorporated long-term retention of radioactive particles in conducting airways into its newly approved respiratory tract dosimetry model (ICRP Report No. 66, 1994). This model is purported to provide a better basis for assessing risk associated with human inhalation exposures to radioactive particles. However, applying the new model requires an understanding of particle retention patterns in conducting airways of the lung. Studies are being conducted at ITRI to quantify long-term retention patterns for particles deposited at specific sites in conducting airways of Beagle dogs. The dog was selected as a model because long-term retention and clearance patterns for particles deposited in the lungs of dogs and humans are similar (Snipes, M. B. *CRC Crit. Rev. Toxicol. 20*: 175, 1989).

Adult male and female dogs from the Institute's closed colony were used in these studies. A fiberoptic bronchoscope was used to position the dosing device, a microspray nozzle (Hoover, M. D. *et al. J. Aerosol Med. 6*: 67, 1993), in specific airway sites in dog lungs. A bronchial nomenclature system (Amis, T. C and B. C. McKiernan. *Am. J. Vet. Res. 47*: 2649, 1986) was used to facilitate consistent identification of airway deposition sites designated as RB2, RPB, and RB4. The dosing sites were a 4-mm location in the right cardiac lobe (RB2) and a 15-mm site in the right principal bronchus (RPB). In earlier studies, we also used an 8-mm site in the right diaphragmatic lobe (RB4). One site was dosed per test of airway clearance, but comparative data are being collected for all designated dosing sites. Radiolabeled test particles were sprayed into the airways at these designated locations to allow quantitation of retained amounts of particles using *in vivo* whole-body counting. Alternatively, fluorescent particles were used to allow direct visualization of the locations of retained particles in lung tissue collected from sacrificed dogs.

Details about the procedures used to spray particles into airways of dogs, whole-body *in vivo* counting procedures, sacrifice and histopathological evaluations of lungs, and some results relevant to clearance and retention of particles sprayed into specific airways have been described (1989–90 Annual Report, p. 49; 1990–91 Annual Report, p. 59; 1991–92 Annual Report, p. 77; 1992–93 Annual Report, p. 40). Our previous studies using 3–4 $\mu$m polystyrene latex microspheres or radiolabeled fused aluminosilicate particles indicated that the dogs varied considerably with respect to airway clearance patterns. Between 2% and 86% of the particles sprayed into the lung airways were retained for 3 d or longer. Examination of lung tissue revealed that most of the long-term retained particles were in pulmonary airspaces distal to the dosing sites. Retrograde movement of the particles immediately after dosing appeared to be the reason for alveolarization of the test particles. The number or mass of test particles, as well as the volume of test suspension, were important factors that influenced initial dispersion patterns and alveolarization of the test particles. Importantly, results suggested that alveolarization of the test particles might be avoided if the mass and number of particles could be kept small, and if the dosing volume was reduced.

As a continuation of the work described above, a study was conducted using a small number of highly radioactive particles administered using 6 $\mu$L of dosing suspension. High-specific-activity $^{111}$In (a photon-emitter with a 2.8-d physical half-life) was mixed in solution with the minimum mass of stable In needed to produce an $In_2O_3$ aerosol. The radioactive and stable In were converted to a colloidal hydroxide, and an aerosol was produced by nebulizing the colloid and heat-treating the particles of In hydroxide at 1100°C as they were passed through a tube furnace. The resulting poorly soluble particles of radioactive $In_2O_3$ were collected on filters. The filters were immersed in $H_2O$,

and $In_2O_3$ particles were removed from the filter and suspended in the $H_2O$ using ultrasonication. The $In_2O_3$ particles in $H_2O$ suspension had activity median aerodynamic diameters of 0.2 $\mu$m, with a geometric standard deviation of 1.6. Dosing volumes were 6 $\mu$L and contained about $10^5$ $^{111}$In-oxide particles, with an average total radioactivity content of 2100 Bq (56 nCi). Minimum detectable true activity (MDTA) for the *in vivo* photon-counting system used to whole-body count the dogs was 67 Bq (1.8 nCi). Therefore, retained amounts of $^{111}$In in excess of 3% of the amount sprayed into the airways could be measured.

Two male and two female dogs were dosed in 4-mm airways, and two males and two females were dosed in 15-mm airways using the procedures previously described. The dogs were whole-body counted immediately after dosing, then on days 1, 2, 3, 4, 5, and 8 after instillation. The physical half-life of 2.8 d for $^{111}$In limited our ability to quantitate the radiolabel to 8 d. Physical clearance of particles from the conducting airways results in passage of the particles through the gastrointestinal (GI) tract, which requires at least 1 d for dogs. Therefore, our whole-body counts for the first day after dosing, and sometimes for 2 or 3 d, detected radioactivity that cleared from the lung airways, but was still present in the dog's GI tract. Our previous studies using particles labeled with longer-lived radionuclides indicated that any radioactive particles retained at or near the dosing sites for 3 d or longer after dosing would clear slowly and could be detected by whole-body counting.

All radioactivity counts for the dogs dosed in 15-mm airways were below the MDTA 2 d after dosing, indicating that most or all of the radioactive particles were cleared rapidly from the 15-mm conducting airway sites. Counts for three dogs dosed in the 4-mm airways were below the MDTA 2 d after dosing, but one dog retained about 15% of the instilled $^{111}$In longer than 3 d. The retained $^{111}$In was detectable in all whole-body counts through day 8, when 9% of the initial dose was still present. The radioactive particles may have been retained in the dosed airway, but our previous experience suggests that about 15% of the dosing volume reached pulmonary airspaces as a result of retrograde movement. It appears that even using a 6-$\mu$L dosing volume can result in alveolarization of test particles sprayed into 4-mm diameter conducting airways of dogs using the Lovelace microspray procedure. Additionally, with the exception of long-term retention in one airway, clearance reduced the amounts of radiolabeled particles to below the MDTA by 2 d after dosing. This strongly suggests that not more than a few percent of particles deposited on conducting airways were retained for more than a few days. Therefore, our results do not support the assumption of the ICRP 66 Model that 20% (or more) of particles deposited on conducting airways clear with half-times of 20–30 d. Quantitative data for particle retention in conducting airways are still needed to allow more accurate radiation dose calculations for bronchi and bronchioles of humans following inhalation of radioactive particles.

(Research supported by the Office of Health and Environmental Research, U.S. Department of Energy, under Contract No. DE-AC04-76EV01013.)

# III. METABOLISM AND MARKERS OF INHALED TOXICANTS

# METABOLISM OF MODEL ORGANIC POLLUTANTS IN CANINE RESPIRATORY TRACT MUCOSA SLICES

*Janice R. Thornton-Manning, Per Gerde*, Susan T. Chen, and Alan R. Dahl*

The high incidence of human bronchial tumors has been correlated with the high fractional deposition of inhaled particles in the bronchi (Schlesinger, R. B. and M. Lippmann. *Environ. Res. 15*: 424, 1978). Polycyclic aromatic hydrocarbons (PAHs) are frequently bound to airborne particles due to their low vapor pressures (Yamasaki H. *et al. Environ. Sci. Technol. 16*: 189, 1982). It is thought that tumorigenicity may result from the release and subsequent bioactivation of these particle-associated organic compounds in the respiratory tract.

Previous studies at ITRI (Gerde, P. *et al. Toxicol. Appl. Pharmacol. 121*: 328, 1993) examined the clearance of organic toxicants from various regions of the canine respiratory tract. Their results indicated that, while clearance of a highly lipophilic PAH such as benzo(a)pyrene (BaP) from the thin alveolar epithelium took only a few minutes, clearance through the thicker epithelium of the conducting airways took hours. Slower, diffusion-limited clearance results in higher concentrations of lipophilic compounds in the epithelium of the bronchi. Hence, the ability of these tissues to metabolize organic compounds to water-soluble metabolites or reactive intermediates may be extremely important in their clearance from the respiratory tract and the potential susceptibility of this region of the respiratory tract to cancer. The purpose of the present study was to evaluate the ability of bronchial mucosa to metabolize a model organic pulmonary carcinogen, BaP, to reactive and nonreactive metabolites and to evaluate the diffusion of the parent compound and metabolites through the bronchial mucosa.

In this study, the metabolism of BaP was evaluated *in vitro* in slices of canine bronchial mucosa. BaP is an extremely lipophilic PAH which has been shown to be carcinogenic in many different species (Stowers, S. J. *et al. Environ. Health Perspect. 62:* 31, 1985). All airborne BaP has been reported to be associated with particles (Miguel A. H. and S. K. Friedlander. *Atmos. Environ. 12*: 2407, 1978). The primary enzyme responsible for the metabolism of BaP in most tissues studied is cytochrome P450 1A1 (Wood, J. *et al. J. Biol. Chem. 251*: 4882, 1976), and activation by this enzyme in pulmonary tissues has been suggested to be of major importance in the etiology of lung cancer (McLemore T. E. *et al. J. Natl. Cancer Inst. 82*: 1333, 1990). The lipophilic nature and potential for bioactivation make BaP an ideal model compound for this study. Furthermore, the metabolic pathway for BaP has been reported, and metabolite standards are available from commercial sources.

In preliminary experiments, metabolism of BaP in lung mucosa slices taken from a single dog was examined after various incubation times. Lung tissue had previously been removed from a 2-y old male dog immediately after sacrifice and was stored at -80°C for approximately 6 mo. The tissue was slowly thawed, maintained on ice, and 0.5 – 1 $cm^2$ slices of bronchial mucosa were isolated. The tissue weights were approximately 0.2 g each and differed by less than 2%. $^3$HBaP was placed on glass coverslips, then applied to the luminal surface of the mucosa slices which were maintained on ice for 20 min in a desiccator. The glass coverslips were removed and counted. Between 2–5 pmol $^3$HBaP were applied to the luminal surface of the mucosa slices. While this method of dosing results in some variability in the amount of compound applied to each tissue, it allows accurate quantification of the actual dose the tissue receives. These low doses of BaP were chosen in order to mimic realistic exposure concentrations and because they do not exceed the solubility of BaP in the aqueous upper layer of the bronchial mucosa. The tissue slices were next placed in Ham's media and incubated for 5, 10, and 100 min at 37°C under 5% carbon dioxide. After incubation, the tissue was extracted with

*Also at the National Institute of Occupational Health, S-171 84 Solna, Sweden

ethyl acetate, while the aqueous media was cryogenically distilled *in vacuo* to remove $^3H_2O$. The dried residue was resuspended in 55% aqueous methanol and analyzed by high pressure liquid chromatography (HPLC).

The production of $^3H_2O$, a general indicator of metabolic activity, was approximately 5.9 nCi/g after 5 min incubation (data not shown). This increased to 7.3 nCi/g at both 20 and 100 min incubation times suggesting that the metabolism of $^3$HBaP and $^3$HBaP metabolites at C-H bonds was completed between 5 and 20 min after initiation of the incubation. The tissue and media extracts from the tissues incubated with $^3$HBaP for 20 and 100 min were analyzed for BaP metabolites using HPLC. The extracts from tissues incubated for 5 min were not analyzed because of the low levels of radioactivity in these samples. The major metabolites formed in the 100- and 20-min incubations were very similar, suggesting that most metabolism was completed within 20 min. The largest portion of metabolites was assigned to a chromatogram peak known to be composed of water-soluble conjugates (Table 1). Tetrahydrotetrols, 4,5- and 7,8-dihydrodiols, quinones, and 9-hydroxy-BaP were also found in both incubations indicating that substantial metabolism of BaP was occurring after only 20 min. Small amounts of *trans*-9,10-dihydrodiol and 3-hydroxy-BaP were detected in the 100-min incubation, suggesting that the formation of these metabolites was less efficient.

Table 1

Benzo(a)pyrene Metabolites in Media and Tissue After
20- and 100-Min Incubations with Canine Bronchial Mucosa Slices[a]

| | Metabolite (% of Total Metabolites Recovered in Tissue and Media) | | | |
|---|---|---|---|---|
| | 20-Min Incubation | | 100-Min Incubation | |
| BaP tissue dose[b] | 2.4 pmols | | 4.3 pmols | |
| Metabolites[c] | Tissue | Media | Tissue | Media |
| Water-soluble conjugate[d] | 6.8 | 49.7 | 8.5 | 49.3 |
| Tetrahydrotetrols | 3.1 | 4.9 | 2.8 | 2.8 |
| Trans 9,10-dihydrodiols | ND[e] | ND | 1.4 | 1.4 |
| 4,5 and 7,8-dihydrodiols | 4.9 | 4.9 | 2.8 | 4.2 |
| Quinones | 2.5 | 4.9 | 2.8 | 8.5 |
| 9-hydroxy | ND | 10.43 | 2.8 | 11.3 |
| 3-hydroxy | ND | ND | ND | 1.4 |

[a]Tissue slices were taken from the same dog
[b]Total dose to tissue slices; each slice weighed approximately 0.2 g
[c]Metabolites were identified by coelution with standards
[d]Tissue data may include $^3H_2O$
[e]ND = Not detected

Further studies were conducted using bronchial mucosa from multiple dogs. Bronchial mucosa was isolated from lungs taken from three female and one male dog, all 15-17 y of age, immediately after sacrifice. These mucosa samples were either placed on ice and used immediately or were frozen for

approximately 24 h at -80°C, then allowed to thaw on ice before use. All four slices were treated with approximately 10.9 to 11.3 pmols of BaP, resulting in concentrations of 37.9 to 128.8 pmols BaP/g tissue. This higher dose of $^{3}$H-BaP was achieved by allowing the glass coverslips to remain on the luminal side of the tissue for the entire 100-min incubation. Again, this dose did not exceed the solubility of BaP in the upper aqueous layer of bronchial mucosa.

The amount of $^{3}$HBaP metabolite covalently bound to tissue macromolecules ranged from 0.21 to 0.77 pmol/g tissue (Table 2). When this amount was expressed relative to the absorbed dose of BaP, these amounts were 0.5 to 0.82% of dose. This value was indicative of BaP metabolites that were primarily bound to proteins. It is possible that significant amounts of metabolite became bound to lipids or nucleic acids, but these were not evaluated in this study. Tissue taken from the first dog appeared to have greater metabolic activity, based on the production of covalently bound metabolite, specific BaP metabolites from HPLC analysis, and production of $^{3}H_2O$, than those taken from the other three dogs. This probably reflects interindividual variation. The bronchial mucosa slices taken from the third and fourth dog were frozen 24 h prior to use in these experiments. However, this freezing process did not appear to have had obvious effects on the metabolic activity of these tissues.

Detectable levels of BaP metabolites were produced in all the tissues (Table 2). As seen in preliminary experiments, the major metabolites were water-soluble conjugates. Although the specific conjugates have not been identified, previous studies with explants or subcellular fractions of bronchi from other species have shown that glutathione, sulfate, and glucuronide conjugates can be formed by bronchial enzymes (reviewed by Cohen, G. M. *Environ. Health. Perspect. 85*: 31, 1990). Relatively large amounts of tetrols also formed in all the incubations. These are the ultimate metabolites of BaP metabolism and are generally considered to be nontoxic. However, the presence of tetrols and dihydrodiols indicates that the toxic epoxide and diol-epoxide intermediates were formed and subsequently served as substrates for epoxide hydrolase. The large amounts of tetrols and dihydrodiols relative to the dihydroepoxide suggest that epoxide hydrolases may be important enzymes for detoxication of PAHs in the bronchial mucosa. The substantial metabolism of BaP in dog bronchial mucosa suggests that the cytochrome P450 enzymes were present which metabolized this compound. Interestingly, S9 preparations from canine bronchial mucosa were reported to have undetectable levels of ethoxyresorufin-O-deethylase, an activity indicative of CYP1A1, the P450 with the greatest BaP-metabolizing ability (Bond, J. A. *et al. Drug Metab. Dispos.* 16: 116-124, 1988). This suggests that the canine lung has other enzymes capable of metabolizing BaP. In future studies, the bronchial mucosa for a variety of xenobiotic-metabolizing enzymes will be evaluated using immunohistochemical methods. Furthermore, the effect of age on xenobiotic metabolism will be explored because older dogs were used in the present investigation.

This study shows that the bronchial mucosa may be an important site for xenobiotic metabolism in the respiratory tract. This may have some important implications for risk assessment of inhaled pollutants, particularly with regard to lipophilic PAHs, such as BaP.

Table 2

Metabolism of Benzo(a)pyrene in Canine Bronchial Mucosa Slices[a]

| Dog # | Gender | Tissue Weight (g) | Dose BaP (pmols/g) | pmols Bound Bap Metab/g[c] | $3H_2O$ | pmol BaP Metabolites/nmol BaP Dose/g Tissue[b] | | | | | | |
|---|---|---|---|---|---|---|---|---|---|---|---|---|
| | | | | | | $H_2O$-Soluble Conjug[d] | Tetrahydro-tetrols | Dihydro-diols | Quinones | Dihydro-epoxide | 9-OH-BaP | 3-OH-BaP |
| 1 | Female | 0.15 | 7.43 | 0.61 (0.82)[e] | 7.7 | 7.67 | 4.85 | 2.83 | 5.25 | 0.77 | ND[f] | 0.713 |
| 2 | Male | 0.09 | 120.8 | 0.77 (0.64) | 7.1 | 5.46 | 1.24 | 1.90 | 1.25 | .51 | ND | 0.513 |
| 3 | Female[g] | 0.13 | 87.2 | 0.44 (0.50) | 3.3 | 2.98 | 1.09 | 1.72 | 1.38 | 0.57 | ND | 0.519 |
| 4 | Female[g] | 0.29 | 37.9 | 0.21 (0.55) | — | 2.9 | 1.27 | 2.19 | 1.58 | ND | 0.74 | ND |

[a]All incubations were carried out for 100 min and were conducted identically to one another.

[b]Calculation of pmol quantities of metabolites did not take into account possible $^3H$ loss into media. These were metabolites extracted from the tissue slice following the incubation. Metabolites present in the media are not shown.

[c]Data represent pmol covalently bound BaP metabolite/g tissue presented as BaP equivalents. The washing process removed lipids, and the contribution of metabolites bound to nucleic acids is believed to be negligible (Lutz, W. F. *Mutat. Res.* 65: 289, 1979). Hence, these data are largely representative of BaP metabolites covalently bound to proteins.

[d]This value may include a small amount of $^3H_2O$. It is likely that conjugates will be found in the media extract.

[e]Percent of dose that became covalently bound to protein.

[f]ND = Not detected

[g]These tissues were frozen for 24 h prior to the metabolism experiment.

(Research sponsored by the PHS/NIH under Grant RO1-ES05910 from the National Institute of Environmental Health Science with the U.S. Department of Energy, under Contract No. DE-AC04-76EV01013.)

# ANALYSIS OF VOLATILE BUTADIENE METABOLITES IN BLOOD BY GAS CHROMATOGRAPHY/GAS CHROMATOGRAPHY/MASS SPECTROSCOPY

*William E. Bechtold, Michael R. Strunk, Janice R. Thornton-Manning, Alan R. Dahl, and Rogene F. Henderson*

1,3-Butadiene (BD) is a monomer used in the production of synthetic rubber. The carcinogenicity of BD has been determined in life-span inhalation studies in Sprague-Dawley rats and B6C3F$_1$ mice (Melnick, P. L. *et al. Environ. Health Perspect. 100*: 227, 1993). Results from these studies suggest a marked species difference in the carcinogenic effects of BD, with mice demonstrating far greater sensitivity than rats. This disparity between species may in part result from differences in the metabolism of BD to reactive intermediates. Studies at our Institute are exploring species differences in the metabolism of BD to volatile metabolites in blood. Methods were needed that allowed the selective and sensitive determination of specific BD metabolites in blood and tissue. The purpose of this paper was to report the development of such a method for the analysis of volatile metabolites of BD in blood and tissues, and the results of application of the method to the analysis of blood from rats and mice exposed to 100 ppm BD for 4 h.

The method was first validated by removing blood from control animals and adding analyte at expected levels to stoppered and evacuated round-bottomed flasks. An internal standard solution of BDO-$d_6$ and $BDO_2$-$d_6$, and aliquots of diluted BD-$d_6$ gas were added, and the contents were well mixed. Graded levels of unlabeled analytes were introduced similarly and the contents mixed well and frozen on liquid nitrogen.

The volatile BD metabolites were isolated from nonvolatile impurities by vacuum-line distillation. Contents of the round-bottomed flask were distilled through a U-tube modified with a sampling port (septaport U-traps). The metabolites were then held at –196°C by liquid nitrogen. The contents of the traps were analyzed for BD, butadiene monoepoxide (BDO), and butadiene diepoxide ($BDO_2$) using gas chromatography/gas chromatography/mass spectroscopy (GC/GC/MS). Preliminary experiments showed that BD and BDO partitioned significantly into the septaport U-trap headspace, while $BDO_2$ remained in the water that had co-distilled. BD and BDO were measured from the head space of the septaport U-traps held at room temperature by removing an aliquot (2–5 mL) with a glass syringe and injecting it directly onto the GC column.

The aqueous phase remaining in the septaport U-trap was removed for analysis of the $BDO_2$. The aqueous phase was extracted with ethyl acetate, and the organic phases were pooled and reduced in volume by passing a stream of nitrogen gas over the sample at room temperature. The organic extract (5 $\mu$L) was analyzed for $BDO_2$ by GC/GC/MS.

The MS was operated in the selected ion mode. Peaks were integrated, and ion ratios were calculated to both internal standards and to each of the other ions from the same analyte. The former set of ion ratios was used for quantitation, while the latter set was used for confirmation of analyte identity. Results of the method validation experiments are shown in Table 1. In general, the method gave values within 25% of those expected.

The consistency for internal ion ratios confirms the identity of the analytes as BD and metabolites. Overall, distillation efficiencies varied between about 40 and 60%, as measured by the internal standard recoveries. The limits of sensitivity for the assay were 100, 20, and 10 pmol/mL for BD, BDO, and $BDO_2$, respectively.

Table 1

Method Validation for BD, BDO, and $BDO_2$ in Blood

| Analyte | Spike Levels (nmol) | Analyte Recovery (% ± SD) | Analyte Ion Ratios: Standards vs. Samples | Internal Standard Recoveries (% ± SEM) |
|---|---|---|---|---|
| BD | 4.96 | 95.6 ± 17.7 | 1.30 vs. 1.25[a] | 41 ± 9.0[b] |
| BDO | 3.42 | 124.6 ± 14.5 | 7.63 vs. 8.25[c] | 52 ± 9.8[d] |
| $BDO_2$ | 0.545 | 98 ± 12 | 2.24 vs. 1.88[e] | 62 ± 15[f] |

[a]Ion pair 39/54
[b]$n$ = 9; based on ion 42
[c]Ion pair 39/69
[d]$n$ = 9; based on ion 46
[e]Ion pair 29/55
[f]$n$ = 6; based on ion 58

The stabilities of BDO and $BDO_2$ were determined in blood for short time periods (1 h) when held at room temperature. Knowledge of the short-term stability of BDO and $BDO_2$ in blood was important because at least some time elapsed (2–5 min) between when animals were sacrificed on the inhalation exposure plenum and when internal standard was added to the blood. Because of the potentially reactive nature of these epoxides, degradation could occur in the interim and artificially lower the observed values. To determine the stabilities, control blood was spiked with BDO and $BDO_2$, and aliquots were removed at specified times and placed in round-bottomed flasks. Internal standard was added, the mixture was distilled on the vacuum line, and the distillate was analyzed for BDO and $BDO_2$. Results showed no significant degradation of the metabolites after 1 h.

Next, both mice and rats were exposed by inhalation in nose-only chambers to approximately 100 ppm BD for 4 h. BD atmospheres were generated directly from commercially available cylinders of BD. BD concentrations in the exposure chambers were quantitated by a GC equipped with a flame ionization detector and were continuously monitored by infrared spectroscopy. The wavelength was set at 3.4 $\mu$m. The target exposure concentration was 100 ppm, while the actual measured values varied between 92 and 101 ppm. The stability of this generation was evaluated at least every 15 min over the 4-h exposure period and typically varied less than ± 20% of the mean concentration.

At the end of the exposure, six exposed and six control mice and rats (exposed to filtered air in nose-only chambers) were anesthetized while breathing the exposure atmosphere, and blood was withdrawn by heart puncture, through a special port in the exposure tube, by a syringe.

Blood was analyzed for chemical-specific metabolites as described above. Results from the exposure are shown in Table 2. In all cases in which values are reported for BD and metabolites in blood, measured values for exposed animals were significantly different than those for controls (Student's $t$-test, $p < 0.05$). The consistency between analyte ion ratios (column 4) confirms the identity of the respective analytes. Internal standard recoveries (column 5) were in general similar to those reported in the validations.

Table 2

Summary of Exposure Results: Analysis of BD, BDO, and $BDO_2$ in the Blood of Mice and Rats Exposed by Inhalation to BD

| Analyte | | Exposure Levels (ppm) (mean ± SD) | Analyte Blood Level (nmol) (mean ± SD) | Analyte Ion Ratios: Standards vs. Samples | Internal Standard Recoveries (% ± SEM) |
|---|---|---|---|---|---|
| BD | Rats | 96.5 ± 5.5 | 4.1 ± 1.0 | 1.3 vs. 1.3 | 28 ± 2.7[a] |
| | Mice | 101 ± 4 | 2.9 ± 1.3 | 1.2 vs. 1.2[b] | 36 ± 4.8[c] |
| BDO | Rats | 96.5 ± 5.5 | 0.10 ± 0.06 | 7.4 vs. 7.2 | 32 ± 2.6 |
| | Mice | 101 ± 4 | 0.38 ± 0.14 | 8.1 vs. 7.5[d] | 48 ± 5.0[e] |
| $BDO_2$ | Rats | 93 ± 13 | Not Detected (ND) | ND | 75 ± 3.3 |
| | Mice | 93 ± 13 | 0.33 ± 0.19 | 1.3 vs. 1.5[f] | 68 ± 4[g] |

[a] $n$ = 6 for both rats and mice
[b] Ion pair 39/54
[c] $n$ = 12; based on ion 42
[d] Ion pair 39/69
[e] $n$ = 12; based on ion 46
[f] Ion pair 29/55
[g] $n$ = 12; based on ion 58

The levels of BDO and $BDO_2$ measured in the blood of exposed mice compare reasonably well with our previously reported values as determined by vacuum line distillation and analysis of $^{14}C$ (Bond, J. A. *et al. Toxicol. Appl. Pharmacol. 84*: 617, 1985). In the earlier studies, levels of BDO in rats and mice were 0.95 and 2.14 pmol/mL/ppm/h, respectively, vs. 0.25 and 1.0 pmol/mL/ppm/h in the present study. Levels of $BDO_2$ in rats and mice were 0.24 and 0.24 pmol/mL/ppm/h, respectively, vs. Not Detected (less than 0.03) and 0.83 pmol/mL/ppm/h in the present study. In the previous study, radioactivity due to butenediol was expected to co-distill with $BDO_2$ and may therefore have contributed to the minimal value observed.

Of particular importance is the comparison of blood levels of $BDO_2$ between rats and mice. The limits of detection for our assay were about 10 pmol/mL. Therefore, for a given level of exposure and time of collection, mice had at least a 30-fold excess of $BDO_2$ relative to rats. In experiments described elsewhere (this report, p. 62), we determined levels of these reactive metabolites in the blood and tissues from mice and rats exposed to 60 ppm BD. Results were consistent with those described here and extended the conclusions over a much broader time, including measurements both during and after exposures. Taken together, these results suggest that $BDO_2$ may contribute to the marked species difference in the carcinogenicity of BD.

(Research sponsored by the Chemical Manufacturers' Association under Funds-in-Agreement No. DE-FIOY-91AL66351, and by the Office of Health and Environmental Research, U.S. Department of Energy, under Contract No. DE-AC04-76EV01013.)

# ANALYSIS OF BUTADIENE MONOEPOXIDE AND BUTADIENE DIEPOXIDE IN VARIOUS TISSUES OF SPRAGUE-DAWLEY RATS AND B6C3F$_1$ MICE FOLLOWING LOW-LEVEL EXPOSURES TO 1,3-BUTADIENE

*Janice R. Thornton-Manning, William E. Bechtold, Alan R. Dahl, and Rogene F. Henderson*

1,3-Butadiene (BD) is used extensively in the production of styrene-butadiene rubber, polybutadiene elastomers, and other polymers. Occupational exposures of workers in areas with concentrations of up to 374 ppm BD have been documented in U.S. plants (Fajen, J. M. *et al. Environ. Health Perspect. 86*: 11, 1990). Additionally, BD is present in cigarette smoke, gasoline vapors, and automobile exhaust resulting in exposures of this chemical to most of the U.S. population (Miller, L. M. EPA-560/2-78-008). Epidemiological studies have revealed increased incidences of mortality due to lymphatic and hematopoietic cancers among rubber industry workers exposed to BD (Mantanoski, G. M. *et al. Environ. Health Perspect. 86*: 107, 1990). However, because these workers were most likely exposed to a wide variety of potentially harmful compounds, the contribution of BD to increased carcinogenic risk is uncertain.

Long-term animal studies have revealed that BD is carcinogenic in both Sprague-Dawley rats and B6C3F$_1$ mice (Huff, J. E. *et al. Science 227*: 548, 1985; Melnick, P. L. *et al. Cancer Res. 50*: 6592, 1990; Owen, P. E. *et al. Am. Ind. Hyg. Assoc. J. 48*: 407, 1987). These studies have shown profound species differences in the potency and organ-site specificity of BD carcinogenesis. In mice, hemangiosarcomas, lymphomas, and lung, forestomach, liver, ovary, and mammary gland tumors were observed. Most notable was that lung tumors resulted from exposures as low as 6.25 ppm. In rats, chronic exposures of 1000 and 8000 ppm resulted in tumors of the thyroid, testis, uterus, mammary gland, and pancreas, although the data suggested that some of the tumors may not have been treatment-related. These species differences in tumorigenic responses to BD have made extrapolation of these data to humans difficult.

*In vivo* and *in vitro* studies have indicated that BD is metabolized by identical oxidative pathways in both rats and mice. The initial step of BD metabolism is oxidation by a cytochrome P450 enzyme(s) to butadiene monoepoxide (BDO). BDO is then further metabolized by a cytochrome P450 enzyme(s) to butadiene diepoxide ($BDO_2$). These epoxides are substrates for the detoxication enzymes, epoxide hydrolases, and glutathione *S*-transferases. $BDO_2$, and to a lesser extent BDO, are mutagenic in bacterial systems (Wade, M. J. *et al. Mutat. Res. 66*: 367, 1979; Voogd, C. E. *et al. Mutat. Res. 89*: 269, 1981). Recent studies measuring the mutagenicity of the epoxides at the *tk* and *hprt* loci in cultured human lymphoblasts indicated that $BDO_2$ was mutagenic at concentrations 100-fold lower than BDO (Cochrane, J. E. and T. R. Skopek. *Carcinogenesis 15*: 713, 1994). Based on these studies and others which have indicated that the epoxides are genotoxic, it is thought that these metabolites may be responsible for the carcinogenicity of BD. The purpose of the present investigation was to examine the production and disposition of BDO and $BDO_2$ in several target tissues in rats and mice during and following 4-h exposures to a low level (62.5 ppm) of BD.

Eleven- to 14-wk-old male Sprague-Dawley rats and B6C3F$_1$ mice were exposed to 62.5 ppm BD by nose-only inhalation for 4 h. Controls were exposed simultaneously to house air on a separate exposure plenum. In order to increase the sensitivity of these methods, tissues from three rats and nine mice were pooled for each determination. Exposures were conducted on eight separate days and included 69 rats and 194 mice (controls and exposed). The animals were anesthetized, and blood was removed by heart puncture through a special port in the exposure tube that allowed the animals to continue breathing the exposure atmosphere while the sample was being removed. The blood was immediately frozen in liquid nitrogen and amended with internal standards (deuterated BDO and

$BDO_2$). The animals were then removed from the exposure plenum; several other tissues, including bone marrow, heart, spleen, thymus, and lungs were removed and immediately frozen in liquid nitrogen. Bone marrow was removed by placing a tube on the end of the femur and expelling the marrow with saline. Internal standards were immediately added, and the bone marrow was frozen. The remaining tissues were stored in liquid nitrogen until prepared for analysis, at which time, they were pulverized under liquid nitrogen and placed in flasks containing internal standard. The samples were distilled *in vacuo* into two U-tubes to separate the epoxide metabolites and internal standards from the tissues. The first tube was immersed in a xylene slush (–48°C) and the second, a septaport U-tube, in liquid nitrogen (–196°C). The metabolites and internal standards were distilled into the septaport U-tube and were analyzed by multidimensional gas chromatography/mass spectroscopy. Method detection limits for BDO were 30.7, 36.9, and 61.5 for blood, heart, and lung, respectively. Limits of detection for $BDO_2$ were 1.6, 30.9, and 26.4 for these tissues. These were determined by methods approved by the U.S. Environmental Protection Agency (40 CFR 136, Appendix B).

Levels of the epoxides in the blood of rats and mice during and following the 4-h exposure are shown in Figure 1. Both metabolites increased at 2 and 4 h, then decreased to control levels by 5 h (1 h after cessation of the exposure). Immediately after the exposure, concentrations of BDO in mouse blood were about 5-fold greater than those in rat blood. This is similar to other reports from this laboratory that showed BDO was present in mouse blood at levels 2- to 4-fold greater than those present in rat blood immediately following low-level exposures to BD (Bond, J. A. *et al. Toxicol. Appl. Pharmacol. 84:* 617, 1985; this report, p. 59).

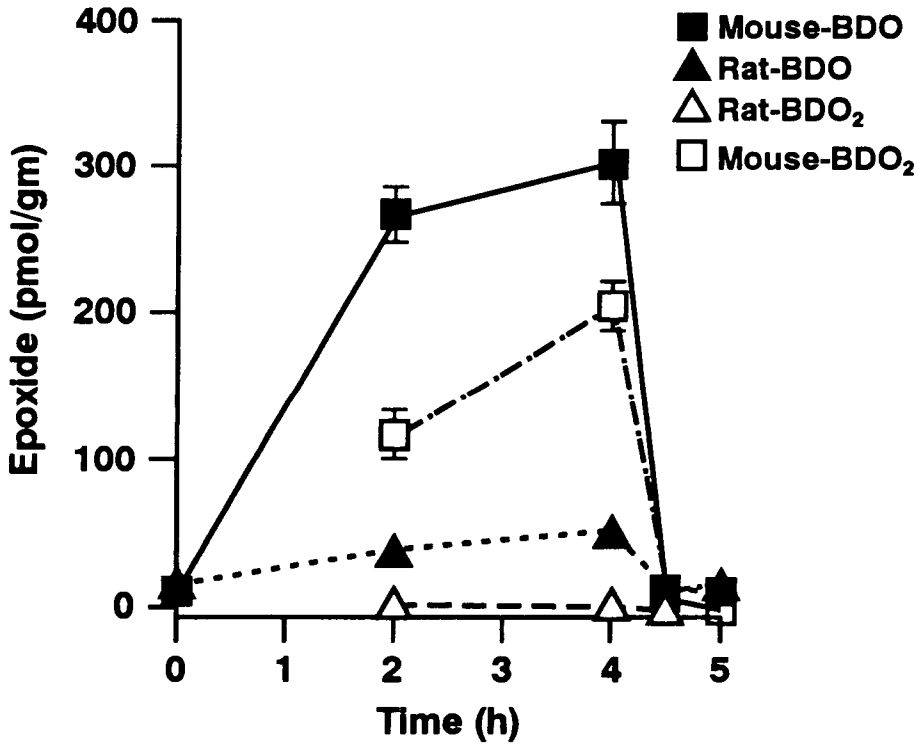


Figure 1. Concentrations of BDO and $BDO_2$ present in the blood of rats (n = 3 to 6) and mice (n = 3 or 4) during and following a 4-h exposure to BD (mean ± SE). (In the 0 h [control] samples, $BDO_2$ levels were not detectable.)

Levels of $BDO_2$, the more mutagenic of the two epoxides, were approximately 100-fold greater in the blood of mice at 4 h than in rats at this time point. $BDO_2$ was present in rat blood at a

concentration of 2.1 ± 0.78 pmol/gm. These data are notable because a recent study (Himmelstein, M. W. *et al. Carcinogenesis 15*: 1479, 1994) in which rats were exposed to a 20-fold higher exposure concentration of BD reported that $BDO_2$ was not quantifiable in rat blood. The increased sensitivity of our methods enabled us to quantify this metabolite in rat blood, and the data agree with other recent studies from this laboratory in which $BDO_2$ concentrations were determined to be below a detection limit of 10 pmol/gm after a 4-h exposure to 100 ppm BD (this report, p. 59).

The levels of the epoxides found in other tissues of rats and mice reflected similar quantitative differences to those seen in blood (Table 1). BDO was present in mouse tissues at levels that were from 3- to 14-fold greater than those present in rat tissues following a 4 h exposure to BD. BDO was not detected in rat lungs at levels that exceeded background levels. $BDO_2$ was present in all the mouse tissues examined, while levels in rat tissues were below detection limits for all the tissues examined.

Table 1

Tissue Levels of BDO and $BDO_2$ in Rats and Mice
Following a 4-h Exposure to 62.5 ppm 1,3-Butadiene by Inhalation

| | BDO[a,b] | | $BDO_2$[a] | |
|---|---|---|---|---|
| Tissue | Rats | Mice | Rats | Mice |
| Heart | 39.8 ± 14.8 | 120.2 ± 11.4 | 1.6 ± 0.5 | 139.1 ± 17 |
| Lung | nd[c] | 32.8 ± 8 | nd | 111.8 ± 38 |
| Fat | 266.7 ± 13.5 | 1301.9 ± 212.6 | 2 ± 0.5 | 91.1 ± 14.9 |
| Spleen | 7.1 ± 3.8 | 39 ± 5.8 | nd | 88 ± 12.5 |
| Thymus | 12.5 ± 2.7 | 104.3 ± 54.4 | nd | 92.7 ± 20.1 |
| Bone marrow[d] | 0.16 ± 0.12 | 2.3 ± 1.5 | nd | 0.93 ± 0.3 |

[a]Mean ± SE, pmol/gm tissue.
[b]Background levels of a "BDO-like" analyte present in controls were subtracted from these values.
[c]nd = not detected; indicates that analyte was not detected or was not above background levels.
[d]Bone marrow data are presented as pmol/mg protein.

In this investigation, levels of BD epoxides were compared in seven tissues from rats and mice. Consistently, the concentrations of the two epoxides were greater in mouse tissues than rats. The lack of quantifiable levels of either BDO or $BDO_2$ in rat lungs may be particularly significant, because tumors occur in murine lungs at exposure levels lower than those used in the current investigation. This study suggests that production of these mutagenic metabolites may play a role in the greater sensitivity of mice to BD-induced carcinogenicity.

(Research supported by the Chemical Manufacturers' Association under Funds-In-Agreement No. DE-FI04-91AL66351 with the U.S. Department of Energy, under Contract No. DE-AC04-76EV01013.)

# BIOCHEMICAL MARKERS IN BUTADIENE-EXPOSED WORKERS

*William E. Bechtold, Janice R. Thornton-Manning, Richard B. Hayes*, and Rogene F. Henderson*

1,3-Butadiene (BD) is used to manufacture a wide range of polymers and copolymers including styrene-butadiene rubber, polybutadiene, and acrylonitrile-butadiene-styrene resins. The carcinogenicity of BD has been determined in life-span inhalation studies in both Sprague-Dawley rats and $B6C3F_1$ mice. Results suggest a marked species difference in the carcinogenic effects of BD. For example, female mice exposed to as low as 6.25 ppm BD exhibited increased alveolar/bronchiolar neoplasms. In contrast, BD was only a weak carcinogen in Sprague-Dawley rats. Rats were observed to have an increase only in mammary tumors after exposure to 1000 ppm.

One possible explanation for the disparity between species in their carcinogenic response may be differences in the metabolism of BD to reactive intermediates. BD is initially metabolized to butadiene monoxide (BMO). BMO is inactivated by epoxide hydrolases and glutathione-S-transferases. Mice, rats, and humans may differ significantly in their relative capacities to metabolize BD and its reactive intermediates. Mice have been shown to form the highly mutagenic butadiene diepoxide ($BDO_2$) after BD exposure, while rats form this intermediate at far lower levels. Whether humans exposed to BD form the $BDO_2$ is unknown. In addition, subsets of human populations may differ in susceptibility to the carcinogenic effects of BD metabolites. For example, although a population bimodal distribution exists for the development of *in vitro* sister chromatid exchange after exposure of peripheral blood lymphocytes to the $BDO_2$, this and other cytogenetic markers have not been studied *in vivo* in humans.

While exposure to BD is common in the U.S., the levels of exposure are low (generally less than 2 ppm). In contrast, exposures outside of the U.S. are often higher. A biochemical study of highly exposed BD workers and unexposed controls is providing valuable information on BD metabolism in humans, and how this relates to the development of intermediate biologic effects. A group of heavily exposed workers was identified in a BD production facility in China. Preliminary studies indicated workers at this facility were exposed to 0 to 100 ppm time weighted average (TWA) over an 6-h day. Based on these initial findings, the workers are being studied more extensively by the National Cancer Institute with collaborators from the Chinese Academy of Preventive Medicine, ITRI, and the University of California at Berkeley. The principal sampling trip, completed in the first quarter of 1994, examined workers at the Yian Shan Chemical Company in Yian Shan, China, where the BD isolation and polymerization facility is located. The purpose of this paper is to report the initial results from the sampling trip.

Three distinct sections could be differentiated at this facility. The first section received a hydrocarbon stream from a pipeline consisting of mainly alkanes and alkenes with three to five carbon atoms. BD was isolated from the hydrocarbons by distillation and a proprietary process based on dimethylformamide (DMF) extraction. This process resulted in a stream of BD over 95% pure. From here, the BD was transported to the next section, the recovery unit, where it was further distilled to a purity of over 99%. The BD was then transported to polymerization vats for synthesis of polybutadiene, in section three. Any BD remaining was returned to the recovery unit, where it was mixed with incoming BD from the DMF recovery facility, repurified, and repolymerized.

The workers acquired samples of the process streams from a number of locations for the purpose of purity analysis. The BD process lines were fitted with sampling valves. Workers opened the valves and filled syringes with the expelled process streams. The syringes were capped and returned to the lab for analysis by gas chromatography (GC).

*National Cancer Institute, Bethesda, Maryland

BD exposure was established by grab sampling, and personal and environmental monitoring. Grab samples were taken at the breathing zone using 50-mL glass syringes. The syringes were capped, returned to the lab, and analyzed by GC. BD gas from a standard cylinder containing 200 ppm BD was used to calibrate the GC. Personal and environmental monitoring samples were taken by drawing atmospheres through charcoal tubes using personal sampling pumps. Flow rates were 35 mL/min. Two traps were combined in series to ensure that all BD was retained. Side-by-side samplers were collected for comparative analysis, both in China and later in the U.S. The two side-by-side sampling trains were connected through a glass "T" to allow the use of a single personal pump. Environmental samples used the same arrangement except that the sampling trains were placed in various fixed locations and allowed to operate for 6 h. Charcoal tubes were analyzed for BD by NIOSH Method 1024 in the U.S., and a variation of Method 1024 in China. However, analyses in China did not use GC columns suitable for separating all other hydrocarbons from BD. Because considerable concentrations of other hydrocarbons were expected, particularly in the DMF facility, these values were used mainly for estimations.

Urine samples were collected during work (0–3, 4–6 h of a 6-h shift) and at 24 h (generally just before beginning the subsequent work shift). Post-shift blood (27 mL) samples were also collected. In one experiment, two volunteers were exposed to BD while wearing personal sampling devices. Blood samples were collected immediately, prior to, and at 2, 5, and 10–20 min after exposure. Study participation was entirely voluntary.

Results from grab samples and observation of work habits suggested a consistent exposure pattern for the workers. After workers arrived for a shift, they immediately sampled the process streams, typically at three to six positions. Individual samples took about 30–60 sec. During the sampling, workers were exposed to dense plumes of BD, hydrocarbons, or both. Overall, this sampling venture took about 30–45 min. Grab sampling and environmental monitoring established that workers receive little exposure over the remainder of the day. Concentrations in the grab samples varied from 0 to about 3000 ppm BD.

Results for individual exposure monitoring are shown in Figure 1. Over the duration of the study, 19, 32, and 19 samplers were analyzed from workers in the DMF extraction, recovery, and polymerization facilities, respectively. For reasons described above, results are reported for analyses from the U.S. laboratory only. The median TWA exposure concentrations for workers in the DMF, recovery, and polymerization facilities were 80, 4.4, and 3 ppm, respectively. Grab samples were consistent with these trends.

Volatile BD metabolites will be measured in blood as previously described (Bechtold, W. E. *et al. Chem. Res. Toxicol.*, in press), with alterations. The measurement of BD metabolites (mercapturic acid conjugates of butanediol [M1]) in blood and urine are in progress. Results of these studies will more clearly describe the relationship between BD exposure and levels of excretion of M1 in urine. We will qualitatively monitor for the presence of a second urinary metabolite found in rodent species, the mercapturic acid conjugate of buteneol (M2). Presence of this metabolite would suggest that metabolism in Orientals differs from Caucasians. Because time-course information will be gathered for excretion of M1, these studies should give an estimation of the excretion half-life. Finally, analysis of blood samples may suggest whether humans produce the highly toxic metabolite $BDO_2$. This metabolite may account for the marked species difference in the toxicity between mice and rats.

In other experiments associated with this study, the relationship between BD exposure and the development of intermediate markers, including chromosomal abnormalities, sister chromatid exchanges, glycophorin A mutation, genetic mutations, adducts, and possibly other markers will be determined. Finally, we will relate these findings to genetic polymorphisms possibly related to BD metabolism.

Taken together, these investigations should provide better estimates of risk associated with human exposures to BD.

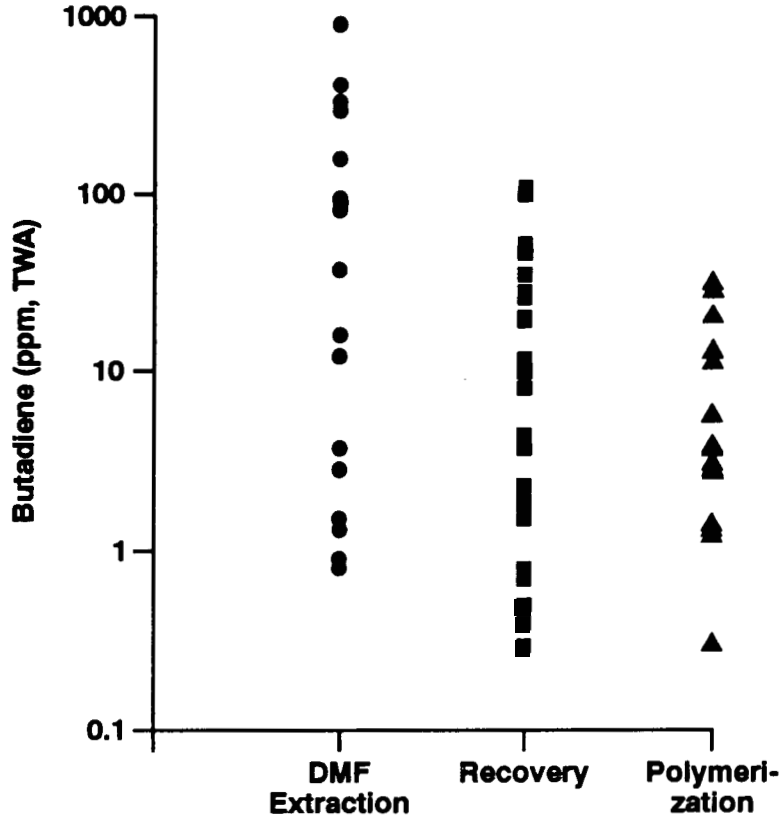


Figure 1. Individual TWA exposures of workers to BD (6-h). The three categories represent three distinct sections of the BD processing plant.

(Research sponsored by the National Cancer Institute under IAG Y01-CP4-0580 with the U.S. Department of Energy, under Contract No. DE-AC04-76EV01013.)

# INDUCTION OF EXPRESSION OF TWO PHENOTYPIC MARKERS OF PULMONARY TYPE II CELLS IN A CULTURED CELL LINE

*Rogene F. Henderson, James J. Waide, and Gary G. Scott**

The functions of pulmonary type II cells, such as synthesis of pulmonary surfactant and metabolism of inhaled xenobiotics, can be studied in primary isolates of lung cells. However, isolated type II cells, when cultured, quickly lose the phenotypic expressions characteristic of type II cells, including surfactant lipid and protein synthesis and alkaline phosphatase (AP) activity. A cultured cell line that maintained expression of type II cell markers of differentiation would be advantageous for the study of such functions as surfactant synthesis and secretion. Such a cell line would allow generation of a large number of homogenous cells for study. The purpose of the current study was to induce markers of differentiated type II cells in a cultured cell line to facilitate studies of factors that control surfactant synthesis and secretion.

Fetal rat lung epithelial (FRLE) cells, a spontaneously immortalized cell line of fetal rat lung type II cell origin, were used in the present study (Leheup, B. P. *et al. Lab. Invest. 60*: 791, 1989). The cells have a stable chromosome number of 44. Passage 90 cells were incubated in RPMI-1640 with 10% calf serum and 1% penicillin-streptomycin solution (basal medium). Cells were treated with inducers of differentiation while growing on either plastic Petri dishes or dishes coated with a commercial form of basement membrane material (Matrigel®).

Treatment of the FRLE cells for up to 3 d with hydrocortisone (0.01 mM), dexamethasone (0.1 mM ), or dibutyryl cAMP (0.5 mM ) did not induce AP activity. However, treatment with 2 mM sodium butyrate for 72 h increased the AP activity from a baseline of 3.8 mIU/$10^6$ cells to 26.1 mIU/$10^6$ cells (Fig. 1). The amount of sodium butyrate required to induce AP activity was determined by treatment of the FRLE cells with varying concentrations of sodium butyrate for 48 h; 2 mM butyrate was sufficient to induce AP in the cells. Using this concentration of butyrate, a time course for the induction of AP activity in the cells was determined. Induction was evident after approximately 30 h but was 10-fold higher after 80 h. If butyrate was removed from the media, the AP activity in the cells declined with a half-life of approximately 12 h.

The AP induced in FRLE cells by butyrate treatment had a similar isoelectric focusing pattern to that found in freshly isolated type II cells. The magnitude of inhibition of the enzyme activity by amino acids, chelating agents, and heat was also similar to that observed for AP from type II cells.

The effect of Matrigel®, a basement membrane preparation known to induce differentiation (Levebuga-Mukasa, J. S., *Am. Rev. Respir. Dis. 144*: 452, 1991), on the synthesis of surfactant lipid in FRLE cells was determined. Surfactant lipid has a high content of disaturated phospholipid (DSPL), and the synthesis of surfactant was monitored by assaying for DSPL. Cells grown on Matrigel® without butyrate had only a slight increase in DSPL content (within cells) and a modest increase in AP activity (Fig. 1). However, cells grown on Matrigel® in the presence of butyrate had three times the amount of DSPL and four times the amount of AP activity as cells grown on Matrigel® alone (Fig. 1). The amount of DSPL in cells grown on Matrigel® with butyrate represented 59% of the total phospholipids in the cells, a value that is similar to that found in surfactant (Rooney, S. A. *Am. Rev. Respir. Dis. 131:* 439, 1985).

*UNM/ITRI Inhalation Toxicology Graduate Student

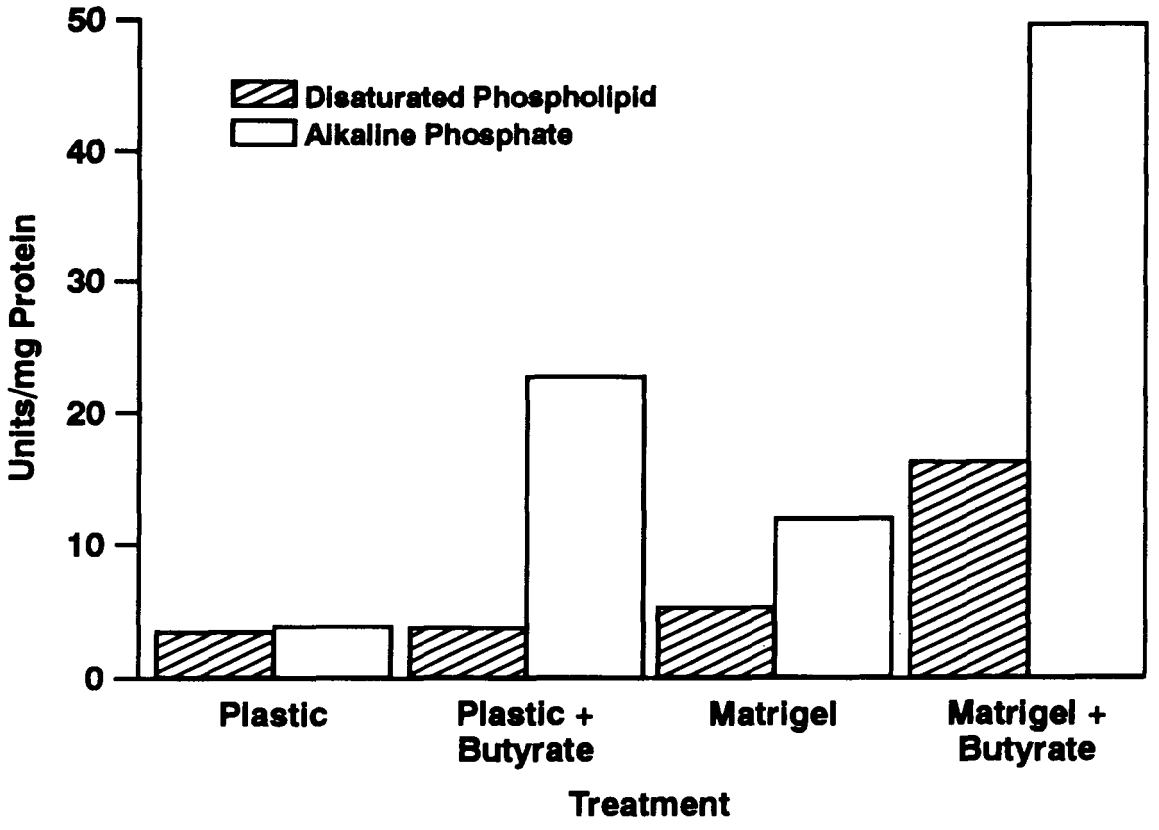


Figure 1. Disaturated phospholipid and AP induction in FRLE cells. One million cells per plate were cultured on plastic or Matrigel® for 24 h and induced or not induced with 2 mM butyrate for 48 h. Clear bars represent AP activity (mIU/mg protein); the cross-hatched bars represent disaturated phospholipid phosphorus ($\mu$g/mg protein). The results are based on a single experiment.

The induction of the expression of two characteristics of type II cells suggests that the FRLE cell line may be a model to study factors influencing the synthesis and secretion of surfactant from type II cells. Additional work is required to confirm that the culture conditions described above will reproducibly increase AP activity and DSPL synthesis. Further work will also determine if the same culture conditions have also induced the synthesis of the surfactant proteins that are associated with the DSPL.

(Research sponsored by the Office of Health and Environmental Research, U. S. Department of Energy, under Contract No. DE-AC04-76EV01013.)

# IV. CARCINOGENIC RESPONSES TO TOXICANTS

# EXPOSURE OF F344 RATS TO AEROSOLS OF $^{239}PuO_2$ AND CHRONICALLY INHALED CIGARETTE SMOKE

*Gregory L. Finch, Kristen J. Nikula, Edward B. Barr, William E. Bechtold, Bean T. Chen, William C. Griffith, Charles H. Hobbs, Mark D. Hoover, and Joe L. Mauderly*

Nuclear workers may be accidentally exposed to radioactive materials such as $^{239}PuO_2$ by inhalation, and thus have increased risk for lung cancer compared to the general population. Of additional concern is the possibility that interactions between radionuclides and other carcinogens may increase the risk of cancer induction. An important and common lung carcinogen is cigarette smoke. This study is being conducted to better determine the combined effects of inhaled $^{239}PuO_2$ and cigarette smoke on the induction of lung cancer in rats.

Three individual exposure blocks (Blocks A, B, and C) of from 690 to 790 male and female CDF®(F-344)/CrlBR rats (Charles River Laboratories, Raleigh, NC) were placed on study during September 1991, February 1992, and May 1992. Rats were received at 4 ± 1 wk of age, held in Hazleton H-2000 chambers (Lab Products, Inc., Maywood, NJ) for 2 wk, and assigned to one of six experimental groups (see Table 1). Beginning at 6 wk of age, groups of rats were exposed by the whole-body mode to either filtered air (FA) or to mainstream cigarette smoke (generated from 1R3 research cigarettes, Tobacco Health Research Institute, Lexington, KY; as described by Chen, B. T. *et al. J. Aerosol Med. 5(1)*: 19, 1992) diluted to concentrations of either 100 or 250 mg total particulate matter (TPM)/$m^3$ (LCS or HCS groups, respectively). Rats were exposed for 6 h/d, 5 d/wk, for 6 wk, at which time they were removed from the chambers and exposed nose-only to either FA or to a $^{239}PuO_2$ aerosol for 25 min (nominal mean values of activity median aerodynamic diameter = 1.0 $\mu$m, geometric standard deviation = 1.6, and $^{239}Pu$ air concentration = 960 Bq/L). One week later, the rats were returned to the H-2000 chambers for continued exposure to FA or cigarette smoke. The rats were whole-body counted weekly for 6 wk for the radiolabel $^{169}Yb$, which was fused into the $^{239}PuO_2$ particles. This technique yielded estimates of initial lung burden of about 440 Bq and clearance half-times of 31, 51, and 64 days for the FA, LCS, and HCS groups, respectively.

Rats are being exposed for 30 mo, at which time final sacrifices will be conducted. Rats are weighed and observed monthly for clinical abnormalities. Moribund rats are euthanized. A full necropsy is performed on all dead animals. As shown in Table 1, approximately two-thirds of the rats are being observed for life. The remaining one-third of the rats are designated for interim sacrifices which are conducted principally to (1) collect lung and lesion tissue for histopathological and morphometric analysis, (2) quantitate epithelial cell proliferation in selected rats using a 5-bromodeoxyuridine labeling technique, (3) measure amounts of $^{239}Pu$ in lung for dosimetric evaluations, and (4) collect frozen lung and blood samples for future molecular biological and biomarker studies.

Additional in-life endpoints not reported here are being examined in selected groups of rats. These endpoints include (1) the periodic assessment of respiratory function, (2) the quantitation of clearance of inert radiolabeled $^{85}Sr$-fused aluminosilicate tracer particles administered after 3 and 18 mo of smoke exposure, and (3) the measurement of nicotine and cotinine in urine at various times after initiation of exposure.

Mean cigarette smoke concentrations have been within 5% of the targeted levels for all chambers, and the composition of the exposure atmospheres is consistent with our previous observations (Chen, B. T. *et al. Inhal. Toxicol. 1*: 331, 1989). As of September 30, 1994, the exposures and final sacrifices of rats from Blocks A and B have been completed, and rats in Block C have been exposed to cigarette smoke for 28½ mo. Six percent of the rats in the study are still alive as of 9/30/94.

Table 1

Experimental Design for the Chronic Study of the Combined Effects of Exposure to Cigarette Smoke and $^{239}PuO_2$ on Lung Cancer in Rats

| | | Approximate $^{239}PuO_2$ ILB[a] | | |
|---|---|---|---|---|
| | | 0 Bq | 400 Bq | Total |
| Cigarette Smoke TPM[c] | 0 mg/m$^3$ | 237[b] (life)<br>114 (sac) | 234 (life)<br>108 (sac) | 471 (life)<br>222 (sac) |
| | 100 mg/m$^3$ | 353 (life)<br>115 (sac) | 346 (life)<br>110 (sac) | 699 (life)<br>225 (sac) |
| | 250 mg/m$^3$ | 163 (life)<br>115 (sac) | 163 (life)<br>107 (sac) | 326 (life)<br>222 (sac) |
| | Total | 753 (life)<br>344 (sac) | 743 (life)<br>325 (sac) | 1496 (life)<br>674 (sac) |
| | | | Experiment Total | 2165 |

[a]ILB = Initial lung burden.
[b]Number of rats included for either life-span exposure and observation (life) or for assignment to serial sacrifice (sac) groups. Numbers do not include 5 rats removed from study (died either during $^{239}PuO_2$ exposure or during in-life procedures).
[c]TPM = Total particulate matter.

Survival has not been markedly affected by cigarette smoke exposure. As expected, the median survival time (MST) of control females is longer than that of control males (835 vs. 777 d of age, respectively). Estimates of MST for both male and female rats across all exposure groups range from 90 to 106% of controls. Cigarette smoke-exposed rats gained less weight than chamber control rats. For the first two exposure blocks, the maximum weights achieved for LCS and HCS group male rats were 88 and 75% that of controls, and 80 and 78% that of controls for LCS and HCS group females, respectively. No other clinical abnormalities have been associated with cigarette smoke and/or $^{239}PuO_2$-exposure to date.

Findings at necropsy include gray mottling of the lungs and hypertrophy of bronchial lymph nodes in rats exposed to cigarette smoke. Histopathological examination of a small number of rats exposed to cigarette smoke revealed alveolar macrophage pigmentation and hyperplasia, chronic-active inflammation, alveolar epithelial hyperplasia, interstitial fibrosis, and bronchial mucous cell hyperplasia in the lungs. The severity of these lesions appeared to increase with exposure time and concentration.

Histologic examination of lung tissue has been conducted on a number of rats having a suspected lung tumor at the time of necropsy. A total of 104 and 107 lung tumors (either benign or malignant) have been diagnosed to date in male and female rats, respectively. The tumor phenotypes have included adenomas, adenocarcinomas, squamous cell carcinomas (all common types of radiation- or chemical-induced lung tumors in rats), a bronchial papilloma, and a carcinosarcoma (both rare lung tumors in rats).

Most of the lung tumors have occurred in rats exposed to both cigarette smoke and $^{239}PuO_2$. Figure 1 illustrates the prevalence (number of rats with lung tumors divided by the total number of rats examined at necropsy) of lung tumors observed in female rats exposed to smoke for at least 12 mo, the approximate time at which the first tumor was observed. A similar trend holds for male rats (data not shown). Lung tumor prevalence has reached as high as 74% in females exposed to HCS plus $^{239}PuO_2$. Interestingly, the combined exposures have produced bronchiolar tumors and a greater proportion of squamous cell carcinomas, compared with adenocarcinomas. These tumor patterns are not typical among rat carcinogenicity studies.

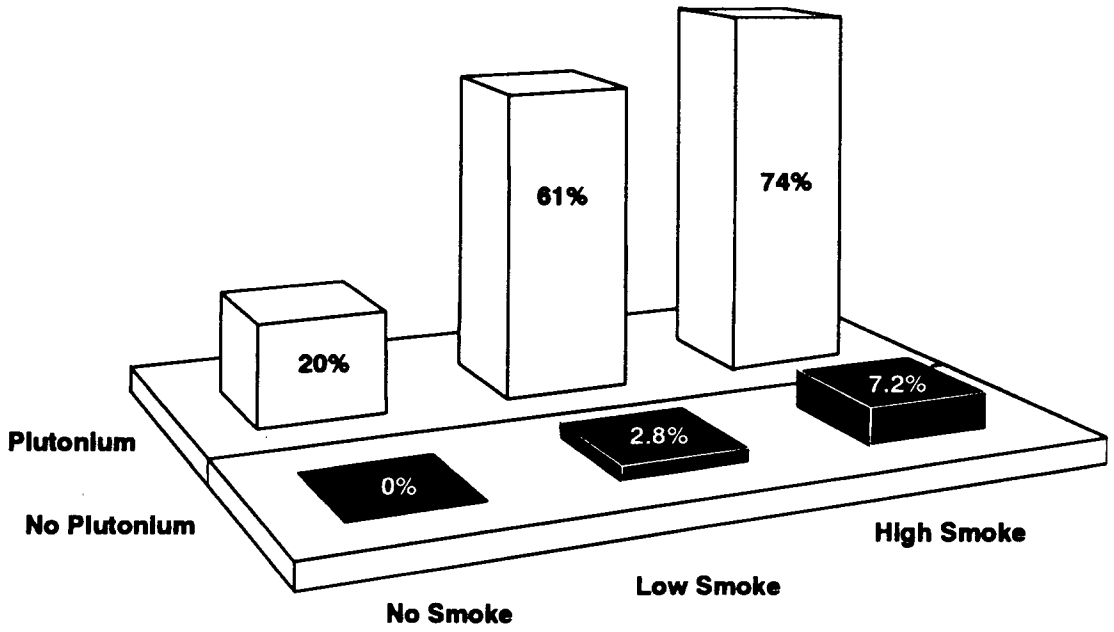


Figure 1. Prevalence of female rats with benign or malignant lung tumors as a function of exposure group for animals on study for at least 12 mo.

Clearly, the present indications are that cigarette smoke and $^{239}Pu$ are interacting synergistically. Data for the amounts of $^{239}Pu$ in the lung are not yet available. As noted above, the whole-body counting of $^{169}Yb$ indicates that exposure to cigarette smoke reduces the lung clearance of $^{239}Pu$. When direct radiochemical measurements of the amounts of $^{239}Pu$ in the lung become available, the data may reveal more about the role of cigarette smoke-induced decreased $^{239}Pu$ lung clearance (with the associated increased radiation dose) in the observed synergism.

This study is still in progress. At the conclusion of this study, we anticipate that significant new information will be generated regarding the induction of cigarette smoke-induced lung cancer in rats, and the potential for interaction between cigarette smoke and $^{239}PuO_2$ exposure in the induction of lung cancer.

(Research sponsored by the Assistant Secretary for Defense Programs, U.S. Department of Energy, under Contract No. DE-AC04-76EV01013).

# EFFECTS OF COMBINED EXPOSURE OF F344 RATS TO INHALED $^{239}PuO_2$ AND A CHEMICAL CARCINOGEN (NNK)

*David L. Lundgren, Steven A. Belinsky, Kristen J. Nikula, William C. Griffith, and Mark D. Hoover*

Workers in nuclear weapons facilities have a significant potential for exposure to chemical carcinogens and to radiation from external sources or from internally deposited radionuclides such as $^{239}Pu$. Although the carcinogenic effects of inhaled $^{239}Pu$ and many chemicals have been studied individually, very little information is available on their combined effects (Fry, R. J. M. and R. L. Ullrich. In *Radiation Carcinogenesis,* Elsevier, New York, p. 437, 1986). One chemical carcinogen that workers could be exposed to, via tobacco smoke, is the tobacco-specific nitrosamine 4-(N-Methyl-N-nitrosamino)-1-(3-pyridyl)-1-butanone (NNK), a product of the curing of tobacco and pyrolysis of nicotine in tobacco (Hoffman, D. and S. S. Hecht. *Cancer Res. 45*: 935, 1985). NNK causes lung tumors in rats, regardless of the route of administration (Rivenson, D. *et al. Cancer Res. 48*: 6912, 1988) and to a lesser extent tumors in the liver, nasal passages, and pancreas.

The purpose of this study is to characterize the effects of combined exposure of rats to NNK and internally deposited plutonium, as well as to these agents alone. The rats are being observed to determine whether specific doses of NNK and internally deposited $^{239}PuO_2$ interact to increase cancer risk. Data are being collected on age-specific cancer incidence rates for cancers that occur spontaneously and as a result of exposure to alpha radiation of the lung with or without exposure to NNK. This information will aid in determining the appropriateness of different mathematical cancer risk models based upon observations of large populations of laboratory animals. A model for the development of lung tumors, illustrating the various rates to be taken into account in predicting the occurrence of lung tumors, has been presented (1986-87 Annual Report, p. 318). Our primary interest in this model is the rate at which the rats develop lung tumors and whether the combined exposure to radiation and a chemical carcinogen alters this rate.

The experimental design for this study has been previously summarized (1991-92 Annual Report, p. 118). Briefly, a total of 740 male 4 ± 1-wk-old CDF®(F344)/CrlBR rats purchased from Charles River Laboratories (Kingston, NY) are being used in two blocks of 370 rats each. The blocks of rats were entered into this study in FY92 and FY93. Rats were randomized by weight for assignment to dose groups within each block. Low, medium, and high doses of NNK, dissolved in physiological saline, were given by subcutaneous injection three times per week for 20 wk. The doses were selected to result in a 15%, 50%, or 90% incidence of lung tumors (Belinsky, S. A. *et al. Cancer Res. 50*: 3772, 1990). The high-dose NNK group (50 mg $kg^{-1}$; 90% lung tumor incidence expected) not exposed to $^{239}PuO_2$, was included to provide tumors for molecular biological studies.

The NNK injections began when the rats were 6 wk of age, and $^{239}PuO_2$ exposures occurred when the rats were 12 wk of age. For this study, the alpha dose to lungs was expected to induce a 15% incidence of lung tumors (1987-88 Annual Report, p. 245; Lundgren, D. L. *et al. Human Exp. Toxicol., 9*: 295, 1990: Lundgren, D. L. *et al. Health Physics 60*: 353, 1991). The methods used for the inhalation exposures of rats to $^{169}Yb$-labeled $^{239}PuO_2$ have been described (Lundgren *et al.,* 1991).

Because exposure to the combination of $^{239}PuO_2$ and NNK may alter the lung tumor incidences and/or death rates, it was necessary to include interim sacrifices to determine the rate at which animals develop lung tumors (1986-87 Annual Report, p. 318; McKnight, B. and J. Crowely *J. Am. Stat. Assoc. 79*: 639, 1984). Four rats per group exposed to $^{239}Pu$ were sacrificed at each of eight time intervals from 8 through 450 d after exposure to obtain more detailed information on the clearance of $^{239}Pu$ for dosimetry purposes. Some rats from each group are also being sacrificed late in life to

obtain data on the prevalence of lung tumors at different times after exposure. Additional data on $^{239}Pu$ retention are being obtained from these rats and from those that die spontaneously. At death, all rats are necropsied, and major organs and all lesions are fixed in 4% buffered paraformaldehyde for histologic examination.

Rats treated with 50 mg NNK $kg^{-1}$ body mass had a slower rate of body weight gain than the other groups of rats in this study. The injections of the lower doses of NNK and exposure to $^{239}PuO_2$ have not affected body weight gain.

As of September 30, 1994, 66 rats had died spontaneously, 288 had been euthanized when moribund, 119 had been sacrificed for dosimetry or to obtain data on the late-in-life prevalence of lung tumors, three had been removed from study for reasons unrelated to this study, and 119 remained alive (Table 1; Fig. 1). There were no significant (Mantel-Cox statistic; $p > 0.05$) differences in the survival of rats treated with either 0.3 or 1.0 mg NNK $kg^{-1}$ body weight. Survival of rats treated with 50 mg NNK $kg^{-1}$ was markedly reduced. Exposure to aerosols of $^{239}PuO_2$ did not significantly alter the survival of rats treated with NNK relative to those treated with NNK and not exposed to $^{239}Pu$. Also, the survival of the rats exposed to $^{239}PuO_2$ with or without treatment with NNK was not significantly different.

Table 1

Survival of Male F344 Rats in the Study of Combined Exposure to Inhaled $^{239}PuO_2$ and A Repeated Subcutaneous Injection of a Chemical Carcinogen (NNK)[a] (as of September 30, 1994)

| Experimental Group Numbers | Exposure | | Number Exposed | Number Alive | Median Survival Time (days) | Survival as a Percentage of Group I |
|---|---|---|---|---|---|---|
| | $^{239}Pu$ ILB[b] | NNK[c] | | | | |
| I | Sham | Sham | 100 | 52 | 702 | – |
| II | 480 ± 70 Bq[d] | Sham | 140 | 51 | 650 | 93 |
| III | Sham | 0.3 mg $kg^{-1}$ | 110 | 39 | 651 | 93 |
| IV | 470 ± 68 Bq[d] | 0.3 mg $kg^{-1}$ | 150 | 59 | 658 | 94 |
| V | Sham | 1.0 mg $kg^{-1}$ | 80 | 28 | 602 | 85 |
| VI | 460 ± 76 Bq[d] | 1.0 mg $kg^{-1}$ | 120 | 35 | 614 | 88 |
| VII | None | 50 mg $kg^{-1}$ | 40 | 0 | 281 | 40 |
| Total | | | 740 | 264 | | |

[a]NNK = 4-(N-methyl-N-nitrosamino)-1-(3-pyridyl)-1-butanone.
[b]ILB = Mean initial lung burden ± SD.
[c]Dose of NNK in saline given by subcutaneous injection three times/wk for 20 wk.
[d]Four rats from each group exposed to $^{239}Pu$ were serially sacrificed at eight time points between 8 and 450 d after exposure for dosimetry.

At its conclusion, this study will provide information on whether exposure to a chemical carcinogen (NNK) in combination with alpha radiation from inhaled $^{239}PuO_2$ acts in an additive, synergistic, or antagonistic manner in inducing lung cancer in rats.

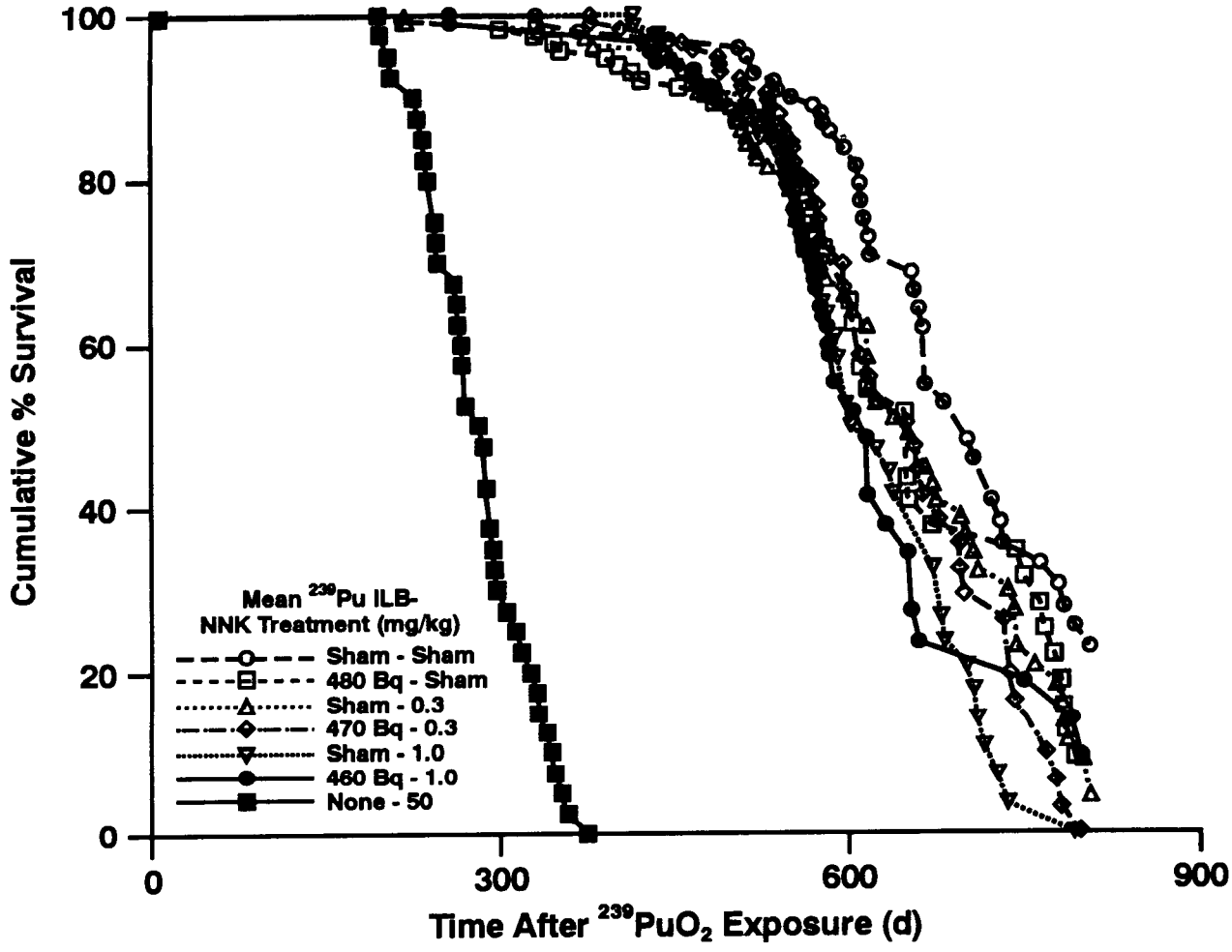


Figure 1. Cumulative percent survival of male F344 rats after exposure by inhalation to aerosols of $^{239}PuO_2$ with and without repeated subcutaneous injections of NNK.

(Research sponsored by the Assistant Secretary for Defense Programs, U.S. Department of Energy, under Contract No. DE-AC04-76EV01013.)

# COMBINED EXPOSURE OF F344 RATS TO BERYLLIUM METAL AND $^{239}PuO_2$ AEROSOLS

*Gregory L. Finch, Fletcher F. Hahn, William W. Carlton*, Alan H. Rebar*, Mark D. Hoover, William C. Griffith, James A. Mewhinney**, and Richard G. Cuddihy*

Nuclear weapons industry workers have the potential for inhalation exposures to plutonium (Pu) and other agents, such as beryllium (Be) metal. Inhaled Pu deposited in the lung delivers high linear energy transfer alpha particle radiation and is known to induce pulmonary cancer in laboratory animals (Biological Effects of Ionizing Radiation-IV, National Academy of Sciences, 1988). Although the epidemiological evidence implicating Be in the induction of human lung cancer is weak and controversial, various studies in laboratory animals have demonstrated the pulmonary carcinogenicity of Be; Be is currently classified as a suspect human carcinogen (Health Assessment Document for Beryllium, U.S. EPA/600/8-84/026F, 1987) in the United States and as a demonstrated human carcinogen by the Internation Agency for Research on Cancer (IARC, Vol. 58, 1993). The purpose of this study is to investigate the potential interactions between Pu and Be in the production of lung tumors in rats exposed by inhalation to particles of plutonium dioxide ($^{239}PuO_2$), Be metal, or these agents in combination.

This study is being conducted in two phases; the experimental design is shown in Table 1. In Phase I, 2856 rats (F344/N; both male and female; 12 ± 1 wk old at exposure) reared at this Institute were exposed once pernasally in eight blocks of 354 or 360 animals. Blocks were entered into the study over a 15-mo period (October 1987 to January 1989). Groups of 60 rats received $^{239}PuO_2$ (activity median aerodynamic diameter = 0.7 $\mu$m, geometric standard deviation [$\sigma_g$] = 1.7, exposure duration = 5 to 25 min, $^{239}$Pu air concentration = 630 Bq/L), followed immediately by exposure to Be metal (mass median aerodynamic diameter = 1.4 $\mu$m, $\sigma_g$ = 1.9, exposure duration = 8 to 50 min, Be air concentration = 200 to 1200 mg/m$^3$), or the appropriate air control. Rats received one of two target initial lung burdens (ILBs) of $^{239}PuO_2$ (56 or 170 Bq), and/or one of three target ILBs of Be metal (50, 150, or 450 $\mu$g).

Rats were designated for either serial sacrifice or for life-span observation. At death, a complete necropsy was performed, and lungs, other selected tissues, and all lesions were fixed in formalin for histological analysis. Lungs of all exposed rats were analyzed for Be and/or $^{239}$Pu as appropriate. All Phase I rats were dead as of March 1991.

Results indicated that Be exposure significantly retarded the clearance of $^{239}$Pu (1989-90 Annual Report, p. 125). Significant mortality from acute pneumonitis was observed in 33 and 64% of the male and female rats in the 450 $\mu$g group of Be metal within 3 wk of exposure. Regarding longer term survival, it was found that for a given $^{239}PuO_2$ exposure group, increased levels of Be metal increased the mortality rate (1990-91 Annual Report, p. 99).

Histological evaluation of the lungs of the rats is in progress. As of September 30, 1994, lung tissues from all control rats and those exposed to Be metal only have been examined. The crude incidence of lung tumors (combined benign and malignant) conditional upon the sacrifice schedule is shown in Table 2. The most prevalent malignant neoplasm observed thus far is the bronchiolar/alveolar adenocarcinoma having alveolar, papillary, or tubular patterns. Other tumor types observed include adenosquamous carcinomas and squamous cell carcinomas. These results demonstrate a

*Purdue University, Lafayette, Indiana

**Currently at the Waste Isolation Pilot Plant Program Office, Carlsbad, New Mexico

substantial incidence of Be metal-induced lung tumors in all exposure groups; in addition, a number of the Be-metal-exposed rats have multiple tumors (data not shown). Approximately 25% of the lungs of rats in the combined exposure groups have been histologically examined; crude incidences of malignant lung tumors conditional upon the sacrifice schedule in this group were given in the 1991-92 Annual Report (p. 112).

Table 1

Experimental Design to Study the Combined Effects of $^{239}PuO_2$ and Be Metal in Rats

| Be metal ILB | Numbers of Rats by Experimental Group | | | | | |
|---|---|---|---|---|---|---|
| | $^{239}PuO_2$ ILB[a] | | | | | |
| | 0 Bq | 60 Bq | 170 Bq | 230 Bq | 460 Bq | Total |
| 0 μg | 478[b]: (208[I]; 270[II]) | 240[I] | 240[I] | 288[II] | 156[II] | 1402 |
| 0.3 μg | 288[II] | - | - | - | - | 288 |
| 1.0 μg | 288[II] | - | - | 288[II] | - | 576 |
| 3.0 μg | 288[II] | - | - | - | - | 288 |
| 10 μg | 288[II] | - | - | 288[II] | - | 576 |
| 50 μg | 406: (240[I]; 156[II]) | 240[I] | 240[I] | - | - | 886 |
| 150 μg | 240[I] | 240[I] | 240[I] | - | - | 720 |
| 450 μg | 240[I] | 240[I] | 240[I] | - | - | 720 |
| Total | 2516 | 960 | 960 | 864 | 156 | 5456 |

[a]ILB = Initial lung burden.

[b]Number of rats per group. Equal numbers of males and females. Superscripts (I) and (II) refer to phase of the study; Phase I exposures conducted October 1987 to January 1989; Phase II exposures conducted April 1993 to November 1994 (planned).

Our results to date reveal significantly higher incidences of Be metal-induced lung tumors than expected based on extrapolations from a limited data base in the literature (Sanders, C. L. *et al. Health Phys. 35*: 193, 1978; Groth, D. H. *Environ. Res.* 21: 84, 1980; Nolibe, D. *et al. Commissariat A L'Energie Atomique 1984 Annual Report*, CEA, France, 1984). Because interactions between two carcinogens are best analyzed when lung tumor incidences from the individual agents are relatively low, Phase II of this study was initiated using lower ILBs of Be.

CDF®(F344)/CrlBR rats purchased from Charles River Laboratories (Raleigh, NC) are being used in Phase II. Significant design features (see Table 1) include (1) the use of relatively large numbers of rats exposed to Be metal only to define dose-response relationships for Be metal-induced carcinogenicity, (2) the combined exposure of two Be metal dose groups with $^{239}PuO_2$, (3) the addition of a group of rats exposed only to $^{239}PuO_2$ at a relatively higher initial dose rate (to mimic the increased cumulative radiation dose caused by reductions in the lung clearance of $^{239}Pu$ likely to occur as a result of exposures to Be in the combined exposure groups), and (4) use of four exposure blocks.

As of September 30, 1994, 75% of the rats (n=2088) comprising Phase II of the study have been exposed. Of these rats, 80% remain alive, 18% have been sacrificed for Be and/or $^{239}Pu$ dosimetry and histologic lung changes, and 2% have died or been euthanized as moribund. Exposure of rats in the fourth exposure block is planned for November 1994. Properties of the exposure atmospheres are similar to those in Phase I, except that the Be metal exposure occurs 1 d after the $^{239}PuO_2$ exposure, and the exposure mass concentrations of Be range from 0.8 to 140 $mg/m^3$. As before, the $^{239}PuO_2$ particles are labeled with $^{169}Yb$ (< 3% by mass) to permit periodic external radioactivity counting through 42 d after exposure for determination of $^{239}PuO_2$ ILB. Early results indicate that exposure to Be metal decreased $^{239}PuO_2$ clearance compared to controls over this 42-d period. Clearance half-times for males and females combined were 39 ± 7 (S.D.), 76 ± 10, or 137 ± 17 d for groups of rats receiving 0, 1, or 10 $\mu g$ target ILBs, respectively.

As noted above, this study is in progress. As the data are obtained and analyzed, this work will serve to define the pulmonary carcinogenicity of Be metal in the rat and will provide information regarding the potential interaction between Be metal and $^{239}PuO_2$ in causing lung cancer.

Table 2

Number of Rats Exposed to Be Metal or Controls
in the Phase I Study Having Lung Tumors[a]

| Exposure Group: | Mean Be lung burden ($\mu$g Be/g lung)[b] | | | | | | | | | |
|---|---|---|---|---|---|---|---|---|---|---|
| | Control | | 17 $\mu$g/g | | 45 $\mu$g/g | | 120 $\mu$g/g | | 450 $\mu$g/g | |
| Gender: | M | F | M | F | M | F | M | F | M | F |
| Number of rats examined: | 107 | 104 | 85 | 63 | 55 | 90 | 77 | 60 | 71 | 54 |
| Number (incidence[c]) with benign and/or malignant lung tumors: | 2 (2%) | 0 (0%) | 49 (58%) | 47 (75%) | 37 (67%) | 81 (90%) | 67 (87%) | 56 (93%) | 65 (92%) | 52 (96%) |
| Number (incidence[c]) with malignant lung tumors: | 2 (2%) | 0 (0%) | 29 (34%) | 43 (68%) | 22 (40%) | 67 (74%) | 40 (58%) | 47 (78%) | 53 (75%) | 43 (80%) |

[a]For rats living 1 y or more after exposure.

[b]Mean values of lung burdens were estimated from measurement of Be burden for each rat at time of death and extrapolation from days after exposure back to exposure date using a single component negative exponential function, the slope of which is determined from Be clearance functions applied to all rats exposed within the target lung burden groups of 50, 150, or 450 $\mu$g Be (Finch, G. L. *et al.* In *Proceedings, 4th International Conference on the Combined Effects of Environmental Factors*, (Fechter, L., ed.), Department of Environmental Health Sciences, Johns Hopkins University, Baltimore, MD; p. 49, 1991). Rats were then divided into four equally sized groups following normalization of each rat's ILB by its body weight at exposure.

[c]Incidence is conditional upon the sacrifice schedule.

(Research sponsored by the Assistant Secretary for Defense Programs, U.S. Department of Energy, under Contract No. DE-AC04-76EV01013.)

# COMPARATIVE PULMONARY CARCINOGENICITY OF INHALED BERYLLIUM IN A/J AND C3H/HeJ MICE

*Kristen J. Nikula, Steven A. Belinsky, Mark D. Hoover, and Gregory L. Finch*

The purpose of these investigations was to compare the pulmonary carcinogenicity of beryllium (Be) metal in A/J and C3H/HeJ mice, strains which are sensitive and resistant, respectively, to pulmonary neoplasia (Malkinson, A. M. *Toxicology 54*: 241, 1989). Lesions in these mice will be used to study the molecular mechanisms of Be-induced carcinogenesis (this report, p. 128). Be, a metal that is generally negative in short-term genotoxicity assays (e.g., Ames test), is a potent pulmonary carcinogen in F344/N rats (1991-1992 Annual Report, p. 112). Although the epidemiological evidence is weak, Be is classified as a suspect human carcinogen (U.S. EPA/600/8-84/026F, 1987).

Be metal (Type I-400, Brush Wellman, Elmore, OH) was continuously fed into a dry powder mill (Jet-O-Mizer, Fluid Energy Processing and Equipment Co., Hatfield, PA), passed through stage 3 of an aerosol cyclone (Southern Research Institute, Birmingham, AL), then delivered to a Lovelace 96-port, rodent nose-only chamber (1984-1985 Annual Report, p. 41). The nominal mass median aerodynamic diameter of the Be metal aerosol produced using this system was 1.4 $\mu$m with a geometric standard deviation of 1.9, as determined using a Mercer cascade impactor (Mercer, T. T. *et al. J. Aerosol Sci. 1*: 9, 1970). Female mice (206 each strain, 6-8 wk old) from Jackson Laboratories (Bar Harbor, ME) were exposed once, nose-only, to Be metal (1 g/m$^3$ for approximately 60 min) to achieve target mean initial lung burdens (ILBs) of approximately 60 $\mu$g Be. Control mice (50 each strain) were sham-exposed to filtered air alone in a separate exposure chamber. The mice were held for up to 23 mo after exposure.

Samples of lung tissue (right intermediate lobe) from mice sacrificed from 7 to 320 days post-exposure (dpe) were analyzed for Be content by flame atomic absorption spectroscopy (Model 306, Perkin-Elmer, Norwalk, CT) following drying, ashing, and dissolution in $HNO_3$. For each mouse analyzed, the quantity of Be measured in the sample was adjusted to total lung Be content using the ratio of total lung weight to sample weight. To determine mean ILBs for both strains for each exposure run, data were plotted as Be content versus dpe, single component negative exponential functions were fitted to the $\log_{10}$-transformed Be content data (BMDP AR, BMDP Statistical Software, Inc., Los Angeles, CA), then these functions were evaluated at zero time. ILBs were normalized by each animal's body weight at exposure, and strain-related differences were examined using student's *t*-tests incorporating a Bonferroni correction for multiple comparisons (BMDP 7D).

To estimate pulmonary clearance of Be, the Be content in each animal's lung at the time of sacrifice was normalized by the appropriate mean ILB. Data from both strains were pooled within strain, plotted as percent ILB versus dpe, then single component negative exponential functions were fitted to the $\log_{10}$-transformed percent ILB data as before. Functions were forced to 100% to account for the entire lung burden. Clearance half-times were estimated by dividing ln(2) by the slope of the exponential. A generalized F-test (Guilmette, R. A. *et al., Radiat. Res. 110*: 199, 1987) was used to determine if the effect of strain on clearance half-time was statistically significant.

Median survival times were estimated using a Kaplan-Meier test (BMDP P1L); sacrificed mice were censored from the analysis. The statistical significance of differences observed was conducted within this procedure using a log-rank method (Breslow test) with the level of significance corrected for multiple comparisons.

Lungs of all mice, except those sacrificed at 7 dpe, were fixed in 4% buffered paraformaldehyde. A standardized scheme, which included sections from every lobe except the right intermediate lobe of mice that died before 320 d, was used to sample the lungs. This sampling was not modified to include observed lung nodules or masses. Therefore, the observation of a lung lesion was based on a uniform sampling of all mice in the study. Histologic slides were prepared from the samples, and neoplastic lesions were classified as adenomas or adenocarcinomas. Mice sacrificed before 11 mo on study were excluded from the preliminary evaluation of incidence, multiplicity, and latency because these sacrifices were done to determine ILBs and to study preneoplastic lesions.

Despite simultaneous exposures, ILBs were 64.0 ± 1.0 (mean ± S.E.M.) $\mu$g Be for C3H/HeJ mice (n = 81) and 47.0 ± 0.8 $\mu$g Be for A/J mice (n = 70). ILBs per gram body weight were 3.37 ± 0.06 $\mu$g Be/g and 2.95 ± 0.12 $\mu$g Be/g for C3H/HeJ and A/J mice, respectively. The difference between strains in body weight normalized ILB was statistically significant ($p < 0.01$). Be clearance half-times, 108 and 97 d for C3H/HeJ and A/J mice, respectively, were also significantly different.

Table 1 lists 50% and 75% quantile survival estimates in days after exposure to Be metal. In addition to the standard median estimate, the 75% quantile is provided because the final sacrifice was conducted before the control A/J mice reached the 50% survival time. Be exposure reduced survival for both strains. This reduction, which was probably due to the marked, granulomatous pneumonia induced by Be, was statistically significant for C3H/HeJ mice ($p = 0.042$), but not for A/J mice ($p = 0.077$). Both exposed and control A/J mice appeared to have slightly greater survival times than C3H/HeJ mice; however, neither of these differences were statistically significant ($p > 0.05$).

Table 1

Survival Analysis of Mice on Study

| Treatment | Quantile | Survival for A/J Strain dpe ± SE[a] | Survival for C3H/HeJ Strain dpe ± SE |
|---|---|---|---|
| Control | 75% | 606 ± 56 | 593 ± 38 |
| | 50% (median) | —[b] | 611 ± 8 |
| Beryllium Exposed | 75% | 499 ± 23 | 466 ± 22 |
| | 50% (median) | 597 ± 15 | 555 ± 14 |

[a]Survival in days post exposure (dpe) ± standard error (SE).
[b]Undetermined; remaining mice sacrificed before median survival was reached.

There was no difference in incidence, multiplicity, or latency of pulmonary neoplasia in Be-exposed C3H/HeJ mice compared to controls. The incidence and multiplicity of pulmonary neoplasia were slightly increased in Be-exposed A/J mice (Table 2). Further analyses are in progress to determine if these increases are statistically significant and if latency was decreased.

The results of this study in two strains of mice contrast sharply to those of a previous study in the F344N/rat (1991-1992 Annual Report, p. 112). In that study, a similar lung burden (50 $\mu$g Be) caused an 80% incidence of pulmonary neoplasms compared to a 1% incidence in control rats. Interestingly, the nonneoplastic lesions differed between mice and rats; although both species developed granulomatous pneumonia, only the mice had significant pulmonary lymphocytic infiltrates. Tissues

from the present study and from the previous study in rats are being used to examine the molecular mechanisms of spontaneous and Be-induced neoplasia in these species.

Table 2

Incidence and Multiplicity of Pulmonary Neoplasms in A/J Mice[a]

| | Control | Beryllium Exposed |
|---|---|---|
| Number of Mice Examined | 35 | 108 |
| Number of Adenomas | 9 | 39 |
| Number (Incidence[b]) of Mice with Adenomas | 9 (26%) | 33 (30%) |
| Number of Adenocarcinomas | 16 | 68 |
| Number (Incidence) of Mice with Adenocarcinomas | 13 (37%) | 50 (46%) |
| Incidence of Mice with Adenoma or Adenocarcinoma | 54% | 61% |
| Number (%) of Mice with More Than One Neoplasm | 2 (6%) | 21(19%) |

[a]Mice sacrificed before 11 mo on study were excluded from this tabulation.
[b]Incidence calculated as (number of mice with observation)/(number of mice examined) x (100%).

(Research sponsored by the Assistant Secretary for Defense Programs and the Office of Health and Environmental Research, U.S. Department of Energy, under Contract No. DE-AC04-76EV01013.)

# LATE BIOLOGICAL EFFECTS OF $^{137}$CsCl INJECTED IN BEAGLE DOGS

*Kristen J. Nikula, Bruce A. Muggenburg, William C. Griffith, Fletcher F. Hahn, and Bruce B. Boecker*

The toxicity of intravenously administered $^{137}$CsCl in the Beagle dog was investigated as part of the ITRI program to evaluate the biological effects of internally deposited fission product radionuclides. The toxicity and health effects of $^{137}$Cs are important to understand because $^{137}$Cs is produced in large amounts in light-water nuclear reactors. Also, large quantities of cesium radioisotopes have entered the human food chain as a result of atmospheric nuclear weapons tests and additional cesium radioisotopes were released during the Chernobyl accident. The intravenous route of exposure was chosen because it was known that after intravenous injection, inhalation, or ingestion, internally deposited $^{137}$CsCl is rapidly absorbed and distributed throughout the body, exposing the whole body to beta and gamma radiation, and because of the reduced radiation protection problems associated with high-level exposure via injection compared to these other routes.

Using equal numbers of both sexes, 54 Beagle dogs 12- to 14-mo old were injected intravenously with $^{137}$Cs to provide one group of six dogs with mean initial body burdens of 141 MBq $^{137}$Cs/kg body mass and four groups of 12 dogs each with mean initial body burdens of 104, 72, 52, and 36 MBq $^{137}$Cs/kg. After injection, the dogs were counted for $^{137}$Cs activity to determine the initial body burden and long-term retention of the $^{137}$Cs. Twelve dogs were injected with isotonic saline (study controls). Because the number of primary control dogs was small, data were also used from an additional 49 controls dogs in other studies at ITRI that were performed over a similar span of years.

The husbandry and veterinary care of the dogs have been described (1989-1990 Annual Report, p. 112). A detailed necropsy was performed on each dog at the time of death or when the dog was euthanized. When all the dogs were dead, one clinical veterinarian reviewed clinical records, and one pathologist reviewed the pathology reports and histopathology from all dogs.

Dogs died from 19 to 5342 d after injection of $^{137}$Cs. Eleven $^{137}$Cs-injected dogs, including all six in the highest initial body burden group, died within 81 d after injection due to hemorrhagic or septicemic complications of severe pancytopenia. An additional 25 dogs had moderate to severe, transient hematologic dyscrasia but survived for long times. The hematologic dyscrasia occurred 7 to 48 d after the cesium injection and lasted approximately 2 mo (14 to 160 d). All dogs that recovered from hematologic dyscrasia survived for long times and died from diseases unrelated to the blood-forming organs, except one dog that died from hemolytic anemia 9 y later. There were no myeloproliferative diseases in $^{137}$Cs-injected dogs.

For statistical analyses, the dogs that survived more than 2 y were divided into three groups: the 21 dogs that received the highest total doses (11.6-23.7 Gy); the 22 dogs that received the lowest total doses (5.9-11.4 Gy); and the 60 pooled controls. The median survival was 4020 d after injection for the high-dose group and 4250 d after injection for the low-dose group. The median survival time of the pooled controls was 4750 d after sham exposure. Overall, there was a significant, dose-dependent decrease in survival of the $^{137}$Cs-injected dogs.

The significant late effects of $^{137}$Cs injection were (1) permanent sterility of male dogs due to testicular atrophy and (2) neoplasia in many different sites. All $^{137}$Cs-injected male dogs had marked damage to the germinal epithelium of the testicular seminiferous tubules with azoospermia in the long-term survivors. Despite this toxic effect, the prevalence of testicular neoplasia was not increased in $^{137}$Cs-injected dogs. Benign and malignant neoplasms occurred in a variety of organs in $^{137}$Cs-injected

dogs, rather than in a single target organ. There was a dose response for the incidence of malignant neoplasms ($p < 0.001$) in $^{137}$Cs-injected male dogs, but not in female dogs. However, when malignant mammary neoplasms were excluded from the analysis, there was no gender difference, and there was a $^{137}$Cs treatment effect ($p < 0.001$) in males and females for the incidence of malignant neoplasms. Figure 1 shows the cause-specific cumulative incidence of malignant neoplasms, excluding mammary neoplasms, in the pooled control dogs and the low- and high-dose $^{137}$Cs-injected dogs. This cause-specific cumulative incidence, which was corrected for competing risks, was estimated by subtracting the Kaplan-Meier estimate for malignant neoplasms excluding mammary neoplasms from a value of 1.

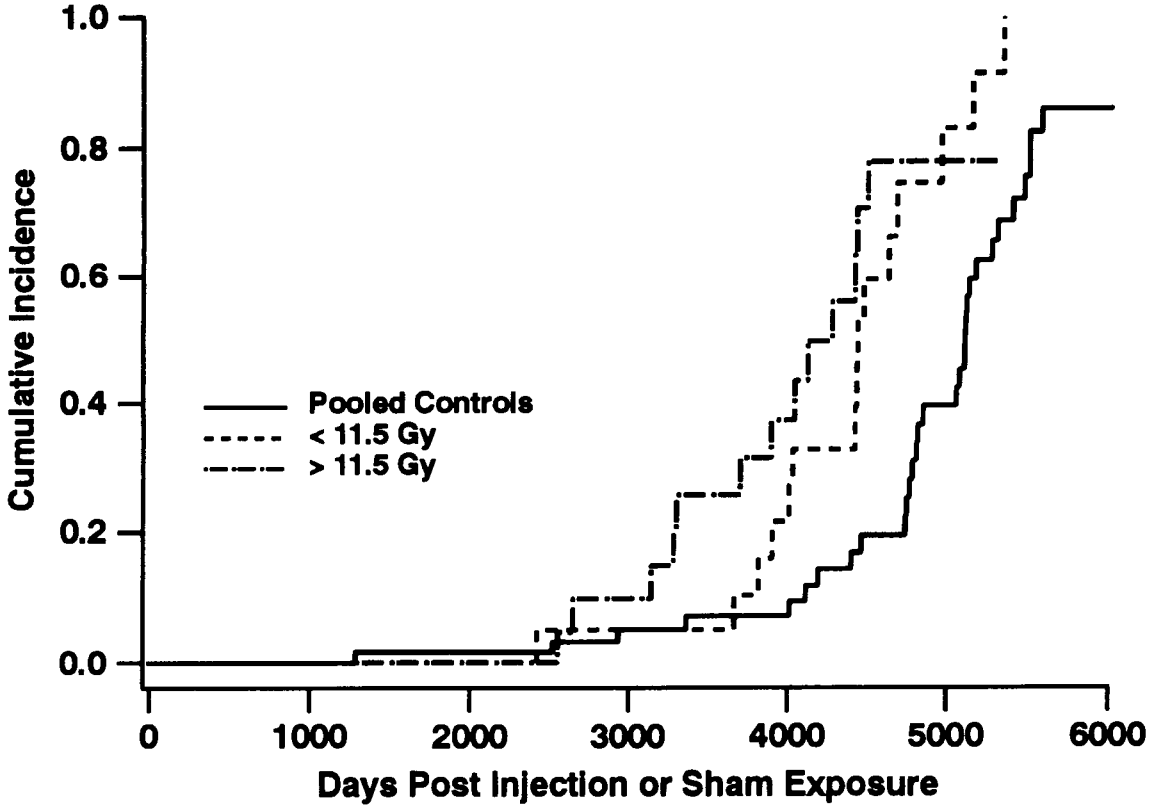


Figure 1. Cause-specific cumulative incidence of malignant neoplasms, excluding mammary neoplasms, in the pooled control dogs and the low-dose and high-dose $^{137}$Cs-injected dogs.

Figure 2 presents some of the more interesting results for the low-dose and high-dose groups compared to the pooled controls in terms of the relative risk (proportional hazards model) or the odds ratio (logistic regression model). When individual organs were considered, the incidence of malignant neoplasms was increased in the liver, and in the nasal cavity and paranasal sinuses. Leiomyomas, benign neoplasms of smooth muscle, were analyzed by occurrence of the general category of neoplasm, rather than specific organ involved. The prevalence of leiomyomas was significantly increased in the $^{137}$Cs-injected dogs. Interestingly, the dose to smooth muscle is thought to be twice the average whole-body dose because the dose to skeletal muscle is twice the whole body dose. The prevalences of hemangiomas in the lymph nodes and spleen, benign urinary tract neoplasms, and benign thyroid neoplasms were also significantly increased in $^{137}$Cs-injected dogs.

The grouping of all malignant neoplasms except mammary neoplasms makes for an interesting comparison between our study in dogs and estimates for the same grouping of people in BEIR V

(*BEIR V, Health Effects of Exposure to Low Levels of Ionizing Radiation*, Committee on the Biological Effects of Ionizing Radiations, National Research Council. National Academy Press, Washington, DC, 1990). For total-body, acute, external, gamma exposures at 25 y of age, BEIR V predicts 1026 excess malignant neoplasms excluding mammary neoplasms in females and 921 excess malignant neoplasms in males per $10^5$ individuals receiving 0.1 Sv. Using the results based upon the proportional hazards model for $^{137}$Cs-injected dogs, 462 and 329 excess malignant neoplasms excluding mammary neoplasms were estimated for the low- and high-dose groups, respectively, for $10^5$ dogs receiving 0.1 Sv. BEIR V estimates that the risk is reduced by a factor of two to four for protracted delivery of dose. If this factor is applied to the risk estimates for people, then the results for the two species show a great similarity in response when large groupings of malignant neoplasms are compared.

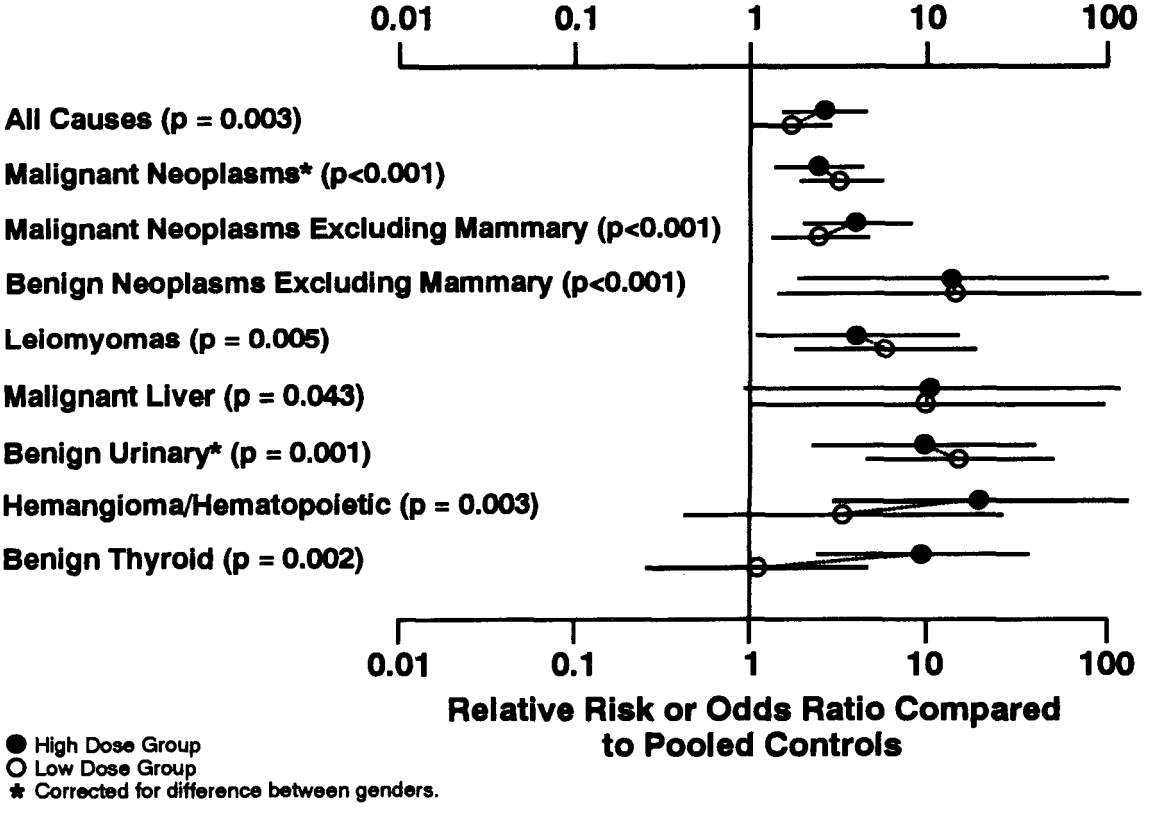


Figure 2. Estimated relative risk in a proportional hazards model for neoplasms observable in living dogs or of odds ratio in a logistic regression model for neoplasms observed at death, with 95% confidence intervals. A value of 1 represents no change from controls.

The similarity between the response in dogs exposed to internally deposited $^{137}$Cs and the response predicted for people exposed to external gamma radiation lends strength to the extrapolation of results from dogs to people for internally deposited $^{137}$Cs. Furthermore, one is tempted to speculate concerning the increases in benign neoplasms that occurred in the dog and whether similar increases might occur in people exposed to internally deposited $^{137}$Cs or whole-body, external gamma radiation. Benign neoplasms like those observed in the dogs would be difficult to detect in human epidemiological studies because they are seldom associated with the cause of death. However, benign neoplasms may still be a health concern and might represent a morbidity caused by radiation. Thus, the results from this study suggest another type of risk of radiation exposure that should be considered when the health consequences of exposure of large populations to low levels of radiation are evaluated.

Lastly, the similarity in the neoplastic response when large groupings of malignant neoplasms are compared between the results in dogs and the predicted response in people leads one to wonder if the two major nonneoplastic results of $^{137}Cs$ injection in dogs, shortened life span and testicular degeneration and atrophy, might also be expected late effects in people exposed to internally deposited $^{137}Cs$.

(Research supported by the Office of Health and Environmental Research, U.S. Department of Energy, under Contract No. DE-AC04-76EV01013.)

# THE ROLE OF LABORATORY ANIMALS IN STUDYING BONE CANCER RESULTING FROM SKELETALLY DEPOSITED RADIONUCLIDES

*Bruce B. Boecker, William C. Griffith, Raymond A. Guilmette, Fletcher F. Hahn, Bruce A. Muggenburg, Scott C. Miller*, Ray D. Lloyd*, and Glenn N. Taylor**

There is a continuing need to determine and understand the long-term health risks of internally deposited radionuclides in persons exposed medically or occupationally, or from radionuclides in the environment. A full understanding of these health risks, particularly for exposures involving low doses and dose rates, requires in-depth knowledge of both the dosimetry of a given exposure and the resulting long-term biological effects. Human data on $^{224}$Ra and $^{226,228}$Ra and their decay products are our primary sources of knowledge on the health risks of chronic alpha irradiation of the skeleton and serve as essential segments of our radiation protection practices for internally deposited radionuclides. However, we cannot obtain all of the needed information from these studies. This paper examines the role of laboratory animal studies in complementing and extending the knowledge of radiation-induced bone cancer obtained from studies of humans exposed to $^{224}$Ra or $^{226,228}$Ra.

Many of the life-span studies that have been at the heart of the laboratory animal studies program are completed or are coming to completion soon. These include practically all of the life-span studies in Beagle dogs sponsored by the United States Department of Energy. Because of the relatively long life span of these dogs (median ~ 14 y), the studies being completed now were initiated primarily in the 1970s or earlier. Current efforts are directed to completing the experimental observations, reviewing all the materials and results from these studies, publishing and archiving the basic results, and modeling the dose-response relationships. As this process continues, gaps in the resulting knowledge base may be identified that can be filled by conducting short-term, carefully focused, ancillary studies as time and resources permit. It is vital that efforts continue to determine the best ways to extrapolate experimental results from these studies to the health risks associated with different human exposures to internally deposited radionuclides.

Bone cancer has been the primary long-term biological effect seen in studies of human populations that ingested $^{226,228}$Ra occupationally or were injected with $^{224}$Ra as a treatment for ankylosing spondylitis or skeletal tuberculosis. A number of life-span studies are being conducted in laboratory animals to strengthen the extension of this dose-response information to other possible human exposure situations involving other radionuclides, radionuclide forms, and routes of exposure. Figure 1 illustrates schematically how life-span studies in Beagle dogs relate, or are linked, to the human studies and to each other for bone cancer.

At the center of the linkages shown are the studies conducted with $^{226}$Ra at the University of Utah and the University of California at Davis. These studies, which parallel the human exposure to $^{226,228}$Ra, make it possible to compare directly, in the dog, the life-span biological effects from other types of exposure. The earliest comparison of this type, which was between $^{226}$Ra and $^{239}$Pu, was the basis for establishing the Utah program of life-span studies. By knowing the health effects of $^{226,228}$Ra in humans and the ratio of $^{239}$Pu-induced health effects to $^{226}$Ra-induced health effects in the dog, one can estimate the magnitude of $^{239}$Pu-induced health effects in people. Such a toxicity-ratio approach is quite valuable in the absence of human dose-response data for internal depositions of $^{239}$Pu. The second side-by-side linkages from the human $^{226,228}$Ra studies are the studies of injected $^{226}$Ra and chronically ingested $^{90}$Sr at Davis. This linkage allows comparisons involving different routes of administration (intravenous vs. ingestion) and linear energy transfer (alpha vs. beta).

*Radiobiology Division, University of Utah School of Medicine, Salt Lake City, Utah

The other primary linkage between the human and dog studies of radionuclide-induced bone cancer involves $^{224}Ra$. The study in dogs shown in Figure 1 was initiated at Utah and is being completed at ITRI (this report, p. 95). Because of the short radioactive half life of $^{224}Ra$ (3.62 d), much of the alpha radiation is emitted while the $^{224}Ra$ is on bone surfaces in contrast to $^{226}Ra$, which is primarily a bone-volume seeker. Thus, the results of these studies of two different isotopes of Ra provide a comparison of effects from a surface-seeking and a volume-seeking radionuclide.

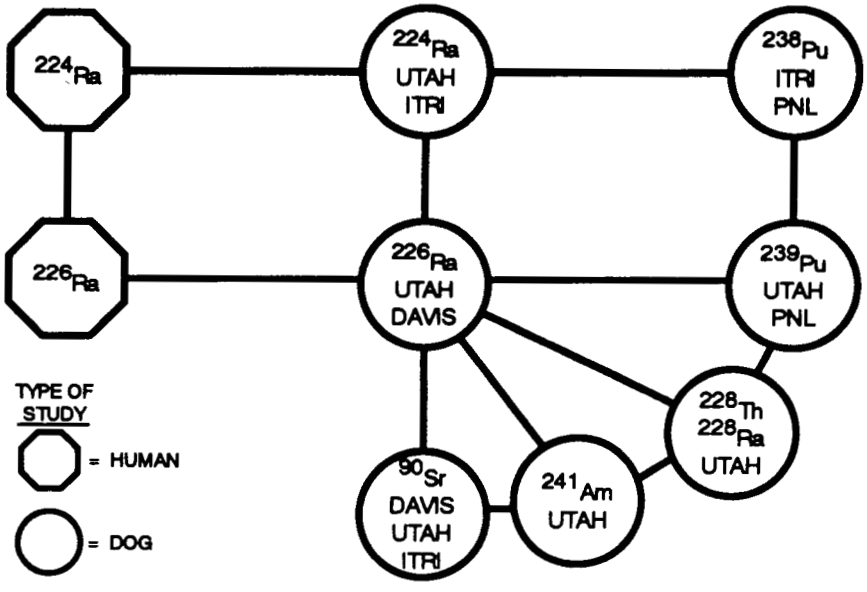


Figure 1. Schematic representation of some important linkages between studies of radionuclide-induced bone cancer in human populations and life-span studies in Beagle dogs. Linkages such as these provide ways to extend the available human data to other potential exposure situations for which few or no human data exist. Utah = University of Utah, Davis = University of California at Davis, ITRI = Inhalation Toxicology Research Institute, and PNL = Pacific Northwest Laboratories.

The studies of inhaled $^{238}PuO_2$ at ITRI and the Pacific Northwest Laboratories (PNL) have involved many bone cancers from skeletal deposition of the $^{238}Pu$ after fragmentation and dissolution of the oxide form in the lung. The linkages shown provide the opportunity to compare $^{238}Pu$-induced bone tumors from two laboratories with results from the $^{224}Ra$ and $^{226}Ra$ studies and the bone tumors induced by $^{239}Pu$ given intravenously at Utah or by inhalation of a soluble form, $^{239}Pu(NO_3)_4$ at PNL.

Other linkages to $^{226}Ra$ and $^{239}Pu$ in the Utah program include studies of $^{228}Th$, $^{228}Ra$, $^{241}Am$, and $^{90}Sr$. Studies of the beta emitter $^{90}Sr$, conducted in three laboratories by three routes of administration (ingestion, inhalation, and intravenous injection), provide opportunities for interstudy comparisons as well as comparisons with other studies involving alpha-emitting radionuclides. Other linkages can also be studied beyond those given as examples here.

As these various studies come to completion, excellent opportunities arise for comparing and contrasting the experimental results. A number of approaches have been and will be used to make these comparisons. Many of the earliest comparisons, which used a toxicity-ratio approach, were made by the late Dr. Charles Mays and associates at Utah for bone cancers produced by skeletally deposited $^{226}Ra$ or $^{239}Pu$ in Beagle dogs. Linear fits were made to grouped data on the incidence of bone cancer for different average doses to the skeleton. When the slopes of the two fitted lines were compared, the fitted line for $^{239}Pu$ was much steeper than that for $^{226}Ra$, reflecting an increased

carcinogenicity of $^{239}Pu$ relative to $^{226}Ra$ by a factor of 16 when the average radiation dose to the skeleton was used (Lloyd, R. D. *et al. Health Phys. 64*: 45, 1993).

Bone cancer ratio values (± 1 S.D.) for other radionuclides relative to $^{226}Ra$ in dogs computed by Lloyd, R. D. *et al.* (*Health Phys. 67*: 346, 1994) are $^{224}Ra$ (50 injections), 16 ± 5; $^{228}Th$, 8.5 ± 2.3; $^{241}Am$, 6 ± 0.8; $^{228}Ra$, 2.0 ± 0.5; and $^{90}Sr$ (> 40 Gy), 1.0 ± 0.5; (5–40 Gy), 0.05 ± 0.03; (< 5 Gy), 0.01 ± 0.01. The value for $^{224}Ra$ given by repeated injections is the same as that for $^{239}Pu$, a result consistent with the mixed bone-surface/bone-volume deposition characteristics of this short-lived radionuclide. Decreasing ratio values are seen for the other radionuclides listed. For $^{90}Sr$, the dose-response curve was nonlinear. Under these conditions, values could be computed at different doses, and three are given to illustrate the decrease in ratio value with decreasing dose. This toxicity ratio method is easy to compute and understand and provides one way of comparing the carcinogenicity of different radionuclides in the same species.

Raabe, O. G. (*Health Phys. Suppl. 1*: 419, 1989) has devised another method for studying the dose-response relationships across species for bone cancers. In general, the method uses log-normal distributions of times to bone cancer expressed as fractions of life span plotted against the average dose rate to skeleton. The result is a power function. When he used this approach for humans, dogs, and mice that had internal depositions of $^{226}Ra$, the curves fell very close to one another, indicating a close interspecies relationship when the data were computed in this way.

A third approach being used to analyze data emerging from the life-span studies involves proportional hazards modeling. Figure 2 illustrates this approach using bone cancer data in Beagle dogs that inhaled relatively soluble forms of $^{90}Sr$ or $^{238}Pu$ at ITRI (Griffith, W. C. *et al. Joint Bone Radiobiology Workshop*, U.S. DOE Report UCD-472-136, 1991). The plots shown on the left side of Figure 2 illustrate the relationship between dose and time to bone cancer in these two studies. This method considers the time-dependent nature of the dose received from an internally deposited radionuclide. These results can then be computed as relative risks based on the hazard rate for bone tumors in control dogs, resulting in the curves shown on the right-hand side of the figure. From these two curves, which were based on average skeletal doses, the alpha emissions from $^{238}Pu$ were over 50 times more effective than the beta emissions from $^{90}Sr$-$^{90}Y$. If an endosteal surface dose were used to describe the alpha radiation from the surface-deposited $^{238}Pu$, the relative effectiveness would be about 5. Both of these results can be compared with the current ICRP radiation weighting factors, $w_R$, for $\alpha/\beta = 20/1 = 20$.

Two new efforts are now in progress to improve our abilities to extrapolate results from studies in laboratory animals to possible human exposure situations. The first of these is an interlaboratory effort being led by risk assessment experts from three DOE laboratories, PNL, ITRI, and Argonne National Laboratory. The specific purpose of this new effort is to conduct cross-laboratory health risk analyses using data from laboratory animals as means of expanding the value of studies conducted within the individual laboratories. The second effort is being conducted by a committee of the National Council on Radiation Protection and Measurements entitled "Extrapolation of Risks from Nonhuman Experimental Systems to Man." This committee is surveying possible extrapolation techniques from the molecular level to the whole animal. Particular emphasis is being placed on those extrapolations that can improve our knowledge of human health risks from ionizing radiation.

From the foregoing information, it is clear that studies in laboratory animals continue to be a vital part of our efforts to expand knowledge on the health risk of internally deposited radionuclides. The role of these studies has changed as the field has matured. Early emphasis was placed on dosimetry and quantitation of early-occurring biological effects. Later emphasis was directed at late-occurring biological effects. Observations of this type are being continued in studies in which animals are still alive. Because many of the studies have reached the time when all of the animals are dead, much

of the current effort is directed to reviews of materials and results, analysis and modeling of the results, and publications of core manuscripts in the open literature. Other efforts are being directed to studies of underlying mechanisms using materials from previous studies or samples obtained from new studies designed to address specific mechanistic questions. At the heart of all of these efforts is the need for appropriate extrapolations of these results to potential human exposures to internally deposited radionuclides.

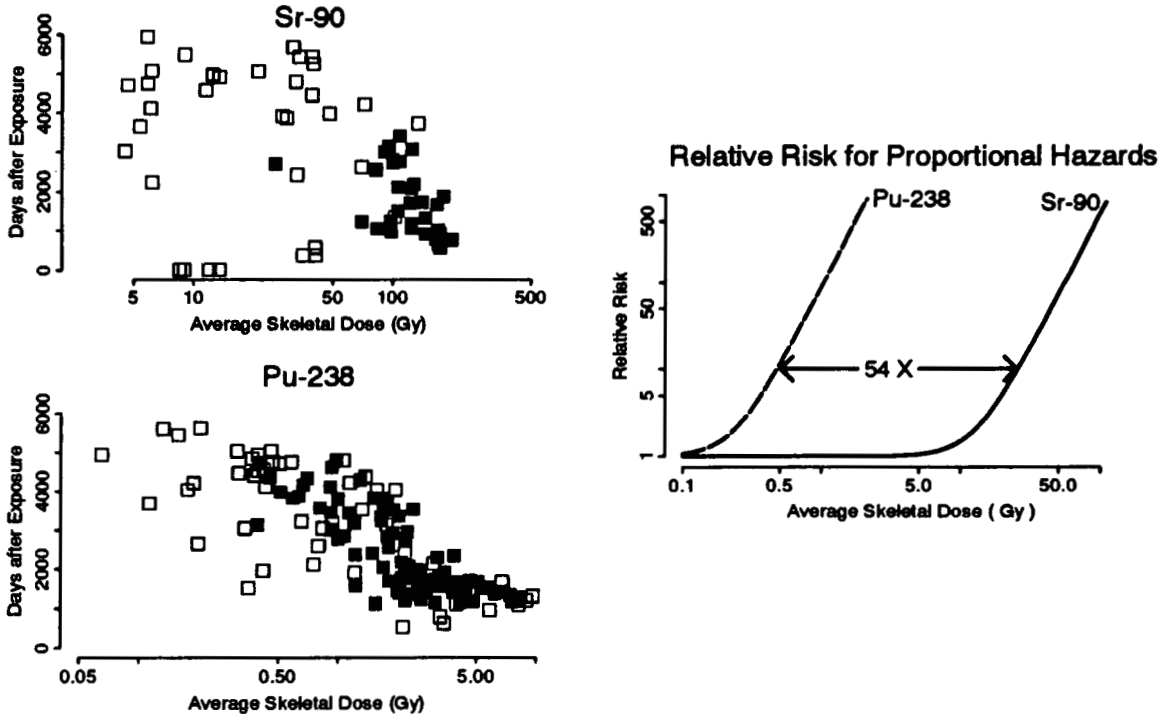


Figure 2. Illustration of the use of a proportional hazards approach for comparing the relative effectiveness of chronic alpha and beta radiations in producing bone cancer in Beagle dogs. When expressed on an average dose to bone basis, the alpha emissions from $^{238}Pu$ were over 50 times more effective in producing bone cancer than the beta emissions from $^{90}Sr$-$^{90}Y$.

(Research sponsored by the Office of Health and Environmental Research, U.S. Department of Energy, under Contract Nos. DE-AC02-76EV00119 and DE-AC04-76EV01013.)

# RADIATION-INDUCED LIVER LESIONS IN BEAGLE DOGS

*Fletcher F. Hahn, Bruce A. Muggenburg, and Bruce B. Boecker*

The risk for liver disease from internally deposited beta-emitting radionuclides is unknown because there are no human populations exposed to hepatotropic beta-emitting radionuclides available for study. In this report, we discuss the hepatic lesions in dogs exposed to a beta-emitting radionuclide, $^{144}CeCl_3$, and held for their life spans.

The experimental design, details of exposure, and dosimetry for this study have been reported (McClellan, R. O. *et al.* In *Life-Span Radiation Effects Studies in Animals: What Can They Tell Us?* [R. C. Thompson and J. A. Mahaffey, eds.], National Technical Information Service, Springfield, VA, p. 74, 1986; Boecker, B. B. and R. G. Cuddihy. *Radiat. Res. 60*: 133, 1974). Fifty-five Beagle dogs (27 females and 28 males) received single, nose-only exposures to aerosols of $^{144}CeCl_3$ (equilibrium mixture of $^{144}Ce$ with its progeny $^{144}Pr$) in a CsCl solution. Fifteen Beagle dogs exposed to stable CsCl aerosols served as controls. Aerosol concentration and exposure times were varied to achieve long-term retained burdens that ranged from 0.096–13.3 MBq/kg body weight. The initial body burden of $^{144}Ce$ and pattern of long-term radionuclide retention were determined for each dog by whole-body counting. Each dog was observed twice daily and examined thoroughly at least annually to determine health status. All dogs were maintained to their natural death or euthanasia. Complete necropsies were performed, including gross and microscopic examination of all major organs and all grossly observed lesions.

Lifetime risk factors were calculated by summing the adjusted annual risk factors. These factors were calculated by dividing the number of liver cancers occurring during each year by the total integrated dose to liver received by all dogs alive at the beginning of the year. The annual risk factors were adjusted by the probability of a control dog surviving to that age.

After the inhalation of $^{144}CeCl_3$, there was rapid mucociliary clearance of 40–50% of the material deposited in the respiratory tract. What remained was the long-term retained burden, much of which was redistributed via the blood and deposited in the liver and skeleton. Concentration of $^{144}Ce$ in the liver and skeleton peaked at 8 d after exposure with a subsequent clearance half-time of about 280 d, the physical half-life of $^{144}Ce$. For dogs that lived longer than 5 y, the average cumulative beta dose for the liver was calculated at 60 Gy per MBq $^{144}Ce$/kg body weight.

Hepatocellular degeneration or hepatic atrophy with fibrosis and hepatic failure was the primary cause of death or contributed to death in 18 of the 45 dogs surviving longer than 308 d after exposure (Table 1). Deaths from hepatic atrophy generally occurred early (309 to 874 d after exposure). Hepatocellular degeneration, primarily fatty change, resulted in increases above the normal range in serum alkaline phosphatase and serum alanine aminotransferase, indicative of functional hepatocellular lesions.

Primary liver tumors were the most common neoplasms in the dogs exposed to $^{144}CeCl_3$ (Table 2). Eighteen of 41 dogs (44%) surviving 2 or more years after inhalation exposure (long-term survivors) had liver neoplasms. Three dogs had two neoplasms. Eleven of the neoplasms (in 10 dogs) were benign, and 10 of these were biliary cystadenomas. Nine of the 41 long-term survivors (22%) had malignant primary liver neoplasms. These include seven hepatic hemangiosarcomas, one hepatocellular carcinoma, one cholangiocarcinoma, and one neurofibrosarcoma. Microscopically cavernous, capillary, and solid patterns of neoplastic endothelial cells were seen in the hemangiosarcomas. Immunohistochemical staining of the tissue for Factor VIII (a blood-clotting factor characteristically produced by normal endothelial cells) showed tumor cell staining in four of six

hemangiosarcomas. The four positive samples included examples of each phenotype, cavernous, capillary, and solid. This result provides evidence that these tumors arise from endothelial cells. The hepatocellular carcinoma was presented as multiple nodules throughout the liver and was poorly differentiated. It was composed of irregular masses of pleomorphic cells without a recognizable pattern of cell arrangement. Tumor tissue infiltrated the parenchyma at the periphery of the tumors, and central areas of tumor masses were often necrotic. The cholangiocarcinoma, which was also present as multiple nodules, was composed of epithelial cells arranged in a tubular pattern. The relationship between cumulative liver beta dose and the time of death from liver tumors is shown in Table 2.

Table 1

Nonneoplastic Liver Lesions in Beagle Dogs that Inhaled $^{144}CeCl_3$

| Liver Lesions | Number of Dogs | LTRB[a] (MBq/kg) | Range of Survival Times (DPE)[b] | Liver Dose to Death (Gy) |
|---|---|---|---|---|
| Exposed (45)[c] | | 0.096–7.8 | 309–5498 | 5.7–280 |
| Atrophy, primary cause of death | 4 | 0.23–5.5 | 309–3117 | 14–200 |
| Degeneration, primary cause of death | 1 | 0.11 | 3392 | 6.4 |
| Degeneration, contributed to death | 13 | 0.17–3.5 | 1759–5139 | 10–210 |
| Controls (15)[c] | | 0 | 2545–6016 | 0 |
| Degeneration, contributed to death | 4 | 0 | 5116–5974 | 0 |

[a]LTRB = Long-term retained burden.
[b]DPE = Days post inhalation exposure.
[c]Number of dogs surviving > 308 DPE.

The relatively high radiation doses to the liver over a prolonged period from the $^{144}Ce$ deposited in the liver resulted in hepatocellular degeneration, or hepatic atrophy in 18 dogs. Hyperplastic hepatocellular nodules and biliary cystadenomas were frequently associated with these degenerative lesions in animals that died more than 9 y after exposure. Although the biliary cystadenomas were frequently large and caused clinical signs, they did not appear to be precursor lesions for cholangiocarcinoma.

At ITRI, 88 control dogs on life-span studies have developed four primary liver tumors, three biliary adenomas, and one mast cell tumor. Although liver tumors observed in dogs exposed to $^{144}CeCl_3$ were not different in appearance from spontaneously occurring hepatic tumors in dogs, the very high incidence of these tumors and the preponderance of hemangiosarcomas suggested a causal relationship between $^{144}Ce$ exposure and the occurrence of liver tumors.

Our studies clearly demonstrate that inhalation of $^{144}CeCl_3$ resulted in an increased incidence of primary hepatic neoplasms, especially hemangiosarcomas, in Beagle dogs. The studies also suggest that the latent period of primary hepatic hemangiosarcomas was related to the beta dose to the liver and that an absolute latent period of approximately 1800 d preceded death from these tumors. These hemangiosarcomas developed in livers unburdened by the heavy particle loads seen in the Thorotrast injection cases (Kojiro, H. and Y. Ito. In *Risks from Radium and Thorotrast* [D. M. Taylor, C. W. Mays, G. B. Gerber, and R. G. Thomas, eds.], BIR Report 21, British Institute of Radiology, London, p. 119, 1989). Also, these livers were affected by hepatocellular degeneration, not inflammation with

accompanying vasoproliferation. Thus, the hepatic hemangiosarcomas in these dogs appear to be a direct result of the beta irradiation of the liver.

Table 2

Neoplastic Liver Lesions in Beagle Dogs that Inhaled $^{144}CeCl_3$

| Liver Neoplasms | Number of Dogs[a] | LTRB[b] (MBq/kg) | Survival Time (DPE)[c] | Liver Dose to Death (Gy) |
|---|---|---|---|---|
| Exposed (41)[d] | | 0.096–5.2 | 799–5498 | 5.7–270 |
| Malignant | | | | |
| Hemangiosarcoma[e] | 7 | 0.17–4.1 | 1735–4878 | 10–240 |
| Neurofibrosarcoma | 1 | 3.5 | 1759 | 210 |
| Cholangiocarcinoma | 1 | 0.26 | 5137 | 15 |
| Hepatocellular Carcinoma[f] | 1 | 0.30 | 5485 | 18 |
| Benign | | | | |
| Biliary Cystadenoma | 10 | 0.11–1.6 | 3494–5485 | 6.4–68 |
| Fibroma | 1 | 2.5 | 1735 | 150 |
| Control (15)[g] | | 0 | 2545–6016 | 0 |
| Benign | | | | |
| Biliary Adenoma | 2 | 0 | 5116–5974 | 0 |

[a]Number of dogs with neoplasms.
[b]LTRB = Long-term retained burden.
[c]DPE = Days post inhalation exposure.
[d]Number of dogs at risk (surviving > 2 y after inhalation exposure).
[e]Two dogs with hemangiosarcoma had second tumors as incidental findings, one a neurofibrosarcoma and another a fibroma.
[f]One dog with hepatocellular carcinoma had biliary cystadenoma as a major contributing disease.
[g]Number of control dogs (surviving > 2 y after inhalation exposure).

The lifetime risk factor for hepatic cancers in these dogs was 80 ± 15 cancers/$10^4$ dog Gy. This is one tenth of the risk factor for $^{238}$Pu-induced liver cancers in dogs (Muggenburg, B. A. *et al. Ann. Occup. Hyg.*, in press). The risk ratio of 1/10 can be applied to data from human populations exposed to Thorotrast to derive a risk for hepatic cancers for people with internally deposited beta-emitting radionuclides. Because the risk factor for Thorotrast is about 300 cancers/$10^4$ Gy (BEIR IV. *Health Risks of Radon and Other Internally Deposited Alpha Emitters*, 1988), this risk ratio comparison technique results in a lifetime population risk of hepatic cancer from beta emitters in people of 30 cancers/$10^4$ person Gy.

(Research sponsored by the Office of Health and Environmental Research, U.S. Department of Energy, under Contract No. DE-AC04-76EV01013.)

# THE BIOLOGICAL EFFECTS OF $^{224}$Ra INJECTED INTO DOGS

*Bruce A. Muggenburg, Fletcher F. Hahn, William C. Griffith, Bruce B. Boecker, and Ray D. Lloyd**

The purpose of this study was to investigate the toxicity of injected $^{224}$Ra in the dog. Radium-224 is a short-lived isotope of radium with a half-life of 3.62 d. When administered parenterally, it deposits on bone surfaces; because of its short half-life, most of its energy is deposited on bone surfaces, in a manner similar to plutonium (Mays, C. W. *et al.* In *Risks from Radium and Thorotrast* [D. M. Taylor *et al.*, eds.], British Institute of Radiology, London, p. 47, 1989).

The experimental design included a comparison to the exposed human population (Schales, F. *Health Phys. 35*: 25, 1978). Instead of using a single injection of $^{224}$Ra, groups were included in which dogs were injected once, 10 times, or 50 times. This design provided groups that could be compared to the multiple injections often used in people for the treatment of ankylosing spondylitis.

The $^{224}$Ra used in this study was purchased as pure $^{224}$Ra chloride from Amersham-Buchler, Braunschweig, Germany, or made by the same methods (Delikan, O. *Health Phys. 35*: 21, 1978). This material was the same as that used in patients for the treatment of ankylosing spondylitis. The activities of the impurities $^{226}$Ra, $^{228}$Ra, $^{227}$Ac, and $^{228}$Th were negligible, each being about $10^{-7}$ of the $^{224}$Ra activity. The radium was administered in a citrate buffer (pH 3.5) by single or multiple weekly intravenous injections.

The study was conducted in 128 Beagle dogs from the University of Utah colony (Rehfeld, C. E. *et al.* In *Radiobiology of Plutonium* [B. J. Stover and W. S. S. Jee, eds.], The J. W. Press, Salt Lake City, p. 47, 1972). The dogs were divided into four activity levels and one group of controls that were given only the citrate solution (Table 1). A major objective of this study was to evaluate the effect of dose protraction by dividing the activity given into one, 10, or 50 injections.

The dosimetry for $^{224}$Ra in dogs was determined in a parallel study conducted in six adult Beagle dogs (Lloyd, R. D. *et al. Radiat. Res. 92:* 280, 1982).

At the conclusion of this study, all pathology findings were reviewed by one pathologist, and all clinical records were reviewed by one veterinary clinician to provide uniform terminology and criteria for diagnosis for the entire study.

The dose-response relationship for bone tumors from injected $^{224}$Ra was analyzed using a proportional hazards model. This type of model uses the time to tumor and corrects for competing risks by considering dogs that die without tumors as censored observations. The time-dependent incidence of bone tumors is modified by a relative risk that is a function of the average skeletal dose in Gy

$$\lambda(t,r) = \lambda_o(t)\exp(\beta_j r) \quad j = 1,2,3, \tag{1}$$

where $t$ is the time on study; $r$ is the average skeletal dose in Gy; $\lambda(t,r)$ is time-specific incidence of bone tumors at time $t$; dose $r$, $\lambda_o(t)$ is the estimated time-specific incidence of bone tumors at time $t$ in the control dogs; and $\exp(\beta_j r)$ is the relative risk for bone tumors at dose $r$. $\beta_j$ are the dose-response coefficients estimated in the model for a single injection, $\beta_1$; 10 injections, $\beta_2$; or 50

*Radiobiology Division, University of Utah School of Medicine, Salt Lake City, Utah

injections, $\beta_3$. In this study, the time dependence of the radiation dose to the bone was not important to specify in the above model because the radiation dose was completely delivered before the occurrence of any bone tumors. In applying the proportional hazards model, $\beta_j, j = 1,2,3$ and $\lambda_0(t)$ were all estimated simultaneously.

Table 1 – Experimental Design

Dogs Injected Intravenously Once, 10 Times, or 50 Times with $^{224}$Ra Citrate

| Weekly Injections | Level | Mean Age at First Injection (d) | Mean Body Weight at First Injection (kg) | Mean Summed $^{224}$Ra Injection Activity (kBq/kg) | Mean Skeletal Dose (Gy) | Number of Dogs |
|---|---|---|---|---|---|---|
| 50 | 5.0 | 646 ± 2.8 | 10.0 ± 0.5 | 343 | 2.78 | 6 |
| | 4.0 | 647 ± 2.1 | 10.6 ± 0.6 | 117 | 0.95 | 6 |
| | 3.0 | 640 ± 5.1 | 10.6 ± 0.4 | 39 | 0.32 | 12 |
| | 2.0 | 634 ± 6.3 | 10.1 ± 0.3 | 13 | 0.11 | 12 |
| | 0.0 | 595 ± 29.9 | 10.7 ± 0.3 | 0 | 0 | 6 |
| 10 | 5.0 | 653 ± 11.4 | 10.3 ± 0.6 | 351 | 2.85 | 6 |
| | 4.0 | 656 ± 11.8 | 9.7 ± 0.4 | 121 | 1.00 | 6 |
| | 3.0 | 633 ± 10.0 | 8.8 ± 0.4 | 40 | 0.34 | 12 |
| | 2.0 | 629 ± 11.5 | 9.2 ± 0.3 | 13 | 0.11 | 12 |
| | 0.0 | 641 ± 6.5 | 9.5 ± 0.4 | 0 | 0 | 6 |
| 1 | 5.0 | 673 ± 12.9 | 9.5 ± 0.5 | 382 | 3.00 | 8 |
| | 4.0 | 662 ± 15.2 | 10.0 ± 0.6 | 121 | 0.98 | 6 |
| | 3.0 | 661 ± 11.1 | 9.7 ± 0.2 | 42 | 0.34 | 12 |
| | 2.0 | 655 ± 9.4 | 10.2 ± 0.4 | 13 | 0.11 | 12 |
| | 0.0 | 619 ± 13.1 | 9.9 ± 0.5 | 0 | 0 | 6 |

Three dogs died from 9 to 16 d after injection from severe hematologic dyscrasia. Eighteen dogs developed bone tumors, 15 dogs had a single tumor, two had two tumors, and one dog had three tumors. Seventeen of these tumors were osteosarcomas. The majority of the tumors were the cause of death, and about half were found to have metastasized to other organs.

The relationship of the total average alpha dose to bone and time from beginning of injections to death and bone tumor occurrence is shown in Figure 1. The higher incidence of bone tumors in the 50-injection group compared to the incidence of tumors in the 10- and single-injection groups was statistically significant. No difference was detected between the 10-injection and single-injection group. The tumor incidences in all three groups of dogs injected with $^{224}$Ra were different from that seen in the controls.

The use of four levels of injected activity and three different time intervals for the administration of the $^{224}$Ra resulted in significantly different dose-rate patterns in this study. The injection of $^{224}$Ra produced a significant dose response for bone tumors, $p < 0.001$ (likelihood ratio test of $\beta_j = 0$), in the three injection groups. There was also a significant effect of dose protraction with the dogs receiving 50 injections having a significantly larger dose response than the other groups, $p < 0.001$ (likelihood ratio test of $\beta_1 = \beta_2 = \beta_3$). The single- and 10-injection groups could not be distinguished from each other, $p = 0.17$ (likelihood ratio test of $\beta_1 = \beta_2$).

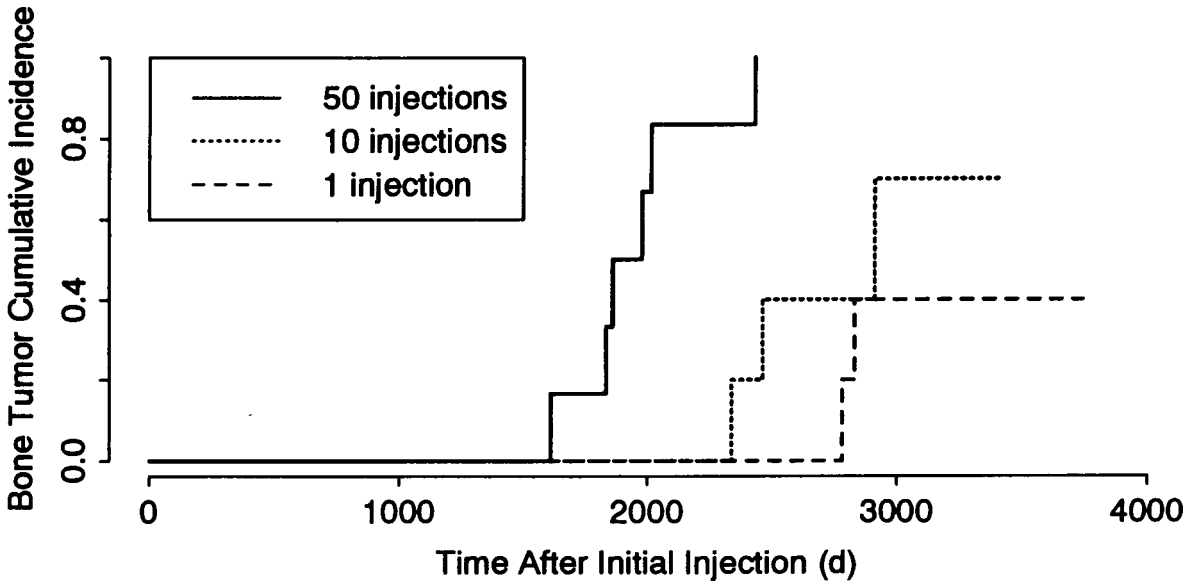


Figure 1. Estimated cumulative incidence of bone tumors in the high dose group of dogs (2.4–3.0 Gy). The cumulative incidence was estimated by subtracting the Kaplan-Meier estimator for bone tumors from 1.

This reverse protraction effect for bone tumors has also been reported in people treated with $^{224}Ra$ for ankylosing spondylitis (Chmelevsky, D. *et al. Radiat. Res. 124*: S69, 1990). In the present study, protraction of the dose over 3 mo, however, did not result in a significant increase in incidence of bone tumors over that in the single-injection group, but none of these dogs died from hematologic disease.

The number of tumors per Gy was also estimated for each injection group. This was calculated by dividing the number of dogs with bone tumors in a given year after the initial injection by the total radiation dose in all dogs surviving to the start of that year, and multiplying the result by the estimated survival of the control dogs for that year.

The risk estimate derived in this study over the lifetime for the dogs given 50 injections is 8400 bone tumors per $10^4$ Gy, a value similar to the lifetime estimate of 6200 bone tumors per $10^4$ Gy for dogs that inhaled $^{238}PuO_2$ (Muggenburg, B. A. *et al. Ann. Occup. Hyg.*, in press), and 7500 bone tumors per $10^4$ Gy for dogs injected with $^{239}Pu$ (Lloyd, R. D. *et al. Health Phys. 64(1)*: 45, 1993). The tumor risk estimate for dogs injected with $^{226}Ra$, where the dose is delivered over a long period of time but much of the dose is delivered to the bone volume, is 470 bone tumors per $10^4$ Gy (Lloyd, 1993). Because most of the dose from $^{224}Ra$ is delivered to bone surface, as is the case with plutonium, it seems reasonable that the risk estimates for protracted irradiation from $^{224}Ra$ would be similar to plutonium. Mays, C. W. *et al.* (*Strahlentherapie (Sonderb) 80*: 27, 1985) estimated the lifetime risk of 170 bone tumors for patients injected with $^{224}Ra$. This lower risk of bone tumors indicates a significant difference in the sensitivity between dogs and humans in the development of bone tumors from alpha radiation.

(Research sponsored by the Office of Health and Environmental Research, U.S. Department of Energy, under Contract Nos. DE-AC02-76EV00119 and DE-AC04-76EV01013.)

# V. MECHANISMS OF CARCINOGENIC RESPONSE TO TOXICANTS

# CHARACTERIZATION OF A UNIQUE MUTATION OF p53 IN A RAT EPITHELIAL CELL STRAIN

*Thomas R. Carpenter*, Deborah S. Swafford*, Albert W. Hickman*, and Neil F. Johnson*

The tumor suppressor gene p53 is the most commonly mutated gene known in human cancer. Mutational alteration of p53 function appears to be an important carcinogenic event in a wide variety of tumor types. Altered activity caused by mutation results in reduction of the following: transcriptional activity, nuclear localization, growth suppression, and cell cycle inhibitory activities (Reviewed in Prives, C. and J. J. Manfredi. *Genes & Dev. 7*: 529, 1993). Wild-type p53 protein has been shown to accumulate in cells exposed to a variety of DNA-damaging agents, including ionizing radiation, primarily through protein stabilization (Kastan, M. B. *et al. Cancer Res. 51*: 6304, 1991). Mutant forms of p53 fail to accumulate after irradiation indicating a failure to respond to upstream regulatory actions (Kastan *et al.*, 1991). The accumulation of p53 protein may serve as a sensitive biologic indicator of DNA damage.

To assess the potential use of the p53 response as an indicator of DNA damage, a spontaneously immortalized rat lung epithelial cell (LEC) strain developed by Li, A. P. *et al.* (*Toxicology 27*: 257, 1983) was used to measure p53 response to alpha-particle radiation (Hickman, A. W. *et al. Cancer Res. 54*: 5797, 1994). This cell strain has an ultrastructure consistent with an origin from alveolar type II cells (Li *et al.*, 1983). Elevations in p53 protein content are demonstrable after alpha-particle doses as low as 6 mGy and X-ray doses as low as 100 mGy (Hickman *et al.*, 1994). The LEC cells responded to radiation doses far below those reported previously to elevate cellular levels of p53 (Kuerbitz, S. J. *Proc. Natl. Acad. Sci. 89*: 7491, 1992). However, attempts to demonstrate a $G_1$ arrest were unsuccessful. Since induction of $G_1$ arrest is dependent upon a functional p53, the LEC p53 was suspected to be mutated.

The purpose of these investigations was to establish the mutational state of the LEC p53 gene and to characterize some of the consequences of such a mutation. DNA sequence analysis of the LEC gene (Sanger, F. *Proc. Natl. Acad. Sci. USA. 74*: 5463, 1977) revealed a mutation at codon 257 that results in the substitution of aspartate → glutamate. Despite the conservative nature of the LEC mutation, prediction of protein secondary structure (Chou, P. Y. and G. D. Fasman. *Adv. Enzymol. Relat. Areas Mol. Biol. 47*: 45, 1978) indicated an increased alpha-helical forming property in the region of the mutation. This finding suggested an altered conformation in a region of the protein responsible for sequence-specific DNA binding.

The promoter function of the LEC p53 protein was next examined because the mutation may alter its *trans-activating* capability. Increased levels of wild-type p53 are known to induce the oncogene mdm2 by binding to a response element within the first intron of the mdm2 gene (Juven, T. *Oncogene 8*: 3411, 1993). LECs were grown as previously reported (Hickman *et al.*, 1994). In order to determine if mdm2 could be induced in LEC cells after X-irradiation, cells were exposed to either 0 or 4 Gy X rays using a Philips RT 250 Radiotherapy Unit (Philips Medical Systems, Shelton , CT) and were harvested 2, 6, 12 or 24 h later. Total RNA was collected by the guanidine thiocyanate, phenol/chloroform method and analyzed by Northern blot analysis using a rat cDNA mdm2 probe (Sambrook, J. *Molecular Cloning: A Laboratory Manual 2nd Ed.*, Cold Spring Harbor Laboratory Press, Cold Spring Harbor, NY, 1989). Densitometric measurements of the autoradiographs were normalized to glyceraldehyde phosphate dehydrogenase (GAPDH) expression. The expression of mdm2 is shown in Figure 1. LEC mdm2 message levels were compared to message levels in the FRLE cell

*UNM/ITRI Inhalation Toxicology Graduate Student

strain, which was known to express wild-type p53 (this report, p. 102). While a moderate increase in mdm2 mRNA expression was seen in LECs, it was about half the increase evident in the FRLEs.

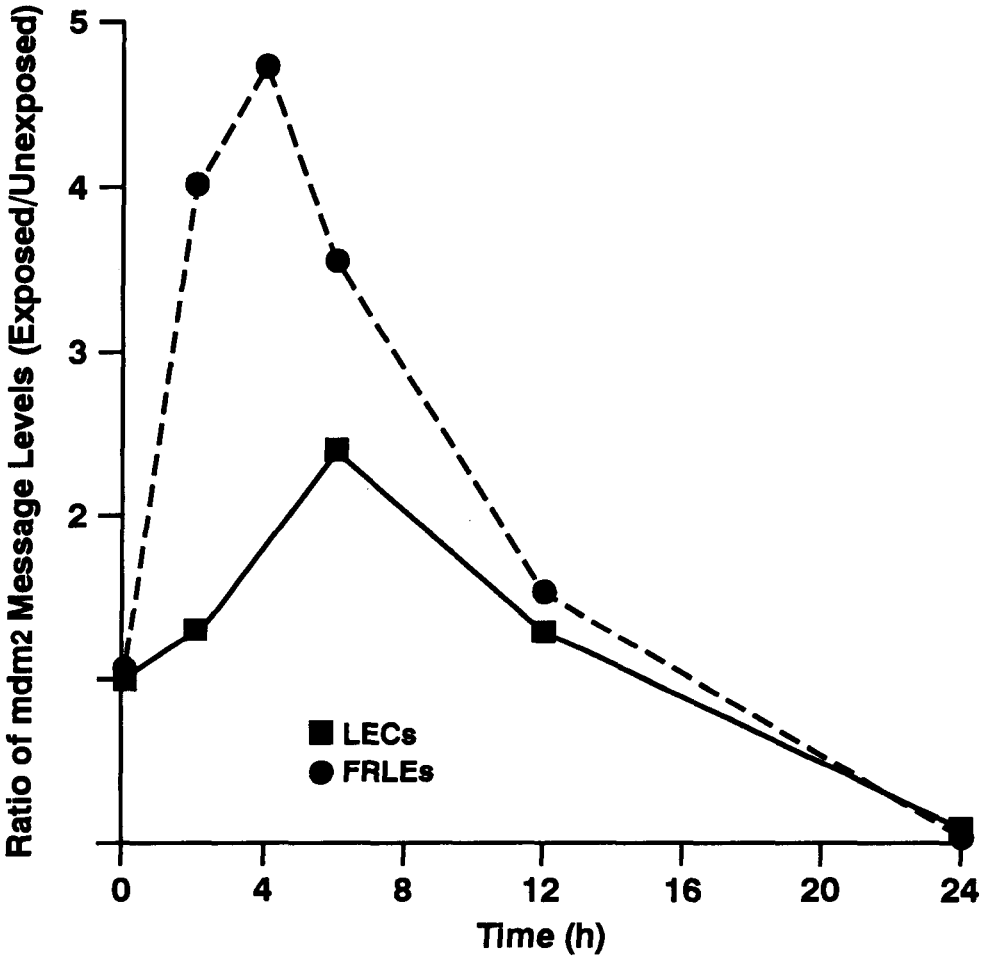


Figure 1. The message level of mdm2 in LECs (■) and FRLEs (●) expressed as a ratio of exposed (4 Gy X rays) to unexposed cells versus time after irradiation. All levels were normalized to GAPDH expression. Data are taken from a single Northern blot.

The induction of p53 is temporally associated with the radiation-induced $G_1$ arrest which occurs presumeably to allow time for DNA repair before commitment to S-phase (Kastan *et al.*, 1991). The ability of LEC p53 to arrest cells in $G_1$ after X-irradiation was examined in cells partially synchronized by maintenance in culture at confluence for 72 h. Maintenance at confluence for 72 h eliminated entry into S-phase and enriched the population of cells in $G_1$ (data not shown). The synchronized cells were harvested, split into two fractions and were transferred to fresh dishes. After replating, 20-40% of the cells entered S-phase within 24 h (data not shown). To determine the extent of radiation-induced $G_1$ arrest, cells were synchronized and replated, then were irradiated as above 2 h after transfer to fresh plates; controls were brought out of the incubator for a similar time to control for ambient light and temperature effects. Twenty-two hours after irradiation, all cells were treated with 100 $\mu$M 5-bromo-2′-deoxyuridine (BrdU) for 2 h, then harvested and fixed in 70% methanol. Arrest in $G_1$ was demonstrated as a failure to enter into S-phase as determined by flow cytometric measurements of the number of cells immunostained for BrdU incorporation. Figure 2 shows the cell-cycle data from confluence-arrested LECs compared to data from confluence-arrested FRLEs. No reduction in cells incorporating BrdU (S-phase) after irradiation was detectable in confluence-arrested populations of LECs, indicating a failure of radiation-induced $G_1$ arrest. FRLEs displayed a 75%

reduction in the number of cells entering S-phase after irradiation, indicative of an intact radiation-induced $G_1$ arrest.

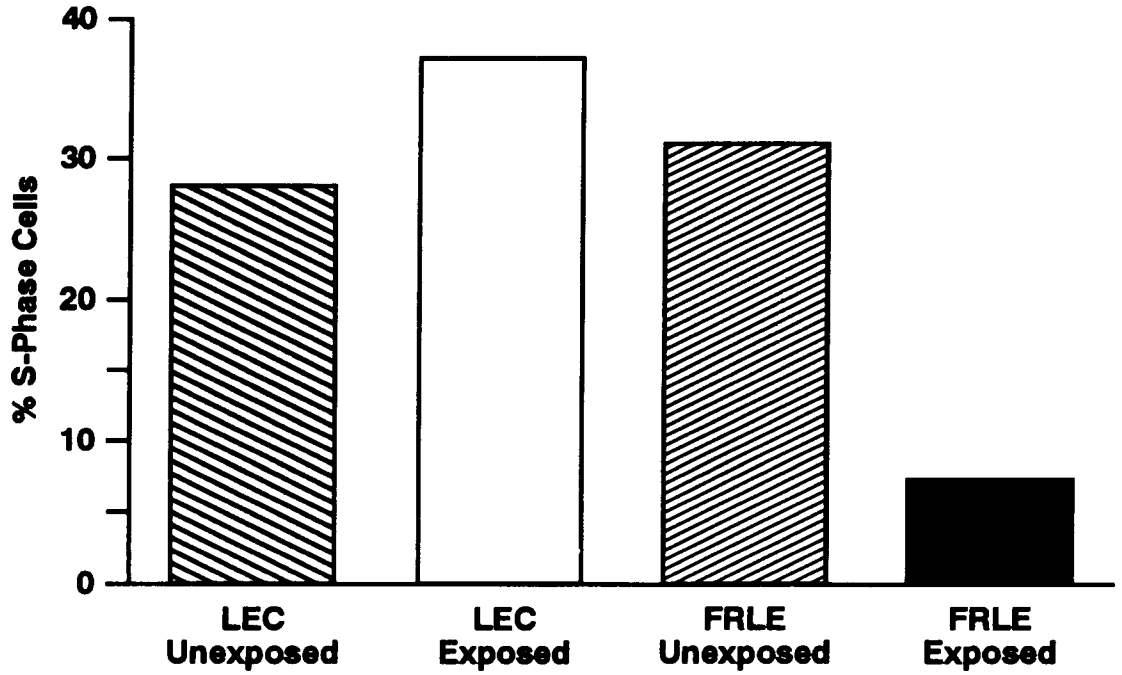


Figure 2. Percentage cells in S-phase of unexposed LECs, exposed (10 Gy X rays) LECs, unexposed FRLEs, and exposed (10 Gy X rays) FRLEs. Cells were collected 6 h after irradiation. The reduction of S-phase cells indicates $G_1$ arrest (n = 1).

These experiments have shown that the LEC p53 mutant accumulated in the cells after irradiation; however, the mutant p53 was unable to induce mdm2 nor was it able to induce $G_1$ arrest. The accumulation of the p53 protein indicated upstream regulators responsible for p53 accumulation were able to impart post-translational modifications necessary to stabilize the protein. The LEC p53 mutation appeared to separate the response of increased p53 protein from cell-cycle arrest. Despite increases in p53 protein exceeding those reported for other cell systems, the LEC mutant p53 caused smaller increases in mdm2 message than those caused by FRLE wild-type p53. It appeared the LEC mutant retained some promoter activity, as no p53-independent activation of mdm2 has been demonstrated in the literature. The LEC mutation occurred in the region of the protein required for sequence-specific DNA binding and thus may have altered affinity for the p53-binding region in the mdm2 gene. Despite retaining some promoter capability, the LEC mutant p53 was unable to induce $G_1$ arrest. This failure to arrest may have resulted from an inability to induce the p53-regulated $cip1^{p21}$ gene, which is responsible for causing $G_1$ arrest through complexes with cyclin, CDK and PCNA (Waga, S. *et al. Nature 369*: 574, 1994). Future work will examine the expression of $cip1^{p21}$ in response to irradiation as well as the p53-regulated gene GADD45. The p53-response elements in these genes may have differing abilities to bind to p53 and may thus be differently regulated by the LEC mutant.

(Research sponsored by the Office of Health and Environmental Research, U.S. Department of Energy, under Contract No. DE-AC04-76EV01013.)

# VALIDATION OF AN *IN VITRO* MODEL OF RAT p53 REGULATION AND FUNCTION

*Thomas R. Carpenter*, Robin P. Groch**, Albert W. Hickman*, and Neil F. Johnson*

Public and governmental concern about the cancer risks associated with indoor exposure to alpha particle-emitting radon progeny is growing. Such concern arises from the exposure-dependent elevation in cancer risk seen in underground miners, most notably uranium miners. Risk estimates for the general population are derived from extrapolations of risk estimates for the uranium miners. The ability to compare data from the numerous retrospective population studies, animal model experiments, and *in vitro* experiments is based upon dose-conversion factors that indicate equivalent detrimental endpoints due to certain exposure levels. Recently, efforts to use cytotoxic endpoints such as cell survival, micronucleus formation, and mitotic delay as biologic dosimeters have been compared *in vivo* and *in vitro* to obtain dose conversion ratios (Thomassen, D. G. *et al. Radiat. Prot. Dosim. 38*: 65, 1991; Johnson, N. F. and G. J. Newton. *Radiat. Res. 139*: 163, 1994). While these efforts are successful in cumulative exposure levels of 75-1000 working level months (WLM), such biological dosimeters are insensitive to the cumulative exposure levels found in indoor environments (1-50 WLM). More sensitive indicators of radiation damage/effect are needed to improve dose conversion factors and to better understand how alpha-emitters such as radon cause cancer.

More recently, changes in p53 expression following radiation exposure are shown to be responsive to radiation doses comparable to the cumulative exposure levels encountered indoors (Hickman, A. W. *et al. Cancer Res. 54*: 5797, 1994). While this work supports using changes in radiation-induced gene expression as a more sensitive biological dosimeter, the cell line used contains a mutation in the p53 gene. Therefore, the purpose of this investigation was to obtain and validate a model for the expression of p53 and associated genes in response to alpha irradiation. Such a model cell strain should express a wild-type p53, demonstrate radiosensitivity typical of other rat lung cells or cell strains, and exhibit an X-ray-induced p53 response similar to that reported in the literature. The fetal rat lung epithelial (FRLE) cell strain (Leheup, B. P. *et al. Lab. Invest. 60*: 791, 1989), derived from spontaneously immortalized alveolar type II cells, was evaluated as a model for studying the p53 response to radiation.

FRLEs were grown in RPMI 1640 media containing 10% fetal bovine serum, 292 μg/ml L-glutamine and 50 μg/ml gentamicin in incubators at 37°C with 5% carbon dioxide. RNA was extracted by the guanidine thiocyanate, phenol/chloroform method (Sambrook, J. *Molecular Cloning: A Laboratory Manual 2nd Ed.* Cold Spring Harbor Laboratory Press, Cold Spring Harbor, 1989). p53 cDNA exons 4–10 were amplified by the polymerase chain reaction (Innis, M. A. *et al. PCR Protocols: A Guide to Methods and Applications.* Academic Press, Inc., San Diego, 1990). The amplification product was ligated into the PCRII plasmid (Invitrogen, San Diego, CA), and sequenced by the dideoxynucleotide method (Sanger, F. *Proc. Natl. Acad. Sci USA. 74*: 5463, 1977). No mutations were detected in exons 4–10.

To determine radiosensitivity, FRLEs were grown to confluence, then exposed to graded doses of X rays (0, 0.1, 0.5, 1.0, 1.5, 2.0, 4.0, 6.0, 8.0, 10.0, 15.0, and 20.0 Gy) using a Philips RT 250 Radiotherapy Unit (Philips Medical Systems, Shelton, CT). Known cell numbers of viable exposed or unexposed cells were then transferred to 60 mm Petri dishes and allowed to incubate for 5 d as

*UNM/ITRI Inhalation Toxicology Graduate Student

**Department of Energy/Associated Western Universities Teacher Research Associates Program (TRAC) Participant

above with media exchanged every 48 h. Plates were then fixed in 70% methanol and stained with Giemsa. Colonies containing at least 50 cells were counted, and cell survival was expressed as colonies + (number cells plated x plating efficiency). Alpha-particle exposures were performed in Mylar®-bottomed dishes with cells grown to confluence as above. Cells were then exposed to an electroplated $^{238}Pu$ source with a dose delivery rate of either 0.90 or 0.11 Gy/min to achieve graded doses of alpha particles (0, 0.01, 0.05, 0.1, 0.25, 0.5, 1.0, 2.0, 3.0, 4.0, or 5.0 Gy). The cells were replated and colonies counted as above. Figure 1 depicts the cell survival curves for both X-ray and alpha-particle exposure. The X-ray survival curve revealed a shoulder extending to 4 Gy followed by a dose-dependent exponential decrease in cell survival. The $D_{10}$ (dose yielding 10% survival) for X-ray survival was 13 Gy. The survival curve to alpha-particle irradiation demonstrated a dose-dependent exponential decrease in cell survival with a $D_{10}$ of 4 Gy.

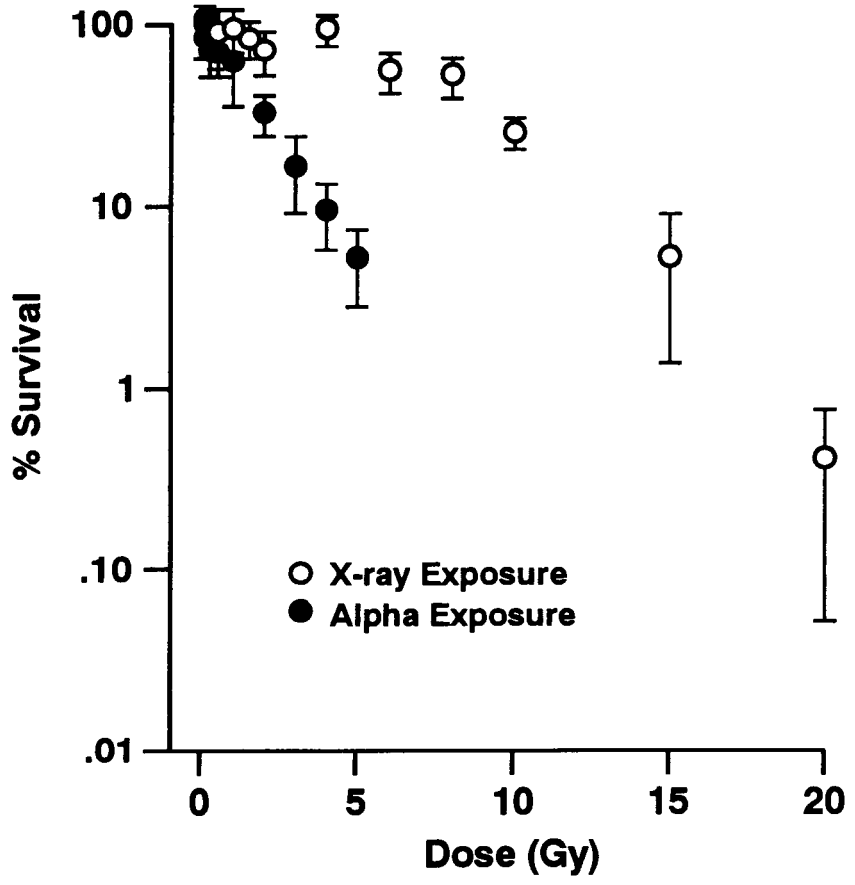


Figure 1. Percent survival of X-irradiated (○) and alpha-irradiated (●) FRLE cells. Error bars represent plus or minus one standard deviation from five trials done on triplicate plating.

p53 protein is induced by protein stabilization after DNA damage caused by ionizing radiation (Kastan, M. B. *et al. Cancer Res. 51*: 6304, 1991). In order to verify p53 protein induction in FRLEs exposed to graded doses of X rays, total protein was extracted at 6 h post-irradiation, separated by acrylamide gel electrophoresis, and transferred to polyvinyldifluoride (PVDF) membrane (Sambrook, 1989). p53 protein was visualized by immunoblot technique using an anti-p53 monoclonal antibody and compared to protein from a rat cell line with a human p53 cDNA expressed under a constitutive promoter. The resulting immunoblot demonstrated a dose-dependent increase in p53 protein expression to doses as small as 2 Gy, expressed as densitometric absorption ratios (results not shown).

In order to assess the ability of FRLE p53 to act as a transcriptional promoter, total RNA was extracted as above from cells exposed to 4 Gy X rays and was subjected to Northern blot or slot blot analysis as outlined in Sambrook (1989). The blots were probed with rat cDNA probes to p53, mdm2, and glyceraldehyde phosphate dehydrogenase (GAPDH) and autoradiographs were quantified by densitometry. Figure 2 depicts data normalized to the GAPDH expression and expressed as the ratio of exposed to control cells. p53 message levels were unchanged over the first 24 h. mdm2 was induced as early as 2 h and peaked at 4 h. Levels of mdm2 message actually fell below controls by 24 h.

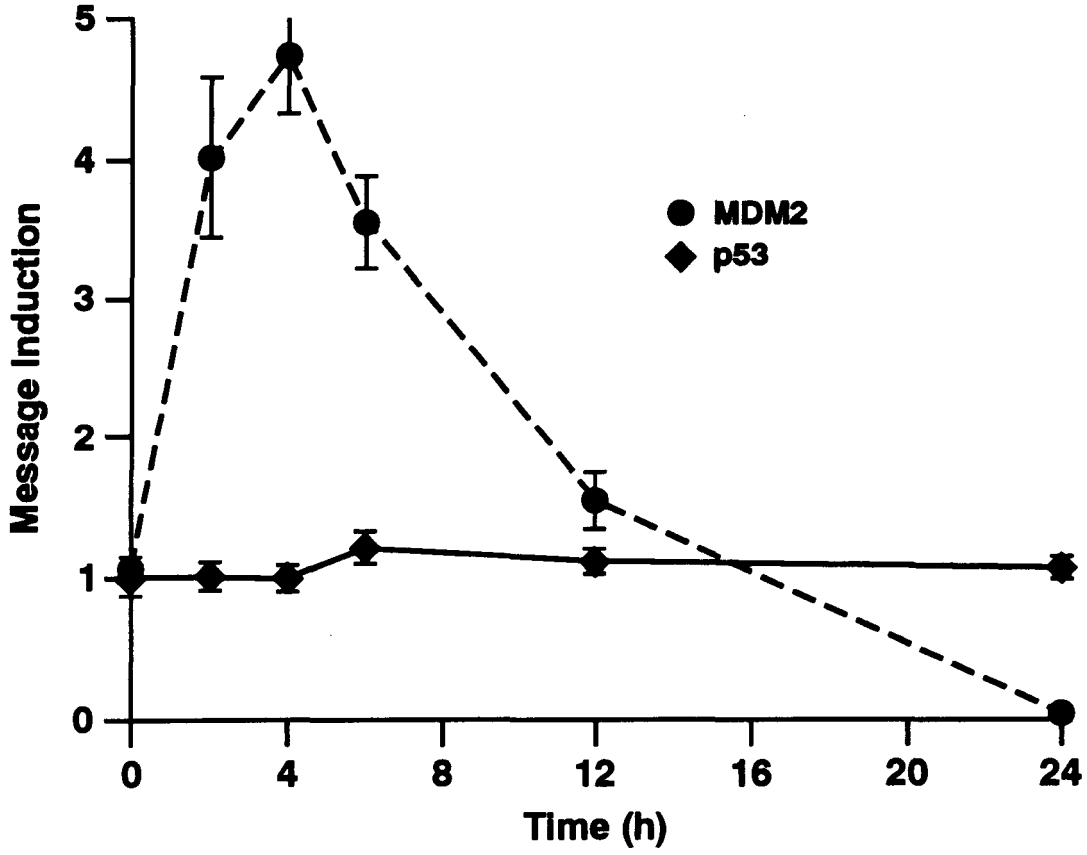


Figure 2. Message expression of p53 (♦) and mdm2 (●) in FRLEs irradiated with 4 Gy X rays. Values represent ratio of exposed to unexposed cells normalized to GAPDH expression. Error bars represent plus or minus one standard deviation of two trials.

One result of p53 induction is arrest in the $G_1$ phase of the cell cycle in order to repair DNA damage (Nelson, W. G. and M. B. Kasten *Mol. Cell Biol. 14*: 1815, 1994). FRLEs were arrested by incubation at confluence for 72 h, replated at 60% confluence, exposed to graded doses of X irradiation after 6 h, and allowed to incubate 24 h. After 24 h, the cells were treated with 100 $\mu$M 5-bromo-2'-deoxyuridine (BrdU) for 2 h, then harvested and fixed in 70% methanol. Incorporation of BrdU was measured by direct immunostaining and flow cytometric analysis. Exposure to X-irradiation reduced the fraction of cells entering S-phase to <10% of unexposed cells at doses above 4 Gy (data not shown).

The FRLE cell strain appeared to be appropriate for the study of the p53 response. First the cells were shown to express a non-mutated form of the p53 gene. Second, the cell strain demonstrated radiosensitivity typical for that reported for rat lung epithelial cells and cell lines (Biard, D. S. F. *et al. Cancer Res. 54*: 3361, 1994; Ford, J. R. and M. Terzaghi-Howe *Radiat. Res. 136*: 89, 1993;

Brooks, A. L. *et al. Int. J. Radiat. Biol. 58*: 799, 1990). Next, the cell strain was shown to respond to X irradiation by increasing p53 protein, suggesting that upstream post-translational modifiers of p53 function were intact. Also, the lack of induction of p53 message was consistent with post-translational induction seen by other investigators (Nelson and Kastan, 1994). The induction of the p53-regulated gene mdm2 indicated FRLE p53 assumed the normal conformation required for its transcriptional promoter role. Finally, because a series of events are required to induce cell cycle arrest, the presence of $G_1$ arrest indicated intact downstream function of p53 in FRLEs. The validation of this cell strain as a good model for detecting low dose radiation-induced gene expression may allow measurement of the radiation dose received by respiratory epithelial cells exposed to the low levels of radon progeny experienced indoors.

(Research sponsored by the Office of Health and Environmental Research, U.S. Department of Energy, under Contract No. DE-AC04-76EV01013.)

# p53 PROTEIN EXPRESSION VERSUS MICRONUCLEUS INDUCTION AS AN INDICATOR OF DNA DAMAGE

*Albert W. Hickman*, Thomas R. Carpenter*, and Neil F. Johnson*

*In vitro* assays for detecting DNA damage play an important role in evaluating the possible adverse health effects of chemical compounds. Exposure to many DNA-damaging agents *in vitro* has been shown to cause elevated levels of the tumor-suppressor protein p53 (Fritsche, M. *et al. Oncogene 8*: 307, 1993; Nelson, W. G. and M. B. Kastan. *Mol. Cell Biol. 14*: 1815, 1994). Work in our laboratory has shown that induction of the p53 protein is useful as a biodosimeter for determining the radiation dose to cells (Hickman, A. W. *et al. Cancer Res. 54*: 5797, 1994). The purpose of this investigation was to compare the sensitivity of this assay to that of micronucleus induction, which is commonly used as a marker of radiation-induced damage.

In these studies, a rat lung epithelial cell (LEC) strain previously isolated from male F344 rats and characterized by Li, A. *et al.* (*Toxicology 27:* 257, 1983) was exposed to graded doses of X rays. For the micronucleus assay, cells were plated onto 225-$cm^2$ tissue culture flasks at a density of $2 \times 10^6$ per flask. After 24 h, cells were exposed to graded doses of X rays (0, 0.1, 0.25, 0.5, 1.0, 2.5, 5.0, or 7.5 Gy) using a Picker Vanguard Console Therapy Unit (Picker X-Ray Corp., Cleveland, OH). Cells were allowed to grow a further 24 h, treated with 3 $\mu$g cytochalasin B/mL media to block cytokinesis, incubated for an additional 24 h, harvested, and fixed in 3:1 methanol:acetic acid. Fixed cells were air-dried on glass slides, stained with Diff-Quik (Baxter Healthcare Corp., Miami, FL), and scored by light microscopy for the presence of micronuclei.

For the p53 protein assay, cells were grown to confluency on 225-$cm^2$ tissue culture flasks, exposed to graded doses of X rays (0, 0.05, 0.1, 0.5, 1.0, or 2.0 Gy), harvested 6 h after exposure, and fixed in 70% methanol. The p53 protein in fixed cells was labeled immunofluorescently using a monoclonal antibody directed against p53, a biotinylated secondary antibody, and streptavidin-conjugated fluorescein isothiocyanate. The percentage of cells having increased amounts of p53 protein due to irradiation was determined by flow cytometric analysis (Hickman *et al.*, 1994). Figure 1 depicts the results of the two assays. p53 protein induction was a more sensitive assay than was micronucleus formation by over an order of magnitude. Whereas an increase in the number of p53-positive cells over control numbers was detectable following a dose of 0.1 Gy ($p < 0.001$), an X-ray dose of 5.0 Gy (an increase of a factor of 50) was required to achieve the same level of statistical significance for micronucleus formation.

Micronucleus formation is a widely used test for chemical genotoxicity as well as radiation-induced DNA damage (Fenech, M. In *Mutation and the Environment, Part B* [M. L. Mendelsohn and R. J. Albertini, eds.], Wiley-Liss, New York, p. 195, 1991). Although a number of studies have investigated p53 protein induction *in vitro* following exposure to genotoxic chemicals, no studies have yet compared the sensitivity of p53 protein induction versus that of other tests following exposure to low doses of these agents. To make this comparison, LECs were exposed to several chemicals reported to cause micronucleus formation in other cell types (Table 1); the concentrations used were at the low end of concentrations reported to induce micronuclei.

Treatment with bleomycin (BLM), mitomycin C (MMC), or 4-nitroquinoline-1-oxide (4-NQO) resulted in an increase in the number of p53-positive LECs, as analyzed using flow cytometry. BLM causes single- and double-strand DNA breaks at the C3′-C4′ bond of the deoxyribose backbone,

*UNM/ITRI Inhalation Toxicology Graduate Student

preferentially at G-C and G-T sites. Strand breaks are also a consequence of DNA repair following exposure to MMC or 4-NQO. MMC is reductively metabolized and preferentially alkylates the N2 positions of two guanine residues in separate DNA strands, causing crosslinks. 4-NQO, after reductive metabolism, forms bulky adducts on guanine and adenine residues. The DNA strand breakage caused by these agents is believed to be an important signal in initiating p53 protein induction.

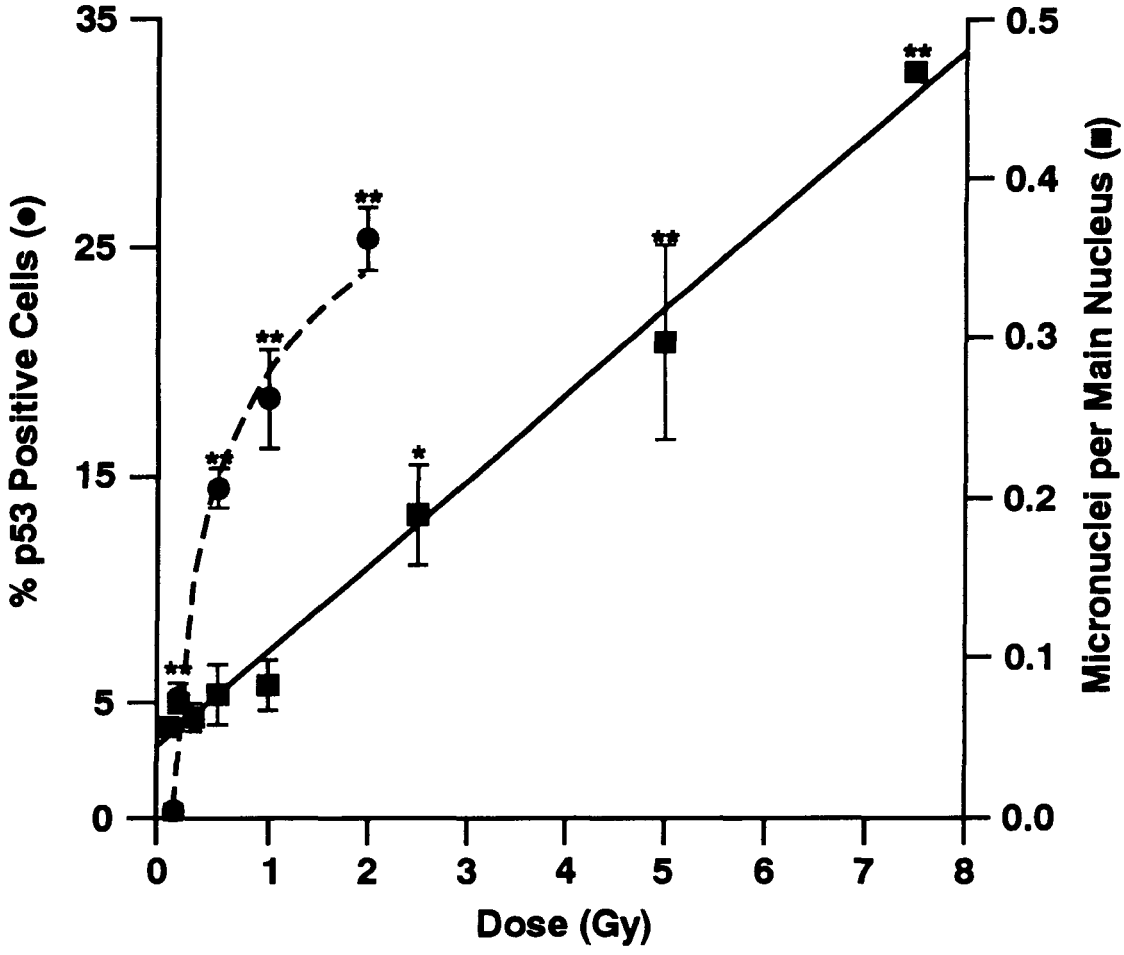


Figure 1. Micronucleus formation (■) and p53 protein induction (●) in LECs following exposure to X rays. Values are means ± standard errors for three experiments. The lines through the data points represent the best fits to the experimental data. * = significantly different from controls, $p < 0.05$; ** = significantly different from controls, $p < 0.001$.

In contrast, exposure to dimethyl sulfoxide (the vehicle for 4-NQO and methyl methanesulfonate [MMS]) or ethanol, neither of which has been shown to be genotoxic, did not cause any elevation in p53 levels. Interestingly, exposure to MMS, a direct-acting agent which methylates primarily the N7 of guanine and the N3 of adenine, did not cause an increase in the number of p53-positive cells. This could be either because methylation is not a signal for the induction of p53 or because DNA damage (e.g., depurination and subsequent repair) that occurred during the exposure was insufficient to cause increases in p53. The present results suggest that this p53 assay could be used to evaluate the low-dose effects of exposure to environmental chemicals. Continuing investigations are focused on determining the limits of sensitivity of the p53 protein assay, in terms of both the types of DNA damage and concentrations of test chemicals studied.

Table 1

p53 Protein Induction by X rays and Chemical Genotoxins

| Exposure | p53 Induction |
|---|---|
| X rays (0.1 Gy) | + |
| Bleomycin (10 μg/mL) | + |
| Mitomycin C (0.5 μg/mL) | + |
| 4-Nitroquinoline-1-oxide (0.1 μg/mL) | + |
| Methyl Methanesulfonate (0.5 μg/mL) | – |
| Dimethyl Sulfoxide (0.1%) | – |
| Ethanol (10 mM) | – |

(Research sponsored by the Office of Health and Environmental Research, U.S. Department of Energy, under Contract No. DE-AC04-76EV01013.)

# p53 TUMOR SUPPRESSOR GENE AND PROTEIN EXPRESSION IS ALTERED IN CELL LINES DERIVED FROM SPONTANEOUS AND ALPHA-RADIATION-INDUCED CANINE LUNG TUMORS

*Lauren A. Tierney*, Neil F. Johnson, and John F. Lechner*

Mutations in the p53 tumor suppressor gene are the most frequently occurring gene alterations in malignant human cancers, including lung cancer (Hollstein, M. *et al. Science*: 49, 1991; Chiba, I. *et al. Oncogene 5*: 1603, 1990). In lung cancer, common point mutations within conserved exons of the p53 gene result in a stabilized form of mutant protein which is detectable in most cases by immunohistochemistry (Bartek J. *et al. Oncogene 6*: 1699, 1991; Bodner, S. M. *et al. Oncogene 7*: 743, 1992). In addition to point mutations, allelic loss, rearrangements, and deletions of the p53 gene have also been detected in both human and rodent tumors (Caamano, J. *et al.* In *Comparative Molecular Carcinogenesis* [J. P. Andres *et al.*, eds.], Wiley-Liss, New York, p. 331, 1992). It has been suggested that for at least some epithelial neoplasms, the loss of expression of wild-type p53 protein may be more important for malignant transformation than the acquisition of activating mutations (Reiss, M. *et al. Oncol. Res. 4*: 349, 1992). Mechanisms responsible for the loss of expression of wild-type protein include gene deletion or rearrangement, nonsense or stop mutations, mutations within introns (Takahashi, T. *et al. J. Clin. Invest. 86*: 363, 1990) or upstream regulatory regions of the gene, and accelerated rates of degradation of the protein by DNA viral oncoproteins (Harris, C. C. *et al. N. Engl. J. Med. 329*: 1318, 1993).

With the exception of small cell lung cancer (SCLC) in which p53 gene deletions and rearrangements have been identified (Nigro, J. M. *et al. Nature 342*: 705, 1989), gene alterations other than allelic loss and mutation are infrequently reported in human lung cancers. Homozygous deletions, rearrangements, intron mutations, and the presence of abnormally spliced p53 RNA transcripts have been reported in both SCLC cell lines (Takahashi, T. *et al. Science 246*: 491, 1989) and non-small cell lung cancer cell lines (Caamano, J. *et al. Am. J. Pathol. 139*: 839, 1991).

Previous work on the Beagle dog from this laboratory (Tierney, L. A. *et al.*, unpublished), examined aberrant p53 protein expression in lung tumors from $^{239}PuO_2$-exposed dogs. Results by immunohistochemistry, suggested that point mutations, as reflected by nuclear accumulation of the p53 protein (Iggo, R. *et al. Lancet 335*: 675, 1990), were far less frequent in canine than in human lung cancers. These results also contrasted with the findings of Vähäkangas *et al.* (*Lancet 339*: 576, 1992) who identified a high proportion of p53 mutations in lung cancers from individuals who smoked and/or were exposed to high-linear energy transfer (LET) radiation through the inhalation of radon progeny.

Disparate results between lung cancers from high-LET-exposed dogs and humans suggested alternative mechanisms of p53 gene inactivation or alternatively other oncogene targets in high-LET-radiation-induced lung cancers. In the dog, lack of genomic p53 sequence data and availability of fresh tissue for the isolation of RNA from primary tumors necessitated an indirect approach to the question of alternative mechanisms of p53 inactivation. The existence of established canine lung tumor cell lines derived from alpha-radiation-induced and spontaneously occurring canine lung tumors provided a means to determine the mechanism underlying p53 dysfunction. The intent of this study was to examine canine lung tumor cell lines for altered p53 protein expression and for the presence of abnormally spliced or lost p53 messenger RNAs.

*UNM/ITRI Inhalation Toxicology Graduate Student

Cell lines were harvested at confluence, and $2 \times 10^6$ cells were injected in the presence of Matrigel® (Becton Dickinson, Bedford, MA) into nude mice. Tumors were subsequently harvested for immunohistochemical analysis of p53 protein (Tierney *et al.*, unpublished). An SV40 large-T antigen immortalized canine tracheal epithelial cell (ACT-8/SV40) and parent cell line (ACT-8) were used as positive and negative controls, respectively, for both northern analysis and immunohistochemistry. Messenger RNA was isolated from subconfluent cells using oligo(dT) cellulose spin columns (Invitrogen, San Diego, CA), and 2 $\mu$g of mRNA was electrophoresed on a 1% formalin agarose gel. Following transfer to a nylon membrane (Hybond, Amersham, U.K.), a human p53 cDNA probe (2.0 kb) (American Tissue Type Collection) was used to identify the canine p53 transcript under stringent hybridization conditions (1% SDS, 40 mM $Na_2HPO_4$ at 65°C).

Neither, the canine tracheal cell line (ACT-8) nor the SV40 immortalized tracheal cell line (ACT-8/SV40) produced tumors in nude mice. All lung tumor cell lines when transplanted into nude mice, formed tumors which, with one exception, recapitulated the histotype of the primary lung tumor (Table 1).

Table 1

Summary of Canine Lung Tumor Cell Line Characteristics

| Cell Line | Passage No. | Exposure | Tumor Histology | | p53 Immunohistochemistry | | |
|---|---|---|---|---|---|---|---|
| | | | Primary | Nude Mouse | p53 Primary | p53 Cell Line | p53 mRNA[a] |
| ACT-8 | p23 | *[b] | N/A | Not tumorigenic | N/A | – | + |
| ACT-8/SV40 | – | **[c] | N/A | Not tumorigenic | N/A | + | + |
| 978B | p9 | $^{239}PuO_2$ | Squamous cell carcinoma | Squamous cell carcinoma | – | – | – |
| 1025B | p10 | Unexposed | Adenosquamous carcinoma | Adenosquamous carcinoma | + | + | + |
| 1061T | p8 | $^{239}PuO_2$ | Papillary adenocarcinoma | Papillary adenocarcinoma | – | – | + |
| 1124A | p14 | Unexposed | Bronchioloalveolar carcinoma | Adenocarcinoma | – | – | + |
| 770S | p21 | Unexposed | Adenosquamous carcinoma | Adenosquamous carcinoma | + | + | + |
| 724S | p22 | $^{238}PuO_2$ | Fibrosarcoma | Squamous cell carcinoma | – | – | – |
| 1222T | p15 | $^{239}PuO_2$ | Solid carcinoma | Solid carcinoma | – | – | – |
| 1100B | p17 | $^{239}PuO_2$ | Adenosquamous carcinoma | Adenosquamous carcinoma | – | – | + |

[a]Cellular mRNA was analyzed for the presence of p53-specific transcript by northern blot.
[b]Canine tracheal epithelial cells transformed by direct acting carcinogen, N-methyl-N'-nitrosoguanidine (MNNG).
[c]Canine tracheal epithelial cell line (ACT-8) immortalized by infection with a recombinant retrovirus (pZipNeOSV(X)) containing the SV40 large T-antigen gene.

Three of five alpha-radiation-induced lung tumors lacked detectable transcript for canine p53, while all spontaneous canine lung tumors had a normal-sized transcript (Fig. 1 and data not shown). On the other hand, two of three spontaneously occurring lung tumor cell lines had evidence of p53 gene dysfunction by immunohistochemistry, while none of the cell lines derived from alpha-exposed primary tumors showed evidence of nuclear p53 accumulation (Table 1). Staining results in canine lung tumor cell lines paralleled those found in primary lung tumors (Table 1), indicating that aberrant nuclear p53

accumulation was not an artifact of *in vitro* culture. As expected, the SV40 immortalized canine cell line showed marked levels of stabilized nuclear p53 protein by immunohistochemistry, while the parent cell line (ACT-8) showed no p53 protein expression, but exhibited a normal 2.0 Kb-sized transcript by northern analysis (Fig. 1 and data not shown). In total, 5/8 (63%) of lung tumor cell lines had altered p53 expression at either the transcript or protein level.The loss of p53 gene expression detected in these canine cell lines might be a direct effect of high-LET radiation. High-LET radiation induces genomic instability which is manifested by a high proportion of chromosomal aberrations and SCEs (Nagasawa, H. *et al. Radiat. Res. 126*: 280, 1991). High-LET radiation is thought to exert its clastogenic effect through the formation of double-stranded DNA breaks that may result in gene deletions and rearrangements (Ritter, M. A. *et al. Nature 266*: 653, 1977). On the other hand, alpha-particles have been shown to induce a high frequency of nonclonal cytogenetic aberrations which result in the transmission of chromosomal instability to their progeny (Kadhim, M. A. *et al. Nature 355*: 738, 1992). Conceivably, alpha-particle-induced chromosomal instability might be further propagated by long-term cell culture resulting in loss of the p53 gene.

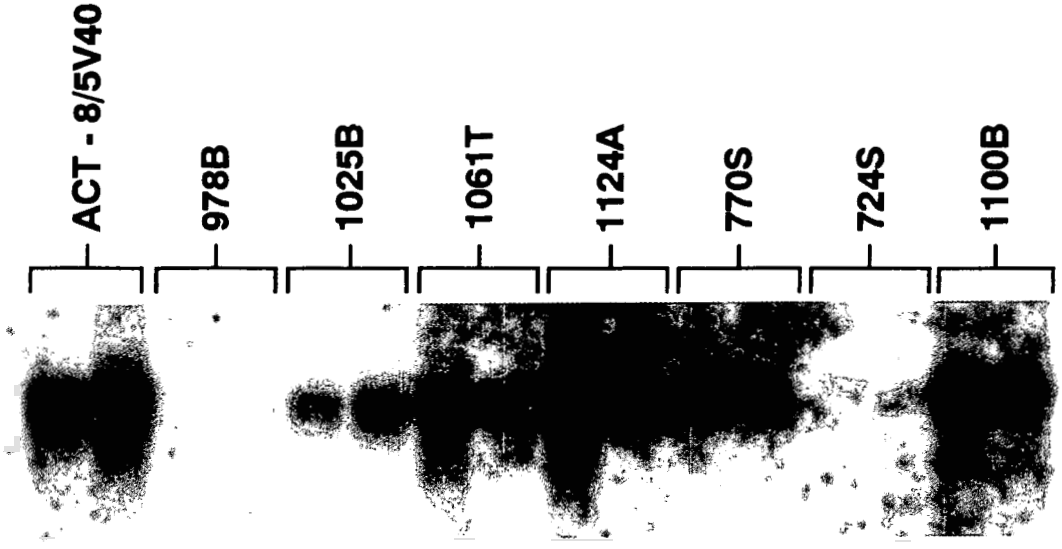


Figure 1. p53 mRNA expression in cell lines derived from spontaneous and α-radiation-induced canine lung tumors. No p53 specific transcripts were detectable in RNA from cell lines 978B and 724S.

Lastly, the loss of p53 transcripts in canine lung tumor cell lines may represent an artifact of passage in cell culture. Culture-associated gene loss has been suggested for another tumor suppressor gene, the cyclin-dependent kinase inhibitor, p16. (Cairns, P. *et al. Science 265*: 415, 1994)

Although these data were based on a limited number of cell lines, the absence of mRNA transcript in lung tumors of plutonium-exposed animals suggested that p53 inactivation in high dose alpha-radiation-induced lung tumors might be a result of gene deletion or rearrangement. Demonstration of somatically acquired p53 gene alterations in primary canine lung tumors will be required to further evaluate these findings.

(Research sponsored by the Office of Health and Environmental Research, U.S. Department of Energy, under Contract No. DE-AC04-76EV01013.)

# GENE ALTERATIONS IN RADIATION-INDUCED F344 RAT LUNG TUMORS

*Gregory Kelly and Fletcher F. Hahn*

The p53 tumor suppressor gene is frequently altered in all major histopathologic types of human lung tumors (Nigro, J. M. *et al. Nature 342*: 705, 1989). Reported p53 mutations include base substitutions, allelic loss, rearrangements, and deletions (Harris, C. C. *Science 262*: 1980, 1993). Point mutations resulting in base substitutions are clustered within a highly conserved region of the gene encoding exons 5-8, and mutations in this region substantially extend the half-life of the p53 protein. (Finlay, C. A. *et al. Mol. Cell. Biol. 8*: 531, 1988).

In addition to its prominent importance in lung carcinogenesis, the p53 gene plays a critical role in the cellular response to genetic damage caused by radiation. Specifically, the protein product of p53 induces a pause or block at the $G_1$ to S boundary of the cell cycle following radiation-caused DNA damage (Kastan, M. B. *et al. Cancer Res. 51*: 6304, 1991; Lane, D. P. *Nature 363*: 849, 1993). This $G_1$ block may allow the cell time to repair the damaged DNA prior to replication. Cells lacking a functional p53 protein fail to pause for repair and consequently accumulate mutations in the genome at an accelerated rate (Lowe, S. W. *et al. Nature 362*: 847, 1993). p53 has also been implicated as a controlling factor in apoptosis or in programmed cell death induced by DNA-damaging agents, such as ionizing radiation (Lowe *et al.*, 1993; Clarke, A. R. *et al. Nature 362*: 849, 1993).

The p53 gene is mutated in approximately 50% of squamous cell carcinomas from uranium miners who inhaled high doses of radon daughters (Vähäkangas, K. H. *et al. Lancet 339*: 576, 1992; Taylor, J. A. *et al. Lancet 343*: 86, 1993). The purpose of the present study was to determine if a similar percentage of squamous cell carcinomas with p53 mutations developed in the lungs of rats exposed to aerosols of $^{239}PuO_2$.

Aberrations in the p53 gene were investigated using an immunohistochemical (IHC) assay on 38 primary lung tumors (26 squamous cell carcinomas, nine adenocarcinomas, and three adenosquamous carcinomas) from rats that had inhaled $^{239}PuO_2$ aerosols. Animal exposures, necropsies, and tissue preparations have been previously described (Herbert, R. A. *et al. Radiat. Res. 134*: 29, 1993). Four-micrometer thick sections of 38 primary lung tumors were deparaffinized in xylene, rehydrated through a graded series of alcohol washes, and rinsed in automation buffer (Biomed, Inc., Foster City, CA). p53 specific immunoreactivity was determined by incubating each slide with anti-p53 antibody in PBS overnight at 4°C (CM1 polyclonal or DO7 monoclonal antibodies, Vector Laboratories Inc., Burlingame, CA). Bound primary antibody was detected by using a Vectastain® avidin-biotin complex kit (Vector Laboratories, Inc. Burlingame, CA) according to the manufacturer's directions. Slides were read in a blinded fashion and graded from 0 (no staining) to 4 (marked staining) according to the intensity of the staining pattern. Lesions with a staining intensity of 2 or greater were considered immunohistochemically positive.

Two large, well-differentiated squamous cell carcinomas (tumor numbers 460 and 551) were positive for nuclear staining (Fig. 1). The positive antibody staining was nuclear with patchy immunoreactivity of groups of cells throughout the neoplasm. Only the basilar, less well-differentiated, nonkeratinized cells stained with a score of 2 or more.

DNA for PCR amplification and sequencing was isolated from formalin-fixed lung tumor tissue embedded in paraffin histology blocks. A 4-$\mu$m section was stained with hematoxylin and eosine to permit histological classification of the tumor, and to guide dissection of the tumor from surrounding normal stroma. A 12-$\mu$m unstained adjacent section was then freed of normal stroma using a razor

blade. After deparaffinazation in xylene and ethanol, the DNA was extracted from the tissue by methods previously described (Ausubel, F. M. *et al. Current Protocols in Molecular Biology.* J. Wiley and Sons, New York, NY, 1987). Exons 5-7 of the rat which correspond to exons 5-8 in humans were amplified by PCR using a GeneAmp® DNA amplification kit and DNA thermocycler (Perkin-Elmer Cetus Corp., Norwalk, CT). Amplification primers and conditions have been previously described (Nickell-Brady, C. *et al. Carcinogenesis 15*: 257, 1994). DNA sequence analysis of the PCR products was performed using an Applied Biosystems 373 DNA sequencer (Applied Biosystems Inc., Foster City, CA) or traditional dideoxy-chain terminating sequencing (Sanger, F. S. *et al. Proc. Natl. Acad. Sci. USA 74*: 5463, 1977).

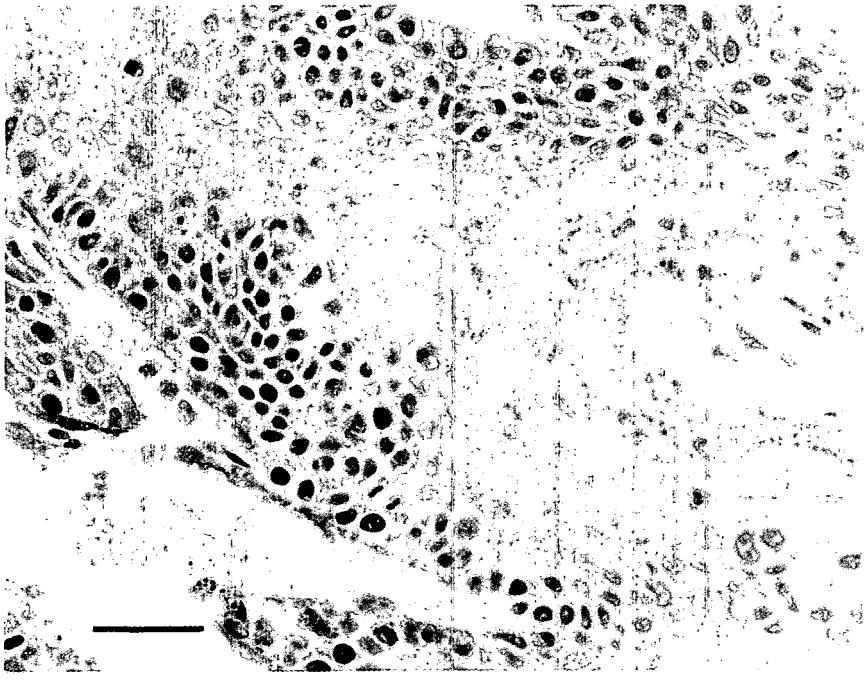

Figure 1. Photomicrographs of $^{239}$Pu-induced squamous cell carcinomas immunostained with an anti-p53 antibody. A) Tumor 551, IHC score of 4; and B) tumor 460, IHC score of 2; showing p53 specific immunoreactivity within the neoplastic epithelial cells. Bar equals 50 $\mu$m (Stain: avidin-biotin immunoperoxidase with hematoxylin counterstain). Magnification 520X.

Direct DNA sequencing was completed for six of the squamous cell carcinomas (four negative by IHC plus the two positives). No alterations in exons 5-7 were found in those tumors that were negative for elevated levels of the protein by IHC. Tumor 460 contained a G→A transition in the first position of codon 283, resulting in a lysine for glutamine substitution. Tumor 551 also contained a G→A transition, at the second position of codon 280 resulting in a histidine to arginine substitution.

Although mutation of the p53 gene is common in human lung tumors associated with excessive inhalation of radon daughters, only two of the 38 rat tumors examined exhibited abnormal p53 properties. Both IHC-positive tumors contained G→A transitions, which have been seen previously in this same collection of tumors for activating mutations in the Ki-*ras* protooncogene (Stegelmeier, B. L. *et al. Mol. Carcinogenesis 4*: 43, 1991). G→A transitions are also the most frequent mutation induced by α-particles *in vitro* using human lymphoblastoid cells (Jaberaboansari, A. J. *et al. Radiat. Res. 127*: 202, 1991). Such mutations may be the result of indirect oxidative damage mediated by hydroxyl radicals (Ward, J. F. *Prog. Nucleic Acid Res. Mol. Biol. 35*: 95, 1988). One possible

mechanism producing G→A transitions is the formation of apyrimidinic sites following removal of damaged cytosines. Under these circumstances, an adenine would be preferentially incorporated opposite the noninstructional base (Loeb, L. A. and B. D. Preston. *Annu. Rev. Genet. 20*: 201, 1986). Another possibility involves the deamination of cytosine to uracil resulting in a C→T base substitution (G→A on the opposite strand) (Tindall, K. R. *et al. Genetics 118*: 551, 1988). This latter suggestion is somewhat controversial, as cytosine deamination by ionizing radiation has been observed *in vitro*, but uracil has not been detected in mutagenized DNA *in vivo* (Breimer, L. E. *Br. J. Cancer 57*: 6, 1988).

The low number of tumors with p53 alterations in rats exposed to $^{239}PuO_2$ indicate that, compared to humans, rats commonly use molecular mechanisms for cell transformation processes that do not involve the p53 tumor suppressor gene. The nature of the cells at risk in the two species is also in keeping with the possibility of inherent differences in carcinogenesis mechanisms between rats and humans. In the lungs of uranium miners, most of the tumors are thought to have arisen in the secretory epithelium of the central airways (Panel of Dosimetric Assumptions Affecting the Application of Radon Risk Estimates, *Comparative Dosimetry of Radon in Mines and Homes.* National Academy Press, Washington DC, 1991). In contrast, the primary cell at risk for $^{239}PuO_2$-caused rat lung tumors is the type II pneumocyte (Herbert, R. A. *et al. Vet. Pathol. 31*: 366, 1994).

(Research sponsored by the Office of Health and Environmental Research, U.S. Department of Energy, under Contract No. DE-AC04-76EV01013.)

# DOSE-DEPENDENT *IN VIVO* CELL-CYCLE CHANGES FOLLOWING RADON PROGENY EXPOSURE

*Neil F. Johnson, Thomas R. Carpenter*, Albert W. Hickman*, Richard J. Jaramillo, and Debbie M. Gurule***

Exposures to low concentrations of alpha-emitting radon progeny are reported by the U. S. Environmental Protection Agency to be the second leading cause of lung cancer. Current risk estimates for lung cancer from the inhalation of radon progeny are based on data from underground uranium miners. To produce such risk estimates, calculations are based on several assumptions concerning exposure-response relationships rather than dose-response relationships. A better understanding of the mechanisms of interactions between alpha particles, the cells of the respiratory tract, and the progression toward cancer may validate the mathematical models used to derive risk estimates.

Recent work using sparsely ionizing radiation has shown a cascade of gene expression following exposure of cells *in vitro* (Kastan, M. B. *et al. Cancer Res. 51*: 6304, 1991). Levels of the p53 tumor suppressor gene protein are elevated after exposure to X rays and gamma radiation. The increase in p53 protein is triggered by DNA strand breaks and is temporally associated with arrest of the cell in the $G_1$ phase of the cell cycle (Nelson, W. G. and M. B. Kastan. *Mol. Cell Biol. 14*: 1815, 1994). This arrest is thought to provide time for the cell to repair the DNA damage. Much of this radiobiology has been conducted with established cell lines. However, a recent report shows that p53 protein is induced in basal keratinocytes of the intact human skin following exposure to ultraviolet radiation (Hall, P. A. *et al. Oncogene 8*: 203, 1993).

Work from our laboratory has recently demonstrated that alpha particles also induce elevated levels of p53 protein in irradiated cultures of a rat lung epithelial cell strain (Hickman, A. W. *et al. Cancer Res. 54*: 5797, 1994). The purpose of the present study was to determine whether exposure of rats to radon progeny results in measurable cell-cycle effects. The cells of the lateral wall of the anterior nose were chosen because of their accessibility and the ease of isolating them for cell-cycle analysis by flow cytometry.

Male Fischer 344/N rats (8-10 wk) were exposed to radon progeny and a vector aerosol in a closed-loop exposure system (Johnson, N. F. and G. J. Newton. *Radiat. Res. 139*: 163, 1994). In the first experiment, the time course of cells undergoing cell division was determined in 25 rats exposed to 1000 WLM using a vector aerosol of $10^4$–$10^5$ cigarette smoke particles per cubic meter, and in 10 rats exposed to vector aerosol alone. Following removal of the rats from the exposure chambers, groups of five exposed rats were injected intraperitoneally with 5-bromo-2′-deoxyuridine (BrdU) (50 $\mu$g/g body wt) immediately after exposure (approximately 2 h post exposure) or 2, 4, 8, and 16 d after exposure. The rats exposed to vector aerosol alone were injected with BrdU immediately after exposure and 16 d post exposure. The animals were sacrificed 2 h following BrdU exposure and the heads removed and decalcified in formic acid. The anterior nasal cavity was sectioned transversely at the level of the front incisor, and the tissue was embedded in paraffin wax; 5-$\mu$ sections were deparaffinized, and the cells containing BrdU were indirectly immunostained with a monoclonal antibody (Johnson, N. F. *et al. Toxicol. Appl. Pharmacol. 103*: 143, 1990). The number of cells incorporating BrdU was counted over the entire length of the lateral wall; the number of positive cells were expressed per mm of basement membrane (Johnson *et al.*, 1990). The data were tested for

*UNM/ITRI Inhalation Toxicology Graduate Student

**Minority High School Student Program Participant

equality of group means using the Tukey Studentized Range Method; the criteria for statistical significance was set at $p < 0.05$.

The second experiment determined the dose-dependent nature of any cell proliferation. Groups of six rats were exposed to 100, 250, 500, or 1000 WLM as described above, and groups of three rats were exposed to vector aerosol alone to correspond with each exposure level. After removal from the exposure chambers, the rats were injected with BrdU and sacrificed 2 h later. The rats and tissue were treated as above to determine the number of cells undergoing cell division. In the third experiment, temporal cell-cycle changes were delineated in 24 rats exposed to 1000 WLM, and six rats exposed to vector aerosol alone. Groups of six exposed rats were sacrificed immediately after removal from the exposure chamber and 2, 4, and 8 d post exposure. The epithelium of the lateral wall was removed and enzymically digested to form a single cell suspension (1989–90 Annual Report, p. 182). The suspension was fixed in 70% methanol and stained with Hoechst 33342 for flow cytometric cell-cycle analysis.

In the first experiment, the number of cells labeled with BrdU showed a significant decrease 2, 4, and 8 d after exposure (data not shown); the decrease in cell numbers was most marked 2 d post exposure. The number of cells labeled with BrdU in rats sacrificed immediately after exposure and 16 d post exposure showed no significant difference from the control values. In the second experiment, the number of cells labeled 2 d post exposure showed a dose-dependent decrease (Fig. 1). In the third experiment, the number of cells in the $G_1$ phase of the cell cycle showed a significant increase 8 d post exposure (Fig. 2).

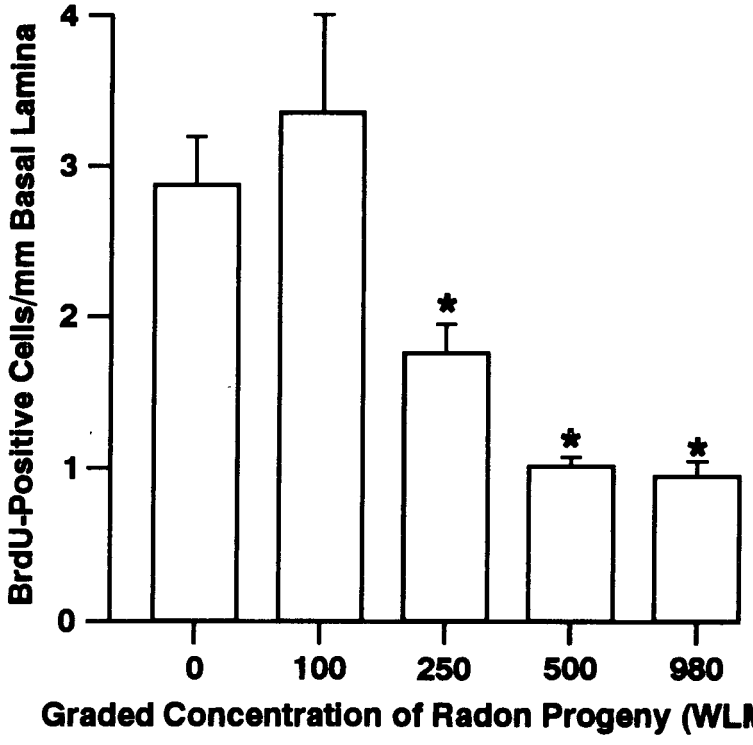


Figure 1. Number of BrdU-labeled cells per mm of basal lamina 2 d after exposure to graded concentrations of radon progeny. * represents a significant difference from the control value (Mean ± S.D.).

The results showed that inhalation of radon progeny by rats causes cell-cycle arrest. This arrest was evidenced by an increased number of cells in the $G_1$ phase of the cell cycle and a significant decrease in the number of cells synthesizing DNA following exposure to 500 WLM. An exposure to 500 WLM is equivalent to 1.2 Gy of alpha radiation, assuming a dose conversion factor of 2.4 mGy/WLM (Johnson and Newton, 1994). This dose is associated with a significant reduction in the colony-forming ability of cultured nasal epithelial cells (Johnson and Newton, 1994). These results show that epithelial cells exposed *in vivo* behave in a similar fashion to cells in culture with respect to radiation-induced, cell-cycle arrest. Whether the pattern of gene expression is also similar for *in vivo* and *in vitro* exposures to alpha radiation is the focus of our current investigation. If this pattern of gene expression is similar, a biodosimetric approach will be pursued to determine radiation dose to cells at cumulative exposures typical of the indoor environment.

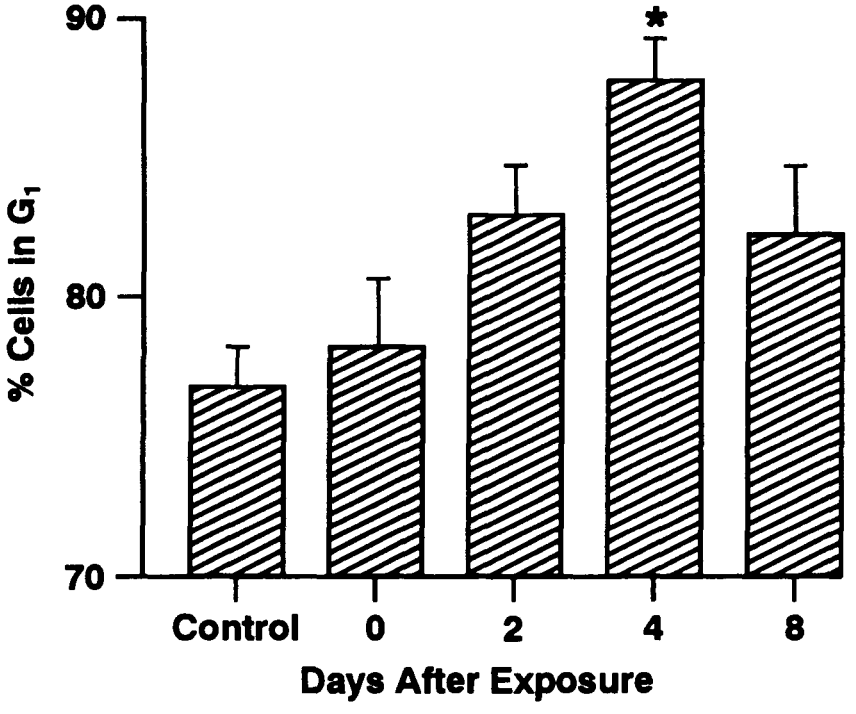


Figure 2. Fraction of cells in the $G_1$ phase of the cell cycle at various times after exposure to 1000 WLM. * represents a significant difference from the control value (Mean = ± S.D.).

(Research sponsored by the Office of Health and Environmental Research, U.S. Department of Energy, under Contract No. DE-AC04-76EV01013.)

# CELL-CYCLE SPECIFIC EXPRESSION OF A SMALL PROLINE-RICH PROTEIN IN CHINESE HAMSTER OVARY CELLS

*Johannes Tesfaigzi*

Squamous metaplasia of the bronchial epithelium is generally believed to be involved in the neoplastic progression toward squamous cell carcinomas. Thus, it is important to understand the mechanisms controlling this type of differentiation. The induction of two families of cDNAs encoding a small proline-rich protein (sPRP), sprI and sprII, was first identified in human keratinocytes exhibiting squamous differentiation (Kartasova, T. and P. van de Putte. *Mol. Cell. Biol. 8*: 2195, 1988). cDNAs similar to sprI have also been identified in cultured tracheal epithelial cells undergoing squamous differentiation (An, G. *et al. Am. J. Respir. Cell Mol. Biol. 7*: 104, 1992; Tesfaigzi, J. *Am. J. Respir. Cell Mol. Biol. 9*: 1434, 1993). The first step during the squamous differentiation process is the inhibition of cell growth (Masui, T. *et al. Proc. Natl. Acad. Sci. 83*: 2438, 1986); it has also been noted that sPRP mRNA in CHO cells is induced 10-fold just before the cultures reach confluence (unpublished data). Thus, sPRP may stop cell division in cells undergoing squamous differentiation. In support of this possibility are the recent investigations correlating expression of sPRP with cell morphology. Specific immunoreactivity to sPRP, using affinity-purified antibodies, showed a strong immunostaining in cells with a round configuration, while less staining was observed in other cells (unpublished data). The major part of the CHO population showed no immunoreactivity. One interpretation of this observation is that the expression of sPRP may be cell-cycle regulated.

The purpose of this investigation was to determine the phase of the cell cycle where induced synthesis of sPRP mRNA occurs. In order to determine levels of sPRP synthesis during cell division, CHO cells were first synchronized in $G_0/G_1$ phase of the cell cycle by maintaining confluent cells in 0.5% FBS containing medium for several days. This procedure resulted in an enriched population of $G_0/G_1$ cells (60%). The cells were then released from the $G_0/G_1$ block by passing cells at low density and increasing the serum content of the medium to 20%. After 14 h, 28% of the cell population was in $G_1/G_0$, and 60% of the population had reached the S-phase. Northern analysis of RNAs isolated from the cells harvested 0, 4, 8, 14, 26, and 30 h after release from $G_0/G_1$ showed that sPRP mRNA levels were high at the timepoint of release (0 h) until 8 h after release (Fig. 1). sPRP mRNA levels decreased by 90% at 14 h after release. Because the formation and activation of cyclin D1 are restricted to the $G_1$ phase of the cell cycle (Toyoshima, H. and T. Hunter. *Cell 78*: 67, 1994), the Northern blot was hybridized to cyclin D1 cDNA as control for transit through $G_1$. The levels of cyclin D1 mRNA increased 7-fold after 4 h and, similar to sPRP mRNA, were down-regulated once 60% of the cells entered the S-phase (Fig. 1). Hybridization to a GAPDH cDNA probe showed that similar amounts of mRNA were present in all lanes.

The results of this study show that the expression of the sprI gene is induced when CHO cells are in $G_0$ and during the $G_1$ phase of the cell cycle. The relationship of sPRP mRNA increase just before confluence and increased synthesis after release from $G_0/G_1$ is not clear. Cells enter $G_0$ after contact inhibition (Ciccarela, C. *et al. Mol. Cell. Biol. 4*: 1525, 1990). It is possible that increased synthesis of sPRP may be involved in the mechanisms of entering and exiting the $G_0/G_1$ phase. Further experiments are being conducted to clarify the expression of sprI mRNA and its relation to transit through the $G_0$ phase of the cell cycle. Thus, the role of sPRP in squamous differentiation may be to cause cells to enter $G_0$, so that mechanisms leading to terminal differentiation can occur.

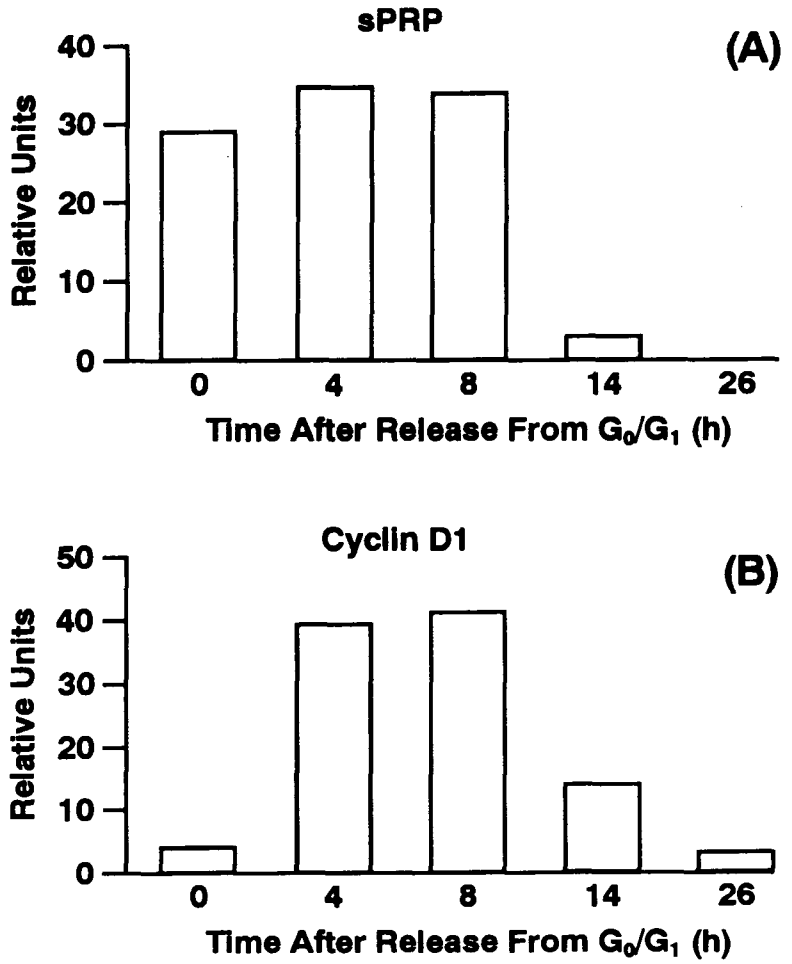


Figure 1. Relative expression of sPRP mRNA determined from Northern analysis of RNAs isolated from CHO cells after release from the $G_0/G_1$ block. (A) Levels of sPRP mRNA decreased 10-fold 14 h after release from the $G_0/G_1$ block; (B) cyclin D1 mRNA increased 7-fold 4 h after release and after 14 h decreased 6-fold. Data are from one experiment.

(Research sponsored by the Office of Health and Environmental Research, U.S. Department of Energy, under Contract No. DE-AC04-76EV01013.)

# DETECTION OF GENOMIC INSTABILITY IN NORMAL HUMAN BRONCHIAL EPITHELIAL CELLS EXPOSED TO $^{238}$Pu α-PARTICLES

*Christopher H. Kennedy, Noelle H. Fukushima*, Robin E. Neft, and John F. Lechner*

Alpha particle-emitting radon daughters constitute a risk for development of lung cancer in humans (Whittemore, A. S. and McMillan, A. *J. Natl. Cancer Inst. 71*: 489, 1983). The development of this disease involves multiple genetic alterations. These changes and the time course they follow are not yet defined despite numerous *in vitro* endeavors to transform human lung cells with various physical or chemical agents (Harris, C. C. *Cancer Res. 51*: 5023s, 1991). However, genomic instability, characterized both by structural and numerical chromosomal aberrations and by elevated rates of point mutations, is a common feature of tumor cells. Further, both types of genomic instability have been reported in the noncancerous progeny of normal murine hemopoietic cells exposed *in vitro* to α-particles (Kadhim, M. A. *et al. Nature 355*: 738, 1992; Wright, E. G., personal communication). The purpose of this investigation was to determine if genomic instability is also a prominent feature of normal human bronchial epithelial cells exposed to α-particle irradiation from the decay of inhaled radon daughters.

NHBE cells from a nonsmoking, 15 y-old male were purchased (Clonetics, San Diego, CA). The cells were cultured and passed to sample cups with a bottom surface consisting of a 1.5 μm thick Mylar® film to facilitate exposure to $^{238}$Pu α-particles, which have a track length of approximately 35 μm in soft tissue (Walsh, P. J. *Health Physics 19*: 312, 1970). NHBE cells were exposed six times over a 17 d period to a dose of either 0.33 Gy or 0.67 Gy of α-particles emanating from a stainless steel disk that had been electroplated with sufficient $^{238}$Pu to provide 0.857 Gy min$^{-1}$ of α-particle energy. One week after the final exposure, foci of PACs (characterized by a distinct colony of cells with a high mitotic index) were detected in 40 of 64 (63%) cultures of NHBE cells exposed to a total of 4.0 Gy of α-particle energy and in 14 of 68 (21%) cultures exposed to a total of 2.0 Gy of α-particle energy. The PACs were passed into plastic dishes and continuously passaged as the cultures became confluent. Approximately six to eight population doublings transpired with each sequential subculturing.

Evidence for structural genomic instability was assessed by two assays in individual cultures of phenotypically altered cells (PACs). The first assay detected binucleated cells (Tolbert, P. E. *et al. Mutat. Res. 271*: 69, 1992); the second identified cells containing micronuclei (Heddle, J. A. *et al. Mutat. Res. 123*: 61, 1983). Samples of cells from passages three through six were fixed in Shandon's Cytospin Collection Fluid® (Shandon, Pittsburgh, PA) and cytospun onto a microscope slide. To assay for binucleated cells, the cells were stained with the Hema 3 Staining System® (Curtis Matheson Scientific, Houston, TX), a colorimetric nuclear stain. Propidium iodide (Sigma, St. Louis, MO), a fluorescent dye, was used for the micronuclei assay. The samples was scored blind. Five hundred cells per sample were counted to score binucleated cells. One thousand cells per sample were counted to score micronucleated cells.

Figure 1A shows the relationship between the percentage of binucleated cells and radiation dose. The results showed an increase in the number of binucleated cells in a portion of the PAC progeny of NHBE cells exposed to α-particles. Thus, by this assay, 24% percent of the PAC cultures scored exhibited genomic instability many (> 30) cell divisions post irradiation. Figure 1B shows the relationship between the percentage of micronucleated cells and radiation dose. This form of genomic

*Department of Energy/Associated Western Universities Summer Student Research Participant

instability was present in 62% of the PACs analyzed after radiation exposure. Further, the experiment showed evidence that some PACs exhibit delayed genomic instability.

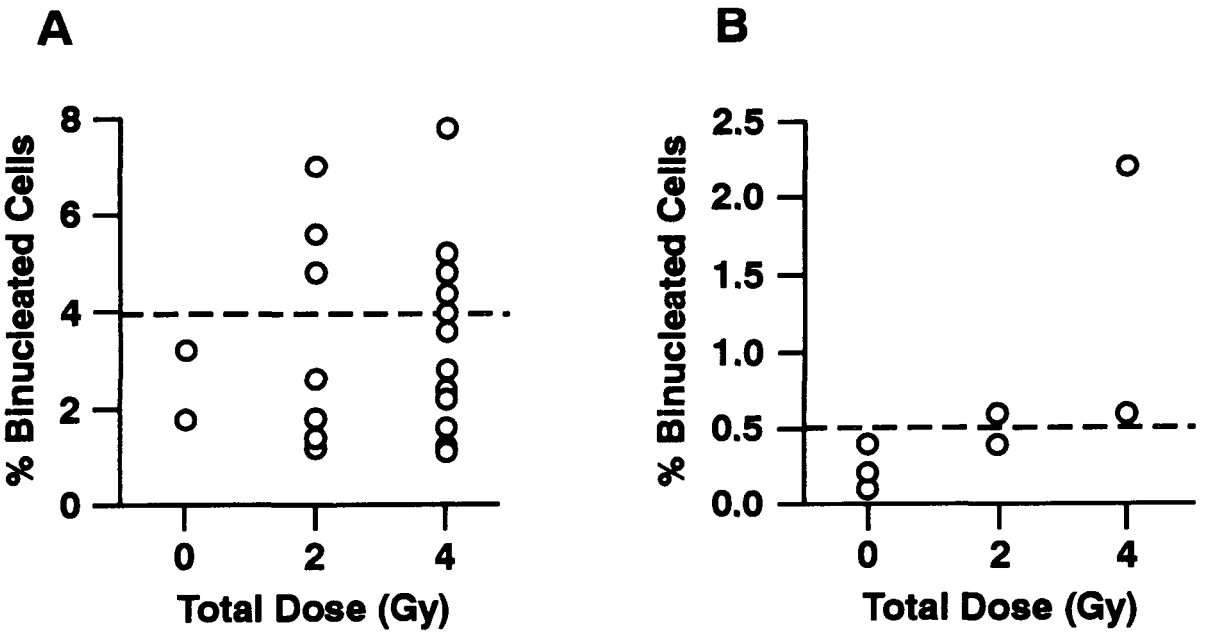


Figure 1. Relationship between the level of either (A) binucleated cells or (B) micronucleated cells and dose of α-particles. Cells were fixed in 4th passage. The dashed line denotes the cutoff value for identification of a cell culture as being phenotypically altered.

The fact that elevated levels of binucleated and micronucleated cells were detected in the extended progeny of NHBE cells exposed to α-particles indicates that these chromosomal aberrations were not a direct consequence of damage induced by ionizing radiation. Rather, some cells apparently survive α-particle-induced DNA damage and give rise to progeny that exhibit genomic instability. Future experiments will evaluate whether the progeny of α-particle-exposed NHBE cells also exhibit genomic instability exemplified by higher mutation rates, and if this kind of genomic instability is independent of chromosomal instability. Phenotypically altered cells determined to exhibit genomic instability after exposure to α-particles will ultimately be used to identify loss of a gene or genes responsible for maintaining genomic stability. Mutation or deletion of stability genes is believed to be responsible for the development of a mutator phenotype that ultimately develops into a malignant phenotype (Loeb, L. A. *Cancer Res. 54*: 5059, 1994). Since the development of a mutator phenotype appears to be an early event in carcinogenesis, identification of stability genes in NHBE cells will provide markers for early genetic alterations/dysfunctions involved in the development of lung cancer.

(Research sponsored by the Office of Health and Environmental Research, U.S. Department of Energy, under Contract No. DE-AC04-76EV01013.)

# ANALYSIS OF GENOMIC INSTABILITY IN BRONCHIAL CELLS FROM URANIUM MINERS

*Robin E. Neft, Steven A. Belinsky, Frank D. Gilliland*, and John F. Lechner*

Epidemiological studies show that underground uranium miners have a radon progeny exposure-dependent increased risk for developing lung cancer (Saccomanno, G. C. *et al. Health Phys. 50*: 605, 1986). The odds ratios for lung cancer in uranium miners increase for all cumulative exposures above 99 Working Level Months. In addition, there is a strong multiplicative effect of cigarette smoking on the development of lung cancer in uranium miners (*Radon and Lung Cancer Risk, NIH/NCI,* Publication # 94-3644, 1994). The purpose of this investigation was to determine whether or not early genetic changes, as indicated by genomic instability, can be detected in bronchial cells from uranium miners. Investigations of this nature may serve as a means of discovering sub-clinical disease and could lead to earlier detection of lung cancer and a better prognosis for the patient.

There is evidence that high-linear-energy-transfer (LET) radiation produces genomic instability (Kadhim, M. A. *et al. Nature 355*: 738, 1992) which leads to chromosome damage and increases the risk of developing cancer. One assay to detect genomic instability is to determine the frequency of micronuclei (MN), which are extranuclear chromosomes or chromosome fragments. Formation of MN is thought to occur through chromosome breakage or interference with the mitotic spindle apparatus (Krepinsky, A. B. and J. A. Heddle. *Radiation Induced Chromosome Damage In Man,* Alan R. Liss, Inc., New York, NY, 1983). Airway epithelial cells can be obtained from uranium miners by bronchial brushing at various time points post-exposure to radon and used to study genomic instability over time.

Through a collaboration with the University of New Mexico, bronchial epithelial cells were obtained by fiberoptic bronchoscopy of four areas (left upper and lower lobe, right upper and lower lobe) in the lungs of 10 healthy former uranium miners who have not mined uranium for the past 15 years (eight ex-smokers and two nonsmokers). The cells were cultured in 60-mm tissue culture dishes coated with fibronectin (BRFF, Ijamsville, MD) in Bronchial Epithelial Cell Growth Medium (Clonetics, San Diego, CA). Cytospins were prepared from ethanol-fixed bronchial cells obtained from cultures at passage 1, 2, or 3. The cells were washed with 1x Sodium Chloride/Sodium Citrate (SSC), then incubated overnight in 0.001M SSC (pH 10) at 55°C. Next, the bronchial cells were washed successively in cold 1xSSC, Dulbecco's Phosphate Buffered Saline (DPBS)/0.5% Brij (Sigma, St. Louis, MO) and finally in DPBS alone. DNA was visualized with propidium iodide (Sigma) which stains DNA. Using a confocal microscope, MN per 1000 cells were scored on coded slides.

To date, bronchial cells obtained from one site each from two former uranium miners were found to contain 10 MN per 1000 cells. Examination of two different lung sites in another uranium miner suggested that genomic instability was evident in one brushed area of the lung, but not in the other. In this miner, bronchial cells from one area of the lung contained 43 MN per 1000 cells, a frequency several fold higher than baseline values. Published values for MN in different cell types from unexposed individuals range from 1-10/1000 (Titenko-Holland, N. *et al. Mutat. Res. 312*: 39, 1994; da Cruz, A. D. *et al. Mutat. Res. 313*: 57, 1994). Bronchial cells from another area of the same miner's lungs contained only 6 MN per 1000 cells. This suggests that differences in genomic stability exist in distinct areas of the lung and could mark areas of increased susceptibility to lung cancer development. In order to test this hypothesis, MN formation is being quantitated in cells propagated from all four sites from the 10 former uranium miners.

---

*University of New Mexico, Albuquerque, New Mexico

This investigation may lead to a better understanding of the early genetic changes that occur following exposure to high-LET radiation and a better identification of persons at greatest risk of developing lung tumors.

(Research sponsored by the Office of Health and Environmental Research, U.S. Department of Energy, under Contract No. DE-AC04-76EV01013).

# CLONING OF THE RAT *Waf1/Cip1* GENE

*Steven A. Belinsky and Susan K. Middleton*

The progression of eukaryotic cells through the cell cycle involves the sequential expression of specific genes. This process is regulated by both external and internal stimuli that prevent the cell from prematurely entering the next phase before all macromolecular events have been completed. The activation and subsequent inactivation of cyclin dependent kinases (Cdks) represent one internal stimuli required to regulate the transit of cells from one stage of the cell cycle to the next (Sherr, C. J. *Cell 73*: 1059, 1993). Another member of this regulatory cascade is the p*53* tumor suppressor gene, which controls a $G_1$ checkpoint at which the cell cycle can be arrested prior to the initiation of DNA synthesis (Lin, D. *et al. Proc. Natl. Acad. Sci. (USA) 89*: 9210, 1992). Following DNA damage, p*53* protein levels rise, and entry into S phase is delayed, presumably to allow time for repair of the lesions (Kastan, M. B. *et al. Cell 71*: 587, 1992). When p*53* function is lost, cells containing damaged DNA template enter S phase leading to fixation and propagation of genetic alterations. Recently, evidence linking the growth-suppressing activity of p*53* and inactivation of Cdks has been provided by the cloning of the *Waf1/Cip1* gene (El-Deiry, W. *et al. Cell 75*: 817, 1993). *Waf1/Cip1* encodes a protein of $M_r$ 21,000 (p*21*), which inhibits Cdks *in vitro* (Xiong, Y. *et al. Nature (Lond.) 366*: 701, 1993). The overexpression of *Waf1/Cip1* in cells inhibits cell growth, suggesting that p*21* is a downstream mediator of p*53* function. Loss of *Waf1/Cip1* gene function could lead to deregulation of the cell cycle and contribute to the development of the neoplastic phenotype in tumors that do not contain mutations in the p*53* gene.

Previous investigations have examined the prevalence for alteration of the p*53* gene in lung tumors induced in the F344/N rat by fractionated exposure to X-rays. Three of 18 squamous cell carcinomas, but none of 17 adenocarcinomas showed nuclear p*53* immunoreactivity (1992-1993 Annual Report, p. 87). Single-strand conformation polymorphism analysis of exons 4-9 of the p*53* gene detected only an exon 9 mutation in one squamous cell carcinoma. These results indicate that mutations in the p*53* gene are infrequent in X-ray-induced lung tumors. The purpose of the present investigation was to clone the rat *Waf1/Cip1* gene, then determine the frequency for alteration of this gene in lung tumors induced by X-rays.

The *Waf1/Cip1* gene contains three exons of 68, 450, and 1600 bp (exon 1, 2, and 3, respectively) as depicted in Figure. 1. The translation initiation signal was contained in exon 2 (Sterner, D. A. and S. M. Berget *Mol. Cell Biol. 13*: 2677, 1993). The termination signal was located 49 bp inside of the 5' end of exon 3. Thus, the major coding portion of this gene is contained within exon 2. Primers to amplify the rat *Waf1/Cip1* sequence by the polymerase chain reaction (PCR) were designed based on regions within exon 2 which exhibited maximum homology between the published human and mouse sequences. The 5' primer was located at nucleotide 108, and the position of the 3' primer was at nucleotide 429 of exon 2. Primer sequences were as follows: 5' primer, 5'-CAGTTGAGCCGTGATTGC-3', and 3' primer, 5'-GGTCTGCCTCCGTTTTCG-3'. This portion of the rat *Waf1/Cip1* exon 2 was amplified using 200 ng of genomic template DNA by PCR. Amplification was carried out for 35 cycles consisting of 96°C for 30 sec, 52°C for 30 sec, and 72°C for 30 sec. The PCR product, a 352 bp DNA fragment was electrophoresed through a 1.5% agarose gel and visualized by ethidium bromide staining. This PCR product was then cloned using the TA Cloning™ system (Invitrogen, San Diego, CA). The clones containing this insert were sequenced using a Sequenase kit® (United States Biochemicals Co., Cleveland, OH). Single strand conformation polymorphism analysis (SSCP) was used to screen lung tumors for possible mutations within this portion of exon 2. SSCP detects single base substitutions within DNA fragments up to 350 bp in

length as shifts in electrophoretic mobility. Details of this procedure have been described by Suzuki, Y. *et al.* (*Oncogene 5*: 1037, 1990).

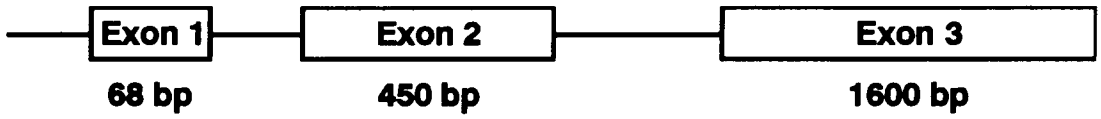


Figure 1. Schematic of the coding regions of the *Waf1/Cip1* gene.

The sequence of codons 35 - 139 of exon 2 from the rat *Waf1/Cip1* gene is depicted in Table 1. Nucleotide homology of 75% and 89% was observed between rat and human or mouse sequences, respectively. Amino acid homology to human and mouse sequences was reduced to 57% and 64%, respectively. Nucleotide homology degenerated at the 3' portion of this fragment (codons 105 - 139). Two of 23 tumors examined by SSCP exhibited polymorphisms within this region of exon 2. Sequencing of the entire *Waf1/Cip1* cDNA and identifying the mutations are underway. Once sequenced, codons 1-34 and 140-150 will also be examined for mutations by SSCP analysis. The present results indicate that the *Waf1/Cip1* gene is conserved across species and that inactivation of this gene by mutation is not common in lung tumors induced in the rat by X-rays.

Table 1

Nucleotide Sequence (Codons 35 - 139) of the Rat
*Waf1/Cip1* Gene Beginning at Nucleotide 103

| | | | | | | | | | | | | | | | | |
|---|---|---|---|---|---|---|---|---|---|---|---|---|---|---|---|---|
| 103 | GAT | GCG | CTC | ATG | GCG | AGC | TGT | CTC | CAG | GAG | GCC | CGA | GAA | CGG | TGG | ACC | TTT | GAC |
| 157 | TTC | GCC | ACT | GAG | ACG | CCA | CTG | GAG | GGC | AAC | TAC | GTC | TGG | GAG | CGT | GTT | CGG | AGC |
| 211 | CCA | GGG | CTG | CCC | AAG | ATC | TAC | CTG | AGC | CCT | GGG | TCC | CGC | CGC | CGT | GAT | GAC | CTG |
| 265 | GGA | GGG | GAC | AAG | AGG | CCC | AGT | ACC | TCC | TCG | GCC | CTG | CTG | CAG | GGC | CAG | GGC | CAG |
| 319 | CTC | CGG | AGG | ACC | ACG | TGG | CCT | TGT | CGC | TGT | CTT | CGA | CTC | TGG | TGT | CTC | ACG | CCC |
| 373 | CTG | AGA | GGC | CTG | AAG | ACT | CCC | GGG | CGG | GAC | CGG | GAC | ATC | TCA | GGG | C | | |

(Research sponsored by the Office of Health and Environmental Research, U.S. Department of Energy, under Contract No. DE-AC04-76EV01013.)

# LOSS OF HETEROZYGOSITY ON CHROMOSOME 15 IN HUMAN LUNG CARCINOMAS

*Charles E. Mitchell, William A. Palmisano, and John F. Lechner*

Loss of heterozygosity (LOH) in tumors may be associated with the inactivation of tumor suppressor genes. A tumor suppressor gene for lung cancer may reside on chromosome 15, because deletions in this chromosome are frequently observed (Testa, J. R. and J. M. Siegfried. *Cancer Res. 52:* 2702, 1992).

Recently, it was reported that a newly discovered gene, GTPase-activating protein-3 (GAP3) maps to chromosome 15 (Benards, A., personal communication). GAP3 is a member of a family of GAP-related genes (Boguski, M. S. and F. McKormick. *Nature 366*: 643, 1993). Although the precise function of GAP3 is not known, it is thought that GAP3 is involved in the regulation of *ras*-like GTPase activities (Boguski and McKormick, 1993). *Ras* proteins have a low intrinsic activity, and their inactivation is dependent on GAPS *in vivo*. Oncogenic mutants of *ras* proteins, for example, at codons 12, 13, or 61, are resistant to GAP-mediated GTPase stimulation and are constituitively locked in their active, GTP-bound states (Trahey, M. and F. McKormick. *Science 238*: 542, 1987).

The finding that *ras* interacts with GAP through its effector domain raised the possibility that the GAP protein may be an immediate target for the *ras* protein. On the other hand, the finding that overexpression of GAP protein induced reversion in NIH3T3 cells transformed by an overexpressed c-*ras* gene seems to support the hypothesis that GAP is an upstream regulator for *ras*. It has been suggested that one possible hypothesis to explain the different GAP-related activities is that GAP has two functions: the complex of GAP with Krev-1 (a gene overexpressed in cells transformed by a mutated ras oncogene) plays a positive role in reversion, and at the same time GAP shuts off the growth signal transduced through *ras* (Noda, M. *et al. Proc. Natl. Acad. Sci. 86*: 162, 1989). In any event, a loss of GAP interactions through either a deletion, a mutation, or a rearrangement in the GAP gene, such as GAP3 will likely affect *ras*—related activities. The purpose of this investigation was to determine the frequency and extent of the LOH of GAP3 in a group of patients with lung cancer.

Thirty samples of tumor tissue and corresponding normal tissue were obtained from the New Mexico Tumor Registry. All tissues were quickly frozen in liquid nitrogen and stored at –80°C until analyses. DNA was isolated from tissue using a standard phenol-chloroform extraction method. Ten micrograms of high molecular DNA was digested with *Hpa 1* or *Rsa 1* restriction endonucleases (New England Biolabs, Beverly, MA) and subjected to electrophoresis through an 0.8% agarose gel. DNAs were transferred by capillary action to a Zeta-Probe GT blotting membrane (Bio-Rad, Hercules, CA) using 0.4 M NaOH. Prehybridization was carried out for 2 h at 65°C in 7%SDS/0.25 M $Na_2PO_4$. The GAP3 DNA probe was kindly provided by Dr. Andre Benards (Massachusetts General Hospital, Boston, MA). The GAP3 probe was labeled with [$^{32}$P] dCTP by random primer extension. The probe ($1 \times 10^9$ DPM) was added to the hybridization buffer and hybridized overnight at 65°C. The membrane was washed for 30–60 min in 5% SDS/20 mM $Na_2PO_4$ at 45°C. Autoradiography was performed for 24–72 h at –70°C. To quantitate the changes affecting GAP3, audioradiographs of the blots were scanned with a laser densitometer to determine the ratios of hybridization of restriction fragments obtained from normal and tumor DNA. A LOH was scored when the ratio of the allele fragment in the tumor DNA was less than 50% of the signal seen in normal tissue. The ratios were also used to obtain a factor to correct for differences in DNA loading.

Normal DNA from four individuals was screened initially with a large number of restriction endonuclease enzymes to identify informative alleles, i.e., two fragments or more present in DNA from

normal individuals. Loss of one of these fragments in DNA from the tumor would indicate an allelic deletion. Two restriction endonucleases, *Rsa 1* and *Hpa 1*, produced informative alleles, thus; they were used in the initial screening of tumor DNAs for LOH. Of the nine tumor-normal DNA pairs analyzed after *Rsa 1* digestion and GAP3 hybridization to date, one was uninformative, i.e., DNA degraded with the appearance of light bands, or DNA was homozygous with the appearance of only one allele in DNA from normal individuals. Of the eight informative sample pairs, one demonstrated an LOH as shown in Figure 1. Two major and one minor allele fragments of 1.6 Kb, 1.8 Kb, and 1.1 Kb were observed following *Rsa 1* digestion and GAP3 hybridization. The major alleles (more intense bands) are thought to represent a higher sequence homology between the allele and the probe. The tumor DNA showed a reduced intensity of the 1.1 Kb fragment. The remaining band in the tumor sample was probably contributed by normal tissue. Of the nine tumor-normal DNA pairs digested with *Hpa 1* and probed with GAP3, three were informative. One of the three DNA samples showed a potential rearrangement of the GAP3 gene with the appearance of a 8 Kb fragment.

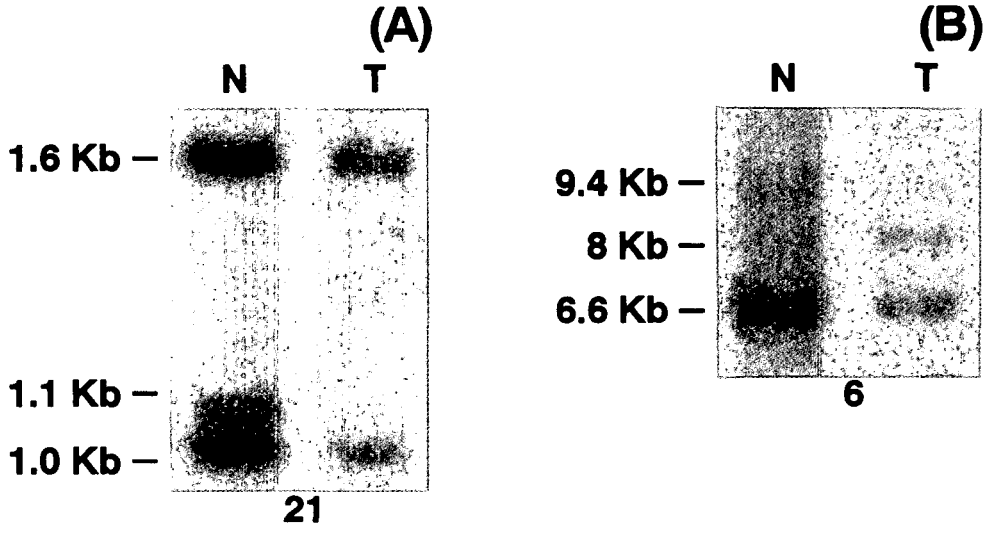


Figure 1. Representative Southern analysis of DNA from normal lung (N) and tumor (T) tissue. DNA was digested with restriction enzymes *Rsa 1* (A) and *Hpa 1* (B), electrophoresed, blotted, and hybridized to the GAP3 cDNA probe. Arrows point to gene fragments that are deleted or rearranged.

In the small sample set analyzed to date, the frequency of LOH ranged from 10%–25%; however, a larger sample set is necessary to obtain a more reliable estimate of the frequency of the genetic alteration that occurs on the GAP3 gene in lung cancer. The actual frequency of LOH or rearrangements may also change, due to the fact that only a portion of the GAP3 gene (5′ cDNA fragment) is available at this time for use as a probe. Further analysis will also use a probe containing the 3′ cDNA fragment.

Future studies will focus on a thorough analysis of the structural alterations of the GAP3 gene and the relationship of these alterations to the development and progression of lung cancer.

(Research sponsored by the Office of Health and Environmental Research, U.S. Department of Energy, under Contract No. DE-AC04-76EV01013.)

# K-ras MUTATIONS IN BERYLLIUM-INDUCED MOUSE LUNG TUMORS

*Steven A. Belinsky and Charles E. Mitchell*

Previous studies at ITRI have shown that single, nose-only exposure of F344/N rats to beryllium metal (Be) produced a 64% incidence of lung tumors over the lifetime of the rat (1992-93 Annual Report, p. 53). Lung tumors induced by Be metal were subsequently analyzed for alterations in the K-*ras* and p*53* genes. Mutation of the K-*ras* gene was both a rare (2 of 24 tumors) and late event in Be-induced carcinogenesis (Nickell-Brady, C. *et al., Carcinogenesis 15*: 257, 1994). In addition, no mutations were detected in exons 5 - 8 of the p53 gene. These results indicated that the mechanisms underlying the development of Be-induced lung cancer in rats did not involve gene dysfunctions commonly associated with human non-small-cell lung cancer.

The A/J mouse strain is not only susceptible to lung tumor induction by chemical carcinogens but also has a high incidence of spontaneous pulmonary tumors (Shimken, M. and G. Stoner, *Adv. Cancer Res. 21*: 1, 1975). Characterization of both spontaneous and chemically induced tumors indicated that activation of the K-*ras* protooncogene was involved in cell transformation. The activating mutations in this gene could be ascribed to the inducing carcinogen (e.g., methyl-N-nitrosourea, benzo(a)pyrene, or dimethylnitrosamine), because the mutation profiles were unique for each class of compound and for the spontaneous tumors (You, M. *et al., Proc. Natl. Acad. Sci. (USA) 86*: 3070, 1989; Belinsky, S. A. *et al., Cancer Res. 49*: 5305, 1989). These studies indicate that the A/J mouse is a sensitive system to study the mechanism of *ras* oncogene activation by chemicals. Moreover, for chemicals such as Be which induce tumors but are nonmutagenic in Salmonella assays (Ashby, J. M. *et al., Mutat. Res. 240*: 217, 1990), the comparison of molecular lesions in tumors from control and treated animals could help elucidate whether the "nongenotoxic" chemical is acting *in vivo* by a direct or indirect mechanism (e.g., as a promoter or via cytotoxicity) to activate a protooncogene. The purpose of this study was to determine and compare the prevalence and specificity for mutation of the K-*ras* gene in lung tumors induced in the A/J mouse by Be to mutations present in spontaneous tumors.

Lung tumors were induced in A/J mice by a single, nose-only exposure to Be metal as described in detail by Nikula, K. J. *et al.* (this report, p. 81). DNAs were prepared by the method of Levi, S. *et al.* (*Cancer Res. 51*: 3497, 1991) from 23 Be-induced and four spontaneous tumors. Tumor tissue was microdissected from 5 $\mu$m unstained, paraffin sections. K-ras exons 1 and 2 were amplified as previously described (Nickell-Brady *et al.*, 1994). Direct sequencing of the polymerase chain reaction products was performed using the dideoxy chain termination method with Sequenase$^{TM}$DNA polymerase (Tindall, K. and L. Stankowski. *Mutat. Res. 220*: 241, 1989). An additional 18 spontaneous tumors with previously characterized K-*ras* mutations were included in this investigation to facilitate comparisons with Be-induced tumors. Statistical analysis was performed using a two-sided Fisher Exact test.

Mutation of the K-*ras* gene was detected in 18 of 23 Be-induced lung tumors (Table 1). Sixty-seven percent of the mutations were localized to codon 12; however, no hotspot for activation was observed. The mutation profile within codon 12 did not differ between Be-induced and spontaneous lung tumors (Table 1). Four different nucleotide substitutions were observed in codon 61 in Be-induced tumors. In spontaneous tumors, CAA to CGA transversions comprised 78% of the codon 61 mutations, while only one of six (17%) of the codon 61 mutations detected in Be-induced tumors involved this nucleotide substitution. Twenty-two percent of the Be-induced tumors did not contain a mutation within exon 1 or 2.

Table 1

Patterns of Mutations in the K-*ras* Gene in Spontaneous and Beryllium-Induced Adenocarcinomas in the A/J Mouse by NNK

| | | Codon 12 | | | | | Codon 61 | | | | |
|---|---|---|---|---|---|---|---|---|---|---|---|
| | | Normal | Mutations | | | | Normal | Mutations | | | |
| Treatment | Frequency of Activated K-*ras* | GGT Gly | GTT Val | GAT Asp | CGT Arg | TGT Cys | CAA Gln | CGA Arg | CAT His | CTA Leu | CAC His |
| None[a] | 22/22 | | 6 | 5 | 1 | 1 | | 7 | 2 | 0 | 0 |
| Beryllium | 18/23[b] | | 3 | 6 | 2 | 1 | | 1[c] | 2 | 2 | 1 |

[a]Data from Belinsky *et al.* (1989) and You *et al.* (1989), four spontaneous tumors from the current study.
[b,c]$p < 0.05$ as compared to no treatment.

The lack of specificity for mutation of the K-*ras* gene by Be supports the hypothesis that this carcinogen may be acting through nongenotoxic mechanisms. The promotion of spontaneous K-*ras* mutations by Be metal could result from the chronic inflammatory response that ensues following the deposition of Be particles in the lung. The recruitment of macrophages, neutrophils, and lymphocytes and the potential for the release of cytokines and oxygen radicals by these cells could induce cellular damage, cell proliferation, and altered homeostasis. The fact that 22% of the Be-induced tumors did not contain mutations within exon 1 or 2 also suggests that other oncogenes could be involved in tumor induction by this carcinogen.

(Research sponsored by the Office of Health and Environmental Research, U.S. Department of Energy, under Contract No. DE-AC04-76EV01013.)

# INCREASED CYTOSINE DNA-METHYLTRANSFERASE ACTIVITY IN A/J MOUSE LUNG CELLS FOLLOWING CARCINOGEN EXPOSURE AND DURING TUMOR PROGRESSION

*Steven A. Belinsky, Jean-Pierre J. Issa*, and Stephen B. Baylin**

Considerable evidence has accumulated that 5-methylcytosine modification of mammalian DNA, both in exons and CpG rich islands located in promoter regions, is important in gene regulation (Holliday, R. *Science 267*: 163, 1987). For example, a decrease of 5-methylcytosine in 5' flanking regions or exons of genes has been associated with increased gene transcription (Holliday, 1987). In addition hypermethylation at specific regions of chromosomes 17p and 3p have also been observed in lung and colon cancer (Makos, M. *et al., Proc. Natl. Acad. Sci. [USA] 89*: 1929, 1992). During colon cancer development, these hypermethylation changes precede allelic loss (Makos *et al.*, 1992). In addition, the activity of the enzyme which maintains the methylation status at CpG dinucleotides, DNA methyltransferase (MT), has been shown to increase during colon cancer progression (Issa, J. P. J. *et al., J. Natl. Cancer. Inst. 15*: 1235, 1993). These observations suggest changes in methylation patterns within specific genes could result in either inappropriate gene expression or gene deletion, both of which would contribute to the establishment of the malignant phenotype.

Recent investigations by our laboratory have used inbred strains of mice as a model for identifying progenitor cells and for studying the development and progression of pulmonary neoplasia (Belinsky, S. A. *et al., Cancer Res. 52*: 3164, 1992). Following treatment of A/J mice with the tobacco-specific nitrosamine 4-methylnitrosamino-1-(3-pyridyl)-1-butanone (NNK), pulmonary tumors developed as a focal proliferation of the alveolar type II cell. These hyperplasias subsequently progressed to adenomas and ultimately carcinomas. The purpose of this investigation was to determine if DNA MT activity is elevated in target (alveolar type II), but not in nontarget (Clara, endothelial, macrophage) lung cells isolated from the A/J mouse following exposure to NNK. In addition, the activity of this enzyme during tumor progression was examined.

Mice (6-8 wk old) were treated three times (every other day) with NNK (50 mg/kg, i.p.) dissolved in saline. Animals were sacrificed 1, 3, 7, and 14 d after treatment. Lung tumors were induced by treatment of mice three times a week for 7 wk with NNK (50 mg/kg, i.p.). Lungs from 18 mice were pooled for each cell isolation. Alveolar macrophages were obtained by pulmonary lavage. Small cells (endothelial cells and lymphocytes), type II, and Clara cells were obtained by centrifugal elutriation following protease digestion of the lungs. (Belinsky *et al.*, 1992). Purity of type II and Clara cell preparations was 71% ± 2 and 72% ± 2, respectively. A fraction of the isolated lung cells ($1 \times 10^6$) was fixed in 4% paraformaldehyde, incubated with RNase, and the DNA stained with propidium iodide. The percent of cells in S phase was determined by a flow cytometric analysis.

A modification of the assay developed by Adams, R. L. P. *et al.* (*J. Biochem. Biophys. Meth. 22*: 19, 1991) was used to determine DNA MT activity. Cell lysates containing 5 $\mu$g of protein were incubated for 2 h at 37°C with a dI-dC template and $^3$H S-adenosyl methionine. Reactions were stopped, protein extracted, and deoxyinsosine-deoxycytidine template recovered by ethanol precipitation. RNA was removed by resuspension of the precipitates in NaOH, DNA was spotted on Whatman filters, dried, then washed with TCA followed by 70% ethanol. Filters were placed in scintillation cocktail, and MT activity was determined by scintillation counting. Results are expressed as dpms/$\mu$g protein. Statistical analysis was performed using a Student's *t*-test.

*Johns Hopkins University, Baltimore, Maryland

Endogenous activity of MT was similar between the isolated cell fractions. One day following treatment with NNK, MT activity was increased significantly in both type II cells and macrophages (Table 1). Enzyme activity declined in macrophages to endogenous rates by 14 d post treatment. In contrast, MT activity continued to increase in type II cells for at least 1 wk. No effect on MT activity following NNK treatment was observed in Clara cells. Moreover, enzyme activity was three-times greater in type II cells than Clara cells 1 wk after cessation of NNK (Table 1). The percentage of type II, Clara, and small cells in S phase 3, 7, or 14 d post NNK treatment did not differ from cells isolated from unexposed mice (data not shown).

A role for aberrant MT activity in cellular transformation has been described (Wu, J. *et al., Proc. Natl. Acad. Sci. [USA] 90:* 8891, 1993). The overexpression of an exogenous mouse DNA MT gene in NIH 3T3 cells caused a marked increase in overall DNA methylation which was accompanied by tumorigenic transformation. At present, the mechanism underlying the increase in MT activity in type II cells is not known. DNA MT is induced to maintain the DNA methylation pattern during cell replication (Szyf, M. *et al., J. Biol. Chem. 260*: 8653, 1985); however, no increase in cell replication was observed following NNK treatment. In addition, in colon cancer, there is no relationship between cell replication and DNA MT activity of normal colonic mucosa versus progressive stages of colon cancer (Camplejohn, R. S., *Cancer Res. 83*: 21, 1982; Issa *et al.*, 1993). The repair of DNA damage can lead to tracts of hemimethylated DNA that would be templates for methylation. However, the concentration of the $O^6$-methylguanine DNA adduct and rates of adduct removal were similar in both type II and Clara cells (Belinsky *et al.*, 1992; Devereux, T. R. *et al. Mol. Carcinogenesis 8*: 177, 1993), yet no increase in MT activity was observed in the Clara cells.

Table 1

Effect of NNK Treatment on DNA Methyltransferase Activity in Lung Cells From A/J Mice

| | | Days Post NNK Treatment | | | |
|---|---|---|---|---|---|
| Cell Type | Control | 1 | 3 | 7 | 14 |
| Type II | 24 ± 11 | 77 ± 20[a] | 84 ± 7[a] | 123 ± 35[a] | 66 ± 13[a] |
| Clara | 16 ± 10 | 9 ± 9 | 42 ± 14 | 35 ± 30 | 36 ± 13 |
| Small cell | 70 ± 17 | 86 ± 21 | 88 ± 4 | 76 ± 21 | 73 ± 20 |
| Macrophage | 23 ± 11 | 211 ± 85[a] | 99 ± 15[a] | 66 ± 37 | 32 ± 16 |

Values with mean ± SEM are from 3 – 5 cell isolations.
[a]$p < 0.01$ with respect to control.

Pulmonary lesions were microdissected from lungs 28, 36, 44, and 52 wk after initiation of treatment. The mass distribution of lesions analyzed for MT activity varied from 0.3 to 5.0 mg. Based on the tumor progression model established previously (Belinsky *et al.*, 1992; Belinsky, S. A. *et al., Cancer Res. 53*: 410, 1993), lesions with the smaller mass (0.3 to 0.5 mg) were predominantly hyperplasias and small adenomas; adenomas and carcinomas were most prevalent in the 0.6 to 1.5 mg and 3.1 to 5.0 mg size range, respectively. MT activity for the various lesions grouped by size is shown in Table 2. The enzyme activity increased in direct proportion to the size of the lesions from 144 dpms/$\mu$g to greater >300 dpms/$\mu$g (Table 2).

Table 2

DNA Methyltransferase Activity in A/J Mouse Lung Tumors

| Lesion Mass (mg) | Methyltransferase Activity (dpms/$\mu$g protein) | Sample Size |
|---|---|---|
| 0.3 – 0.5 | 114 ± 19 | 10 |
| 0.6 – 1.0 | 177 ± 28[a] | 10 |
| 1.1 – 1.5 | 167 ± 22[a] | 10 |
| 1.6 – 3.0 | 312 ± 38[a,b] | 10 |
| 3.1 – 5.0 | 333 ± 28[a,b] | 16 |

Values are means ± SEM
[a]$p < 0.01$ with respect to lesions 0.3 to 0.5 mg.
[b]$p < 0.01$ with respect to lesions 0.3 to 0.5 mg or 0.6 to 1.5 mg.

The earliest known oncogene mutation associated with NNK exposure to A/J mice is mutation of the K-*ras* gene in alveolar hyperplasias (Belinsky *et al.*, 1992). The mutation formed, a GGT to GAT transition in codon 12, is consistent with the base mispairing properties of the $O^6$-methylguanine DNA adduct formed during metabolism of NNK. Thus, it is likely that this mutation may be one of the initiating events, occurring at the time of replication of the damaged DNA template. The marked increase in MT activity in type II cells following NNK treatment may modulate the methylation state of key regulatory genes and promote the selective clonal expansion of *ras* initiated cells. The increase in MT activity during murine lung tumor progression parallels that observed in human colon cancer (Issa *et al.*, 1993). DNA MT activity was also found to be elevated in rat hepatic neoplasms compared to adjacent normal tissue (Miyoshi, E. *et al.*, *Carcinogenesis 14*: 603, 1993). The detection of increased MT activity in the murine lung cancer model used in this investigation provides further support of the hypothesis that the deregulation of this pathway may serve to promote genomic instability and contribute to the progressive chromosomal losses detected in human lung cancer.

(Research sponsored by the Office of Health and Environmental Research, U.S. Department of Energy, under Contract No. DE-AC04-76EV01013 at ITRI and Contract No. 1-P50-CA58184 at Johns Hopkins.)

# BIOCHEMICAL MECHANISMS INVOLVED IN THE ENDOTOXIN-INDUCED TYPE II CELL HYPERPLASIA IN F344 RAT LUNG

*Johannes Tesfaigzi, Neil F. Johnson, and John F. Lechner*

Proliferative lesions and pulmonary epithelial neoplasms induced in the rat by plutonium inhalation have been shown to be of type II cell origin (Herbert, R. A. *et al. Vet. Pathol. 31*: 366, 1994). Defining the gene changes responsible for the development of the type II proliferative lesions would help to elucidate the genetic events involved in the expansion of initiated type II cells into fully transformed tumor cells. One problem in identifying these gene alterations is dissociating changes in gene expression linked to cell replication or repair from those involved in tumor initiation and progression. The long-term goals of these investigations are to first develop and characterize a model of transient type II cell hyperplasia. Second, changes in gene expression associated with remodeling epithelium will be compared to gene changes exhibited by the $^{239}$Pu-induced hyperplastic lesions.

Two approaches will be used. One will be to evaluate the expression of candidate protooncogenes and tumor suppressor genes. The other approach will be to use the technique of subtraction hybridization to identify novel changes in gene expression that are specifically altered in the $^{239}$Pu-induced hyperplastic lesions. The purpose of this investigation was to develop an efficient method of inducing transient alveolar type II cell hyperplasia in the rat lung and to begin examining the expression of protooncogenes associated with the cell cycle.

Previous investigations by Harkema, J. R. and J. A. Hotchkiss (*Am. J. Pathol. 141*: 307, 1992) showed that endotoxin, a lipopolysaccharide that constitutes a major part of the gram-negative bacterial cell wall, induces hyperplasia of secretory cells. Therefore, endotoxin instillation has been evaluated as a probable means to induce transient type II cell hyperplasia as well. Amplification and overexpression of the EGF receptor and c-erb B-2 genes have been found in many different human primary tumors including non-small cell lung cancer. Therefore, EGF receptor and c-erb B-2 genes are postulated to be important in human carcinogenesis (DiFiori, P. P. *et al. Lung Cancer 4*: 135, 1988). They belong to the same family of transmembrane receptors and both have intrinsic tyrosine kinase activity (Peles, E. *et al. Cell 69*: 205, 1992). Whether the expression of these receptors also occurs during a transient type II cell hyperplasia was investigated.

Male F344/N rats, 8–10 wk of age (Taconic Laboratories, Germantown, NY) received a single intratracheal instillation 0.5 mg endotoxin (lipopolysaccharide from *E. coli* 0111:B4, Sigma Chemicals Co., St. Louis, MO) in pyrogen-free saline. Control rats were similarly instilled with 0.5 mL pyrogen-free saline. All rats were injected intraperitoneally (IP) with 5-bromo-2'-deoxy uridine (BrdU) (Sigma) at 50 $\mu$g/g body weight in saline 2 h prior to sacrifice to label cells undergoing DNA synthesis as described previously (Johnson, N. F. *et al. Toxicol. Appl. Pharmacol. 103*: 143, 1990). At least six rats were killed at each time point 3, 6, 12, 24, 48, 96, and 168 h after instillation by IP injection of sodium pentobarbital. Lung tissues were prepared and analyzed by electron microscopy as described previously (Harkema and Hotchkiss, 1992).

Serial sections adjacent to histologically classified sections of normal lung and hyperplastic regions were immunostained using affinity-purified rabbit polyclonal antibodies raised against synthetic peptides corresponding to amino acid sequences of the human EGF receptor and human erbB-2 glycoprotein 185 and the corresponding peptides (Santa Cruz Biotechnology, Inc., Santa Cruz, CA). EGF receptor and erbB-2 were detected essentially as described by the manufacturer.

Intratracheal instillations of endotoxin induced parenchymal changes in the rat lung 3 h post instillation (PI), the earliest time point examined. At this time the influx of cells were primarily polymorphonuclear cells (PMNs), which were found in the alveolar airspace in both the endotoxin-treated and the saline-treated rats. Twelve hours PI a significant increase in the number of PMNs and other inflammatory cells was observed, but only in the endotoxin-instilled rats. The inflammatory response was most evident in rats sacrificed 24 and 48 h PI.

Hypertrophy of type II cells was observed in rats 48 h PI, and hyperplasia of epithelial cells lining the alveoli was evident in rats sacrificed 96 h PI. These changes were predominantly found in areas of extensive inflammation, which in most rat lungs occurred in areas surrounding the conducting airways. Electron microscopic studies showed that the proliferating cells lining the airspace contained numerous lamellar bodies and cell junctions, both of which are characteristic for type II cells. The hyperplasia was less pronounced in rats sacrificed 7 days PI where only few focal lesions were evident.

The number of cells which had incorporated BrdU into the nuclei increased significantly in the lungs of endotoxin exposed rats 1 to 7 d PI. However, 48 h PI the number of BrdU-labeled cells had increased at least five times the number observed at 24 h or 96 h (Fig. 1). The majority of labeled cells appeared to be lining the alveolar air spaces and in the interstitium. The number of BrdU-labeled cells did not increase in saline-instilled rats (Fig. 1).

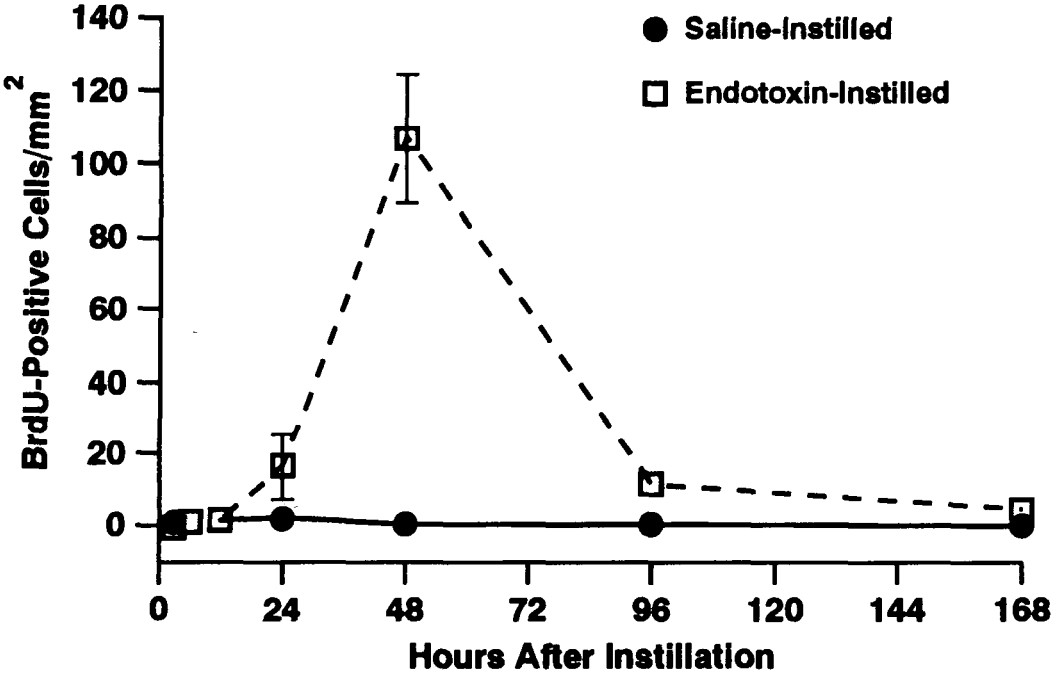


Figure 1. The portion of cells per unit area labeled with BrdU in saline-exposed (filled circle) and endotoxin-exposed (open squares) rats. Each data point represents data from six rats, the error bars represent one standard deviation; where no error bars are shown the values were smaller than the size of the symbol.

In saline-instilled control rats, a weak positive staining for the EGF receptor was seen in almost all type II cells 4 d after instillation. The type II cells exhibited moderate staining 24 h after endotoxin instillation, and about 90% of the PMNs and macrophages in the alveoli reacted with this antibody. After 48 and 96 h, the hypertrophic and hyperplastic type II cells as well as the

inflammatory cells showed extensive staining of EGF receptor. The staining of the membranes became more evident in the hyperplastic cells. After 7 d when the type II cell hyperplasia had regressed, most of the type II cells and macrophages still stained for the EGF receptor.

The antibody to erbB-2 weakly stained the alveolar epithelium of the saline-instilled rats. Some of the inflammatory cells which accompanied the saline instillation and 10% of the type II cells also showed minimal staining reaction. The intensity of staining for erbB-2 in the alveolar epithelium and in the inflammatory cells increased dramatically PI. Two and 4 d PI the type II cells retained a marked expression of the erbB-2 protein. Some of these hyperplastic cells showed the specific membrane staining. After the regression of the hyperplasia, all alveolar epithelial cells exhibited erbB-2 protein.

The primary conclusions of this study were that a single intratracheal administration of endotoxin induced type II cell proliferation in rats and that the expression of the growth factor receptors, EGF receptor and erbB-2, was increased in hyperplastic type II cells. The observation that an influx of PMNs into the alveolar space occurred in the rat at early time points after endotoxin instillation was similar to reports involving other species (Brigham, K. L. and B. Meyrick. *Am. Rev. Respir. Dis. 133*: 913, 1986; Hudson, A. R. *et al. Am. Rev. Resp. Dis. 115*: 89, 1977). Endotoxin is known to be a mitogen for certain cells including reticuloendothelial cells, B lymphocytes, and liver cells (Frank, L. *et al. J. Clin. Invest. 65*: 1104, 1980). Likewise, it is possible that endotoxin directly activates a receptor on type II cells and stimulates proliferation. In spite of the massive influx of leukocytes into the bronchoalveolar space after a single dose of lipopolysaccharide, cell injury could not be detected by use of cytosolic enzymes for up to 7 d after the initial PMN exudation (Lopez, A. and S. Yong. *Am. J. Vet. Res. 47*: 1287, 1986). Therefore, it is unlikely that the type II cells proliferate to replace damaged alveolar type I cells, as was reported for studies using oxidant gases such as $NO_2$ (Evans, M. *et al. J. Exp. Mol. Pathol. 22*: 142, 1975).

The levels of EGF receptor and erbB-2 proteins increased during hypertrophy and hyperplasia. This suggests that ligands belonging to families of EGF or TGFα play a role in type II cell proliferation. Because amplification and overexpression of the EGF receptor and c-erbB-2 genes have been found in many different human primary tumors including non-small cell lung cancer, they are postulated to be important in human carcinogenesis (DiFiori, 1988). The increased expression of EGF receptor and TGFα in radiation-induced proliferative foci (Gillett, N. A. *et al. Radiat. Res. 126*: 289, 1992; *Vet. Pathol. 29*: 46, 1991) may, therefore, be associated with general cell replication mechanisms, instead of having a specific role in neoplastic progression.

(Research sponsored by the Office of Health and Environmental Research, U.S. Department of Energy, under Contract No. DE-AC04-76EV01013.)

# MAMMARY GLAND CANCER IN A COLONY OF BEAGLE DOGS: INHERITANCE, AND p53 & erbB-2 EXPRESSION

*Gregory Kelly, William C. Griffith, Bruce A. Muggenburg, Lauren A. Tierney*, John F. Lechner, and Fletcher F. Hahn*

One American woman in nine will be diagnosed with breast cancer in her lifetime. This somber statistic translates into 182,000 new diagnoses and 46,000 deaths per year (American Cancer Society, *Cancer Facts and Figures - 1993*, American Cancer Society, 1993). Efforts to decrease breast cancer mortality, have focused on early detection and improved treatment. Such efforts would be facilitated by the identification of individuals predisposed to the disease. A family history of the disease can increase a woman's risk for developing breast cancer by two- to six-fold (Houlston, R. S. *et al. J. Med. Genet. 29*: 154, 1992; Tulinius, H. *et al. J. Med. Genet. 29*: 158, 1992). Inheritance of this disease is consistent with at least one susceptibility locus on chromosome 17 (17q12-21) with incomplete penetrance (Hall, J. *et al. Science 250*: 1684, 1990; Porter, D. E. *et al. Int. J. Cancer. 53*: 188, 1993). However, other mechanisms of inherited susceptibility also contribute to the high incidence of the disease (Porter, D. E. and C. M. Steel. *Disease Markers 11*: 11, 1993).

Based on the biological characteristics of canine mammary tumors, a number of investigators have suggested that the dog could provide an important model for the study of human breast cancer (Gilbertson, S. R. *et al. Vet. Pathol. 20*: 127, 1983; MacEwen, E. G. *Cancer Metastasis Rev. 9*: 125, 1990). ITRI has maintained a Beagle dog colony for over 30 y to investigate the adverse health effects of inhaled toxicants. To date, nearly 4,000 female descendants have been born from 28 original female dogs. The most recent dogs are the fifth generation descendants of the original females. Two of the founding female dogs in this colony gave rise to offspring that have an exceptionally high incidence of spontaneous mammary cancer. Two other founding female dogs gave rise to offspring that have a very low incidence of spontaneous mammary cancer. The purpose of the present study was to characterize the familial pattern of mammary cancer development in the dog colony. In addition, the expression of the p53 tumor suppressor gene and c-erbB2 ($p185^{erbB2}$) oncogene proteins, which are frequently altered in human breast cancer, were examined in dogs susceptible and resistant to mammary cancer.

To estimate the strength of the familial association with mammary cancer, a proportional hazards analysis was applied to each family within the colony. The rate of development of mammary tumors was regressed on the probability of inheriting an allele at a single locus from each founding dog of the breeding colony. This probability provided a measure of the likelihood that a particular characteristic was inherited from a particular founder. Because it was not based upon any specific genetic markers, it could be regarded as a general measure of the genetic distance between the individual dog and each founder. The probability of inheriting an allele at a single locus was calculated by considering that a dog has a probability of 1/2 of inheriting an allele from each parent. More specifically, a dog has the probability $x_i$ of inheriting an allele from each of the $n$ founding dogs, $i = 1,...,n$. The Cox proportional hazards model, which describes how mammary tumor hazard rates are altered by the probability of an allele at a single locus, is

$$\lambda(t; x_1,...,x_n) = \lambda_b(t) \exp\left(\sum_{i=1}^{n} \beta_i x_i\right),$$

*UNM/ITRI Inhalation Toxicology Graduate Student

where $\lambda_b(t)$ is the baseline (average prevalence for a mammary tumor in this population) hazard rate, $\lambda(t;x_1,...,x_n)$ is the mammary tumor hazard rate for an individual dog with probabilities of inheriting an allele of $x_1,...,x_n$, and $\beta_1,...,\beta_n$ are the coefficients for each founder which are estimated in the regression model. A proportional hazards model corrected for the varying fractions of the life span over which the dogs were observed. The analysis did not attempt to track the inheritance of a particular allele but instead related one characteristic, the time of onset of a mammary tumor, in an individual to a measure of genetic distance of that individual from each founder.

Based on these risks, the ages of onset for mammary tumors associated with these families are shown in Figure 1 using an estimate from the proportional hazards model of $\lambda_b(t)\ \exp(\hat{}\beta_i)$ for the probability of inheriting an allele from the founder of a female family. Two markedly different phenotypes became apparent with this analysis. Resistance to breast cancer was characterized by a very late time of onset, making it unlikely that a mammary tumor would develop before death from other competing causes. In contrast, the susceptible phenotype was characterized by a latency period for a 50% incidence of only 7 y, and all members of this phenotype developed breast tumor by age 10. As illustrated in Figure 1, Families 1 and 26 exhibit the resistant phenotype, while Families 10 and 18 represent the susceptible phenotype.

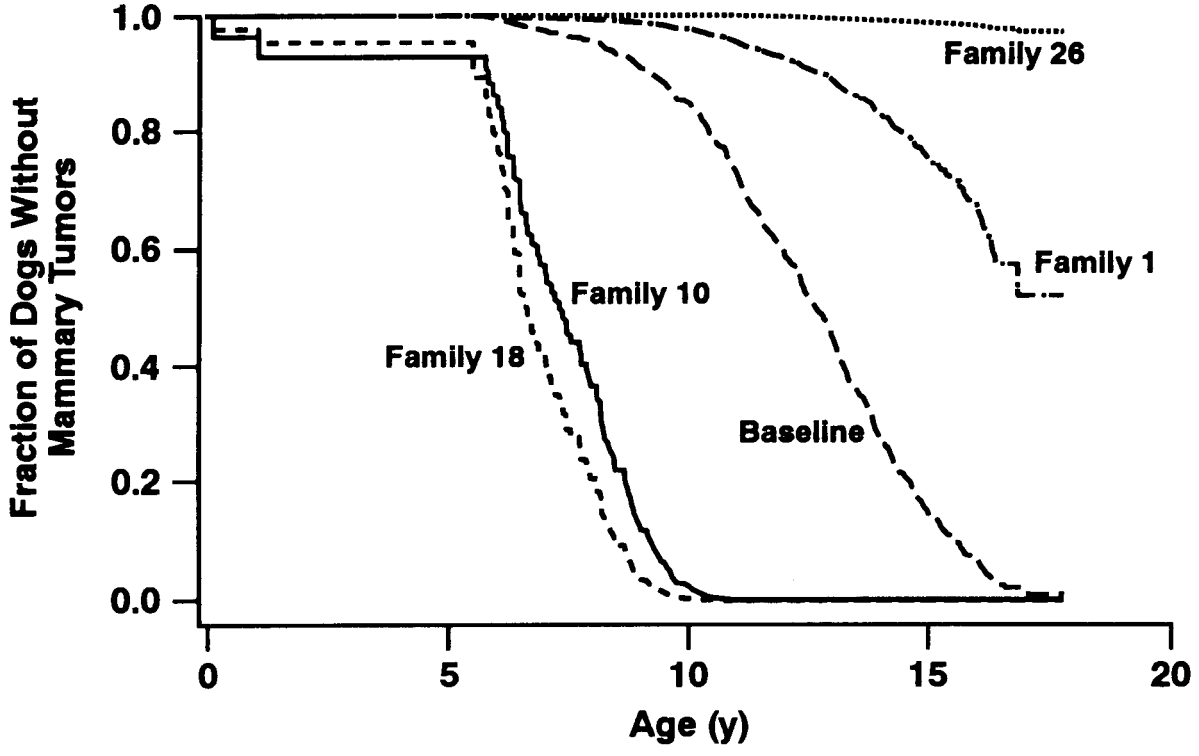


Figure 1. Estimate from the proportional hazards model of age of mammary tumor onset associated with the probability of inheriting an allele from founders of female families.

Thirty-six mammary tumors were examined by immunohistochemistry (IHC) for p53 protein expression and 33 tumors for c-erbB2 receptor protein expression. This sample set included 17 tumors from a susceptible family of dogs and 20 tumors from a family resistant to mammary cancer development. Mammary tumors from the susceptible family included seven solid adenocarcinomas, eight complex adenocarcinomas, one tubular adenocarcinoma, and one carcinosarcoma. Mammary tumors from the resistant family included 13 solid adenocarcinomas, four complex adenocarcinomas, and three papillary adenocarcinomas. The polyclonal antibody CM-1 (Signet Laboratories, Dedham,

MA) was used to detect overexpression of the p53 protein. Expression of $p185^{erbB2}$ was detected using the CB11 monoclonal antibody (Signet Laboratories, Dedham, MA). The results of this analysis are included in Table 1. Detectable p53 expression was infrequent (6/36) in all malignant canine mammary tumors examined. In most cases, p53 staining was focal or regional, but was not evident in all portions of the tumor (data not shown). Forty-two percent (14/33) of all tumors examined had evidence of $p185^{erbB2}$ expression. No family-specific differences in p53 or $p185^{erbB2}$ expressions were noted.

The p53 tumor suppressor gene is expressed in 20-25% of human breast cancers (Davidoff, A. M. *et al. Cancer Res. 51*: 2605, 1991; Ostrowski, J. L. *et al. J. Pathol. 164*: 75, 1991; Spandidos, D. A. *et al. Anticancer Res. 12*: 81, 1992), $p185^{erbB2}$ expression, which correlates with advanced clinical stage, is observed in 17-30% of human tumors examined (Slamon, D. *et al. Science 235*: 177, 1987; van de Vijver, M. *et al. Mol. Cell. Biol. 7*: 2019, 1987; Zhou, O. *et al. Cancer Res. 47*: 6123, 1987; Nagai, M. A. *et al. Oncology 50*: 412, 1993). Sixteen percent of the tumors examined in this study expressed p53 protein. The frequency of $p185^{erbB2}$ expression was higher in the dog (42%) than that usually reported for human breast cancer. However, the difference between the frequencies of tumors expressing these proteins in the two species are not large and can probably be attributed to the relatively small number of canine tumors (32) examined in the present study. The results of the IHC analyses reported here suggest that at least for p53 and $p185^{erbB2}$, the development of mammary cancer in dogs and breast cancer in humans may involve similar mechanisms. These similarities bolster the similarities in morphology, incidence, and metastatic potential reported by other investigators (Fidler, I. H. and R. S. Brodey. *J.A.V.M.A. 151*: 710, 1967; Strandberg, J. D. *Am. J. Pathol. 75*: 225, 1974; Owen, L. N. *Invest. Cell Pathol. 2*: 257, 1979).

As a result of a germ-line mutation in the p53 tumor suppressor gene, Li-Fraumeni syndrome patients are susceptible to a number of neoplasms including breast cancer (Malkin, D. *et al. Science 250*: 1233, 1990). Based on IHC findings, the susceptibility to mammary cancer of Family 10 is probably not the result of a germ-line mutation in the p53 tumor suppressor gene. Amino acid substitutions in the p53 protein alter the conformation of the molecule, resulting in an increased cellular half-life of the protein (Finlay, C. A. *et al. Mol. Cell. Biol. 8*: 531, 1988). Such increased protein levels resulting from missense mutations within the gene have been detected by various techniques including IHC (Takahashi, T. *et al. Science 246*: 491, 1989; Rodrigues, N. R. *et al. PNAS 87*: 7555, 1990; Davidoff, A. M. *et al. PNAS 88*: 5006, 1991; Marks, J. R. *et al. Cancer Res. 51*: 2979, 1991; Kohler, M. F. *et al. Cancer Res. 52*: 1622, 1992). A germ-line mutation in the susceptible family would be expected to produce a situation in which either none of the tumors would express p53 (germ-line deletion of one p53 allele, followed by a somatic mutation deleting the second allele) or all of the tumors would express the protein (a point mutation in each allele or a point mutation in one allele and deletion of the second allele). IHC showed that a few mammary tumors from both the susceptible and resistant dog families expressed detectable levels of the p53 protein.

The families of dogs within the ITRI Beagle colony that develop inherited mammary cancer provide a unique experimental model to identify the genetic alterations responsible for this disease. These same alterations may play a role in the human disease. Ultimately, delineation of the nature of these alterations may provide a means to identify those women susceptible to premenopausal inherited breast cancer. Mortality from breast cancer could be decreased by aggressive early screening and identification of susceptible individuals. Moreover, identifying and characterizing the susceptibility gene may result in an early marker for premalignant disease and a target for intervention therapy. This canine model of inherited mammary cancer may also provide an experimental system with which to evaluate the efficacy of drugs or other treatment regimens that might be used in the prevention or treatment of breast cancer.

Table 1

p53 and p185$^{erbB2}$ Expression in Mammary Tumors from Family 1 and Family 10

| Animal ID | Family | Mammary Gland | Histology | p53 Expression | p185$^{erbB2}$ Expression |
|---|---|---|---|---|---|
| 96F | 1 | L5 | Solid Adenocarcinoma | – | + |
| | | R5 | Solid Adenocarcinoma | – | + |
| 162D | 1 | R4 | Solid Adenocarcinoma | + | + |
| | | R5 | Solid Adenocarcinoma | – | + |
| 708V | 1 | R4 | Solid Adenocarcinoma | – | ND |
| 889U | 1 | L4 | Papillary Adenocarcinoma | – | – |
| | | R5 | Papillary Adenocarcinoma | – | – |
| 929T | 1 | L4 | Solid Adenocarcinoma | + | + |
| | | L4–5 | Solid Adenocarcinoma | + | + |
| 1055W | 1 | L3 | Solid Adenocarcinoma | + | – |
| 1098S | 1 | L4 | Complex Adenocarcinoma | – | – |
| | | L5 | Complex Adenocarcinoma | ND | – |
| 1098T | 1 | L2 | Solid Adenocarcinoma | – | – |
| | | R4–5 | Solid Adenocarcinoma | – | – |
| 1128S | 1 | R5 | Solid Adenocarcinoma | – | ND |
| 1128U | 1 | L4 | Solid Adenocarcinoma | – | – |
| 1152S | 1 | R3 | Solid Adenocarcinoma | – | + |
| 1378U | 1 | L2 | Papillary Adenocarcinoma | – | + |
| | | R3 | Complex Adenocarcinoma | – | + |
| 164E | 10 | L5 | Solid Adenocarcinoma | – | – |
| | | L3 | Solid Adenocarcinoma | – | – |
| 173G | 10 | R1 | Tubular Adenocarcinoma | – | + |
| 274E | 10 | L4 | Complex Adenocarcinoma | – | – |
| 339U | 10 | L5 | Complex Adenocarcinoma | – | ND |
| | | R5 | Solid Adenocarcinoma | + | + |
| 375U | 10 | L5 | Complex Adenocarcinoma | – | – |
| | | R3 | Solid Adenocarcinoma | – | + |
| 375T | 10 | L2 | Complex Adenocarcinoma | – | – |
| | | L5 | Complex Adenocarcinoma | – | – |
| 385T | 10 | L5 | Solid Adenocarcinoma | – | – |
| | | R5 | Solid Adenocarcinoma | – | – |
| 391T | 10 | R3 | Complex Adenocarcinoma | – | + |
| 423U | 10 | L5–R5 | Carcinosarcoma | – | – |
| 429S | 10 | R5 | Complex Adenocarcinoma | – | – |
| 718T | 10 | L4–5 | Complex Adenocarcinoma | – | – |
| Total | | | | 5/34 | 13/32 |

Tissue specimens were subjectively graded positive or negative for protein expression according to the intensity of specific staining relative to background. Several dogs had more than one malignant mammary tumor. Tumors of the same histotype which did not cross the midline (i.e., along the same mammary chain) were counted as a single tumor when tallying for the subtotals and totals. ND = not determined.

(Research sponsored by the Office of Health and Environmental Research, U.S. Department of Energy, under Contract No. DE-AC04-76EV01013.)

# VI. NONCARCINOGENIC RESPONSES TO INHALED TOXICANTS

# ATROPHIC RHINITIS AND OTHER NASAL LESIONS INDUCED BY A 1-MONTH EXPOSURE OF F344 RATS TO 0.25 OR 0.5 ppm OZONE

*Jon A. Hotchkiss, Paul W. Wacnik*, and Jack R. Harkema***

Ozone, the principal oxidant pollutant of photochemical smog, is a common inhaled toxicant for metropolitan area residents. The effects of acute and chronic ozone exposure on inflammatory cell influx, hyperplasia, and secretory cell metaplasia within the surface epithelium lining rat nasal airways have previously been reported (Hotchkiss, J. A. *et al. Exp. Lung Res. 15*: 589, 1991; Harkema, J. R. and J. A. Hotchkiss. *Toxicol. Lett. 68*: 252, 1993). On the other hand, there is a paucity of data describing the effects of ozone exposure on the subepithelial tissues (i.e., lamina propria and bone) of nasal turbinates. However, recently, a significant decrease in nasal turbinate bone area in rats chronically exposed (20 mo) to 1 ppm ozone was reported (Harkema, J. A. *et al. Effects of Chronic Ozone Exposure on the Nasal Mucociliary Apparatus in the Rat*, Report to the Health Effects Institute, in press). The purpose of the present study was to examine the effects of a 1-mo ozone exposure on subepithelial tissue compartments of maxilloturbinates in the anterior nasal cavity of rats.

Eighteen F344/N Hrl male rats (12–14 wk; 170–210 g; Harlan Sprague-Dawley, Indianapolis, IN) were used in this study. The rats were exposed to sea level-equivalent concentrations of 0, 0.25, or 0.5 ppm ozone in whole-body exposure chambers (HC-2000, Hazleton Systems, Aberdeen, MD), 8 h/d, 7 d/wk, from 4:30 p.m. to 12:30 a.m., for 1 mo. Ozone was generated using an OREC Model 03VI-0 ozonizer, and the chamber ozone concentrations were monitored with Dasibi Model 1003AH ambient ozone monitors. Food was removed during exposures. The chamber temperature was maintained between 21° and 25°C, relative humidity was held between 40% and 70%, and a 12-h light/dark cycle was maintained starting at 4:00 a.m. Rats were sacrificed 9 h following the end of the last exposure. Animals were anesthetized with 4% halothane in oxygen and exsanguinated by severing the abdominal aorta or renal artery. Immediately after death, the head of each rat was removed from the carcass, and the lower jaw, skin, and musculature were removed. The nasal cavity was fixed with 10% zinc-formalin and decalcified in 13% formic acid. A tissue block from the anterior nasal cavity was removed by making two transverse cuts, perpendicular to the hard palate, immediately posterior to the upper incisor teeth and immediately anterior to the incisive papilla (Fig. 1).

The nasal tissue blocks were imbedded in paraffin; 5 $\mu$m sections were cut from the anterior block face and were stained with alcian blue (pH 2.5)/hematoxylin and eosin, alcian blue/periodic acid-Schiff or Mason's Trichrome in preparation for light microscopic examination. Morphometric analyses were made using a computerized image analysis system (Hotchkiss *et al.*, 1991). The total turbinate area, surface epithelial area, lamina propria area, bone area, blood vessel lumenal area, and volume density of stored intraepithelial mucosubstances were measured.

Rats exposed to 0.25 ppm ozone displayed no significant morphologic alterations compared to air-exposed control animals. Exposure to 0.5 ppm $O_3$ had no significant effect on total turbinate area or the area of the lamina propria underlying the surface epithelium (Fig. 2). However, there was a significant increase (68%) in epithelial area and volume density of stored mucosubstance (100-fold), and a shift in the morphology of the surface epithelium from simple cuboidal to pseudo-stratified columnar. The blood vessel lumenal area decreased 58%. The decrease in lumenal area was associated with an influx of mononuclear and polymorphonuclear leukocytes and an increase in connective tissue within the lamina propria, and a thickening of the blood vessel wall. Compared to

*Department of Energy/Associated Western Universities Summer Research Participant
**Michigan State University, East Lansing, Michigan

air-exposed controls, there was a 30% decrease in maxilloturbinate bone area. Numerous resorption pits were present around the periphery of the turbinate bones, suggesting an increase in osteoclastic activity.

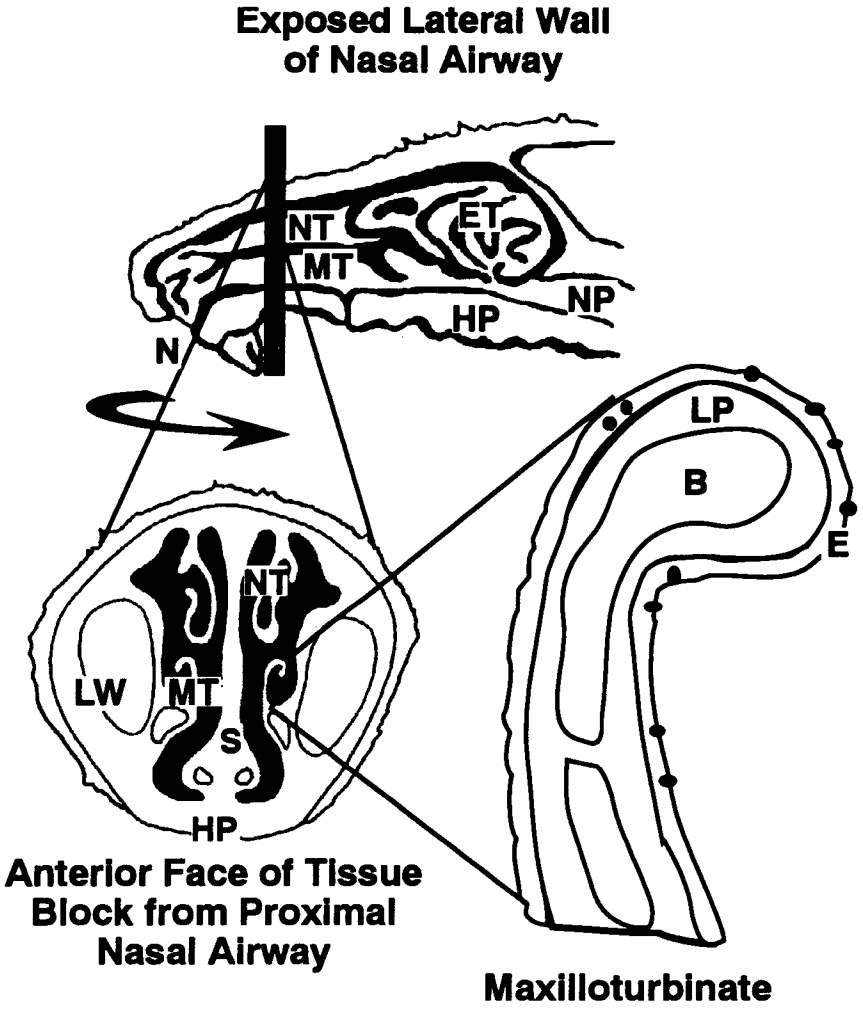


Figure 1. Location of nasal tissue selected for image analysis. B = turbinate bone; E = epithelium; ET = ethmoid turbinate; HP = hard palate; LW = lateral well; MT = maxilloturbinate; N = nares; NP = nasopharynx; NT = nasoturbinate; S = septum.

This is the first study to report significant structural alterations to the turbinates of the anterior nasal cavity as a result of subchronic exposure to ozone. The ozone concentrations selected for use in this study, 0.25 and 0.5 ppm, may be encountered in highly polluted urban centers such as Mexico City. The underlying cellular mechanisms which resulted in the observed morphologic alterations are, as yet, unknown. The epithelial changes (e.g., increased epithelial thickness and increased amounts of stored mucosubstance) may be adaptive responses that help to protect the epithelium from further ozone-induced injury. The bone atrophy may be associated with the ozone-induced influx of inflammatory cells into the lamina propria. Factors thought to influence osteoclast activity, hence bone resorption, include, local acidosis, an increase in free radicals, super oxide anions ($O_2$), and other reactive oxygen species ($H_2O_2$) which have been shown to stimulate osteoclast activity and/or counteract the natural bone resorption inhibitor, nitric oxide (Towhidul, A. *et al. Bioscience Rep. 12*: 369, 1992).

This model of toxicant-induced bony atrophy may aid in the understanding of the pathogenesis of other diseases (e.g., arthritis, periodontal disease) that affect bone integrity. Additionally, a better understanding of the chronic effects of ozone exposure may help in determining if the current ambient air quality standards for ozone exposure are appropriate.

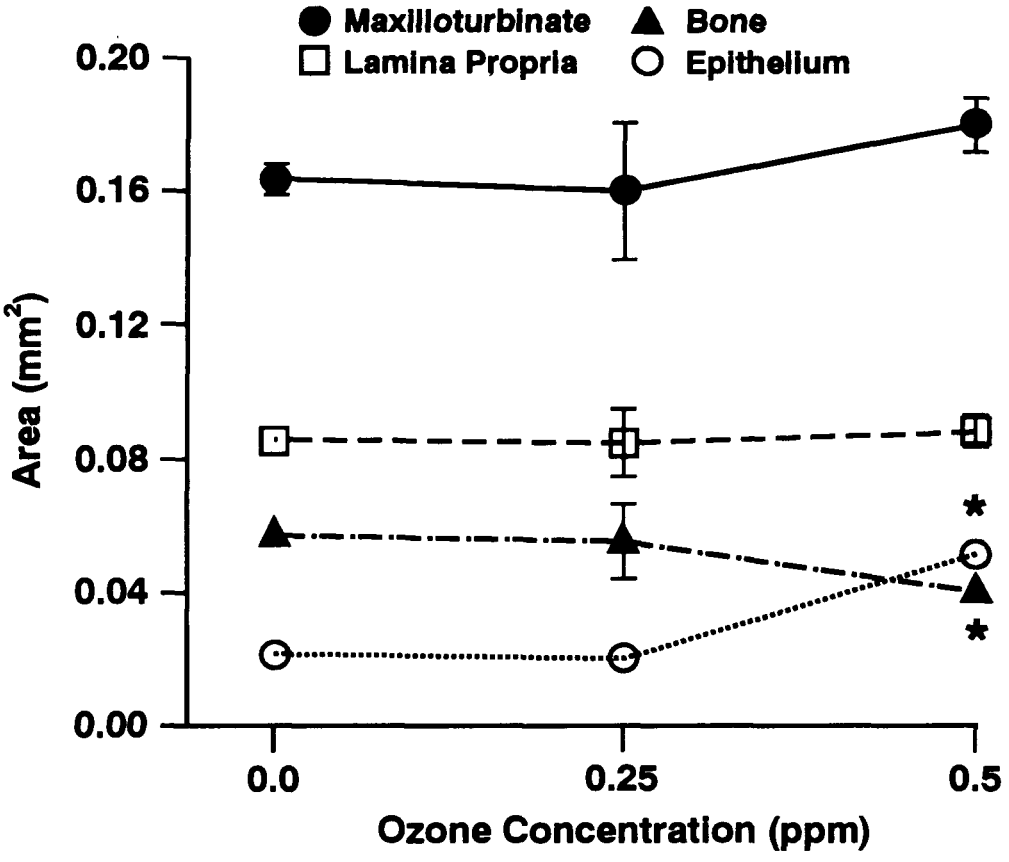


Figure 2. Morphometric quantitation of turbinate area, lamina propria area, bone area, epithelial area, and blood vessel lumenal area in maxilloturbinates of rats exposed to 0.0, 0.25, or 0.5 ppm ozone. Data points represent the mean ± standard error of the mean. * = significantly different than air-exposed controls ($p \leq 0.05$).

(Research sponsored by the Office of Health and Environmental Research, U.S. Department of Energy, under Contract No. DE-AC04-76EV01013.)

# PRELIMINARY CHARACTERIZATION OF THE TOXICITY OF A BERYLLIUM-COPPER ALLOY

*Janet M. Benson and Mark D. Hoover*

Beryllium (Be) is a low-molecular-weight metal with unique strength and nuclear properties. Because of these properties, Be has been used in the production of nuclear weapons and in nuclear reactors. Consequently, thousands of individuals in nuclear weapons facilities may have been exposed to Be. While the need for Be in the nuclear weapons industry has diminished in recent years, industrial applications of Be-containing alloys are increasing. Be-copper (Be-Cu) alloys are used in the electronics industry and are especially useful in spacecraft and aircraft guidance systems. Be-aluminum alloys are lightweight, have structural strength similar to that of pure Be, and are available at lower cost. Potential for human exposure to Be continues with the increasing production and use of Be-containing alloys.

Be also has unique toxicological properties. Individuals exposed to low concentrations of Be (< 100 $\mu$g Be/m$^3$) may develop chronic beryllium disease (CBD), a condition characterized by fibrotic granulomatous lung lesions with infiltrates of lymphocytes and plasma cells. Interestingly, CBD develops in about only 3% of exposed individuals and is thought to be immune-mediated. Several investigations at ITRI and elsewhere have shown that Be can induce granulomatous lung disease in dogs, monkeys, and mice (Haley, P. J. *et al. Lab. Invest. 61*: 219, 1989; *Immunopharmacol. Immunotoxicol.* (in press); 1991-92 Annual Report, p. 169, p. 171) and is highly tumorigenic in rats (1992-93 Annual Report, p. 58; Groth, D. H. *et al. Environ. Res. 21*: 63, 1980). Although data are limited on the pulmonary toxicity of inhaled Be alloys, there is some evidence that inhaled Be-Cu alloy produces CBD in people and is tumorigenic in rats (Hooper, W. F. *N. C. Med. J. 42*: 551, 1981; Groth *et al.*, 1980).

The cytotoxicity of metal particles to alveolar macrophages (AMs) provides information regarding their potential to produce a pulmonary inflammatory response when inhaled (Benson, J. M. *et al. Fundam. Appl. Toxicol. 7*: 340, 1986; *J. Toxicol. Environ. Health 19*: 105, 1986; Finch, G. L. *et al. Toxicol. Lett. 41*: 97, 1988; *Inhal. Toxicol. 6*: 205, 1994). Cytotoxicity of metal particles often is associated with the solubility of the particle, which is determined in part by the particle's surface area. The purpose of this study was to begin evaluation of the cytotoxicity of a Be-Cu alloy (2% Be, 98% Cu) to AMs and to attempt to relate cytotoxicity to the specific surface area of the material. The cytotoxicity and specific surface area of the Be-Cu alloy were compared to those of Be and Cu metal and of copper sulfate ($CuSO_4$).

Be metal powder and Be-Cu alloy were obtained from the Brush-Wellman Co., Elmore, OH. The powdered alloy was prepared by a grinding process and was representative of the kind of powder to which workers might be exposed. Both Be metal and Be-Cu alloy powders had real diameters < 38 $\mu$m and were not size-fractionated before use. Cu powder (nominal 3 $\mu$m diameter as specified by the manufacturer) and cupric sulfate pentahydrate were obtained from standard chemical suppliers.

The cytotoxicity of the Be, Cu, and Be-Cu alloy powders and $CuSO_4$ to Beagle dog AMs was determined using previously described methods (Benson *et al.*, 1986). Each test material was evaluated at four concentrations; samples were run in duplicate, and each experiment was repeated at least twice. The percentage of viable AM in each cell culture was determined following 20 h of incubation with the test materials using the method of trypan blue exclusion. The median lethal concentration ($LD_{50}$) for each material was calculated by probit analysis using SAS statistical software (Cary, NC). The specific surface areas of the Be, Cu, and Be-Cu powders were determined by quantitating the amount

of $N_2$ adsorbed on the particles. This was accomplished by using a Quantasorb/Quantector System (Quantachome Co., Syosset, NY) which measures the thermal conductivity of a $N_2$/He mixture before and after passing over the particles.

Results are summarized in Table 1. The ranking of compounds for cytotoxicity, in decreasing order of toxicity, was: $CuSO_4$ > Cu > Be = Be-Cu alloy. Considering that the Be-Cu alloy contains 98% Cu and that it had twice the specific surface area of the Cu metal, it is surprising that the cytotoxicity of the Be-Cu alloy was a factor of 3 lower than that of the Cu metal. Differences in the size distribution of the Be-Cu alloy and Cu powders, which may affect the relative amounts of particles taken up by the cells, may be responsible for the apparent discrepancy. The specific surface area ($m^2/g$) of the Be metal powder was approximately 4 times greater than that of the Be-Cu alloy and approximately 10 times greater than the Cu metal powder.

Table 1

Specific Surface Area and Median Lethal Concentration ($LD_{50}$) in Canine Alveolar Macrophages for Each of Four Be- and Cu-Containing Materials

| Compound | Specific Surface Area[a] ($m^2/g$) | $LD_{50}$ ($\mu g$ metal/mL medium) |
|---|---|---|
| Be Metal | 5.43 ± 0.09 | 180 (121–375)[b] |
| Be-Cu Alloy | 1.2 ± 0.02 | 182 (146–256) |
| Cu Metal | 0.55 ± 0.01 | 69 (64–74) |
| $CuSO_4$ | NA | 15 (11–19; as Cu) |

[a]Results represent the mean ± SD.
[b]Values in parentheses are 95% confidence intervals.

The results of this study suggest that both $CuSO_4$ (soluble Cu) and Cu metal powder are considerably more cytotoxic to AM than Be metal powder and Be-Cu alloy. However, future work will focus on studies using size-fractionated industrial samples of Be and Cu metal and Be-containing alloys. In these studies, the amounts of metal in the macrophage incubation medium and that taken up by the cells will also be quantitated in order to determine actual metal doses to the cells and to provide more accurate information regarding the relative toxicities of Be, Cu and the Be-Cu alloy.

(Research sponsored by the Office of Health and Environmental Research, U.S. Department of Energy, under Contract No. DE-AC04-76EV01013.)

# PULMONARY RETENTION AND TISSUE DISTRIBUTION OF $^{239}Pu$ NITRATE IN F344 RATS AND SYRIAN HAMSTERS INHALING CARBON TETRACHLORIDE

*Janet M. Benson, Edward B. Barr, David L. Lundgren, and Kristen J. Nikula*

Carbon tetrachloride ($CCl_4$) has been used extensively in the nuclear weapons industry, so it is possible that nuclear plant workers have been exposed to $CCl_4$ and plutonium compounds. Potential for future exposure exists during "cleanup" operations at weapon production sites such as the Hanford, Washington, and Rocky Flats, Colorado, facilities. The current Threshold Limit Value for $CCl_4$ is 5 ppm; however, concentrations of $CCl_4$ occurring in the nuclear weapons facilities over the past 40–50 y are unknown and may have exceeded this value.

The pilot study described in this report is designed to determine whether subchronic inhalation of $CCl_4$ by CDF®(F-344)/CrlBR rats and Syrian golden hamsters, at concentrations expected to produce some histologic changes in liver, alters the hepatic retention and toxic effects of inhaled $^{239}Pu$ nitrate $^{239}Pu(NO_3)_4$. $^{239}Pu(NO_3)_4$ represents moderately soluble Pu compounds in a variety of chemical forms that may have occurred in the weapons plants. In this study, the hamster more closely serves as a model for humans with regard to the tissue distribution and retention of the inhaled moderately soluble $^{239}Pu$. Use of rats allows species comparisons and close examination of potential interactions between $CCl_4$ and moderately soluble $^{239}Pu$ in lung. The endpoints being evaluated in this study include: (1) species differences and dose-response relationships in toxic effects resulting from inhalation of $CCl_4$ by rats and Syrian hamsters, (2) the effect of subchronic inhalation of $CCl_4$ on the pulmonary and whole-body retention and tissue distribution of acutely inhaled $^{239}Pu(NO_3)_4$, (3) effects of subchronic $CCl_4$ inhalation on the pulmonary clearance of an acutely inhaled surrogate insoluble tracer particle ($^{85}Sr$-labeled fused aluminosilicate particles [$^{85}Sr$-FAP]), and (4) the effects of combined exposure to $CCl_4$ and $^{239}Pu$ on histopathological changes occurring in nose, lung, liver, kidneys, and bone marrow, compared to those occurring in rats and hamsters exposed to each agent alone. The results obtained will provide a basis for deciding whether a chronic combined exposure study for this combination of toxicants is warranted.

Groups of CDF®(F-344)/CrlBR rats (36M/36F) and 72 Syrian hamsters (36M/36F) are being exposed in Hazleton H-2000 chambers to air (controls) or to 5, 20, or 100 ppm $CCl_4$ 6 h/d, 5 d/wk, for a total of 16 wk. Subgroups consisting of 30 animals/sex/$CCl_4$ exposure concentration also have been exposed once, nose-only, to aerosols of $^{239}Pu(NO_3)_4$ after 4 wk of exposure to air or $CCl_4$. The remaining six animals/sex/$CCl_4$ level have been exposed once, nose-only, to an aerosol of $^{85}Sr$-FAP to evaluate the effects of $CCl_4$ inhalation on particle clearance from lung. After the nose-only exposures to $^{239}Pu$ or $^{85}Sr$, the animals were held for 1 wk without $CCl_4$ exposure, then returned to the whole-body inhalation chambers for an additional 12 wk of $CCl_4$ exposure. Animals exposed to the $^{239}Pu$ were sacrificed at 4 h and at 2, 4, 6, and 13 wk after the nose-only exposure for quantitation of $^{239}Pu$ in lung, liver, kidney, and femur, and for evaluation of histopathological changes in these tissues. Clearance of the $^{85}Sr$ activity from lungs is determined by whole-body counting of the animals throughout the 13-wk period after the $^{85}Sr$-FAP exposure. At the termination of the $CCl_4$ exposures, the $^{85}Sr$-FAP exposed animals will be sacrificed for determination of histopathological changes in tissue resulting from $CCl_4$ alone. Body weights and clinical signs of toxicity are recorded at the beginning of the $CCl_4$ exposures and monthly thereafter.

Inhalation of $CCl_4$ in combination with $^{239}Pu$ slightly depressed the weight gain of male and female rats exposed to 100 ppm. The weight gain in male and female hamsters was notably depressed in a $CCl_4$ exposure-concentration-dependent manner. By the fourteenth study week, the body weights

for hamsters exposed to 5, 20, and 100 ppm $CCl_4$ were 100, 86, and 68% of controls for males and 88, 74, and 61% of controls for females, respectively. The growth curve for female hamsters is shown in Figure 1. Few clinical signs of toxicity (other than decreased weight gain) attributable to $CCl_4$ exposure were observed in hamsters, and survival was not affected. Clinical signs of toxicity attributable to $CCl_4$ exposure were not observed among the rats on study.

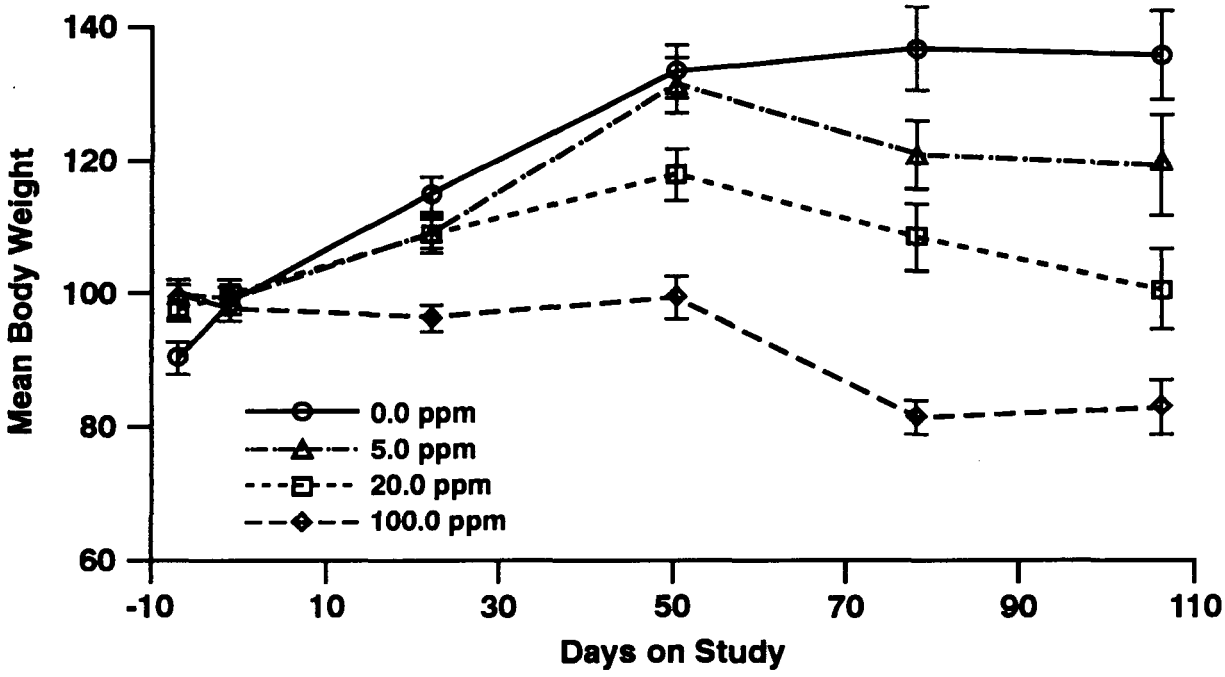


Figure 1. Growth curve for female hamsters exposed to air or $CCl_4$. Error bars represent standard error.

Pale livers were observed in male and female hamsters exposed to 20 or 100 ppm $CCl_4$ and sacrificed 4 and 6 wk after their exposure to $^{239}Pu(NO_3)_4$. This liver lesion was observed in male and female rats exposed to 20 and 100 ppm $CCl_4$ plus $^{239}Pu$ and sacrificed 6 wk after the $^{239}Pu(NO_3)_4$ exposure. Testicular atrophy was present in 5/6 and 2/6 male hamsters exposed to 20 and 100 ppm $CCl_4$ plus $^{239}Pu$ and sacrificed 4 wk after the $^{239}Pu(NO_3)_4$ exposure. The incidence of testicular atrophy in male hamsters sacrificed 6 wk after $^{239}Pu(NO_3)_4$ exposure was 2/6, 5/6, 6/6, and 6/6 for animals exposed to 0, 5, 20, and 100 ppm $CCl_4$ plus $^{239}Pu$. Testicular atrophy was not observed among male rats sacrificed at the same times. The cause of the testicular atrophy among hamsters remains to be determined. The contribution of $CCl_4$ alone to the occurrence of the atrophy will be determined after the terminal sacrifices.

Initial lung burdens of $^{85}Sr$-FAP were 4.3–6.4 kBq/g lung for rats and were 5.6–8.3 kBq/g lung for hamsters. There appears to be no consistent relationship between the exposure level to $CCl_4$ and the amount of $^{85}Sr$-FAP deposited. Pulmonary clearance of the inhaled $^{85}Sr$-FAP could be described by a two-component negative exponential equation. A majority of the inhaled particles cleared the lungs of rats and hamsters with a half-time ($T_{1/2}$) of approximately 1.5 d. The $T_{1/2}$s for long-term clearance of the remaining particles from lungs of male and female control rats were 33 and 41 d, respectively. The ranges of $T_{1/2}$ values for $CCl_4$-exposed males and females were 30–37 d and 35–36 d, respectively. The $T_{1/2}$ values for the longer term clearance of particles from lungs of male and female control hamsters were 53 and 58 d, respectively. The corresponding $T_{1/2}$ values for $CCl_4$-

exposed hamsters were 86–99 d for males and 63–69 d for females. Therefore, the $^{85}$Sr-FAP clearance patterns in rats and hamsters does not appear to be significantly affected by $CCl_4$ inhalation.

The terminal sacrifices for this study will be conducted in October 1994. Radiochemical and histopathological evaluation of tissues will begin in FY–95. Preliminary results indicate that the Syrian golden hamster is more sensitive than CDF®(F-344)/CrlBR rats to inhaled $CCl_4$ and that subchronic inhalation of $CCl_4$ does not affect clearance of poorly soluble particles from lung.

(Research sponsored by the Assistant Secretary for Defense Programs, U.S. Department of Energy, under Contract No. DE-AC04-76EV01013.)

# VII. MECHANISMS OF NONCARCINOGENIC RESPONSES TO INHALED TOXICANTS

# MAINSTREAM CIGARETTE SMOKE EXPOSURE ALTERS CYTOCHROME P4502G1 EXPRESSION IN F344 RAT OLFACTORY MUCOSA

*Jon A. Hotchkiss, Kristen J. Nikula, Johnnye L. Lewis,*
*Gregory L. Finch, Steven A. Belinsky, and Alan R. Dahl*

Inhalation of mainstream cigarette smoke (MCS) by rats results in multifocal rhinitis, mucous hypersecretion, nasal epithelial hyperplasia and metaplasia, and focal olfactory mucosal atrophy. In humans, cigarette smoking causes long-term, dose-related alterations in olfactory function in both current and former smokers (Frye, R. E. *et al. JAMA 263(9)*: 1233, 1990). An olfactory-specific cytochrome P450 has been identified in rabbits (P450NMb; Ding, X. *et al. Arch. Biochem. Biophys. 285(1)*: 120, 1991) and rats (P4502G1; Nef, P. *et al. J. Biol. Chem. 265(5)*: 2903, 1990). The presence of olfactory-specific P450s, as well as relatively high levels of other biotransformation enzymes, such as NADPH-cytochrome P450 reductase and UDP-glucuronosyl transferase, in the olfactory neuroepithelium suggests that these enzyme systems may play a role in olfaction. This hypothesis is strengthened by the observation that, in rats, the temporal gene activation of P4502G1 coincides with the postnatal increase in the sensitivity of olfactory response to odorants (Nef *et al.*, 1990).

The purpose of this investigation was to examine the effect of MCS exposure on P4502G1 protein expression. Male CDF®(F-344)/CrlBR rats (6 wk of age) were exposed to filtered air or 250 mg/m$^3$ MCS, 6 h/d, 5 d/wk, for 10 wk or 30 wk (n = 5/group). All rats were sacrificed 16 h to 18 h after their last day of exposure. The nasal cavities were fixed in 10% neutral buffered formalin and decalcified in 13% formic acid. A tissue block was removed from each nasal cavity by making two transverse cuts perpendicular to the hard palate at the levels of the second palatal ridge and the first upper molar tooth. The tissue blocks were embedded in paraffin; 5-$\mu$m sections from the anterior face of each block were cut and histochemically stained with Alcian Blue (pH 2.5)/hematoxylin and eosin for histopathologic evaluation, or the tissues were immunohistochemically stained (Hotchkiss, J. A. *et al. Toxicol. Appl. Pharmacol. 118*: 98, 1993) to detect immunoreactive rat P4502G1 protein. Immunoreactive rat P4502G1 was detected using an antiserum produced in rabbits against a rat P4502G1 peptide conjugated to keyhole limpet hemacyanin. The peptide that was used as the immunogen corresponded to amino acids 244 through 263 (IEERIQEEAGYLLEELHKVV) as deduced from the published rat P4502G1 cDNA sequence (Nef *et al.*, 1990). This antiserum binds to a 56 Kd protein present in sustentacular cells within the surface epithelium of rat olfactory mucosa and is present in cells of the Bowmen's gland within the lamina propria underlying the olfactory neuroepithelium. This antiserum does not react with other nonolfactory nasal surface epithelia, with bronchial epithelium, nor with nonrespiratory tract tissues such as liver, kidney, or skeletal muscle.

Relative levels of immunoreactive P4502G1 protein in the olfactory surface epithelium were assessed by microdensitometric analysis (Hotchkiss *et al.*, 1993) of immunohistochemically stained nasal tissue sections. To determine the optimal primary antibody concentration, serial sections from one MCS-exposed and one air-exposed rat from each sacrifice time were immunostained with several different concentrations (1:100, 1:200, 1:500, 1:1000, 1:2000, 1:4000) of rabbit anti-rat P4502G1 or normal rabbit serum (specificity control). Based on this dilution series, a primary antibody dilution of 1:1000 was selected for analysis of MCS-induced alterations in P4502G1 protein levels.

Optical densities of the surface epithelium of the olfactory mucosa were measured on both sides of the nasal septum extending from its point of intersection with the dorsal meatus to the approximate mid-point of the septum. A rectangular measurement window was established where height was less than or equal to the thickness of the surface epithelium. Starting at the point of intersection of the

nasal septum with the dorsal meatus, the window was placed over the image of the immunochemically stained section such that one surface was aligned with the lumenal surface of the olfactory neuroepithelium. The total optical density of all pixels within the measurement window was determined. The process was repeated at four more contiguous sites, proceeding ventrally, on one side of the nasal septum; the process was repeated on the opposite surface of the nasal septum. These data were used to devise a single descriptive value (mean total optical density) representing the average density of the immunochemical reaction product for each animal. The mean total optical densities of the following experimental groups (n = 5/group) were compared using a Student's *t* test with Bonfferoni correction for multiple comparisons: (1) 10-wk controls vs. 30-wk controls; (2) 10-wk controls vs. 10 wk MCS-exposed; (3) 30-wk control vs. 30-wk MCS-exposed.

No histopathologic lesions were discerned in the olfactory epithelium of the air-exposed control rats. Rats exposed to MCS for 10 wk were similar to controls; however, occasional focal atrophy of the olfactory epithelium was observed. Rats exposed to MCS for 30 wk had more extensive atrophy of olfactory epithelium, and numerous eosinophilic globules were visible within the surface epithelium of the ethmoid turbinates. In addition, there were occasional unilateral foci where the olfactory neuroepithelium was replaced by a one- to two-cell-layer-thick cuboidal epithelium. In these regions, there were also degeneration/atrophy of the underlying Bowmen's glands and a significant accumulation of neutrophils within the lamina propria.

Compared to control rats sacrificed after 10 wk of exposure, rats exposed to filtered air for 30 wk had 52% more immunoreactive P4502G1 protein within their surface epithelium (Fig. 1). Compared to their respective filtered air controls, MCS exposure reduced the amount of immunoreactive P4502G1 protein in the surface epithelium by 32% and 56% in rats exposed for 10 wk and 30 wk, respectively. There was no quantitative difference in the amount of immunoreactive P4502G1 protein in the surface epithelium between rats exposed to MCS for 10 wk or 30 wk. There were, however, qualitative differences in the distribution of immunoreactive P4502G1. Rats exposed to MCS for 10 wk appeared to have approximately the same number of P4502G1-positive cells as control rats; however, the cells contained less P4502G1 protein (i.e., decreased optical density). After 30 wk of MCS exposure, there appeared to be fewer positive cells, each expressing high levels (comparable to the 30-wk control rats) of immunoreactive P4502G1 protein.

In this study a significant increase in the level of immunoreactive P4502G1 protein expression was observed in air-exposed control rats between 10 wk and 30 wk of exposure. It is not known if this is an age-related phenomenon or if it is due to induction of this xenobiotic-metabolizing enzyme by some factor related to extended housing in whole-body exposure chambers. Analysis of age-matched controls housed under different conditions (i.e., shoe-box type housing) may clarify this observation.

Ten weeks of repeated exposure to MCS resulted in a significant decrease in the expression of immunoreactive P4502G1 protein in the surface epithelium of the olfactory mucosa, a response which preceded any significant MCS-induced morphologic alterations to the olfactory neuroepithelium. Continued MCS exposure resulted in significant structural alterations to the olfactory epithelium resulting in an apparent loss in the number of cells within the surface epithelium expressing P4502G1. If this xenobiotic-metabolizing enzyme does play a role in olfaction, its decreased expression in olfactory neuroepithelium following MCS exposure may contribute to alterations in olfactory function experienced by human cigarette smokers.

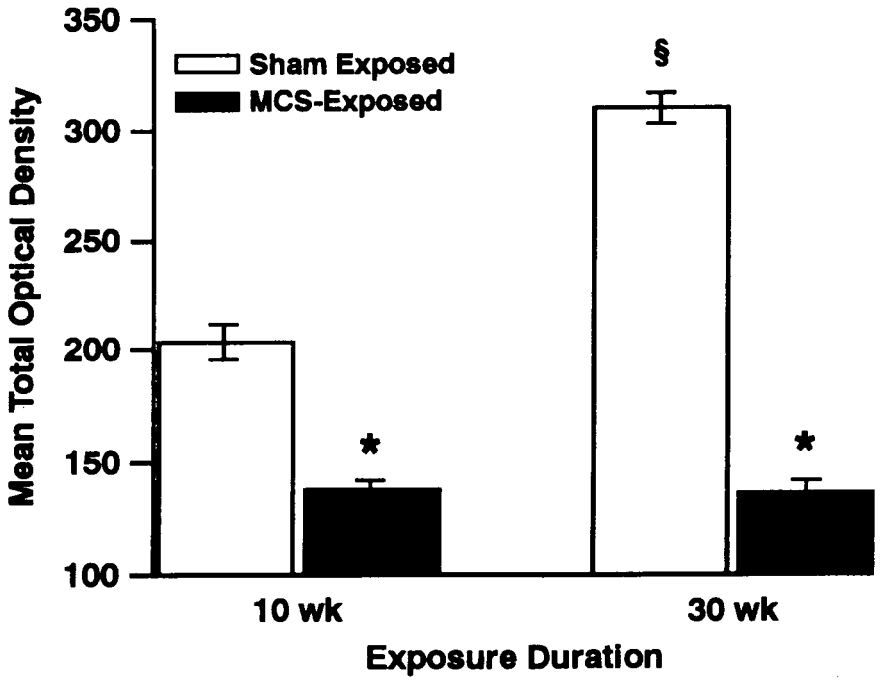


Figure 1. Effect of 10-wk and 30-wk exposures to filtered air or 250 mg/m$^3$ MCS on P4502G1 protein expression in olfactory neuroepithelium. Values are mean total optical density ± standard error of the mean (n = 5/group). § = significantly different from 10-wk controls ($p \leq 0.05$). * = significantly different from respective control group ($p \leq 0.05$).

(Research sponsored by the Office of Health and Environmental Research and Assistant Secretary for Defense Programs, U.S. Department of Energy, under Contract No. DE-AC04-76EV01013.)

# CORRELATION OF PULMONARY EOSINOPHILIA WITH TOTAL SERUM IgE

*David E. Bice, D. David S. Collie*, Douglas J. DeBoer**, Bruce A. Muggenburg, and Fletcher F. Hahn*

Asthma is a serious disease that causes an impaired quality of life, significant financial loss, and death (Weiss, K. B. *et al. N. Engl. J. Med. 326:* 862, 1992). The incidence and severity of asthma, and the mortality it causes have increased during the last 10 y (Evans, R. *et al. Chest 91:* 65S, 1987). Because the reasons for this are not known, studies using experimental animals are needed to determine if environmental factors (e.g., inhaled pollutants) may be important for the increased incidence of asthma.

A phenotypic indication of atopy and allergic asthma is an increased number of eosinophils in blood and lung (Bousquet, J. *et al. N. Engl. J. Med. 323:* 1033, 1990). Recent observations suggest that some dogs in the ITRI colony have large numbers of eosinophils in their blood and lung (Fig. 1). Because eosinophilia and the development of asthma are genetically inherited (Demoly, P. *et al. Presse Med. 22:* 817, 1993), it is possible that these dogs may represent susceptible individuals. The total level of IgE in serum of asthmatics correlates with the number of eosinophils in their blood. Therefore, the purpose of this investigation was to determine if these dogs represent a genetically susceptible population for allergic disease by quantitating the levels of IgE in their serum.

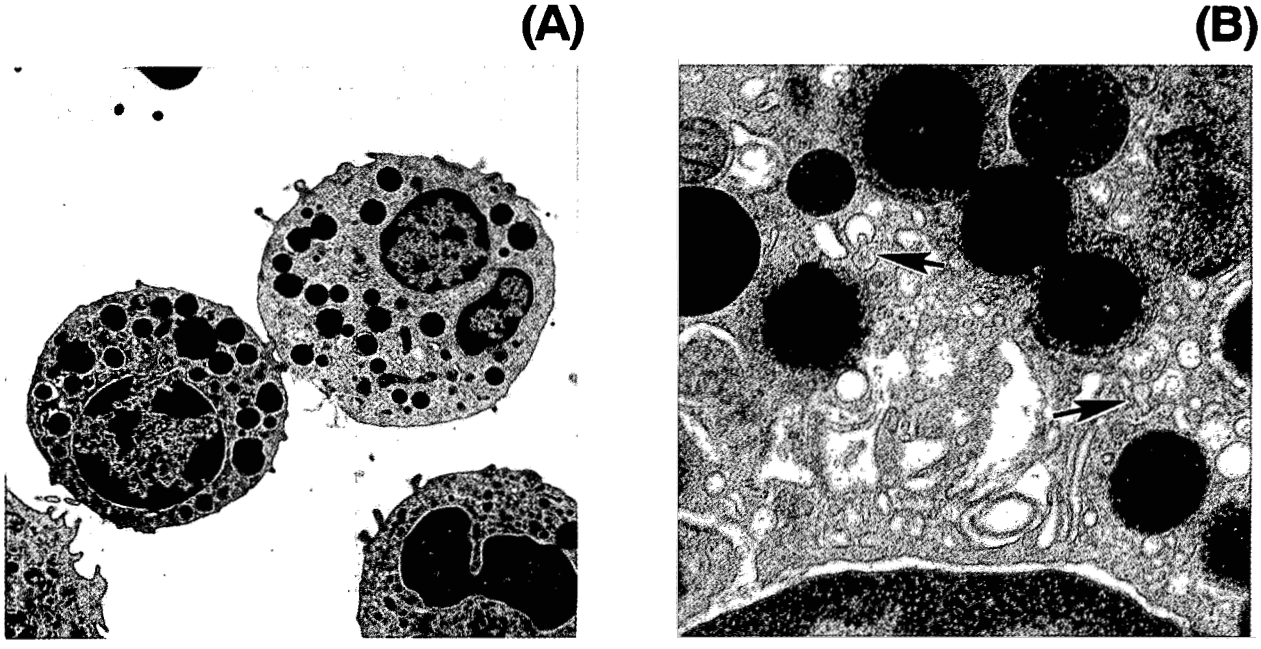


Figure 1. Transmission electron micrograph of cells with eosinophil granules in bronchoalveolar lavage of dog 1523V. (A) Overview of cells showing large oval or bilobed nuclei and abundant cytoplasmic granules; 5,000X. (B) Detail of cytoplasmic organelles showing cytoplasmic granules and specific microgranules; 22,500X.

*Postdoctoral Fellow

**School of Veterinary Medicine, University of Wisconsin, Madison, Wisconsin

A total of 25 dogs from breeders that had or had not produced offspring with eosinophils were used in this study. Because some of these dogs were used in pulmonary immunology studies, data on the number of eosinophils in their lungs were based on lung lavage samples from control lung lobes rather than from lung lobes exposed to antigens. Exposure to antigen increased the number of both eosinophils and neutrophils in lavage fluids. Dogs were anesthetized, and control lung lobes were lavaged by instillation and aspiration of 50 mL normal saline (five, 10 mL washes). Blood samples were taken at the time of lavage. Cytocentrifuge slides were prepared and stained with Diff-Quick. The number of eosinophils in the cytocentrifuge smear was counted and expressed as the total number present in the lavage sample. Serum was removed from the blood samples and the total level of IgE was determined by an enzyme-linked immunosorbant assay. The correlation of the number of eosinophils and the level of IgE in the blood were evaluated by linear regression (MINITAB Software, State College, PA).

Linear regression analysis of the data showed that the total IgE and the number of eosinophils lavaged from the lung were significantly correlated ($r = 0.657$, $p < 0.01$) (Fig. 2). The positive correlation between serum IgE and the number of eosinophils in the lung suggests that these dogs are genetically susceptible for the development of asthma. Because only control lung lobes were lavaged for these evaluations, few or no neutrophils were present in the lavage fluids.

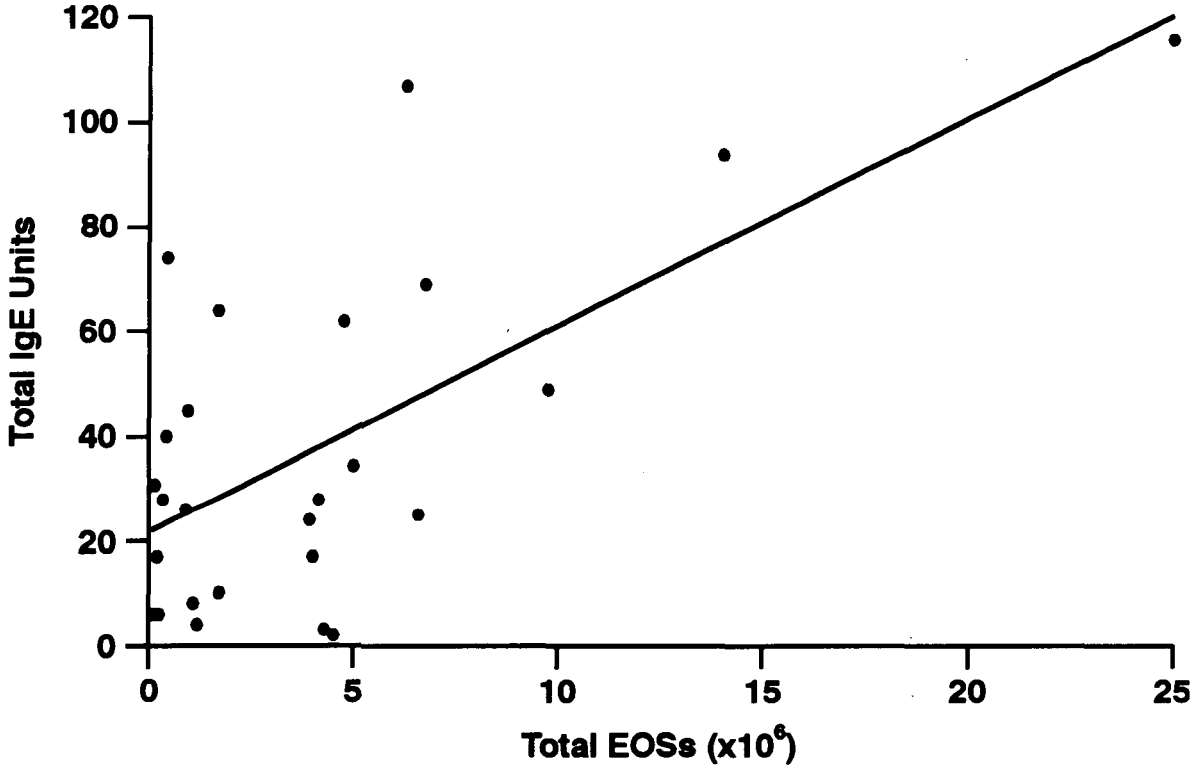


Figure 2. Correlation of the total number of eosinophils obtained by lavaging the lungs of dogs in the ITRI colony with the total level of serum IgE ($p < 0.01$).

Preliminary evaluations by Dr. Fernando Martinez, a collaborator at the University of Arizona, suggest that the eosinophilia in our colony is inherited. However, more data are needed for these comparisons. Therefore, an additional 75 dogs have been lavaged and serum samples taken. The data on eosinophils and the serum levels of IgE in these extra dogs will be included in subsequent genetic evaluations.

Recent studies suggest that pulmonary immune responses that either cause asthma or result in no lung disease are controlled by subclasses of T helper lymphocytes (Robinson, D. S. *et al. N. Engl. J. Med. 326:* 298, 1992). These studies suggest that immune responses in the lungs of asthmatics are produced by Th2 helper lymphocytes, while responses in the lungs of nonasthmatics are produced by Th1 lymphocytes. It is likely that eosinophils are increased in asthmatics because their Th2 immune responses result in the production of IL-4 and IL-5 that recruit eosinophils into the lung and activate these cells. Therefore, the potential identification of inherited eosinophilia in the Beagle dog may provide a model to study the development of Th2 immune responses and asthma. Dogs have been used in asthma studies, usually with immunizations by intraperitoneal injection of allergens in adjuvants (Becker, A. B. *et al. J. Appl. Physiol. 66:* 2691, 1989). However, dogs with pulmonary eosinophilia may develop asthma without the need of adjuvants and therefore represent a more realistic model of asthma.

(Research sponsored by the Office of Health and Environmental Research, U.S. Department of Energy, under Contract No. DE-AC04-76EV01013).

# VIII. THE APPLICATION OF MATHEMATICAL MODELING TO RISK ESTIMATES

# A GENETIC ALGORITHM AS AN AID TO BIOKINETIC MODELING

*Joseph H. Diel*

To describe health effects of inhaled toxicants in a meaningful way, one must have a measure of the dose of the toxicant that caused the effect. For toxicants such as inhaled Pu, the dose is different for different organs and at different times after exposure. The purpose of this investigation was to develop a biokinetic model to simulate the distribution of Pu activity in the tissues and excreta of a dog as a function of time after it is inhaled. Such a model needed to account for all of the substance through a materials balance. It also had to model the amount of material retained in each major organ separately, with each organ divided into multiple compartments to depict different forms of Pu in the organ. Transfer between organs was controlled using transfer coefficients that were either constants, functions of particle size, or functions of time after deposition. This model required a large number of parameters because of its complexity.

A genetic algorithm can optimize large numbers of parameters at one time (Wilson, S. *AI Expert 8(12)*: 21, 1993). This algorithm imitated the processes used in evolution. It consisted of a population that was allowed to evolve using analogues of genetic mutation and genetic information-sharing among individuals. Members of the population who are allowed to contribute to future populations are chosen by some measurement of fit to the system being optimized (Davis, L. *Handbook of Genetic Algorithms*, Van Nostrand Reinholt, New York, 1991).

Genetic algorithms are not normally used alone to solve a given problem because they are often not very efficient, particularly in cases where the number of parameters is large. Methods that incorporate more traditional fitting techniques in addition to a genetic algorithm are known as hybrid genetic algorithms. The hybrid genetic algorithm used for this study consisted of a genetic algorithm with the allowance for the investigator to intervene either by directly changing the parameters of the model or by changing the weights of choices made by the system.

In the experiment modeled, Beagle dogs were exposed by inhalation to one of four monodisperse aerosols of $^{238}PuO_2$ with aerodynamic particle diameters of 1.5, 1.7, 2.7, and 3.0 $\mu$m. The Pu content of excreta was measured periodically, and the Pu content of organs was measured at death. Initial lung burdens were determined for each dog based on the sum of the activity remaining at death and estimates of the amount excreted based on the periodic measurements of activity in excreta. The model predictions were compared to measurements of Pu activity in the different organs of the body at different times after exposure, plus the amounts excreted. All measurements were normalized to the initial lung burden of each dog. All Pu was assumed to be deposited initially in the lung. This Pu was then cleared from the lung either through mechanical clearance of the particles to the gastrointestinal tract or lymph nodes, or dissolution of the particles and transfer through blood to other organs in the body. Dissolution was aided by the fragmentation of the particles resulting from alpha decay energy deposited in the particles. The model used here was a modification of a model used previously to describe this study at an earlier stage in its progress (Mewhinney, J. A. and J. H. Diel. *Health Phys. 45*: 39, 1983). The differences are discussed elsewhere in this report (This report, p. 159).

The number of dogs in the experiment was 178. There was one measurement of Pu activity per organ or group of organs for each dog. Excreta values included 3625 activity measurements for combined urine and feces before 200 d after exposure, and 5268 for feces and 5268 for urine after 200 d.

The genetic algorithm used to fit the model had the following characteristics:

(1) A member of the population consisted of an ordered list of the 47 parameters used in the model that were allowed to vary. The population size could be set by the investigator; 16 members were used for most of the runs of this algorithm.

(2) The function used to measure the fit of the model to the data (fitness) was the weighted sum over all data points of the absolute value of the difference between the logarithm of the measured activity and that of the model prediction normalized by the logarithm of the model prediction. Each datum point within the set of points for an organ or excretion activity measurement was given equal weight. The relative weights for the 10 different organ and excreta groups could be set by the investigator. A smaller fitness value indicated a better fit. This method of evaluation was considered to approximate the visual fitting on a semi-log plot that has been used.

(3) Each potential new member of the population was based on one or two existing members of the population (parents). Members of the population were ranked in reverse order of the magnitude of their fitness. Each parent for the next potential member of the population was chosen using the roulette wheel algorithm. This consisted of summing the ranks of the population, generating a random number between zero and the sum of the ranks, and choosing the first member of the population for whom the sum of the ranks of the preceding members exceeded the random number generated. Using this algorithm, the probability of choice of a member increased with the rank of the member in the population.

(4) The methods used to generate new members included two forms of information interchange (genetic crossover) and one of random changes (mutation).

   (a) Uniform crossover—each parameter of the new member was chosen at random between the values of the same parameter in the two parents.

   (b) Average crossover—each parameter of the new member was the average of the values of the same parameter in the two parents.

   (c) Real number creep—in this form of mutation, the value of each parameter of the new member was a multiple of the value of the same parameter in the single parent.

   The algorithm chose at random among these methods with the relative probability of the choice of the methods set by the investigator.

(5) After a new member was generated, the model was run, and the fitness of the new member was computed. The member was then added to the population, the rank order of the augmented population was determined, and the member of the augmented population with lowest rank was removed to reduce the population back to its original size. This approach is generally referred to as steady-state reproduction.

The genetic algorithm was implemented so that it ran automatically through a preset number of iterations before being interrupted for the evaluation of the results and possible intervention by the investigator. Implementation was on a DEC MicroVAX II minicomputer with 16 Mb of RAM running the VMS operating system. Routines were written in Fortran, DCL (the VMS batch command language), and the Simusolv modeling language (Dow Corning, Midland, MI). The model was run for a total of about 2000 runs; the elapsed time per run was about 15 min. The large amount of computing time required was offset by the small amount of time required for direct intervention by

the investigator, and the ability to run the process during time periods in which there was little other use of the computer.

Fitting the model to the experimental data pointed out several problems that resulted in changes to the model from that previously published (Mewhinney and Diel, 1983). These improvements were based on availability of data to about 5700 d compared to the 1460 d used previously.

As would be expected, improvement of the fit to the model was much greater during the early runs than the later ones (Fig. 1).

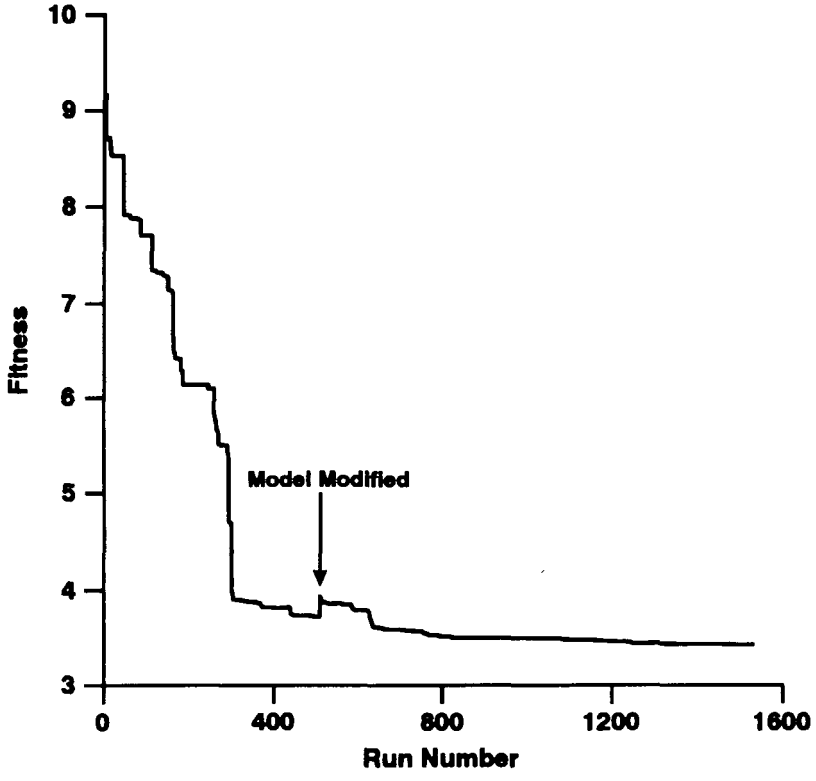


Figure 1. Goodness of fit, fitness of the model to measured activity in different organs and excreta as a function of run number. The measure of goodness of fit is defined in the text.

Neither the population size, nor the relative weights of the fitnesses for the organs and excreta appeared to have much influence on the rate of improvement. All four methods of optimization contributed to the improvement of the fit of the model (Fig. 2). The ability of the investigator to intervene directly in the process was useful for increasing efficiency, particularly at early times in the fitting process. Contrary to expectation based on more traditional genetic algorithms, the mutation function appeared to contribute more to the optimization than did either of the crossover methods.

The hybrid genetic algorithm used in conjunction with the simulation model resulted in an improved ability to describe the organ distribution of Pu in a Beagle dog as a function of time after inhalation of $^{238}PuO_2$. The use of this approach made it possible to optimize all 47 parameters at the same time. The automated features of this algorithm decreased the time needed by the investigator to make routine calculations and allowed a more objective evaluation of the fit of the model to the data.

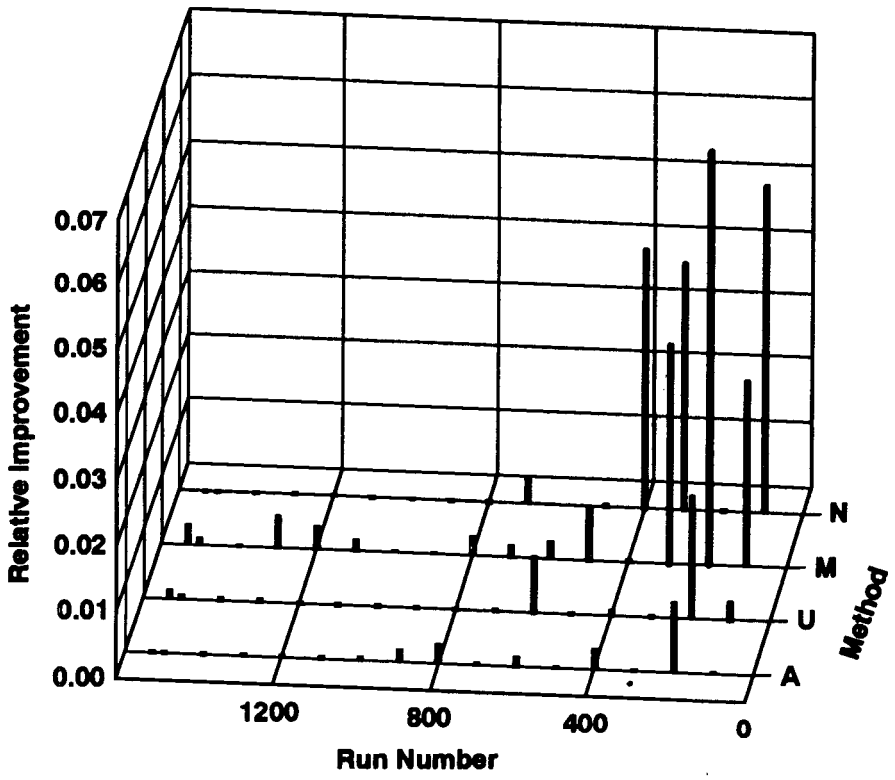


Figure 2. Improvement in the goodness of fit of the model as a function of the run number and the method of modification of the parameters. Improvement is defined as the difference between the previous best value and the new best value divided by the previous best value. Methods used are indicated by A for average crossover, U for uniform crossover, M for mutation, and N for changes in parameters made directly by the investigator. Values plotted are mean and standard deviation for each group of 100 runs.

(Research sponsored by the Office of Health and Environmental Research, U.S. Department of Energy, under Contract No. DE-AC04-76EV01013.)

# BIOKINETICS AND DOSIMETRY OF INHALED $^{238}PuO_2$ IN THE BEAGLE DOG: AN UPDATE

*Raymond A. Guilmette, William C. Griffith, and Joseph H. Diel*

The temporal and spatial distributions of $^{238}Pu$ have been measured during the course of a dose-response study of the biological effects of inhaled $^{238}PuO_2$ in Beagle dogs. These measurements were done on the dose-response study animals, as well as a separate group of dogs exposed to similar aerosols and killed serially out to 4 y after exposure. The data from this latter group provided the basis for the development of a biokinetic/dosimetric model for $^{238}PuO_2$ in dogs (Mewhinney, J. A. and J. H. Diel. *Health Phys. 45*: 39, 1983). Since the publication of this model, several important findings have been made that affected the dosimetric evaluations. The first involved the discovery of significant quantities of natural uranium (U) in the feces samples. The U was measured with the plutonium (Pu), which inflated the values for purported Pu in feces. The second finding involved the addition of Pu biokinetics data from the dose-response dogs, which increased the period of observation from 4 y to 15 y; these later data were not consistent with the earlier model predictions. The purpose of this investigation was 1) to remove the analytical bias in the $^{238}Pu$ radiochemical data due to the U and 2) to modify the original model of Mewhinney and Diel, taking into account all data from both studies.

The biokinetics of inhaled $^{238}PuO_2$ in individual dogs is reconstructed from data obtained from radiochemical analysis of the $^{238}Pu$ content of tissue, urine, and feces samples collected over the experimental life span of each dog. Because institutional resources precluded analyzing all excreta samples, periodic daily collections were made during the course of each animal's experimental lifetime. The total amounts of $^{238}Pu$ excreted in urine and feces were then estimated by fitting mathematical functions to the urine and feces data sets from individual dogs (nonlinear regression, NLIN, SAS statistical software, Cary, NC), and integrating these functions for the experimental observation period (excepting the first 4 d after exposure, which were considered to represent clearance of Pu particles deposited on ciliated airways). The sum of the total tissue content of $^{238}Pu$ at death and the integrated urine and feces excretions comprised the initial lung burden (ILB) for each animal. The ILB was also estimated through a series of whole-body counts of a $^{169}Yb$ gamma-emitting tracer incorporated into the $^{238}PuO_2$ particles during production.

The radiochemical method of Keough, R. F. and G. J. Powers (*Anal. Chem. 42*: 419, 1970) was used for analysis of $^{238}Pu$ in biological samples. Acid-solubilized Pu(IV) was extracted quantitatively from an aqueous acid phase by di-[2-ethylhexyl] phosphoric acid in toluene to produce a two-phase cocktail. The cocktail was counted in a liquid scintillation counter with high efficiency and reasonably low background. During the middle 1980s, it was discovered that this counting method also extracted U(VI) quantitatively. Therefore, because the liquid scintillation technique did not discriminate between Pu and U alpha particles, all Pu measurements (tissue and excreta) were artifactually high due to the presence of U in the individual samples. This counting bias was most problematic in the feces samples because of the significant U content of the dry kibble food used during the study. In addition, the magnitude of the problem increased with decreasing ILBs, as the relative U contribution to the feces increased with decreasing exposure levels of $^{238}Pu$.

To correct for this U bias, an estimate of the U daily excretion rates in urine and feces for individual dogs was needed. The individual daily rates were estimated for the 48 dogs with the lowest lung burdens, using the $^{169}Yb$ radiolabel. The observed fecal excretion pattern was fit by a negative exponential plus a constant, where it was assumed that the slope of the exponential was the same for all dogs. The constant provided the estimated amount of the U excreted in the feces per day, and

the integral of the negative exponential provided an estimate of the amount of $^{238}Pu$ in the feces. The average daily U fecal excretion for this subpopulation was 3.00 ± 0.92 Bq/d.

It was subsequently realized that this method overcorrected for the U contribution in the feces of these 48 dogs because the $^{238}Pu$ contribution to the fecal alpha activity that was due to biliary excretion could not be detected. An additional correction factor was therefore applied by expressing the cumulative biliary excretion as a fraction of the final body burden. This factor was then computed as a function of time using the simulation model for the specific $^{238}PuO_2$ aerosol inhaled, and multiplying it by the final $^{238}Pu$ body burden. This amount was then added into the reconstructed ILB. For dogs that lived more than 5000 d on study, the biliary excretion factor represented about 75% of the Pu body burden at death.

Correcting for the U content in the feces exposed at higher $^{238}Pu$ levels was a simpler process. The average value for daily U fecal excretion from the lower-level dogs (3.00 Bq/d) was used as an estimate of the daily excretion rate for the higher-level dogs. Its time integral (3.00 Bq/d x days on study) was subtracted from the integral of the function fitted to each dog's fecal excretion data (a sum of two or three negative exponentials).

To correct the urinary excretion for U content, it was assumed that the U in the urine was a constant fraction of the daily U fecal excretion for all dogs. This fraction (final value of 0.18) was adjusted so that the ratio of the reconstructed lung burdens to the lung burdens determined by $^{169}Yb$ counting was approximately unity for the average of all dogs on study.

The correction for the U in the feces was the largest factor because for the lowest level dogs, the contribution of the U was about 10 times their ILB. The correction for the U in the urine was smaller but still important, being about two times the ILB for the lowest dogs.

The original $^{238}PuO_2$ biokinetics model was developed based on serial sacrifice data from animals killed ≤ 4 y after exposure. Addition of a significant amount of data from the 144 animals from the dose-response study indicated that the original model of Mewhinney and Diel (1983) needed to be modified. In terms of the structure of the compartmental model, the changes made were to eliminate the transfers of Pu from the "transformed" compartment of the lung to blood and to the tracheobronchial compartment, the Pu transfer from the "transformed" compartment of the tracheobronchial lymph nodes (TBLN) to blood, and the transfer from blood to the small intestine; to change the transfer to blood from (liver, stabile) to (liver, labile); and to add transfer from (kidney, labile) to urine, blood to (lung, labile), and blood to (TBLN, labile). In addition to these modifications, the parameter values were changed. These values were obtained by refitting the model-predicted, organ-specific, and excreta-specific curves to the complete data set from the dose-pattern and dose-response studies. A hybrid genetic algorithm approach (this report, p. 155) was used. The results of the simulation modeling for the retention of $^{238}Pu$ are illustrated in Figure 1.

The radiation doses calculated for the major tissue sites receiving α-radiation dose from $^{238}Pu$ using the Mewhinney-Diel model and the current modification of the $^{238}PuO_2$ model are compared in Table 1. The long-term cumulative doses were significantly different: the lung dose increased 19%, the liver dose decreased 33%, the skeletal dose decreased 44%, and the TBLN dose decreased 170%. The Pu retention in these tissues is described significantly better using the current model based on the goodness of fit of the modeled simulation curves with each tissue-specific radiochemical data set (data not shown). Therefore, we are more confident in using the current dose estimates in determining the dose-response relationships in the dogs that inhaled $^{238}PuO_2$ aerosols as young adult animals.

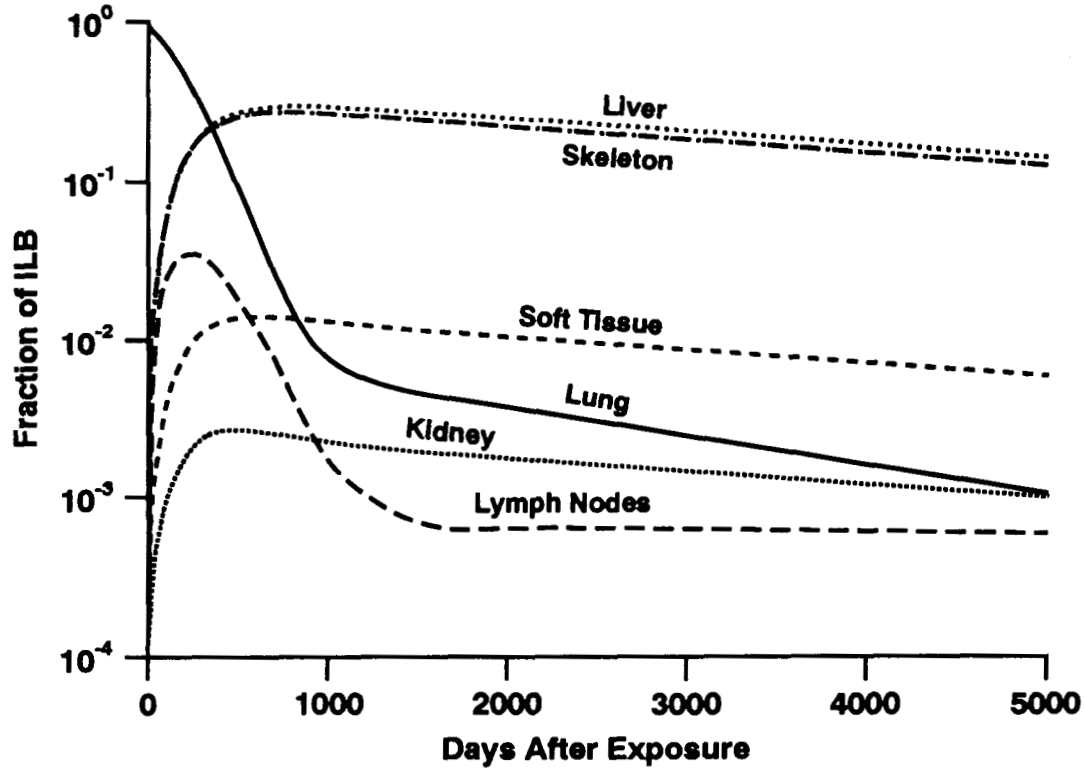


Figure 1. Pu distribution in a Beagle dog after inhalation of $^{238}PuO_2$. Results obtained from a materials balance simulation model fitted to Pu activity measurements in organs at death and in periodically collected excreta.

Table 1

Comparison of 5000-D Cumulative Radiation Doses
For Exposure to 3.0 $\mu$m AMAD $^{238}PuO_2$ Aerosols:
Current Model vs. Mewhinney and Diel (1983)

| | Cumulative Dose (Gy/kBq Initial Lung Burden) | |
|---|---|---|
| Tissue | Mewhinney and Diel | Current Model |
| Lung | 0.16 | 0.19 |
| Liver | 0.24 | 0.16 |
| Skeleton | 0.11 | 0.062 |
| TBLN | 1.35 | 3.70 |

(Research sponsored by the Office of Health and Environmental Research, U.S. Department of Energy, under Contract No. DE-AC04-76EV01013.)

# PARTIAL SPLINE SCORE TEST TO DETERMINE IF TUMORS ARE INCIDENTAL

*William C. Griffith*

A primary consideration in many rodent bioassays is whether a tumor observed in an animal has affected its life span. When tumors are incidental, the natural death times can be regarded as random sampling times unrelated to the presence of the tumor. In this case, animals dying from natural causes and those sacrificed can be combined to estimate the prevalence $p(t)$ of the tumors in the living animals. When tumors are incidental, the tumor incidence rate, $\lambda^T(t)$, is related to the prevalence by

$$\lambda^T(t) = \frac{\dot{p}(t)}{1 - p(t)}, \tag{1}$$

where $\dot{p}(t)$ is the derivative of the prevalence.

The pathologist reading a study will often make a judgement as to whether a tumor is incidental. This may be based upon a general category of tumor types or on an animal-by-animal basis. Many types of tumors appear to arise near the end of the life span and seem to have little effect on the life span even when some of the tumors cause the death of the animal. The pathologist may regard a tumor as not being incidental only if it had some obvious relation to the immediate cause of death, rather than just altering the time of death. Because of the limited information available for the pathologist to consider in a rodent bioassay, this may be the only reasonable basis on which a judgement can be made. When additional information is available, such as a detailed clinical history for larger animals or humans, then the pathologist can better judge when a tumor is incidental to death.

Because such information is lacking in rodent bioassays, it is necessary to have a basis on which to test whether tumors are incidental. One type of test is suggested by comparing equation (1) to the equation for the tumor incidence rate when tumors are not incidental

$$\lambda^T(t) = \frac{\dot{p}(t)}{1 - p(t)} + \lambda^D(t)\frac{r(t) - p(t)}{1 - p(t)}, \tag{2}$$

where $r(t)$ is the prevalence of the tumors in the rodents at the time of death from natural causes and $\lambda^D(t)$ is the mortality rate (McKnight, B. and J. Crowley. *J. Am. Stat. Assoc. 79*: 639, 1984). When $r(t) = p(t)$, then equation (2) reduces to equation (1). The purpose of this paper was to develop a semiparametric test of the equivalence of $r(t)$ to $p(t)$ that tests the assumption of tumors being incidental to the cause of death and minimizes the number of mathematical assumptions. To develop a test, it was necessary to consider the likelihood associated with a rodent bioassay study and the most appropriate forms for $r(t)$, $p(t)$, and $\lambda^D(t)$.

The negative log likelihood for a rodent bioassay can be written as a partial likelihood in order to have three separate sums, each involving only terms with $r(t)$, $p(t)$, or $\lambda^D(t)$. This eliminated cross products between $r(t)$, $p(t)$, and $\lambda^D(t)$ and made it possible to maximize a likelihood term independently for each function. This also made it possible to use techniques of penalized likelihood estimation for each function, which had the advantage of potentially providing a nonparametric estimate of $r(t)$, $p(t)$, and $\lambda^D(t)$. Nonparametric estimates are preferable because there are no known reasons to prefer one particular form of a parametric mathematical function over another for the estimation of

any of these functions. In this application, a semiparametric estimator (a combination of parametric and nonparametric functions) was used instead of a nonparametric estimator because of the practical and technical considerations described below. Because the penalized likelihood was being maximized, the estimator had an easily computable form known as a partial spline. A spline was easily computable because it consisted of a collection of cubic polynomials in time pieced together such that the curve and its first two derivatives were continuous. The reason for using a spline was that as data were collected at a larger number of time points, the splines converged to any curve that had its first two derivatives continuous, even if the curve was not a polynomial. This very rich family of curves forms an infinite dimensional space, a requirement of any nonparametric curve estimator.

The practical consideration for the use of a semiparametric model arose because of the limited number of sacrifice times usually available for estimation of the prevalence in living animals, $p(t)$. The assumptions about the parametric form of the functions could be minimized by jointly estimating $r(t)$ and $p(t)$ with a partial spline, such that the logit of $p(t)$ was a spline and the difference of the logits of $p(t)$ and $r(t)$ was a linear function of time.

The reason for using this partial spline was that in the calculation of the tumor incidence rate by equation (2), the difference, $r(t) - p(t)$, was important in determining the magnitude of $\lambda^T(t)$. Often, there may be relatively few sacrifice times to determine the tumor prevalence $p(t)$, so that the estimation of $p(t)$ may not have a sufficient number of sacrifice times to justify its estimation by a separate spline. The sign of the difference $r(t) - p(t)$ was also important because there were no constraints to force the sign of equation (2) to be positive. By using a partial spline in this manner, both prevalence functions had a common nonparametric component to adjust to whatever shape was observed for the prevalences as a function of time. A nonparametric estimate of the mortality rate, $\lambda^D(t)$, was made using a cubic spline to maximize a penalized partial likelihood.

A score test for incidental tumors based on $r(t) = p(t)$ using the partial spline estimator was equivalent to testing whether the linear function components of the partial spline were zero, i.e., whether the coefficients $\zeta_0 = 0$ and $\zeta_1 = 0$ in $\zeta_0 + \zeta_1 t$. The score test was derived following the usual methods based upon the score and the inverse information matrix (Green, P. J. and B. W. Silverman. *Nonparametric Regression and Generalized Linear Models*, Chapman and Hall, London, 1994). The test had a chi-square distribution with 2 degrees of freedom because it was testing whether two parameters were zero, $\zeta_0$ and $\zeta_1$. The simplicity with which this test could be constructed was the technical reason for use of a semiparametric model for the prevalences. If separate nonparametric estimates were used for $r(t)$ and $p(t)$, then it would not be clear how to define the degrees of freedom for the test.

To illustrate the advantage of this type of proposed score test for incidental tumors, it was compared to one described by Malani, H. M. and J. Van Ryzin (*J. Am. Stat. Assoc. 83*: 1171, 1988), that involved grouping animals dying from natural causes into time intervals between sacrifice times. This could be viewed as a nonparametric test based upon averages across broad time intervals. The power of the two tests was compared using simulated experiments for a test of size 0.05. The simulations were performed for a variety of conditions to compare the power characteristics of the two tests.

The results of the simulations indicated that when the difference between $r(t)$ and $p(t)$ was large, as when tumors were rapidly lethal, both tests had high power even for small experiments with less than 50 animals. In simulations when the difference between $r(t)$ and $p(t)$ was not large, the powers of the two tests depended upon the characteristics of the simulations. When the assumptions of the semiparametric estimator were met, the semiparametric score test had greater power than the test described by Malani and Van Ryzin (1988). When the assumptions of the semiparametric estimator

were not met, because the difference between the prevalences were not linear on a logistic scale, the powers of the two tests appeared to be similar. This is illustrated in Figure 1A. All data points involved 500 replications of the simulations. For these simulations, 5% of the living animals were sacrificed at 200, 300, 400, 500, 600 d, 10% of the living animals were sacrificed at 700 and 800 d, and all remaining animals at 900 d.

In simulations when the assumptions of the partial spline score test were met, the differences in power between the two tests were important because of the much smaller sample sizes needed by the semiparametric test. This can be seen by comparing the sample sizes needed to achieve approximately 80% power, a level sometimes used for the design of studies. When the assumptions of the semiparametric estimators were met, the proposed semiparametric test required about 250 animals compared to about 500 animals for the other test (curves with closed circles in Fig. 1A). For the simulations where the assumptions of the semiparametric estimator were not met, both tests would require about 500 animals (curves with pluses in Fig. 1A).

The power for both tests can be changed by the sacrifice schedule. An alternative to the schedule for the curves in Figure 1A was used to generate the power curves in Figure 1B. In this schedule, 5% of the living animals were sacrificed at 500, 600, 700 d, 10% at 800 d, 20% at 850 d, and all remaining animals at 900 d. With this alternative sacrifice schedule, only about 150 animals were needed to achieve 80% power for the score test based upon the semiparametric estimator and about 250 animals for the test described by Malani and Van Ryzin (1988). The power increased for both tests because the sacrifice times were concentrated into times where there was a high prevalence of tumors in living animals.

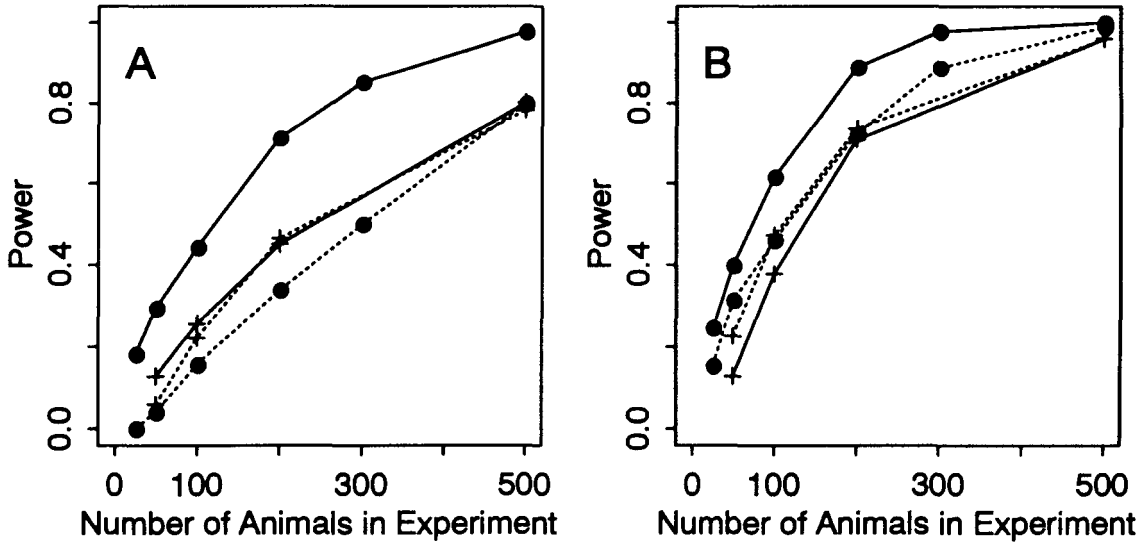


Figure 1. Comparison of power curves for tests of the null hypothesis (at p = 0.05) that tumors are incidental to the cause of death. The solid line is the score test based on the semiparametric estimator, and the dotted line is the test described by Malani and Van Ryzin (1988). The curves with closed circles indicate simulations when the assumptions of the semiparametric estimators are met, and the curves with pluses indicate simulations when the assumptions of the semiparametric estimators are not met. A and B are simulations with two different sacrifice schedules described in the text.

These simulations illustrate the advantage of the proposed partial spline score test for incidental tumors compared to an interval based test. The partial spline score test was more powerful in situations where the assumptions of the estimator were satisfied. When the assumptions were not satisfied, it performed as well as the interval-based test which might be thought to have advantages because no assumptions were made in its derivation about the relationships of the functions between intervals.

Optimizing the power of these tests by the choice of sacrifice schedule would probably not be the only consideration in the design of the sacrifice schedule. Usually one is more concerned about the estimation of the tumor incidence rate, $\lambda^T(t)$, than the determination of whether a tumor is incidental. The best sacrifice schedule for estimation of $\lambda^T(t)$ often would require sacrifices for a broader range of times than would be optimal for the partial spline score test. At the same time, if one could demonstrate that the assumption that tumors are incidental was reasonable, then the estimation of the tumor incidence rate would be greatly simplified and a more precise estimate could be made. The partial spline score test provides a better tool than previously proposed methods for making these decisions and for designing studies from which reasonable decisions can be made.

(Research sponsored by the Office of Health and Environmental Research, U.S. Department of Energy, under Contract No. DE-AC04-76EV01013.)

# CHARACTERIZING ADULT HUMAN NASAL AIRWAY DIMENSIONS

*Raymond A. Guilmette and William C. Griffith*

Respiratory tract models used in calculating radiation dose from exposure to inhaled radioactive aerosols have only recently focused attention on the importance of the nasal airways (NAs). Because the NAs are the first tissues of the respiratory tract available for aerosol deposition in normally nose-breathing people, any deposition of aerosol in this anatomical structure will reduce the amounts available to be deposited in the remainder of the respiratory tract. Thus, uncertainties in estimating the deposition fractions in the NAs will propagate throughout the remainder of the respiratory tract, creating errors in the calculated dose estimates. Additionally, there is evidence that the NAs are also at risk for induction of cancer from exposure to certain occupational aerosols such as wood dust, leather dusts, chromium, and nickel (Roush, G. C. *Head Neck Surg. 2*: 3, 1979).

Cheng, Y. S. *et al.* (*Radiat. Protect. Dosim. 38*: 41, 1991) summarized the human data on NA deposition of both ultrafine and larger sized aerosols, and found a dramatic intersubject variability in the deposition fractions, particularly in the particle-size range from 1–10 $\mu$m. Because the NAs are very complex structures, adequate theoretical models for aerosol deposition in NAs do not yet exist. Nevertheless, we hypothesize that much of the variability that has been observed in NA deposition efficiencies in different humans is due to differences in the size and shape of individual NAs.

The purpose of this investigation was to conduct an anatomical study to assess the variabilities in NA dimensions. Adult, nonsmoking, male and female human subjects, having no notable NA disease or structural pathology, received a magnetic resonance imaging (MRI) scan of their NAs (3-mm contiguous coronal sections taken from the anterior end of the nostrils to the posterior pharynx) using the 1.5 Tesla 55-cm bore Siemens MRI unit at the Veterans Administration Medical Center, Albuquerque, NM. During the course of performing the MRI scan, several anthropometric measurements are also made on each subject. These included (1) height, (2) weight, (3) circumference of the head at the level of the glabella, (4) lateral head width at the glabella, and (5) anterior-posterior head width at the glabella, the smooth area on the frontal bone between the superciliary arches.

The perimeters of left and right NAs were digitized by hand tracing the perimeters of the NAs using a sonic digitizer. The data were stored and analyzed in a computer in terms of both individual airway cross-sectional area and perimeter length. For the present analysis, the cross-sectional areas of all coronal sections from the nares to the posterior end of the nasal septum were summed, then multiplied by 3 mm, the thickness of each section, to obtain a measure of the volume of both NAs. This volume does not include the nasopharynx. Likewise, the perimeter lengths for the same sections were summed and multiplied by the section thickness to obtain the NA surface area. These data were then compared to the various anthropometric measurements by simple linear regression (REG procedure, SAS/STAT software, Cary, NC).

To date, MRI scans of adequate quality for morphometric analysis have been obtained from 49 male and 36 female subjects. Of these, the MR images from 10 males and 10 females have been digitized, and the volume and surface area data regressed against their respective anthropomorphic variables. The results of these preliminary statistical analyses are given in Table 1. Gender-specific analyses will not be done until larger sample sizes are available. However, there are no apparent differences between genders thus far (e.g., Fig. 1).

Based on the current analyses, there are statistically significant relationships of both total NA volume and surface area with subject height, head circumference, and anterior-posterior head width.

No relationships are apparent for weight, height/weight ratio, and lateral head width. As expected with the limited number of data, the uncertainties on the fitted parameters are large, but may be reduced as more data are obtained. If the currently observed relationships between the size of the NAs and certain measures of head and body size are seen in analysis of a larger data set, then the size of individual NAs may be predicted by easily acquired anthropometric measurements. This would provide dosimetry modelers with a practical means of estimating NA dimensions and possibly particle deposition for individuals or populations of individuals.

Table 1

Regression Analyses of Head and Body Size Measures vs. NA Volume and Surface Area Obtained from MRI Scans of Adult Humans

| Variable | Intercept (± SE) | Slope (± SE) | $R^2$ | Pr (Slope = 0) |
|---|---|---|---|---|
| | | Volume | | |
| Height | –31.7 (14.7) | 0.31 (0.08) | 0.403 | 0.0015 |
| Weight | 12.7 (5.7) | 0.13 (0.08) | 0.129 | 0.100 |
| Height/Weight | 30.1 (6.5) | –3.1 (2.6) | 0.069 | 0.24 |
| Circumference | –88.4 (24.0) | 1.92 (0.41) | 0.516 | 0.0002 |
| Lateral Width | 19.5 (7.2) | 0.18 (0.46) | 0.0076 | 0.699 |
| A-P Width[a] | –32.4 (14.3) | 2.85 (0.74) | 0.425 | 0.0010 |
| | | Surface Area | | |
| Height | 18.0 (61.2) | 0.98 (0.35) | 0.279 | 0.012 |
| Weight | 149 (21) | 0.53 (0.29) | 0.142 | 0.084 |
| Height/Weight | 221 (24) | –13.2 (9.6) | 0.0867 | 0.183 |
| Circumference | –135 (108) | 5.61 (1.88) | 0.308 | 0.0073 |
| Lateral Width | 172 (27) | 1.05 (1.74) | 0.018 | 0.555 |
| A-P Width | 10.5 (58.8) | 9.23 (3.06) | 0.313 | 0.0068 |

[a]A-P width is the anterior-posterior width of the head.

Whether the metrics used in this study (total NA volume and surface area) are also predictive of particle deposition efficiencies has not been shown. Other more detailed measures of NA size, such as cross-sectional area at the liminal valve, may be better predictors of particle deposition, particularly for particle sizes > 0.5 $\mu$m. Additional studies are required to determine the relationships between NA size and shapes (probably using *in vitro* approaches) and deposition efficiencies and localized deposition patterns. Results of such studies will improve the basis for developing theoretical deposition models for NAs.

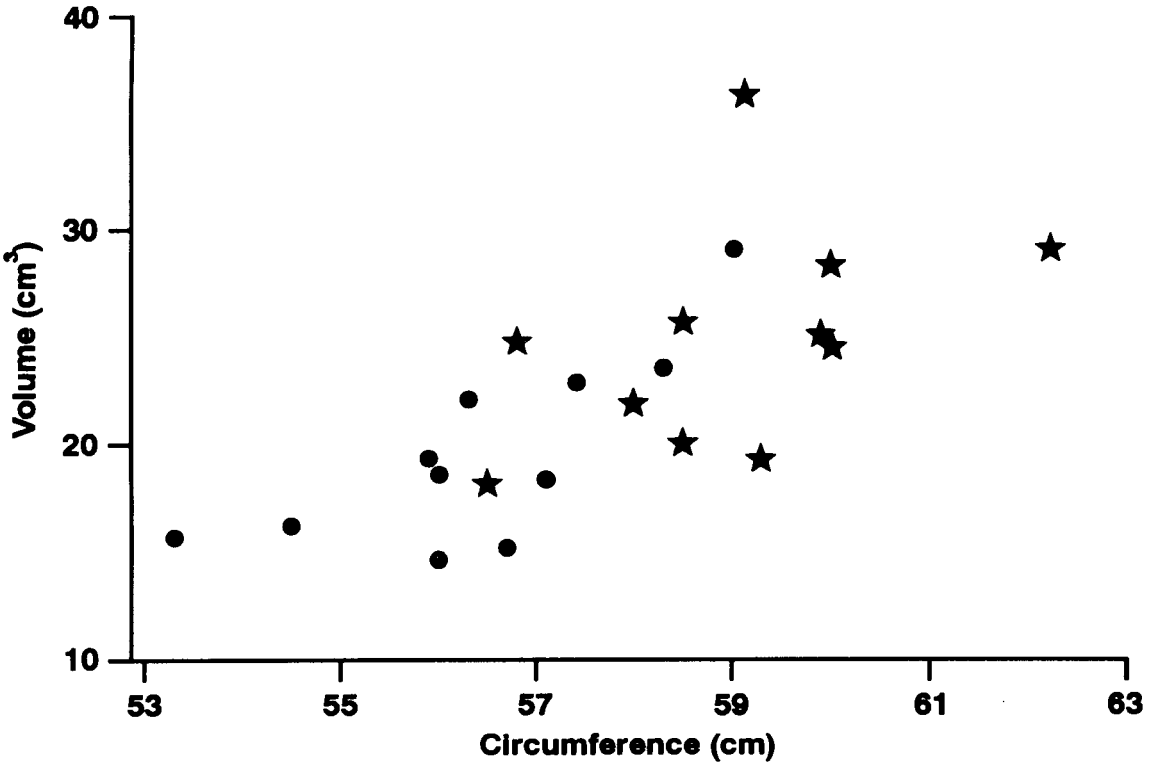


Figure 1. Nasal Airway volume vs. head circumference at the level of the glabella for female (circles) and male (stars) subjects.

(Research sponsored by the Office of Health and Environmental Research, U.S. Department of Energy, under Contract No. DE-AC04-76EV01013.)

# HEMATOLOGICAL RESPONSES AFTER INHALING $^{238}PuO_2$: AN EXTRAPOLATION FROM BEAGLE DOGS TO HUMANS

*Bobby R. Scott, Bruce A. Muggenburg, Colleen A. Welsh*, and David A. Angerstein*

The alpha emitter plutonium-238 ($^{238}Pu$), which is produced in uranium-fueled, light-water reactors, is used as a thermoelectric power source for space applications. Inhalation of a mixed oxide form of Pu is the most likely mode of exposure of workers and the general public. Occupational exposures to $^{238}PuO_2$ have occurred in association with the fabrication of radioisotope thermoelectric generators. Organs and tissue at risk for deterministic and stochastic effects of $^{238}Pu$-alpha irradiation include the lung, liver, skeleton, and lymphatic tissue. Little has been reported about the effects of inhaled $^{238}PuO_2$ on peripheral blood cell counts in humans. The purpose of this study was to investigate hematological responses after a single inhalation exposure of Beagle dogs to alpha-emitting $^{238}PuO_2$ particles and to extrapolate results to humans.

Details on the experimental protocol have been published (Muggenburg, B. A. *et al. 5th International Congress of the International Radiation Protection Association,* Vol. II, p. 115, 1980). The data set used was based on exposure of 144 dogs (ages 12 to 15 mo; both sexes) via nose-only inhalation of monodisperse aerosols of $^{238}PuO_2$; initial lung burdens (ILB) ranged from 1 to 500 kBq. A total of 24 control dogs was also included. White blood cell (WBC), neutrophil, and lymphocyte concentrations in the peripheral blood were analyzed as a function of the ILB and time after inhalation exposure using SAS software (*SAS Procedures Guide, Version 6, Third Edition,* SAS Institute Inc., Cary, NC, 1990; *SAS System for Linear Models, Third Edition,* SAS Institute Inc., Cary, NC, 1991; *SAS Graph Software, Usage Version 6, First Edition,* SAS Institute Inc., Cary NC, 1991).

To compensate for variability in blood cell counts, data were grouped by both ILB (0 [controls], 1 to 9.99, 10 to 19.99, 20 to 49.99, 50 to 99.99, and 100 to 500 kBq) and times after inhalation exposure (consecutive 100-d intervals to 1000 d; followed by consecutive 200-d intervals to 4000 d). Group averages and associated standard deviations were also calculated. These groupings facilitated resolution of both temporal and exposure-related changes in blood cell counts. Data to 6 y (2200 d) post-inhalation exposure were judged to be the most useful for comparative analyses; thus, only results to 6 y post-inhalation exposure are presented here.

In evaluating neutrophil and WBC data, the time course of changes in blood cell counts were evaluated to eliminate any artifacts related to complications associated with the diseases that caused death of the dogs. For 19 dogs, blood cell counts were found to have increased rapidly within about a year prior to their death. Therefore, for the indicated 19 dogs, neutrophils and WBC counts recorded within 1 y of death were excluded in our analyses. Average blood cell counts for control animals progressively decreased with increasing time (age) post-inhalation exposure and were adequately characterized using polynomial regression models. Because of these age-related changes, data for Pu-exposed dogs were not normalized to baseline values but were compared to data for age-matched controls. Average blood cell counts for the 1–2 y post inhalation exposure period were found to be relatively stable and were used to demonstrate exposure-related decrements (depressions) in blood cell counts relative to values for age-matched controls. Depressions were averaged over the 1–2 y post-inhalation exposure period for a given ILB (rather than over ranges of ILB).

*Department of Energy/Associated Western Universities Teacher Research Associates Program (TRAC) Participant

For dogs with ILBs greater than 20 kBq, full recovery to normal lymphocyte, neutrophil, and WBC counts required more than 5 y. Figure 1 shows the average lymphocyte counts (cells per $mm^3$ of blood) as a function of time and ILB range. Note that lymphocyte counts decreased progressively during the first year with increasing ILB. For ILBs greater than about 50 kBq, lymphocyte counts varied over time with average values remaining below control values to at least 6 y post-inhalation exposure. For ILBs greater than about 100 kBq, lymphocyte counts dropped progressively from values close to 4000 per $mm^3$ to about 1000 per $mm^3$ at about 1.5 y, then showed signs of only partial recovery through about 4 y and thereafter a progressive decrease; death prior to the 6-y time point was not uncommon for this high-level group.

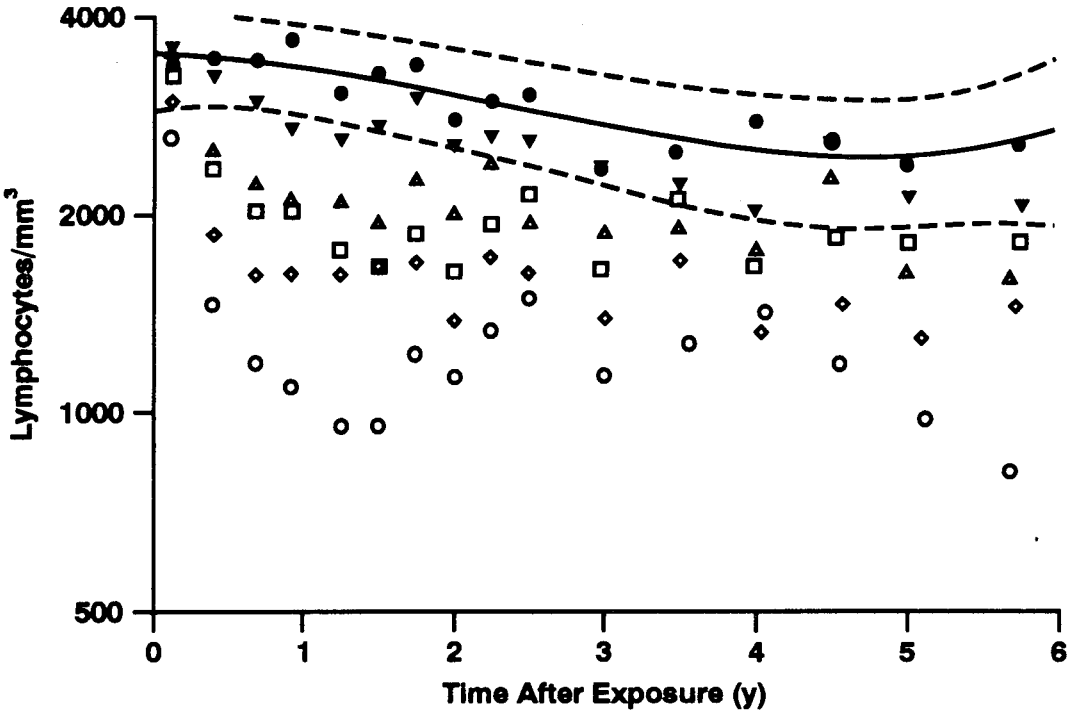


Figure 1. Average lymphocyte counts by ILB range and time after inhalation exposure of Beagle dogs to $^{238}PuO_2$. A cubic regression model was used to fit the data for controls (filled circles, solid line). A 95% confidence region was used for characterizing uncertainty (dashed lines). ILB groups are indicated by the following symbols (●) control; (▽) 0-10 kBq; (△) 10-20 kBq; (□) 20-50 kBq; (◊) 50-100 kBq; and (○) 100–500 kBq.

Depressions in lymphocyte counts during the 1–2 y follow-up period were also evaluated as a function of the ILB. Depression was expressed as a percentage of age-matched control values and averaged over the 1–2 y interval. A 40% depression would correspond to a decrease in blood cell counts to 40% of control values. Depression in lymphocyte counts was found to be strongly correlated ($R = 0.9$) with $\ln(ILB)$ and was highly significant ($p < 0.001$). The dose-response relationship was of the threshold type and was characterized using the equation

$$Y = a + b \ln(ILB) \quad (1)$$

The variable $Y$ represents the percentage depression as a function of the $ILB$ in kBq. The parameter $a$ was found to be –5.9 ± 3.2%; $b$ was found to be 13.7 ± 0.9 % per ln(kBq). With this model, the threshold $ILB$ (indicated by $ILB_o$) is given in kBq by

$$ILB_o = e^{-a/b} . \quad (2)$$

Note that $a/b$ has units of ln(kBq) and that $a$ is negative. $ILB_o$ was found to be 1.5 ± 0.3 kBq. It is useful to re-express Eq. 1 with the normalized lung burden, $X = ILB/ILB_o$, as the independent variable instead of $ILB$. One then gets

$$Y = b \ln(X) . \quad (3)$$

With the normalized lung burden, $X$, interspecies differences in sensitivity are presumed to be factored out so that Eq. 3 should apply to both dogs and humans; however, $ILB_o$ will be different for the two species and should differ for male and female humans because of differences in their lung masses. If $W$ is the mass in g of the lung of a human adult, then $ILB_o$ for that person can be estimated as 1.54 $W$/110, with approximate standard error 0.32 $W$/110, where 110 in the denominator is the average mass in g of the dog lung for our study. This is based on the assumption that the hematological response to inhaled $^{238}PuO_2$ in dogs and humans is directly related to the initial radioactivity concentration in the lung. When $W$ changes with age (e.g., for children), an average value over 1–2 y post-inhalation exposure can be used.

Figure 2 presents a plot of lymphocyte depression (% of control value) as a function of X for the 1–2 y follow-up period. A threshold is indicated at $X = 1$. Figure 2 applies to both dogs and humans. Note that $X$ is plotted on a logarithmic scale. Results presented in Figure 2 and similar results obtained for neutrophils and total WBCs indicate that depression in peripheral blood cell counts could serve as a biological dosimeter for evaluating the intake of large amounts of $^{238}Pu$. Such a biological dosimeter may prove useful in epidemiological studies involving inhalation exposure to Pu, and possibly other radionuclides.

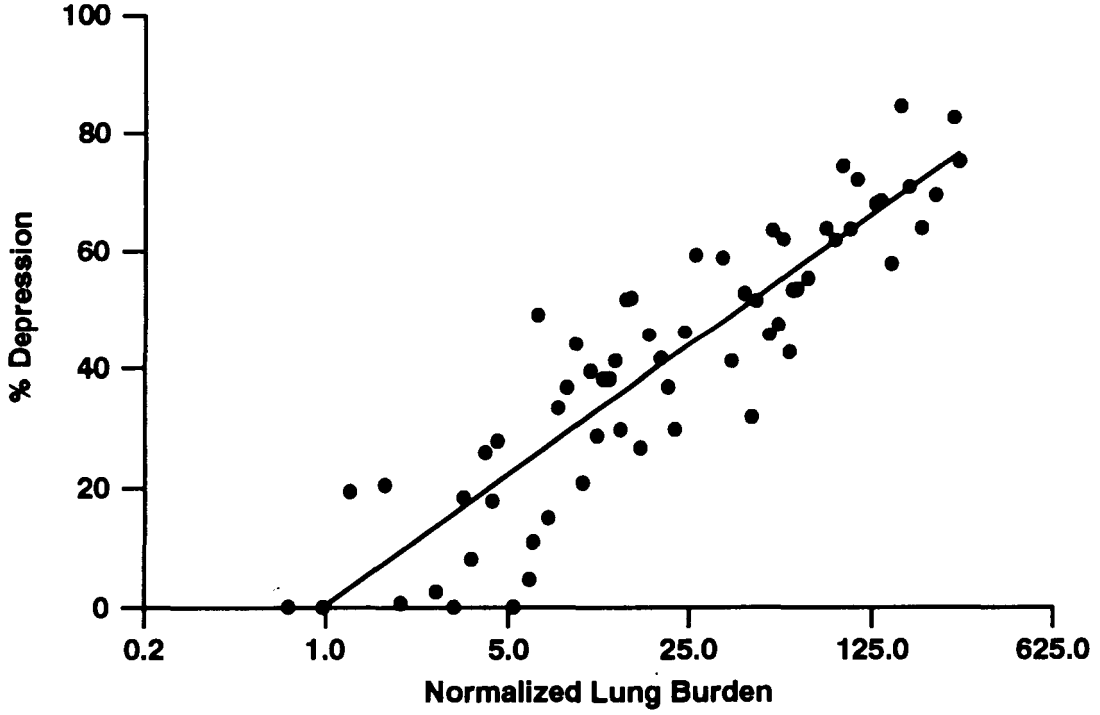


Figure 2. Percentage depression in lymphocyte counts in Beagle dogs exposed by inhalation to $^{238}PuO_2$ as a function of the normalized lung burden $X$. Data were evaluated at 1–2 y after inhalation exposure. $X = 1$ corresponds to $ILB_o$. Results are presumed to also apply to humans.

Our results suggest that blood cell counts after inhalation exposure to $^{238}PuO_2$ can remain depressed for periods of years. This might be confirmed by evaluating possible residual hematological effects in populations exposed in Russia to relatively large levels of Pu. A key question to be addressed in future research is whether a prolonged depression in peripheral blood cell counts similar to those observed in our study could have serious immunological consequences in humans.

(Research sponsored by the Office of Health and Environmental Research, U.S. Department of Energy under Contract No. DE-AC04-76EV01013.)

# IX. APPENDICES

# APPENDIX A

## STATUS OF LONGEVITY AND SACRIFICE EXPERIMENTS IN BEAGLE DOGS

Each annual report of the Inhalation Toxicology Research Institute from 1967 (LF-38) through 1987-1988 (LMF-121) included an appendix containing detailed tabular information on all dogs in the life-span studies of inhaled radionuclides and many sacrifice series associated with these studies. In LMF-121, similar kinds of summary tables were also included for dogs in long-term and life-span studies of injected actinides that were conducted at the University of Utah. All dogs remaining alive in the Utah studies were transferred to ITRI on September 15, 1987, where they are being maintained and studied for the remainder of their life spans. Responsibility for managing the completion of the Utah life-span studies has been assigned to ITRI. A small team of investigators at the University of Utah and investigators at ITRI are working together to complete the observations and summaries.

Along with other changes made in the regular ITRI Annual Report beginning with Report LMF-126, *Inhalation Toxicology Research Institute Annual Report, 1988-1989*, it was decided that the growing body of detailed information on these studies in dogs would no longer be included. Instead, separate periodic reports are being prepared that contain specific updated information on all ITRI and University of Utah long-term and life-span studies in Beagle dogs. The first three of these reports, entitled *Annual Report on Long-Term Dose-Response Studies of Inhaled or Injected Radionuclides*, were published as Report LMF-128 for 1988-1989, as Report LMF-130 for 1989-1990, and as Report LMF-135 for 1990-1991. These reports described the studies, updated experimental design charts, survival plots, pathology summaries and detailed tabular information on all dogs in a manner consistent with past practices. This year, ITRI-139 was published as the *Biennial Report on Long-Term Dose-Response Studies of Inhaled or Injected Radionuclides*, 1991-1993.

Recognizing that these data are of interest to a limited number of individuals, these reports are provided without charge to individuals requesting them. To obtain these reports, please send a request to:

Director
Inhalation Toxicology Research Institute
P. O. Box 5890
Albuquerque, NM 87185-5890

## LOVELACE BIOMEDICAL AND ENVIRONMENTAL RESEARCH INSTITUTE
Directors and Officers

R. O. McClellan, DVM, Chairman
D. J. Ottensmeyer, MD, Vice Chairman
J. L. Mauderly, DVM, President
C. H. Hobbs, DVM, Vice President
B. B. Boecker, PhD, Asst. Secretary/Treasurer (non-director)
J. F. Lechner, PhD, Asst. Secretary/Treasurer (non-director)
J. A. Lopez, BSChE, Asst. Secretary/Treasurer (non-director)

J. P. Bundrant
N. Corzine
J. Doull, MD
B. D. Goldstein, MD
W. A. Gross, PhD
D. E. Kilgore, MD
J. Lovelace-Johnson
D. P. Pasternak, MD
M. W. Twiest, MD
A. C. Upton, MD

## INHALATION TOXICOLOGY RESEARCH INSTITUTE
J. L. Mauderly, DVM, Director
C. H. Hobbs, DVM, Associate Director
B. B. Boecker, PhD, Assistant Director for Research
J. F. Lechner, PhD, Assistant Director for Research
J. A. Lopez, BSChE, Assistant Director for Administration

### Scientific Groups

- Aerosol Science
  H. C. Yeh, PhD
- Chemistry and Biochemical Toxicology
  R. F. Henderson, PhD
- Molecular and Cellular Toxicology
  N. F. Johnson, PhD
- Pathology
  F. F. Hahn, DVM, PhD
- Pathophysiology
  J. M. Benson, PhD

### Office of the Director

- Special Assistant to Director
  R. K. Jones, M.D.
- Administrative Associate
  M. B. Morgan
- Internal Auditor
  E. C. Bankey, MBA
- Education Coordinator
  D. E. Bice, PhD

### Scientific Programs

- Aerosols
  Y. S. Cheng, PhD
- Applied Toxicology
  C. H. Hobbs, DVM
- Cancer Mechanisms
  J. F. Lechner, PhD
- Chemical Toxicology
  A. R. Dahl, PhD
- Pathogenesis
  J. F. Lechner, PhD
- Radiation Toxicology
  R. A. Guilmette, PhD

### Research Support Sections and Units

- Analytical Chemistry
  W. E. Bechtold, PhD
- Animal Care
  D. G. Burt, DVM
- Biomathematics
  B. B. Boecker, PhD
- Chronic Studies
  J. M. Benson, PhD
- Clinic
  B. A. Muggenburg, DVM, PhD
- Clinical Pathology
  F. F. Hahn, DVM, PhD
- Exposure
  E. B. Barr, MSEE
- Histopathology
  F. F. Hahn, DVM, PhD
- Necropsy
  J. Hogan, BA

### Administrative Support Sections and Units

- Computer
  J. H. Diel, PhD
- Engineering, Construction and Environmental Restoration
  A. C. Grace III, MS
- Facility Operations and Maintenance
  W. F. Beierman, BSEE
- Financial Management
  K. M. Aragon, MBA
- Health Protection
  B. B. Boecker, PhD (Acting)
- Human Resources
  B. K. Solari, BA
- Library
  S. E. Spurlock, MLS, MIS
- Procurement
  R. F. Harris, MBA
- Property Management
  P. F. Kaplan
- Quality Assurance
  D. L. Harris, MS
- Technical Communications
  P. L. Bradley, MA

# LOVELACE BIOMEDICAL AND ENVIRONMENTAL RESEARCH INSTITUTE
## INHALATION TOXICOLOGY RESEARCH INSTITUTE
## ORGANIZATIONAL STRUCTURE

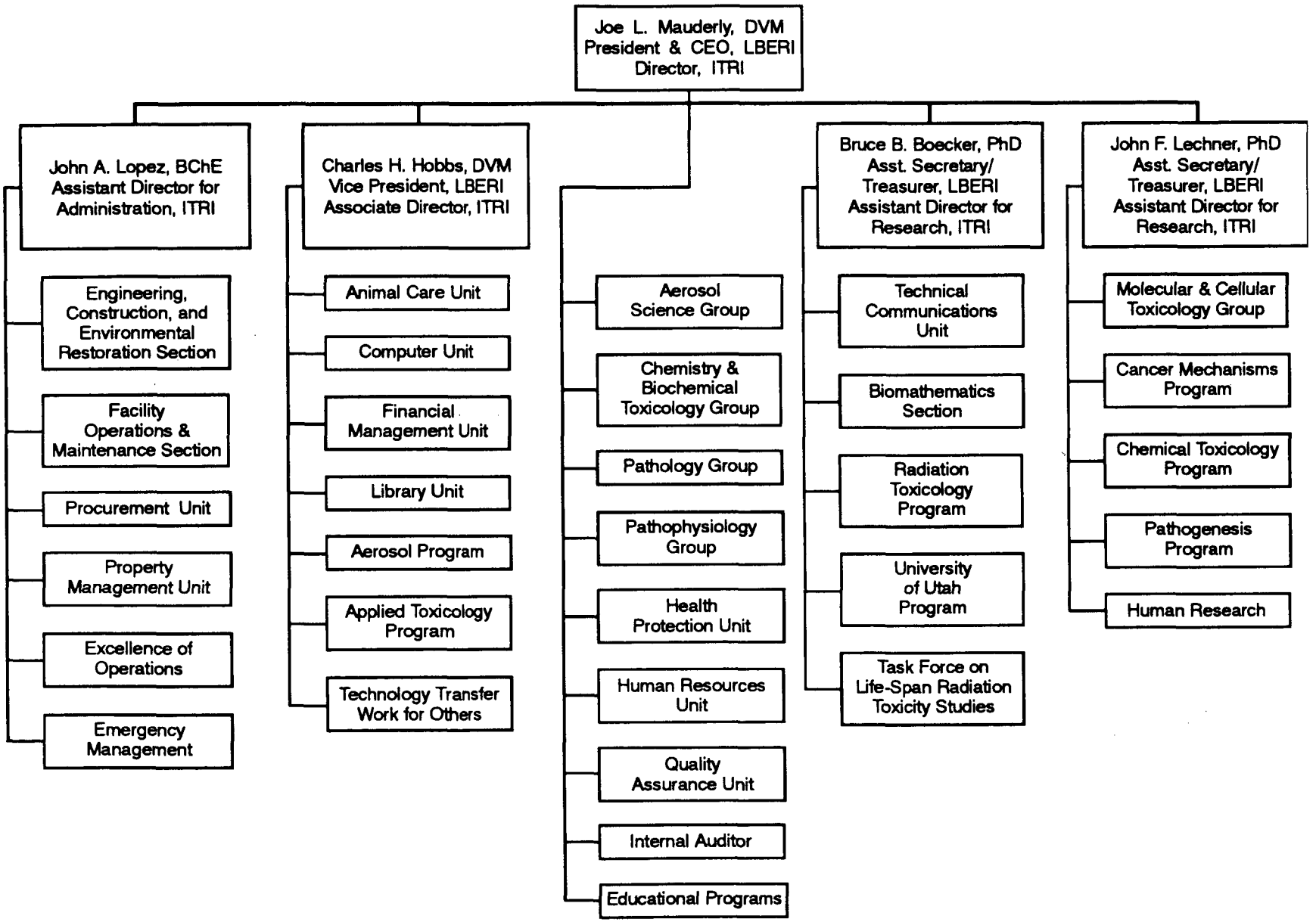

# STAFF OF THE INHALATION TOXICOLOGY RESEARCH INSTITUTE

## ADMINISTRATIVE SUPPORT

| | |
|---|---|
| E. C. Bankey, MBA | Internal Auditor |
| L. L. Burton | Executive Secretary |
| M. G. Campos | Clerical Specialist |
| R. K. Jones, MD* | Special Assistant to the Director |
| M. B. Morgan | Administrative Associate |

## AEROSOL SCIENCE GROUP

| | |
|---|---|
| H. C. Yeh, PhD | Supervisor/Aerosol Scientist |
| B. T. Chen, PhD | Aerosol Scientist |
| T. R. Chen, BS | Graduate Student |
| K. H. Cheng, BS | Graduate Student |
| Y. S. Cheng, PhD | Aerosol Scientist |
| B. Fan, PhD | Postdoctoral Fellow |
| G. A. Feather, BS | Research Technologist |
| A. F. Fencl, BS | Sr. Research Technologist |
| T. D. Holmes, BS | Sr. Research Technologist |
| M. D. Hoover, PhD | Aerosol Scientist |
| M. Marcinkovich | Research Technologist |
| G. J. Newton, BS | Aerosol Scientist |
| K. D. Rohrbacher, BS* | Graduate Student |
| S. M. Smith, BS | Graduate Student |
| D. Yazzie | Research Technologist |

### Exposure Section

| | |
|---|---|
| E. B. Barr, MSEE | Supervisor/Aerosol Scientist |
| R. D. Brodbeck | Technical Specialist |
| R. K. White, BS | Technical Specialist |
| K. L. Williamson | Laboratory Technician |

## BIOMATHEMATICS SECTION

| | |
|---|---|
| B. B. Boecker, PhD | Assistant Director for Research |
| W. C. Griffith, Jr., BS | Biomathematician |
| B. R. Scott, PhD | Biophysicist |

## CHEMISTRY AND BIOCHEMICAL TOXICOLOGY GROUP

| | |
|---|---|
| R. F. Henderson, PhD | Supervisor/Toxicologist |
| M. L. Allen | Research Technologist |
| W. E. Bechtold, PhD | Chemist |
| L. K. Brookins, BS | Sr. Research Technologist |
| S. T. Chen, BS | Research Technologist |
| A. R. Dahl, PhD | Toxicologist |
| P. Gerde, PhD* | Chemical Engineer |
| M. J. Meyer, BS* | Graduate Student |
| L. Pei, PhD | Postdoctoral Fellow |
| M. R. Strunk, BA | Sr. Research Technologist |
| J. R. Thornton-Manning, PhD | Toxicologist |
| J. J. Waide, MS | Sr. Research Technologist |

### Analytical Chemistry Section

| | |
|---|---|
| W. E. Bechtold, PhD | Supervisor/Chemist |
| K. R. Ahlert | Technical Specialist |
| L. I. Archuleta | Laboratory Technician |
| S. N. Lucas | Laboratory Technician |
| A. M. Maestas | Laboratory Technician |
| P. R. Schmidt | Laboratory Technician |
| D. M. Sugino | Laboratory Technician |

*Part-time employee

## MOLECULAR AND CELLULAR TOXICOLOGY GROUP

| | |
|---|---|
| N. F. Johnson, PhD | Supervisor/Exptl. Pathologist |
| S. S. Amershi, BS | Research Technologist |
| S. A. Belinsky, PhD | Molecular Biologist |
| T. R. Carpenter, DVM | Graduate Student |
| N. R. Collinge, BS | Research Technologist |
| D. M. Gurule* | Laboratory Assistant |
| H. J. Harms, BS | Research Technologist |
| A. W. Hickman, Jr., MS | Graduate Student |
| R. J. Jaramillo, BS | Sr. Research Technologist |
| S. E. Jones, DVM | Experimental Pathology Program Graduate Student |
| G. Kelly, PhD | Molecular Biologist |
| C. H. Kennedy, PhD | Molecular Toxicologist |
| D. M. Klinge, BS | Sr. Research Technologist |
| J. L. Lane, BS | Research Technologist |
| F. T. Lauer | Research Technologist |
| T. L. McGlaun, BS | Research Technologist |
| S. K. Middleton, BS | Research Technologist |
| C. E. Mitchell, PhD | Molecular Biologist |
| M. M. Murphy, BS | Research Technologist |
| R. E. Neft, PhD | Cell Biologist |
| W. A. Palmisano, PhD | Molecular Biologist |
| S. E. Phillips, BS | Research Technologist |
| D. S. Swafford, BS | Graduate Student |
| J. Tesfaigzi, PhD | Molecular Biologist |
| L. A. Tierney, DVM | Graduate Student |

## PATHOLOGY GROUP

| | |
|---|---|
| F. F. Hahn, DVM, PhD | Supervisor/Exptl. Pathologist |
| K. Avila, BS | Research Technologist |
| D. E. Bice, PhD | Immunologist |
| D. D. S. Collie, BVM&S, PhD | Postdoctoral Fellow |
| P. Y. Cossey, BS | Sr. Research Technologist |
| K. M. Garcia, BA | Sr. Research Technologist |
| J. A. Hotchkiss, PhD | Cell Biologist |
| D. A. Kracko, BS | Sr. Research Technologist |
| J. L. Lewis, PhD* | Toxicologist |
| K. J. Nikula, DVM, PhD | Experimental Pathologist |
| K. A. Schafer, DVM | Experimental Pathology Program Graduate Student |
| G. G. Scott, BS* | Graduate Student |
| A. J. Williams, II, BS | Sr. Research Technologist |
| M. B. Wood, BS | Administrative Assistant |

*Part-time employee

### Clinical Pathology Section

| | |
|---|---|
| F. F. Hahn, DVM, PhD | Supervisor/Exptl. Pathologist |
| D. A. Angerstein, AA | Research Technologist |

### Histopathology Section

| | |
|---|---|
| F. F. Hahn, DVM, PhD | Supervisor/Exptl. Pathologist |
| S. C. Barnett | Research Technologist |
| Y. N. Knighton | Laboratory Technician |

### Necropsy Section

| | |
|---|---|
| J. Hogan, BA | Supervisor/Chief Res. Technologist |
| J. L. DuBoise | Laboratory Technician |
| B. Pacheco | Laboratory Technician-Trainee |
| R. B. Garlick | Laboratory Technician |
| P. R. Romero-Stagg | Laboratory Technician |

## PATHOPHYSIOLOGY GROUP

| | |
|---|---|
| J. M. Benson, PhD | Supervisor/Toxicologist |
| L. F. Blair | Research Technologist |
| D. C. Esparza, BS | Sr. Research Technologist |
| G. L. Finch, PhD | Toxicologist |
| K. G. Gillett, BS | Sr. Research Technologist |
| R. A. Guilmette, PhD | Radiobiologist |
| A. M. Holmes | Research Technologist |
| D. L. Lundgren, PhD | Radiobiologist |
| E. J. Salas | Research Technologist |
| M. B. Snipes, PhD | Radiobiologist |
| B. M. Tibbetts, BA | Research Technologist |
| C. P. Vigil, BS | Research Technologist |

### Chronic Studies Section

| | |
|---|---|
| J. M. Benson, PhD | Supervisor/Toxicologist |
| C. A. Dison | Research Technologist |

### Clinical Section

| | |
|---|---|
| B. A. Muggenburg, DVM, PhD | Supervisor/Physiologist |
| M. A. Berry, DVM* | Clinical Veterinarian |
| T. R. Carpenter, DVM | Graduate Student |
| M. A. Weinhold, AS | Research Technologist |

## ANIMAL CARE UNIT

| | |
|---|---|
| D. G. Burt, DVM | Supervisor/Attending Veterinarian |
| S. L. Batson, BS | Chief Animal Technologist |
| D. M. Bolton | Animal Technician |
| F. Campbell, Jr. | Animal Technician |
| D. T. Cordaro | Sr. Animal Technician |
| F. E. Delgado | Animal Technician |
| J. M. Duran | Sr. Animal Technician |
| F. B. Kleinschnitz | Animal Caretaker |
| A. D. Murrin | Clerical Specialist |
| J. F. Quintana* | Animal Caretaker |
| C. G. Romero | Animal Technician |
| P. J. Ryan | Animal Technician |
| S. Walker | Animal Technician |
| C. C. Ynostroza, AS | Sr. Animal Technician |

## COMPUTER UNIT

| | |
|---|---|
| J. H. Diel, PhD | Supervisor/Computer Scientist |
| M. F. Conrad, AS | Research Technologist |
| R. L. Lucero-Maldonado* | Laboratory Technician |
| S. C. McLellan | Laboratory Technician |
| E. Taplin, BBA | Software Specialist |

## ENGINEERING, CONSTRUCTION AND ENVIRONMENTAL RESTORATION SECTION

| | |
|---|---|
| A. C. Grace III, MS | Supervisor |
| J. A. Detmer | Technical Secretary |
| R. L. Gonzales* | Laboratory Assistant |
| D. Griego | Research Assistant - Trainee |
| R. E. Harris | Clerical Specialist |
| S. J. Moya* | Laboratory Assistant |
| A. A. Powell* | Laboratory Assistant |
| G. A. Saiz* | Laboratory Assistant |
| J. P. Samora, MS | Project Engineer |

## FACILITY OPERATIONS AND MAINTENANCE SECTION

| | |
|---|---|
| W. F. Beierman, BSEE | Supervisor |
| E. Anzures | Electrical Maintenance Worker |
| R. T. Cossey, ASEE | Instrum. & Controls Maint. Worker/ Technical Specialist |
| F. D. Cox | Sr. Research Technologist |
| A. R. Espalin | General Maintenance Worker |
| E. M. Gallegos* | Laboratory Assistant |
| J. C. Hawkins* | Laboratory Assistant |
| W. J. Jennings | Heating & Refrigeration Maint. Worker |
| T. A. Knowlton* | Laborer |
| A. F. Monnin | Sr. Research Technologist |
| T. B. Orwat | Technical Specialist |
| B. D. Romero | Janitor |
| F. R. Torrez | HVAC Mechanic & Central Plant Operator |

## FINANCIAL MANAGEMENT UNIT

| | |
|---|---|
| K. M. Aragon, MBA | Supervisor/Budget Officer |
| A. I. Medrano | Clerical Specialist |
| P. S. Ohl, BS | Accountant |
| K. J. Rima | Clerical Specialist |

## HEALTH PROTECTION UNIT

| | |
|---|---|
| B. B. Boecker, PhD | Supervisor/Health Protection Mgr. |
| W. M. FitzPatrick* | Graduate Student |
| L. C. Haling | Executive Secretary |
| M. H. LeForce, MS | Environmental Specialist |
| J. R. Lackey | Sr. Research Technologist |
| J. M. Mauser, MS | Environmental Restoration Engineer |
| K. L. Moline, AA | Research Technologist |
| G. R. Moore, BFA | Clerical Specialist |
| C. W. Pohl | Research Technologist |
| P. S. Puckett* | Laboratory Assistant |
| P. E. Sanchez | Clerical Specialist |
| W. C. Schleyer, III, MS | Health Physicist |
| T. T. Simpson, AAS | Research Technologist |
| T. L. Zimmerman | Research Technologist |

*Part-time employee

## HUMAN RESOURCES UNIT

| | |
|---|---|
| B. K. Solari, BA | Supervisor/Human Resources Manager |
| A. F. Baca | Surveillance Worker |
| J. A. Davis, BS | Assistant Human Resources Manager |
| T. J. Hoskins | Clerical Specialist |
| J. T. Nunez | Clerical Specialist |
| P. Padilla | Surveillance Worker |
| G. J. Quintana | Surveillance Worker |
| R. L. Ripple | Clerical Specialist |
| I. J. Salinas | Surveillance Worker |

## LIBRARY UNIT

| | |
|---|---|
| S. E. Spurlock, MLS, MIS | Supervisor/Technical Librarian |
| C. S. Snidow | Clerical Specialist |

## PROCUREMENT UNIT

| | |
|---|---|
| R. F. Harris, MBA | Supervisor |
| V. K. Aragon | Clerical Specialist |
| J. A. Stephens | Sr. Research Technologist |
| L. Vigil | Clerical Specialist |

## PROPERTY MANAGEMENT UNIT

| | |
|---|---|
| P. F. Kaplan | Supervisor |
| A. J. Garcia | Clerical Specialist |
| K. Perales | Clerical Specialist |
| C. R. Shumate* | Laborer |

## QUALITY ASSURANCE UNIT

| | |
|---|---|
| D. L. Harris, MS | Supervisor/Quality Assurance Officer |
| T. A. Ahlert, BA | Administrative Specialist |

## TECHNICAL COMMUNICATIONS UNIT

| | |
|---|---|
| P. L. Bradley, MA | Supervisor/Technical Editor |
| C. M. Herrera | Clerical Specialist |
| S. L. Perez | Clerical Specialist |
| W. L. Piper, BA | Clerical Specialist |
| S. F. Randock, BA | Clerical Specialist |

## TASK FORCE ON LIFE-SPAN RADIATION TOXICITY STUDIES**

| | |
|---|---|
| B. B. Boecker, PhD | Assistant Director for Research |
| M. G. Campos | Clerical Specialist |
| M. F. Conrad, AS | Research Technologist |
| J. H. Diel, PhD | Computer Scientist |
| K. M. Garcia, BA | Sr. Research Technologist |
| K. G. Gillett, BS | Sr. Research Technologist |
| W. C. Griffith, Jr., BS | Biomathematician |
| R. A. Guilmette, PhD | Radiobiologist |
| F. F. Hahn, DVM, PhD | Experimental Pathologist |
| B. A. Muggenburg, DVM, PhD | Physiologist |
| K. J. Nikula, DVM, PhD | Experimental Pathologist |
| B. R. Scott, PhD | Biophysicist |
| M. B. Snipes, PhD | Radiobiologist |

*Part-time employee

**Individuals have primary assignment in Scientific Groups or Units on preceding pages.

## EDUCATIONAL PARTICIPANTS

| Name | School/University | ITRI Group/Unit/Section |
|---|---|---|
| Department of Energy/Associated Western Universities Summer Student Research Participants | | |
| Elizabeth A. Baker | Colorado State University, CO | Chemistry & Biochemical Toxicology Group |
| Jill C. Baran | Syracuse University, NY | Molecular & Cellular Toxicology Group |
| Nicole L. Boudry | Marion College, WI | Chemistry & Biochemical Toxicology Group |
| Kim K. Decatur | New Mexico State University, NM | Pathology Group |
| Noelle H. Fukushima | University of CA-Santa Cruz, CA | Molecular & Cellular Toxicology Group |
| Lori S. Krob | Metropolitan State College, CO | Pathology Group |
| Sean D. Pearson | New Mexico State University, NM | Aerosol Science Group |
| Paul W. Wacnik | University of New Mexico, NM | Pathology Group |
| William B. Wente | Texas A&M University, TX | Aerosol Science Group |
| Department of Energy/Associated Western Universities Teacher Research Associates Program (TRAC) Participants | | |
| Kevin D. Blackstone | Alamogordo High School, NM | Cellular Toxicology Group |
| Robin P. Groch | San Ramon Valley High School, CA | Molecular & Cellular Toxicology Group |
| Stephen P. Schum | Manzano High School, NM | Aerosol Science Group |
| Allen Templeton | Highland High School, NM | Pathophysiology Group |
| Gary L. TenEyck | Kingwood High School, TX | Chemistry & Biochemical Toxicology Group |
| Colleen A. Welsh | McAllen Memorial High School, TX | Biomathematics Section |
| Department of Energy Health/Physics Fellows | | |
| Craig M. Cullen | University of Missouri, MO | Health Protection Unit |
| Minority High School Student Program Participants | | |
| Carlos Gonzales | Rio Grande High School, NM | Chemistry & Biochemical Toxicology Group |
| Debbie M. Gurule | Valley High School, NM | Molecular & Cellular Toxicology Group |

# ITRI EDUCATIONAL PARTICIPANTS

| Name | School/University | ITRI Group/Unit/Section |
|---|---|---|
| Student Employees – 1994 | | |
| Kelley Bell | University of New Mexico | Animal Care Unit |
| Daniel W. Bettinger | Albuquerque T-VI | Engineering, Construction & Environmental Restoration Section |
| Nicole Britnell | University of New Mexico | Animal Care Unit |
| Karen J. Fennell | University of New Mexico | Quality Assurance Unit |
| Ernest M. Gallegos | University of New Mexico | Facility Operations & Maintenance Section |
| Carlos Gonzales | Rio Grande High School | Chemistry & Biochemical Toxicology Group |
| Richard L. Gonzales | University of New Mexico | Engineering, Construction & Environmental Restoration Section |
| Debbie M. Gurule | Valley High School | Molecular & Cellular Toxicology Group |
| Jonathan C. Hawkins | University of New Mexico | Facility Operations & Maintenance Section |
| Thomas A. Knowlton | University of New Mexico | Facilities Operations & Maintenance Section |
| Christine E. Landon | Albuquerque T-VI | Animal Care Unit |
| Carl R. Millegan | University of New Mexico | Animal Care Unit |
| Salomon J. Moya | University of New Mexico | Engineering, Construction & Environmental Restoration Section |
| Adam A. Powell | University of New Mexico | Engineering, Construction & Environmental Restoration Section |
| Paul S. Puckett | University of New Mexico | Health Protection Unit |
| J. Frederic Quintana | University of New Mexico | Animal Care Unit |
| Gregory A. Saiz | University of New Mexico | Engineering, Construction & Environmental Restoration Section |
| Carrie R. Shumate | University of New Mexico | Property Management Unit |
| Kenneth J. Summa | University of New Mexico | Engineering, Construction & Environmental Restoration Section |
| Andrew D. Szydlowski | New Mexico State University | Engineering, Construction & Environmental Restoration Section |
| Brian S. Winkenweder | University of New Mexico | Aerosol Science Group |

UNM/ITRI Inhalation Toxicology Graduate Students

Thomas R. Carpenter, DVM
Albert W. Hickman, Jr.
Mark D. Meyer
Kevin D. Rohrbacher
Gary G. Scott
Shawna M. Smith
Deborah S. Swafford
Lauren A. Tierney, DVM

Postdoctoral Fellows

D. David S. Collie, PhD
Bijian Fan, PhD
Luigi Pei, PhD

Purdue/ITRI Experimental Pathology Graduate Students

Susan E. Jones, DVM
Kenneth A. Schafer, DVM

| PROGRAM AND PROJECT TITLES | SPONSOR* | COORDINATOR |
|---|---|---|
| **BRUCE B. BOECKER, ASSISTANT DIRECTOR** | | |
| Radiation Toxicology - R. A. Guilmette, Program Manager | | |
| Effective Dose from Inhaled Nuclear Energy Materials | DOE/OHER | R. A. Guilmette |
| Dose-Response Relationships for Inhaled Radionuclides | DOE/OHER | B. A. Muggenburg |
| Radiation Dose and Injury to Critical Cells from Radon | DOE/OHER | N. F. Johnson |
| Deposition of Radon and Radon Progeny in the Respiratory Tract | DOE/OHER | H. C. Yeh |
| Toxicity of Injected Radionuclides - ITRI Effort | DOE/OHER | B. B. Boecker |
| Toxicity of Injected Radionuclides - Utah Effort | DOE/OHER | S. C. Miller |
| Low Level Effects of $^{239}Pu$ Oxide | DOE/OHER | B. B. Boecker |
| Statistical Analysis of Data from Radiobiologic Animal Studies | DOE/OHER | W. C. Griffith |
| Improved Exposure Assessment Using $^{210}Pb$ Measurements for Epidemiologic Studies | DOE/OHER | R. A. Guilmette |
| Solubility Measurements for Implementing 10 CFR Part 20 | NRC | R. A. Guilmette |
| INSRP/BEES Panel | BNL | M. D. Hoover |
| Internal Dosimetry | WSRC | R. A. Guilmette |
| **CHARLES H. HOBBS, ASSOCIATE DIRECTOR** | | |
| Aerosols - Y. S. Cheng, Program Manager | | |
| Biologically Relevant Properties of Energy Related Aerosols | DOE/OHER | Y. S. Cheng |
| Dynamics of Radon Daughter Interactions with Indoor Aerosols | DOE/PHYS | Y. S. Cheng |
| Underground Aerosol Characterization at the WIPP Site | DOE/AL | G. J. Newton |
| Y-12 Radiological Protection Program | DOE/Y-12 | M. D. Hoover |
| HQ Health Physics Study | DOE/HQ | M. D. Hoover |
| Inhalation Hazards for Uranium Mill Tailings | DOE/UMTRAP | G. J. Newton |
| Characterization of Aerosols Produced by Surgical Procedures | NIOSH | H. C. Yeh |
| Evaluation of Respirators - II for Asbestos Fibers | NIOSH/CDC | Y. S. Cheng |
| Experimental Tests on Continuous Air Monitors | EG&G | M. D. Hoover |
| Air Sampling Program at SNL Area V | SNL | G. J. Newton |
| Dissolution of Metal Tritides in Biological Systems | SNL | Y. S. Cheng |
| Russian Topaz-II Study | SNL | M. D. Hoover |
| NESHAP Studies | SNL | G. J. Newton |
| Independent Testing and Evaluation of SRS | DOE/WSRC | M. D. Hoover |
| Air Sampling Program | Pantex | G. J. Newton |

| PROGRAM AND PROJECT TITLES | SPONSOR* | COORDINATOR |
|---|---|---|
| Applied Toxicology - C. H. Hobbs, Program Manager | | |
| Effects of L-Deprenyl on Physiologic Functions | DAHI | B. A. Muggenburg |
| Treatment of Chronic Prostatic Hypertrophy | IMI | B. A. Muggenburg |
| Combined Exposure, Plutonium-Cigarette Smoke | DOE/DP | G. L. Finch |
| Combined Exposure, Plutonium-Beryllium | DOE/DP | G. L. Finch |
| Combined Exposure, Plutonium-X Ray | DOE/DP | D. L. Lundgren |
| Combined Exposure, Plutonium-Chemical Carcinogen | DOE/DP | D. L. Lundgren |
| Combined Exposure, Radiation-Fiber | DOE/DP | J. M. Benson |
| Chronic Inhalation of Hygroscopic Material in Rats | P&G | J. M. Benson |
| 90-Day Study of Powdered Detergent Constituents Inhaled by F344 Rats | P&G | M. B. Snipes |
| Effects of Physical/Chemical HMs on Inflammatory and Proliferative Response Induced in the Lung | IPA | R. F. Henderson |
| Evaluation of Bioavailability of Nickel Compounds | EPRI | J. M. Benson |
| Effects of Ozone on Airway Mucous Cells | NIH | J. R. Harkema |
| **JOHN F. LECHNER, ASSISTANT DIRECTOR** | | |
| Cancer Mechanisms - J. F. Lechner, Program Manager | | |
| Links Between Radiation-Induced Lung Cancer in Laboratory Animals and People | DOE/OHER | F. F. Hahn |
| Pre-Malignant Events in Radiation-Induced Lung Cancer | DOE/OHER | J. Tesfaigzi |
| Lung Cancer in Uranium Miners - Gene Dysfunction | DOE/OHER | J. F. Lechner |
| Cellular Models of Radiation-Induced Lung Cancer | DOE/OHER | J. F. Lechner |
| Molecular Mechanisms of Radiation-Induced Cancer | DOE/OHER | G. Kelly |
| Gene Dysfunction in Chemical Induced Carcinogenicity | DOE/OHER | S. A. Belinsky |
| Identification of Intrinsic Human Genes that Govern Susceptibility to Rn-Induced Cancer | DOE/OHER | W. Palmisano |
| Identification of Target Genes Involved in Carbon Black and Diesel Induced Lung Cancer | HEI | S. A. Belinsky |
| Detection of Molecular Markers to Lung Cancer in Uranium Miners | JHU | J. F. Lechner |

| PROGRAM AND PROJECT TITLES | SPONSOR* | COORDINATOR |
|---|---|---|
| Chemical Toxicology - A. R. Dahl, Program Manager | | |
| Influence of Respiratory Tract Metabolism on Effective Dose | DOE/OHER | A. R. Dahl |
| Biological Markers of Human Exposure to Organic Compounds | DOE/OHER | W. E. Bechtold |
| Mechanisms of Granulomatous Disease from Inhaled Beryllium | DOE/OHER | G. L. Finch |
| Study of Biomarkers of Dosimetry from Exposure to 1,3 Butadiene | NCI | R. F. Henderson |
| Nitrogen Heterocycles: Metabolic Effect and Toxicity | WSU | A. R. Dahl |
| Human Sensitivity to Genotoxic Effects of Butadiene | UTMB | W. E. Bechtold |
| Metabolism of 1,3-Butadiene, Butadiene Monoepoxide and Butadiene Diepoxide by Human and Mouse Liver and Lung Tissue Homogenates | CMA | R. F. Henderson |
| Exposure of $B6C3F_1$ Mice to 1,3-Butadiene | CMA | R. F. Henderson |
| Fate of Inhaled Vapors in Rats and Dogs | NIH/NIEHS | A. R. Dahl |
| Carcinogenicity of Inhalants: A Dosimetric Approach | NIH/NIEHS | A. R. Dahl |
| Disposition of Inhaled Toxicants in the Olfactory System | NIH/NIDCD | J. L. Lewis |
| Toxicity of Nickel Compounds to the Respiratory Tract | NiPERA | J. M. Benson |
| Dosimetry of Benzene in Bone Marrow | API | R. F. Henderson |
| Pathogenesis - J. F. Lechner, Program Manager | | |
| Cellular & Biochemical Mediators of Respiratory Tract Disease | DOE/OHER | R. F. Henderson |
| Airway Epithelial Injury, Adaptation and Repair | DOE/OHER | J. R. Harkema |
| Role of Immune Responses in Respiratory Disease | DOE/OHER | D. E. Bice |
| Evaluation of Pulmonary Immune Responses to Viral Agents | UA | D. E. Bice |



* API - American Petroleum Institute
BNL - Brookhaven National Laboratory
CMA - Chemical Manufacturers Association
DAHI - Deprenyl Animal Health, Inc.
DOE/AL - Department of Energy Operations Office, Albuquerque
DOE/DP - Department of Energy, Defense Programs
DOE/HQ - Department of Energy, Headquarters
DOE/OHER - Department of Energy, Office of Health and Environmental Research
DOE/PHYS - Department of Energy, Physical and Technological Research
DOE/UMTRAP - Department of Energy, Uranium Mill Tailings Remediation Action Program
DOE/Y-12 - Y-12 Plant
EG&G - Rocky Flats Plant
EPRI - Electric Power Research Institute
HL - National Heart, Lung and Blood Institutes
HEI - Health Effects Institute
IMI - Indigo Medical, Inc.
IPA - Institute of Polyacrylic Absorbents
JHU - Johns Hopkins University
NCI - National Cancer Institute
NIDCD - National Institute on Deafness and Communicable Diseases
NIEHS - National Institute of Environmental Health Sciences
NIH - National Institutes of Health
NIOSH/CDC - National Institute of Occupational Safety & Health/ Centers for Disease Control
NiPERA - Nickel Producers Environmental Research Association
NRC - Nuclear Regulatory Commission
P&G - Proctor & Gamble
SNL - Sandia National Laboratories
UA - University of Arizona
UTMB - University of Texas Medical Branch at Galveston
WSRC - Westinghouse Savannah River Co.
WSU - Wayne State University

## APPENDIX D

## PUBLICATION OF TECHNICAL REPORTS

## OCTOBER 1, 1993 - SEPTEMBER 30, 1994

Benson, J. M.: *Final Report to the Nickel Producers Environmental Research Association, Inc.*, Durham, NC, 1993.

Benson, J. M.: *Two-Year Repeated Inhalation Exposure of F344 Rats to HM.* Institute for Polyacrylate Absorbents, Washington, DC, 1994.

Harkema, J. R. and J. L. Mauderly: *Respiratory Function Alterations in Rats Following Chronic Ozone Inhalation*, Report to the Health Effects Institute, Cambridge, MA (in press).

Harkema, J. R., K. T. Morgan, E. G. Bermudez, P. T. Catalano and W. C. Griffith: *Effects of Chronic Ozone Exposure on the Nasal Mucociliary Apparatus in the Rat*, Report to the Health Effects Institute, Cambridge, MA (in press).

Mauderly, J. L., M. B. Snipes, E. B. Barr, S. A. Belinsky, J. A. Bond, A. L. Brooks, I. Y. Chang, Y. S. Cheng, N. A. Gillett, W. C. Griffith, R. F. Henderson, C. E. Mitchell, K. J. Nikula and D. G. Thomassen: *Pulmonary Toxicity of Inhaled Diesel Exhaust and Carbon Black in Chronically Exposed Rats*, Report to the Health Effects Institute, Cambridge, MA (in press).

Newton, G. J., M. D. Hoover and R. H. Reif: *Determination of Aerosol Size Distributions at Uranium Mill Tailings Remedial Action Project Sites*, Report to the U.S. Department of Energy – UMTRA Project, Albuquerque, NM.

ITRI-139 - Boecker, B. B., B. A. Muggenburg, S. C. Miller and P. L. Bradley (eds.): *Biennial Report on Long-Term Dose Response Studies of Inhaled or Injected Radionuclides - October 1, 1991 through September 30, 1993*, National Technical Information Service, Springfield, VA 22161.

ITRI-140 - Nikula, K. J., S. A. Belinsky and P. L. Bradley (eds.): *Inhalation Toxicology Research Institute Annual Report - October 1, 1992 through September 30, 1993*, National Technical Information Service, Springfield, VA 22161.

ITRI-141a - 1992 ITRI Site Environmental Report.

ITRI-141b - Evans, J., S. Abrahamson, M. A. Bender, B. B. Boecker, E. S. Gilbert and B. R. Scott: *Health Effects Models for Nuclear Power Plant Accident Consequence Analysis. Part I: Introduction, Integration, and Summary. Rev. 2, Part I (ITRI- 141)*, U.S. Nuclear Regulatory Commission, Washington, DC, 1993.

ITRI-142 - Yeh, H. C., B. A. Muggenburg, D. L. Lundgren, R. S. Turner, R. A. Guilmette, M. B. Snipes and R. K. Jones: *Characterization of Aerosols Produced by Surgical Procedures*, National Technical Information Service, Springfield, VA 22161.

ITRI-143 - 1993 ITRI Site Environmental Report.

# APPENDIX E

# ITRI PUBLICATIONS IN THE OPEN LITERATURE PUBLISHED, IN PRESS, OR SUBMITTED BETWEEN OCTOBER 1, 1993 - SEPTEMBER 30, 1994


Au, W. W., W. E. Bechtold, E. B. Whorton and M. S. Legator: Chromosome Aberrations and Response to Gamma-Ray Challenge in Lymphocytes of Workers Exposed to 1,3-Butadiene. *Mutat. Res.* (in press).

Bechtold, W. E., M. R. Strunk, I. Y. Chang, J. B. Ward and R. F. Henderson: Species Differences in Urinary Butadiene Metabolites: Comparisons of Metabolite Ratios Between Mice, Rats, and Humans. *Toxicol. Appl. Pharmacol. 127*: 44-49, 1994.

Bechtold, W. E. and R. F. Henderson: Biomarkers of Human Exposure to Benzene. *J. Toxicol. Environ. Health 40*: 377-386, 1993.

Bechtold, W. E., J. J. Waide, T. Sändstrom, N. Stjernberg, D. McBride, J. Koenig, I. Y. Chang and R. F. Henderson: Biological Markers of Exposure to $SO_2$: S-Sulfonates in Nasal Lavage. *J. Exposure Anal. Environ. Epidemiol. 3*: 371-382, 1993.

Bechtold, W. E., M. R. Strunk, J. R. Thornton-Manning and R. F. Henderson: Species Differences in the Metabolism of 1,3-Butadiene: Appearance of Butadiene Diepoxide in the Blood of Mice, but not Rats. *Chem. Res. Toxicol.* (submitted).

Belinsky, S. A., J. F. Lechner and N. F. Johnson: An Improved Method for Isolation of Type II and Clara Cells from Mice. *In Vitro* (submitted).

Benson, J. M., E. B. Barr, W. E. Bechtold, Y. S. Cheng, J. K. Dunnick, W. E. Eastin, C. H. Hobbs, C. H. Kennedy and K. R. Maples: The Fate of Inhaled Nickel Oxide and Nickel Subsulfide in F344/N Rats. *Inhal. Toxicol. 6*: 167-183, 1994.

Boecker, B. B., M. D. Hoover, G. J. Newton, R. A. Guilmette and B. R. Scott: Evaluation of Strategies for Monitoring and Sampling Airborne Radionuclides in the Workplace. *Radiat. Protect. Dosim. 53*: 69-71, 1994.

Boecker, B. B., W. C. Griffith, R. A. Guilmette, F. F. Hahn, B. A. Muggenburg, S. C. Miller, R. D. Lloyd and G. N. Taylor: The Role of Laboratory Animals in Studying the Late-Occurring Effects of Radionuclides Deposited in the Liver and Skeleton. In *Proceedings of the International Seminar: Health Effects of Internally Deposited Radionuclides, Emphasis on Radium and Thorium*, held in Heidelberg, Germany, April 18-21, 1994, World Scientific Publishing, River Edge, NJ (in press).

Brain, J. D. and J. L. Mauderly: Animal Studies with Environmental Aerosols. *J. Aerosol Med. 7*: 25-32, 1994.

Buckley, T. J., A. B. Lindstrom, V. R. Highsmith, W. E. Bechtold and L. S. Sheldon: The Time-Course and Sensitivity of Muconic Acid as a Biomarker for Human Environmental Exposure to Benzene. In *Proceedings of the EPA/AWMA International Symposium: Measurement of Toxic and Related Air Pollutants*, pp. 981-986, Air Waste and Management Association, Pittsburgh, PA, 1993.

Chen, B. T., J. V. Benz, G. L. Finch, J. L. Mauderly, P. J. Sabourin, H. C. Yeh and M. B. Snipes: Effects of Exposure Mode on Amounts of Radiolabeled Cigarette Particles in Lungs and Gastrointestinal Tracts of F344 Rats. *Inhal. Toxicol.* (in press).

Chen, B. T., W. E. Bechtold, G. L. Finch, J. A. Lopez, J. J. Thompson and C. H. Hobbs: Thermal Oxidation of Cigarette Smoke Exhaust. *J. Air Waste Manage. Assoc.* (submitted).

Chen, B. T., H. C. Yeh and N. F. Johnson: Design and Use of a Virtual Impactor and an Electrical Classifier for Generation of Test Fiber Aerosols with Narrow Size Distributions. *J. Aerosol Sci.* (submitted).

Cheng, Y. S., C. C. Yu and K. W. Tu: Intercomparison of Activity Size Distributions of Thoron Progeny by Alpha- and Gamma-Counting Methods. *Health Phys. 66*: 72-79, 1994.

Cheng, Y. S., C. C. Yu, C. J. Tung and P. K. Hopke: Neutralization of Thoron Progeny in Gases. *Health Phys. 67*: 155-161, 1994.

Cheng, Y. S.: Denuder Systems and Diffusion Batteries. In *Air Sampling Instruments*, American Congress of Government Industrial Hygienists, Cincinnati, OH (in press).

Cheng, Y. S. and W. E. Bechtold: Incense Smoke: Characterization and Dynamics in Indoor Environments. *Aerosol Sci. Technol.* (in press).

Cheng, Y. S. and B. T. Chen: Aerosol Sampler Calibration. In *Air Sampling Instruments*, American Congress of Government Industrial Hygienists, Cincinnati, OH (in press).

Cheng, Y. S., H. N. Jow and A. R. Dahl: *In Vitro* Dissolution and Radiation Dosimetry of Metal Tritides. To be published in *Proceedings of the Department of Energy Radiation Protection Workshop*, held in Las Vegas, NV, April 13-15, 1993 (in press).

Cheng, Y. S., Q. H. Powell, S. M. Smith and N. F. Johnson: Silicon Carbide Whiskers: Characterization and Aerodynamic Behaviors. *Am. Ind. Hyg. Assoc. J.* (submitted).

Cheng, Y. S., S. M. Smith, H. C. Yeh, D. B. Kim, K. H. Cheng and D. L. Swift: Deposition of Ultrafine Aerosols and Thoron Progeny in Replicas of Nasal Airways of Young Children. *Aerosol Sci. Technol.* (submitted).

Dahl, A. R. and P. Gerde: Uptake and Metabolism of Toxicants in the Respiratory Tract. *Environ. Health Perspect.* (in press).

Dahl, A. R., D. J. Zastrow and J. A. Hotchkiss: Advances in Comparative Nasal Enzymology Between F344 Rats and Humans. *Inhal. Toxicol.* (in press).

Economou, P., J. F. Lechner and J. M. Samet: Familial and Genetic Factors in the Pathogenesis of Lung Cancer. In *Epidemiology of Lung Cancer* (J. M. Samet, ed.), pp. 353-396, Marcel Dekker, Inc., New York, NY, 1994.

Fan, B., Y. S. Cheng and H. C. Yeh: Evaluation of the Performance of an Annular Diffusion Chamber. To be published in *Proceedings of a Scientific Conference on Obscuration and Aerosol Research*, held in Aberdeen, MD, June 2-5, 1994 (submitted).

Finch, G. L.: *In Vitro* Measurement of Macrophage Phagocytosis Using a Sheep Red Blood Cell Assay. In *Methods in Toxicology*, (C. A. Tyson and J. M. Taylor, eds.), Vol. 1B, pp. 279-286, Academic Press, New York, 1994.

Finch, G. L., B. T. Chen, E. B. Barr, I. Y. Chang and K. J. Nikula: Effects of Cigarette Smoke Exposure on F344 Rat Lung Clearance of Insoluble Particles. In *Toxic and Carcinogenic Effects of Solid Particles in the Respiratory Tract* (U. Mohr, D. L. Dungworth, J. L. Mauderly and G. Oberdoester, eds.), pp. 509-511, International Life Sciences Institute Press, Washington, DC, 1994.

Finch, G. L., P. J. Haley, M. D. Hoover, M. B. Snipes and R. G. Cuddihy: Responses of Rat Lungs to Low Lung Burdens of Inhaled Beryllium Metal. *Inhal. Toxicol. 6*: 205-224, 1994.

Finch, G. L., P. J. Haley, M. D. Hoover and R. G. Cuddihy: Responses of Rats Lungs Following Inhalation of Beryllium Metal Particles to Achieve Relatively Low Lung Burdens. *Ann. Occup. Hyg.* (in press).

Finch, G. L., K. J. Nikula, B. T. Chen, E. B. Barr, I. Y. Chang and C. H. Hobbs: Effect of Chronic Cigarette Smoke Exposure on Lung Clearance of Tracer Particles Inhaled by Rats. *Fund. Appl. Toxicol.* (in press).

Gerde, P., B. A. Muggenburg, M. D. Hoover and R. F. Henderson: Clearance of Particles and Lipophilic Solutes from Central Airways. *Ann. Occup. Hyg.* (in press).

Gordon, T. and J. R. Harkema: Effect of Inhaled Endotoxin on Intraepithelial Mucosubstances in F344 Rat Nasal and Tracheobronchial Airways. *Am. J. Respir. Cell Mol. Biol. 10*: 177-183, 1994.

Gordon, T. and J. R. Harkema: Cotton Dust Produces an Increase in Intraepithelial Mucosubstances in Rat Airways. *Am. Rev. Resp. Dis.* (in press).

Guilmette, R. A., W. C. Griffith and A. W. Hickman: Intake Assessment for Workers that Inhaled $^{238}$Pu Aerosols. *Radiat. Protect. Dosim. 53*: 127-131, 1994.

Guilmette, R. A. and T. J. Gagliano: Construction of a Model of Human Nasal Airways Using *In Vivo* Morphometric Data. *Ann. Occup. Hyg.* (in press).

Guilmette, R. A., Y. S. Cheng, H. C. Yeh and D. L. Swift: Deposition of 0.005-12 $\mu$m Monodisperse Particles in a Computer-Milled, MRI-Based Nasal Airway Replica. *Inhal. Toxicol.* (in press).

Hahn, F. F., W. C. Griffith, C. H. Hobbs, B. A. Muggenburg, G. J. Newton and B. B. Boecker: Biological Effects of $^{91}$Y in Relatively Insoluble Particles Inhaled by Beagle Dogs. *Ann. Occup. Hyg.* (in press).

Hahn, F. F., B. A. Muggenburg and B. B. Boecker: Hepatic Lesions Induced by Chronic Beta Irradiation from $^{144}$Ce in Dogs. To be published in *Proceedings of the International Seminar: Health Effects of Internally Deposited Radionuclides, Emphasis on Radium and Thorium*, held in Heidelberg, Germany, April 18-21, 1994, World Scientific Publishing, River Edge, NJ (in press).

Hahn, F. F.: Radiation-Induced Squamous Cell Carcinoma, Lung of Rats. To be published in the *International Life Sciences Institute Press Monograph: Pathology of Laboratory Animals, Respiratory System*, Second Edition (T. C. Jones, ed.), International Life Sciences Institute Press, Washington, DC (submitted).

Hahn, F. F.: Radiation-Induced Adenosquamous Carcinoma, Lung of Rats. To be published in the *International Life Sciences Institute Press Monograph: Pathology of Laboratory Animals, Respiratory System*, Second Edition (T. C. Jones, ed.), International Life Sciences Institute Press, Washington, DC (submitted).

Hahn, F. F.: Radiation-Induced Adenocarcinoma, Lung of Rats. To be published in the *International Life Sciences Institute Press Monograph: Pathology of Laboratory Animals, Respiratory System*, Second Edition (T. C. Jones, ed.), International Life Sciences Institute Press, Washington, DC (submitted).

Hahn, F. F.: Radiation-Induced Sarcoma, Lung of Rats. To be published in the *International Life Sciences Institute Press Monograph*: *Pathology of Laboratory Animals, Respiratory System*, Second Edition (T. C. Jones, ed.), International Life Sciences Press, Washington, DC (submitted).

Haley, P. J., K. F. Pavia, D. S. Swafford, D. R. Davila, M. D. Hoover and G. L. Finch: The Comparative Pulmonary Toxicity of Beryllium Metal and Beryllium Oxide in Cynomolgus Monkeys. *Immunopharm. Immunotox.* (in press).

Harkema, J. R. and J. A. Hotchkiss: Ozone-Induced Proliferative and Metaplastic Lesions in Nasal Transitional and Respiratory Epithelium: Comparative Pathology. *Inhal. Toxicol.* (in press).

Harkema, J. R., C. M. Wierenga, L. M. Herrera, J. A. Hotchkiss, W. A. Evans, D. G. Burt and C. H. Hobbs: Strain-Related Differences in Ozone-Induced Secretory Metaplasia in the Nasal Epithelium of Rats. *Inhal. Toxicol.* (in press).

Harkema, J. R. and J. L. Mauderly: Pulmonary Function Alterations in F344 Rats Following Chronic Ozone Inhalation. *J. Air Waste Manage. Assoc.* (submitted).

Hatch, G. E., J. R. Harkema, C. G. Plopper and L. Harris: Ozone Dosimetry Studies in the Nose and Eye Using Oxygen-18. *Inhal. Toxicol.* (in press).

Henderson, R. F. and J. L. Mauderly: Diesel Exhaust: An Approach for the Study of the Toxicity of Mixtures. In *Toxicology of Chemical Mixtures* (R. S. H. Yang, ed.), pp. 119-133, Academic Press, San Diego, CA, 1994.

Henderson, R. F., W. E. Bechtold, P. J. Sabourin, K. R. Maples and A. R. Dahl: Species Differences in *In Vivo* Metabolism of 1,3-Butadiene. In ***Butadiene and Styrene: Assessment of Health Hazards*** (M. Sorsa, K. Peltonen, H. Vainio and K. Hemminki, eds.), pp. 57-64, International Agency for Research on Cancer, Lyon, France, 1993.

Henderson, R. F., K. E. Driscoll, R. C. Lindenschmidt, J. R. Harkema, E. B. Barr and I. Y. Chang: Response of the Lung to Instilled Versus Inhaled Particles. In *Toxic and Carcinogenic Effects of Solid Particles in the Respiratory Tract* (U. Mohr, D. L. Dungworth, J. L. Mauderly and G. Oberdoester, eds.), pp. 515-517, International Life Sciences Institute Press, Washington, DC, 1994.

Henderson, R. F., P. J. Sabourin, W. E. Bechtold, B. Steinberg and I. Y. Chang: Disposition of Inhaled Isobutene in F344/N Rats. *Toxicol. Appl. Pharmacol. 123*: 50-61, 1993.

Henderson, R. F., K. E. Driscoll, J. R. Harkema, R. C. Lindenschmidt, I. Y. Chang, K. R. Maples and E. B. Barr: A Comparison of the Inflammatory Response of the Lung to Inhaled Versus Instilled Particles in F344 Rats. *Fundam. Appl. Toxicol.* (submitted).

Herbert, R. A., B. L. Stegelmeier, N. A. Gillett, A. H. Rebar, W. W. Carlton, G. Singh and F. F. Hahn: Plutonium-Induced Proliferative Lesions and Pulmonary Epithelial Neoplasms in the Rat: Immunohistochemical and Ultrastructural Evidence for Their Origin from Type II Pneumocytes. *Vet. Pathol. 31*: 366-374, 1994.

Hickman, A. W., W. C. Griffith, G. S. Roessler and R. A. Guilmette: Application of a Canine $^{238}Pu$ Biokinetic/Dosimetry Model to Human Bioassay Data. *Health Phys.* (in press).

Hickman, A. W., R. J. Jaramillo, J. F. Lechner and N. F. Johnson: Alpha Particle-Induced p53 Protein Expression in a Rat Lung Epithelial Cell Strain. *Cancer Res. 54:* 5797-5800, 1994.

Hobbs, C. H., K. M. Abdo, F. F. Hahn, N. A. Gillett, S. L. Eustis, R. K. Jones, J. M. Benson, E. B. Barr, M. P. Dieter, J. A. Pickrell and J. L. Mauderly: Summary of the Chronic Inhalation Toxicity of Talc in F344/N Rats and $B6C3F_1$ Mice. In *Toxic and Carcinogenic Effects of Solid Particles in the Respiratory Tract,* (U. Mohr, D. L. Dungworth, J. L. Mauderly and G. Oberdoester, eds.), pp. 525-528, International Life Sciences Institute Press, Washington, DC, 1994.

Hoover, M. D. and G. J. Newton: Calibration and Operation of Continuous Air Monitors for Alpha-Emitting Radionuclides. To be published in the Proceedings of the *DOE Radiation Protection Workshop*, held in Las Vegas, NV, April 13-15, 1993 (in press).

Hotchkiss, J. A., H. Kim, F. F. Hahn, R. F. Novak and A. R. Dahl: Pyridine Induction of Sprague-Dawley Rat Renal Cytochrome P4502E1: Immunohistochemical Localization and Quantitation. *Toxicol. Letts.* (in press).

Hotchkiss, J. A., J. S. Kimbell, L. K. Herrera, G. E. Hatch, K. T. Morgan and J. R. Harkema: Regional Differences in Ozone-Induced Nasal Epithelial Cell Proliferation in F344 Rats: Comparison with Computational Mass Flux Predictions of Ozone Dosimetry. *Inhal. Toxicol.* (in press).

Hotchkiss, J. A., W. A. Evans, B. T. Chen, G. L. Finch and J. R. Harkema: Regional Differences in the Effects of Mainstream Cigarette Smoke on Stored Mucosubstances and DNA Synthesis in F344 Rat Nasal Epithelium. *Toxicol. Appl. Pharmacol.* (submitted).

Johnson, N. F. and K. R. Maples: Fiber-Induced Hydroxyl Radical Formation and DNA Damage. In *NATO ASI Series, Cellular and Molecular Effects of Mineral and Synthetic Dusts and Fibres* (J. M. G. Davis and M. C. Jaurand, eds.), pp. 23-37, Springer-Verlag, Heidelberg, Germany, 1994.

Johnson, N. F. and G. J. Newton: Estimation of the Dose of Radon Progeny to the Peripheral Lung and the Effect of Exposure to Radon Progeny on the Alveolar Macrophage. *Radiat. Res. 139*: 163-169, 1994.

Johnson, N. F.: Intraphagolysosomal pH and Glass Fiber Dissolution in Cultured Rat Nasal Epithelial Cells and Alveolar Macrophages: A Preliminary Study. *Environ. Health Perspect.* (in press).

Johnson, N. F.: An Overview of Animal Models for Assessing Synthetic Vitreous Fibers (SVFs) Safety. *Reg. Toxicol. Pharmacol.* (in press).

Johnson, N. F.: Radiobiology of Lung Target Cells. *Radiat. Protect. Dosim.* (submitted).

Johnson, N. F. and F. F. Hahn: Mesothelioma Induction Following Intrapleural Inoculation of F344 Rats with Silicon Carbide Whiskers and Continuous Ceramic Filaments. *Carcinogenesis* (submitted).

Kelsey, K. T., J. K. Wienecke, J. B. Ward, W. E. Bechtold and J. Fajen: Cytogenic Sensitivity to Diepoxybutane in Lymphocytes from Butadiene Monomer Production Workers. *Mutat. Res.* (submitted).

Kennedy, C. H., W. E. Bechtold, I. Y. Chang and R. F. Henderson: Effect of Dose on the Disposition of 2-Ethoxyethanol after Inhalation by F344/N Rats. *Fund. Appl. Toxicol. 21*: 486-491, 1993.

Kusewitt, D. F., G. Kelly, C. L. K. Sabourin and R. D. Ley: Cloning and Sequencing of a cDNA from the K-ras Proto-oncogene (KRAS) of the Marsupial Monodelphis Domesrica. *DNA Sequence 4*: 37-42, 1993.

Last, J. A., T. Gelzleichter, J. R. Harkema, W. C. Parks and P. Mellick: Effects of 20 Months of Ozone Exposure on Lung Collagen in Fischer 344 Rats. *Toxicology 84*: 83-102, 1993.

Lechner, J. F. and J. L. Mauderly: Sequence of Events in Carcinogenesis: Initiation and Promotion, Protooncogenes and Tumor Suppressor Genes and Particulates. In *Toxic and Carcinogenic Effects of Solid Particles in the Respiratory Tract* (U. Mohr, D. L. Dungworth, J. L. Mauderly and G. Oberdoester, eds.), pp. 235-251, International Life Sciences Institute Press, Washington, DC, 1994.

Lechner, J. F. and K. A. Elliget: A Protocol for Normal Human Bronchial Epithelial Cell Cultures. To be published in *Protocols in Cell and Tissue Culture*, John Wiley and Sons, Ltd., West Sussex, U. K. (in press).

Lewis, J. L. and A. R. Dahl: Olfactory Mucosa: Composition, Enzymatic Localization, and Metabolism. In *Handbook of Clinical Olfaction and Gustation* (R. L. Doty, ed.), pp. 33-52, Marcel Dekker, New York, 1994.

Lewis, J. L., F. F. Hahn and A. R. Dahl: Transport of Inhaled Toxicants to the Central Nervous System: Characteristics of a Nose-Brain Barrier. In *The Vulnerable Brain and Environmental Risks, Volume 3, Toxins in Air and Water*, Chapter 5 (R. L. Isaacson and K. F. Jensen, eds.), pp. 77-103, Plenum Press, New York, 1994.

Lewis, J. L., K. J. Nikula, R. Novak and A. R. Dahl: Comparative Localization of Carboxylesterase in F344 Rat, Beagle Dog, and Human Nasal Tissue. *Anatom. Rec. 239*: 55-64, 1994.

Lewis, J. L., K. J. Nikula and L. A. Sachetti: Induced Xenobiotic-Metabolizing Enzymes Localized to Eosinophilic Globules in Olfactory Epithelium or Toxicant-Exposed F344 Rats. *Inhal. Toxicol.* (in press).

Lipscomb, M. F., D. E. Bice, C. R. Lyons, M. R. Schuyler, and D. Wilkes: The Regulation of Pulmonary Immunity. To be published in *Advances in Immunology* (F. J. Dixon, ed.), Academic Press, San Diego, CA (in press).

Lloyd, R. D., G. N. Taylor, W. Angus, S. C. Miller and B. B. Boecker: Skeletal Malignancies Among Beagles Injected with $^{241}$Am. *Health Phys. 66*: 172-177, 1994.

Lundgren, D. L., P. J. Haley, F. F. Hahn, W. C. Griffith and B. R. Scott: Pulmonary Carcinogenicity of Repeated Inhalation Exposure of Rats to Aerosols of $^{239}PuO_2$. *Radiat. Res.* (submitted).

Malkinson, A. M. and S. A. Belinsky: The Use of Animal Models in Preclinical Studies Relating to Lung Cancer. To be published in *Lung Cancer: Principles and Practice*, J. B. Lippencott, Philadelphia, PA (in press).

Mauderly, J. L.: Contribution of Inhalation Bioassays to the Assessment of Human Health Risks from Solid Airborne Particles. In *Toxic and Carcinogenic Effects of Solid Particles in the Respiratory Tract* (U. Mohr, D. L. Dungworth, J. L. Mauderly and G. Oberdoester, eds.), pp. 355-365, International Life Sciences Institute Press, Washington, DC, 1994.

Mauderly, J. L.: Noncancer Pulmonary Effects of Chronic Inhalation Exposure of Animals to Solid Particles. In *Toxic and Carcinogenic Effects of Solid Particles in the Respiratory Tract* (U. Mohr, D. L. Dungworth, J. L. Mauderly and G. Oberdoester, eds.), pp. 43-55, International Life Sciences Institute Press, Washington, DC, 1994.

Mauderly, J. L.: Toxicological and Epidemiological Evidence for Health Risks from Inhaled Engine Emissions. *Environ. Health Perspect. 102*: 165-171, 1994.

Mauderly, J. L.: Toxicological Approaches to Complex Mixtures. *Environ. Health Perspect. 101*: 155-165, 1993.

Mauderly, J. L., E. B. Barr, A. F. Eidson, J. R. Harkema, R. F. Henderson, J. A. Pickrell and R. K. Wolff: Pneumoconiosis in Rats Exposed Chronically to Oil Shale Dust and Diesel Exhaust, Alone and in Combination. *Ann. Occup. Hyg.* (in press).

Mauderly, J. L.: Differences in Pulmonary Responses of Rats, Other Animals, and Humans to Chronic Inhalation of Silica and Other Particles. To be published in *Proceedings of the Second International Symposium on Silica, Silicosis and Cancer*, held in San Francisco, CA, October 28-30, 1993 (in press).

Mauderly, J. L.: Current Assessment of the Carcinogenic Hazard of Diesel Exhaust. *Toxicologic and Environmental Chemistry* (in press).

Mitchell, C. E., S. A. Belinsky and J. F. Lechner: Rapid Detection and Quantitation of Mutant Codon 12 Restriction Fragments by Capillary Electrophoresis. *Anal. Biochem.* (in press).

Muggenburg, B. A., R. A. Guilmette, W. C. Griffith, F. F. Hahn, N. A. Gillett and B. B. Boecker: The Toxicity of Inhaled Particles of $^{238}PuO_2$ in Dogs. *Ann. Occup. Hyg.* (in press).

Muggenburg, B. A., F. F. Hahn, W. C. Griffith and B. B. Boecker: The Biological Effects of $^{224}Ra$ Injected into Dogs. To be published in *Proceedings of the International Seminar: Health Effects of Internally Deposited Radionuclides, Emphasis on Radium and Thorium*, held in Heidelberg, Germany, April 18-21, 1994, World Scientific Publishing, River Edge, NJ (in press).

Newton, G. J., W. E. Bechtold, M. D. Hoover, F. Ghanbari, P. S. Herring and H. N. Jow: A Case Study on Determining Air Monitoring Requirements in a Radioactive Materials Handling Area. To be published in the *Proceedings of the DOE Radiation Protection Workshop*, held in Las Vegas, NV, April 13-15, 1993 (in press).

Nickell-Brady, C., F. F. Hahn, G. L. Finch and S. A. Belinsky: Analysis of K-ras, p53, and c-raf-1 Mutations in Beryllium-induced Rat Lung Tumors. *Carcinogenesis 15*: 257-262, 1994.

Nikula, K. J., M. B. Snipes, E. B. Barr, W. C. Griffith, R. F. Henderson and J. L. Mauderly: Influence of Particle-Associated Organic Compounds on the Carcinogenicity of Diesel Exhaust. In *Toxic and Carcinogenic Effects of Solid Particles in the Respiratory Tract* (U. Mohr, D. L. Dungworth, J. L. Mauderly and G. Oberdoester, eds.), pp. 565-568, International Life Sciences Institute Press, Washington, DC, 1994.

Nikula, K. J. and J. L. Lewis: Olfactory Mucosal Lesions in F344 Rats Following Inhalation Exposure to Pyridine. *Fund. Appl. Toxicol.* (in press).

Nikula, K. J., M. B. Snipes, E. B. Barr, W. C. Griffith, R. F. Henderson and J. L. Mauderly: Comparative Pulmonary Toxicities and Carcinogenicities of Chronically Inhaled Diesel Exhaust and Carbon Black in F344 Rats. *Fundam. Appl. Toxicol.* (in press).

Nikula, K. J., B. A. Muggenburg, I. Y. Chang, W. C. Griffith, F. F. Hahn and B. B. Boecker: Late Biological Effects of $^{137}$CsCl Injected in Beagle Dogs. *Radiat. Res.* (submitted).

Nikula, K. J., R. F. Novak, I. Y. Chang, A. R. Dahl, D. A. Kracko and J. L. Lewis: Induction of Nasal Carboxylesterase in F344 Rats Following Inhalation Exposure to Pyridine. *Drug Metab. Dispos. Biol. Fate Chem.* (submitted).

Rothman, N., G. L. Li, R. B. Hayes, M. Dosemeci, W. Bechtold, G. Marti, Y.-Z. Wang, M. Linet, L. J. Xi, W. Lu, M. T. Smith, N. Titenko-Holland, L. P. Zhang, W. Blot and S. N. Yin: Hematotoxicity Among Chinese Workers Heavily Exposed to Benzene. *Am. J. Public Health* (submitted).

Sanders, C. L., R. A. Guilmette and R. L. Kathren: Autoradiographic Examination of Selected Soft Tissue in USTUR Case 246. *Health Phys.* (submitted).

Schuyler, M., B. Edwards, K. Gott and K. J. Nikula: Experimental Hypersensitivity Pneumonitis: Effect of CD4 Cell Depletion. *Am. Rev. Respir. Dis. 149*: 1286-1294, 1994.

Schuyler, M., B. Edwards, K. Gott and K. J. Nikula: Experimental Hypersensitivity Pneumonitis: Effect of CD3 and CD8 Depletion. *Am. J. Respir. Crit. Care Med.* (submitted).

Scott, B. R.: Additional Evidence for Errors in DS86 Neutron Kerma for Hiroshima Based on Biological Dosimetry and Implications for Radiation Protection and Attributable Risk Evaluation. *Radiat. Protect. Dosim. 55*: 87-92, 1994.

Scott, B. R., C. W. Langberg and M. Hauer-Jensen: Models for Estimating the Risk of Ulcers in the Small Intestine After Localized Single or Fractionated Irradiation. *Br. J. Radiology* (in press).

Shyr, L. J., P. J. Sabourin, M. A. Medinsky, L. S. Birnbaum and R. F. Henderson: Physiologically Based Modeling of 2-Butoxyethanol Disposition in Rats Following Different Routes of Exposure. *Environ. Res. 63*: 202-218, 1993.

Simpson, S. Q., R. Singh and D. E. Bice: Heat-killed Pneumococci and Pneumococcal Capsular Polysaccharides Stimulate Tumor Necrosis Factor-Alpha Production by Murine Macrophages. *Am. J. Respir. Cell. Mol. Biol. 10*: 284-289, 1994.

Snipes, M. B.: Biokinetics of Inhaled Radionuclides. In *Internal Radiation Dosimetry, Health Physics Society 1994 Summer School* (O. G. Raabe, ed.), pp. 181-196, Medical Physics Publishing, Madison, WI, 1994.

Snipes, M. B., A. L. Barnett, J. R. Harkema, J. A. Hotchkiss, A. H. Rebar and L. J. Reddick: Specific Biological Effects of an Anti-Rat PNM Antiserum Intraperitoneally Injected into F344/N Rats. *Vet. Clin. Pathol.* (in press).

Stegelmeier, B. L., N. A. Gillett, F. F. Hahn, A. H. Rebar and G. Kelly: Expression of Transforming Growth Factor Alpha and Epidermal Growth Factor Receptor in $^{239}$Plutonium-Induced Rat Lung Neoplasms. *Radiat. Res. 140*: 191-198, 1994.

Stoeber, W. and J. L. Mauderly: Simulation of Particulate Lung Loads in Inhalation Studies with Rats Using a Pulmonary Retention Model: Hypothesis of a Critical Dose for Overload Tumor Induction by Diesel Soot and Carbon Black. *Inhal. Toxicol.* (in press).

Swafford, D. S., K. J. Nikula, C. E. Mitchell and S. A. Belinsky: Low Frequency of Alteration in p53, K-ras, and mdm2 in Rat Lung Neoplasms Induced by Diesel Exhaust or Carbon Black. *Carcinogenesis* (submitted).

Taya, A., J. A. Mewhinney and R. A. Guilmette: Subcellular Distribution of $^{241}$Am in Beagle Lungs Following Inhalation of $^{241}Am(NO_3)_3$ Aerosols. *Ann. Occup. Hyg.* (in press).

Tierney, L. A., F. F. Hahn and J. F. Lechner: p53, erbB2, and K-ras Gene Dysfunctions are Rare in Spontaneous and Plutonium-239-Induced Canine Lung Neoplasia. *Lab. Invest.* (submitted).

Ubels, J. L. and J. R. Harkema: The Rabbit Lacrimal Gland in Vitamin A Deficiency. *Invest. Opthalmol. Vis. Sci. 35*: 1249-1253, 1994.

Ward, J. B., M. M. Ammenheuser, W. E. Bechtold, E. B. Whorton and M. S. Legator: hprt Mutant Lymphocyte Frequencies in Workers at a 1,3-Butadiene Production Plant. *Environ. Health Perspect.* (in press).

Weissman, D., D. E. Bice, R. E. Crowell, and M. R. Schuyler: Intrapulmonary Antigen Deposition in the Human Lung: Local Responses. *Am. J. Respir. Cell Mol. Biol.* (in press).

Yeh, H. C., B. A. Muggenburg, R. A. Guilmette, M. B. Snipes, R. S. Turner, R. K. Jones and J. P. Smith: Characterization of Aerosols Produced During Total Hip Replacement Surgery in Dogs with 51-Cr-Labeled Blood. *J. Aerosol Sci.* (in press).

Yeh, H. C., R. S. Turner, R. K. Jones, B. A. Muggenburg, D. L. Lundgren and J. P. Smith: Characterization of Aerosols Produced During Surgical Procedures in Hospitals. *Aerosol Sci. Technol.* (in press).

# APPENDIX F

## PRESENTATIONS BEFORE REGIONAL OR NATIONAL SCIENTIFIC MEETINGS AND EDUCATIONAL AND SCIENTIFIC SEMINARS

## OCTOBER 1, 1993 - SEPTEMBER 30, 1994

Bechtold, W. E.: Biomarkers of Exposure to Benzene. Thirty-First Hanford Symposium on Health and the Environment, Richland, WA, October 20-23, 1993.

Bechtold, W. E., M. R. Strunk, and R. F. Henderson: Methods for the Analysis of Butadiene and Volatile Metabolites in Blood. Annual Meeting of the Society of Toxicology, Dallas, TX, March 13-17, 1994.

Bechtold, W. E., N. Rothman, S. N. Yin, M. Dosemeci, G. L. Li, Y. Z. Wang, R. B. Hayes, and M. T. Smith: Sixth Conference of the International Society for Environmental Epidemiology and Fourth Conference of the International Society for Exposure Analysis, Research Triangle Park, NC, September 18-21, 1994.

Beierman, W. F.: Student Utilization in Facility Maintenance. U. S. Department of Energy Maintenance Management Workshop, Carlsbad, NM, December 1-3, 1993.

Belinsky, S. A.: p53 Alterations in Lung Tumors Induced in F344/N Rats. Keystone Symposium for Tumor Suppressor Genes, Taos, NM, February 13-20, 1994.

Belinsky, S. A., J. P. Issa, and S. Baylin: Increased Cytosine DNA-Methyltransferase Activity in A/J Mouse Lung Cells Following Carcinogen Exposure and During Tumor Progression. American Association for Cancer Research, San Francisco, CA, April 10-13, 1994.

Belinsky, S. A., K. J. Nikula, C. E. Mitchell, and D. S. Swafford: Identification of Target Genes Induced In Carbon Black and Diesel Exhaust-Induced Lung Cancer. Health Effects Institute Tenth Annual Meeting, Reston, VA, May 1-4, 1994.

Belinsky, S. A.: Gene Dysfunctions in Rodent Lung Tumors. 7th World Conference on Lung Cancer, Colorado Springs, CO, June 26-July 1, 1994.

Belinsky, S. A.: Genetic and Epigenetic Alterations in Human and Rodent Lung Cancer, Lilly Research Laboratories, Greenfield, IN, July 14, 1994.

Benson, J. M., Y. S. Cheng, I. Y. Chang, B. A. Muggenburg, and F. F. Hahn: Fate of Inhaled Nickel Oxide, Nickel Sulfate, and Nickel Subsulfide in Cynomolgus Monkeys. Annual Meeting of the Society of Toxicology, Dallas, TX, March 13-17, 1994.

Berry, M. A., W. C. Griffith, and F. F. Hahn: Pituitary and Adrenal Neoplasia and the Incidence of Hyperadrenocorticism in a Geriatric Beagle Colony. American College of Veterinary Internal Medicine, San Francisco, CA, June 2-5, 1994.

Bice, D. E., M. E. Cunniffe, G. E. Snow, and B. A. Muggenburg: The Development of Pulmonary Immune Memory is Not Antigen-Specific. American Lung Association/American Thoracic Society International Conference, Boston, MA, May 22-25, 1994.

Bice, D. E.: Pulmonary Immune Memory. NIOSH, Morgantown, WV, July 28, 1994.

Bice, D. E.: Immune Responses in the Lung – A Review. Department of Medicine, West Virginia University School of Medicine, Morgantown, WV, July 28, 1994.

Boecker, B. B.: Radiation Science and Politics in the Marshall Islands-Rongelap Atoll. Noontime Seminar, ITRI, October 26 and 29, 1993.

Boecker, B. B.: Comparison of Old and New Lung Models. Symposium on Radiobiology of Inhaled Nuclides, Richland, WA, November 9-10, 1993.

Boecker, B. B., W. C. Griffith, R. A. Guilmette, F. F. Hahn, B. A. Muggenburg, S. C. Miller, R. D. Lloyd, and G. N. Taylor: The Role of Laboratory Animals in Studying the Late-Occurring Effects of Radionuclides Deposited in the Liver and Skeleton. Health Effects of Internally Deposited Radionuclides, Heidelberg, Germany, April 18-22, 1994.

Carpenter, T. R., A. W. Hickman, and N. F. Johnson: Validation of an *In Vitro* Model of the P53 Response to DNA Damage. Mountain West Chapter Society of Toxicology 12th Annual Meeting, Albuquerque, NM, September 29-30, 1994.

Carter, C. A., J. F. Lechner, and C. J. Bresee: Analysis of Cytoskeletal Alterations in Bronchial Carcinoma Cells *In Vitro*: Prospective as a Diagnostic Marker in Sputum Samples. American Association for Cancer Research, San Francisco, CA, April 10-13, 1994.

Chen, B. T. and H. C. Yeh: Design and Use of a Virtual Impactor and an Electrical Classifier for Generation of Test Fiber Aerosols with Narrow Size Distribution. American Association for Aerosol Research Annual Meeting, Oak Brook, IL October 11-15, 1993.

Chen, B. T., R. Irwin, Y. S. Cheng, M. D. Hoover, and H. C. Yeh: Aerodynamic Behavior of Fiber- and Disc-Like Particles in a Millikan Cell Apparatus. American Industrial Hygiene Conference and Exposition, Anaheim, CA, May 21-27, 1994.

Cheng, Y. S., C. C. Yu, P. K. Hopke, and K. W. Tu: Particle Size and Charge Neutralization of Thoron Progeny. American Association for Aerosol Research Annual Meeting, Oak Brook, IL October 11-15, 1993.

Cheng, Y. S., H. C. Yeh, S. Q. Simpson, and D. L. Swift: Deposition of Ultrafine Aerosols in the Nasal Passage of Human Volunteers. American Association for Aerosol Research Annual Meeting, Oak Brook, IL October 11-15, 1993.

Cheng, Y. S. and H. C. Yeh: Deposition Pattern of Airborne Particles in the Respiratory Tract. Program of Environmental Health, National Autonomy, University of Mexico, Mexico City, April 15, 1994.

Cheng, Y. S., H. C. Yeh, and K. D. Rohrbacher: Penetration of Spherical and Fiber Aerosols in Respiratory Filters. American Industrial Hygiene Conference and Exposition, Anaheim, CA, May 21-27, 1994.

Cheng, Y. S., B. Fan, and H. C. Yeh: Application of Computational Fluid Dynamics to Air Sampling Research. Scientific Conference on Obscuration and Aerosol Research, Edgewood, MD, June 20-24, 1994.

Cheng, Y. S., H. C. Yeh, R. A. Guilmette, K. H. Cheng, D. L. Swift, and S. Q. Simpson: Correlation of Airway Geometry and Nasal Deposition in Human Volunteers. Fourth International Aerosol Conference, Los Angeles, CA, August 28 - September 2, 1994.

Cheng, K. H., D. L. Swift, Y. S. Cheng, and H. C. Yeh: A Comparison of Natural and Passive Methods to Measure Nasal Deposition of Ultrafine Aerosols *In Vivo* Using a Replicate Upper Airway Cast. Fourth International Aerosol Conference, Los Angeles, CA, August 28 - September 2, 1994.

Cheng, Y. S., H. C. Yeh, J. Bigu, K. W. Tu, E. O. Knutson, R. Falk, and R. F. Holub: Intercomparison of Measurement of Thoron and Thoron/Radon Mixtures. Fourth International Aerosol Conference, Los Angeles, CA, August 28 - September 2, 1994.

Dahl, A. R., J. A. Hotchkiss, H. Kim, F. F. Hahn, and R. F. Novak: Pyridine Induction of Renal Cytochrome P4502E1 in Sprague-Dawley Rats. Annual Meeting of the Society of Toxicology, Dallas, TX, March 13-17-1994.

Dahl, A. R.: How Inhalants Interact with the Olfactory Mucosa. Human Olfaction and Audition Meeting Parallels and Emerging Research Strategies, England, May 16-18, 1994.

Fan, B. J., A. R. McFarland, and N. K. Anand: Particle Lift Force and Particle Deposition. Fourth International Aerosol Conference, Los Angeles, CA, August 28 - September 2, 1994.

Finch, G. L., E. B. Barr, W. E. Bechtold, B. T. Chen, W. C. Griffith, C. H. Hobbs, M. D. Hoover, J. L. Mauderly, and K. J. Nikula: Life-Span Study of Rats Exposed to Cigarette Smoke and $^{239}PuO_2$. Mountain West Chapter of the Society of Toxicology, Tucson, AZ, October 17, 1993.

Finch, G. L., F. F. Hahn, W. C. Griffith, M. D. Hoover, W. W. Carlton, A. H. Rebar, J. A. Mewhinney, and R. G. Cuddihy: F344 Rat Lung Carcinogenicity from Inhaled Beryllium (Be) Metal. Annual Meeting of the Society of Toxicology, Dallas, TX, March 13-17, 1994.

Finch, G. L.: Life-span Study of Rats Exposed to Cigarette Smoke and $^{239}PuO_2$. California Primate Research Center, University of California, Davis, CA, June 24, 1994.

Finch, G. L., E. B. Barr, W. E. Bechtold, B. T. Chen, W. C. Griffith, C. H. Hobbs, M. D. Hoover, J. L. Mauderly, and K. J. Nikula: Inhaled $^{239}PuO_2$ and Cigarette Smoke Act Synergistically to Produce Lung Cancer Tumors in Rats. Health Physics Society Annual Meeting, San Francisco, CA, June 26-30, 1994.

FitzPatrick, W. M.: Waste Minimization/Resource Recovery of Solvents Used in the Preparation of Histopathology Standard Operating Procedures. Mountain West Chapter Society of Toxicology 12th Annual Meeting, Albuquerque, NM, September 29-30, 1994.

Gerde, P., B. A. Muggenburg, R. F. Henderson, and A. R. Dahl: Particle-Associated Hydrocarbons and Lung Cancer; the Correlation Between Cellular Dosimetry and Tumor Distribution. NATO Advanced Research Workshop, Paris, France, October 11-13, 1993.

Guilmette, R. A., W. C. Griffith, and A. W. Hickman: Intake Assessment for Workers that Inhaled $^{238}Pu$ Aerosols. CEC/DOE Workshop on Intakes of Radionuclides, Bath, UK, September 13-17, 1993.

Guilmette, R. A.: Risks from Radon: What We Know and What We Need to Know. Rensselaer Polytechnic Institute, Troy, NY, February 16, 1994.

Guilmette, R. A., M. B. Snipes, J. W. Spoo, K. J. Nikula, and B. A. Muggenburg: Particle Clearance Studies in a Canine *In Vivo* Model. Symposium on the Fate of Aerosol Particles in the Airways, Frankfurt, Germany, March 25-26, 1994.

Hahn, F. F.: Radiation-Induced Pulmonary Neoplasia, Toxicologic Seminar Program. The University of Texas, Medical Branch, Galveston, TX, October 20, 1993.

Hahn, F. F.: Radiation-Induced Pulmonary Neoplasia. Toxicologic Seminar Program. The University of Houston Medical School, Houston, TX, October 21, 1993.

Hahn, F. F., B. A. Muggenburg, and B. B. Boecker: Hepatic Lesions in Dogs that Inhaled $^{144}$Cerium Chloride., Annual Meeting of the American College of Veterinary Pathologists, San Antonio, TX, December 5-10, 1993.

Hahn, F. F.: Radiation-Induced Pulmonary Cancer. Department of Chemistry and Biochemistry Seminar, California State University, Fullerton, CA, February 3, 1994.

Hahn, F. F., B. A. Muggenburg, and B. B. Boecker: Hepatic Lesions in Dogs Induced by Chronic Beta Irradiation from $^{144}$Cerium. Health Effects of Internally Deposited Radionuclides, Heidelberg, Germany, April 18-22, 1994.

Hahn, F. F.: Liver Tumors in Laboratory Animals Exposed to Radionuclides. Collaborative EULEP/BETG Liver Pathology Workshop, Heidelberg, Germany, April 21-22, 1994.

Harkema, J. R., H. J. Harms, P. W. Mellick, and J. A. Hotchkiss: Effects of Chronic Ozone Exposure on Nasal Airway Mucosubstances in the F344 Rat. Health Effects Institute Tenth Annual Meeting, Reston, VA, May 1-4, 1994.

Harkema, J. R. and J. L. Mauderly: Respiratory Function Alterations in F344 Rats Following Chronic Ozone Inhalation. Health Effects Institute Tenth Annual Meeting, Reston, VA, May 1-4, 1994.

Harkema, J. R., K. T. Morgan, E. G. Bermudez, and W. C. Griffith: Effects of Chronic Ozone Exposure on the Nasal Mucociliary Apparatus in the Rat. Tropospheric Ozone: Critical Issues in the Regulatory Process, Orlando, FL, May 11-13, 1994.

Harkema, J. R. and J. L. Mauderly: Respiratory Function Alterations in Rats Following Chronic Ozone Inhalation. Tropospheric Ozone: Critical Issues in the Regulatory Process, Orlando, FL, May 11- 13, 1994.

Harkema, J. R., H. J. Harms, P. W. Mellick, and J. A. Hotchkiss: Effects of Chronic Ozone Exposure on Nasal Airway Mucosubstances in the F344 Rat. American Lung Association/American Thoracic Society International Conference, Boston, MA, May 22-25, 1994.

Henderson, R. F.: Biomarkers of the Respiratory Tract. World Health Organization's International Program on Chemical Safety, Maclaren Vale, South Australia, October 11-15, 1993.

Henderson, R. F.: Biological Markers in the Respiratory Tract. University of Houston Medical School, Houston, TX, November 17, 1993.

Henderson, R. F.: Species Differences in 1,3-Butadiene Metabolism. University of Houston Medical School, Houston, TX, November 17, 1993.

Henderson, R. F.: Toxicity of Short-Chain Alkenes. Chemical Industry Institute of Technology, Research Triangle Park, NC, December 6, 1993.

Henderson, R. F.: The Use of Biological Markers of Response in Risk Assessment. Society of Risk Analysis, Savannah, GA, December 7, 1993.

Henderson, R. F., G. C. Scott, and J. J. Waide: Alkaline Phosphatase Activity in Lavage Fluid: An Indicator of Type II Cell Secretions? Annual Meeting of the Society of Toxicology, Dallas, TX, March 13-17, 1994.

Henderson, R. F., J. J. Waide, G. Kelly, G. Scott, and S. A. Belinsky: Induction of Alkaline Phosphatase Activity in an Immortalized Fetal Pulmonary Type II Cell Line. American Lung Association/American Thoracic Society International Conference, Boston, MA, May 22-25, 1994.

Hickman, A. W., N. F. Johnson, and J. F. Lechner: Wild-Type p53 Expression Following Alpha Particle Exposure. American Association for Cancer Research, San Francisco, CA, April 10-13, 1994.

Hickman, A. W., R. J. Jaramillo, and N. F. Johnson: A Comparison of Micronucleus Induction and p53 Protein Expression as Indicators of Genotoxicity. Mountain West Chapter Society of Toxicology 12th Annual Meeting, Albuquerque, NM, September 29-30, 1994.

Hoover, M. D. and G. J. Newton: Adjustments to Annual Limits on Intake Based on Particle Size and Solubility. Spring Technical Meeting of the Rio Grande Chapter of the Health Physics Society, Santa Fe, NM, March 4, 1994.

Hoover, M. D. and G. J. Newton: Adjustments to Annual Limits on Intake Based on Particle Size and Solubility. 6th Workshop of the DOE Contractor Air Monitoring User Group, Carlsbad, NM, March 22-24, 1994.

Hotchkiss, J. A., G. L. Finch, and J. R. Harkema: Role of Neutrophils in Recovery from Cigarette Smoke-Induced Nasal Epithelial Lesions in F344 Rats. Annual Meeting of the Society of Toxicology, Dallas, TX, March 13-17, 1994.

Hotchkiss, J. A. and J. R. Harkema: Effect of Neutrophil Depletion on Endotoxin-Induced Mucous Cell Metaplasia in Pulmonary Airways of F344 Rats. American Lung Association/American Thoracic Society International Conference, Boston, MA, May 22-25, 1994.

Johnson, N. F. and K. R. Maples: Fiber-Induced Hydroxyl Radical Formation and DNA Damage. NATO Advanced Research Workshop, Paris, France, October 11-13, 1993.

Johnson, N. F.: Biodosimetry of Inhaled Radon Progeny in the Rat. Biomedical Research Department, AEA Industrial Technology, Didcot, U. K., October 14, 1993.

Johnson, N. F.: Dose and Injury to Critical Lung Cells from Inhaled Radon. DOE/OHER Radon Research Program Contractors Meeting, New York, NY, October 18, 1993.

Johnson, N. F.: Radiobiology of Lung Target Cells. Symposium on Radiobiology of Inhaled Nuclides, Richland, WA, November 9-10, 1993.

Johnson, N. F.: Expression of Endogenous Wild-Type p53 in G1 and G2M in Cultured Lung Epithelial Cells Following Exposure to Alpha Particles and X-Rays. Keystone Symposium for Tumor Suppressor Genes, Taos, NM, February 13-20, 1994.

Johnson, N. F. and F. F. Hahn: Mesothelioma Induction by Silicon Carbide Whiskers after Intrapleural Administration in Rat. Annual Meeting of the Society of Toxicology, Dallas, TX, March 13-17, 1994.

Johnson, N. F., A. W. Hickman, and J. F. Lechner: Differences in Dose-Dependent Increases in p53 Expression Following Alpha- Particle and X-Ray Exposures to Rat Lung Epithelial Cells. Radiation Research Society - 42nd Annual Meeting and North American Hyperthermia Society - 14th Annual Meeting, Nashville, TN, April 29 - May 4, 1994.

Johnson, N. F., R. J. Jaramillo, and A. W. Hickman: Flow Cytometric Analysis of p53 Protein in Rat Lung Epithelial Cells. Rocky Mountain Cytometry Society, Angel Fire, NM, May 27-29, 1994.

Kennedy, C. H., R. E. Neft, N. H. Fukishima, and J. F. Lechner: Induction of Genomic Instability in Normal Human Bronchial Epithelial (NHBE) Cells by Alpha Particles. Mountain West Chapter Society of Toxicology 12th Annual Meeting, Albuquerque, NM, September 29-30, 1994.

Lechner, J. F.: Cell Response Specificity to Dusts. NATO Advanced Research Workshop, Paris, France, October 11-13, 1993.

Lechner, J. F.: Recent Investigations of the Molecular Events Involved in the Development of High-LET Radiation-Caused Lung Cancer in Humans and Animals. Commissariat A L'Energie Atomique, Fontenay-Aux-Roses, France, October 14, 1993.

Lechner, J. F.: Lung Cancer in Uranium Miners: Gene Dysfunctions. DOE/OHER Radon Research Program Contractors Meeting, New York, NY, October 18, 1993.

Lechner, J. F.: Molecular Phenomena in High-LET Radiation-Caused Lung Cancer in Humans and Animals. National Cancer Institute, National Institutes of Health, Washington, DC, November 23, 1993.

Lechner, J. F.: Lung Cancer in Uranium Miners-Gene Dysfunctions. U. S. DOE/Office of Health and Environmental Research, Germantown, MD, December 9, 1993.

Lechner, J. F.: Molecular Phenomena in High-LET Radiation-Caused Lung Cancer in Humans and Animals. Programa De Medico Ambiente, Faculty of Medicine, National University of Mexico, Mexico DF, June 6, 1994.

Lechner, J. F., N. F. Johnson, G. Kelly, and S. A. Belinsky: Molecular Analyses of High-LET Radiation-Caused Lung Cancer in Humans and Animals. Joint Meeting of the Association for Radiation Research and the Irish Radiation Research Society, University College, Dublin, June 23-26, 1994.

Lechner, J. F.: Molecular Analysis of High-LET Radiation-Caused Lung Cancer in Humans and Animals. Association for Radiation Research and the Irish Radiation Research Society Meeting, University College, Dublin, Ireland, June 23-26, 1994.

Lechner, J. F. and S. A. Belinsky: Detection of Molecular Markers in Sputum to Predict Lung Cancer Risk in Uranium Miners. Second Annual SPORE Meeting, Rockville, MD, July 17-19, 1994.

Lechner, J. F.: Detection of Molecular Markers in Sputum to Predict Lung Cancer Risk in Uranium Miners. Second Annual SPORE Investigators Meeting, Rockville, MD, July 17-19, 1994.

Lechner, J. F.: Biomarkers. Radiation Health Effects and Hanford, Spokane, WA, September 9-11, 1994.

Lopez, J. A.: Prioritization of Self-Assessment Results. EFCOG Prioritization Workshop, May 10-11, 1994.

Mauderly, J. L.: Differences in Cancer and Noncancer Responses of Rats, Other Animals, and Humans to Heavy Chronic Inhalation Exposures to Particles. Second International Symposium on Silica, Silicosis, and Cancer, San Francisco, CA, October 28-30, 1993.

Mauderly, J. L. and J. R. Harkema: Respiratory Function Alterations Following Chronic Ozone Inhalation in Rats. National Toxicology Program/Health Effects Institute Collaborative Ozone Study Meeting, Research Triangle Park, NC, November 16, 1993.

Mauderly, J. L.: Implications of the Pulmonary Carcinogenicity of Carbon Black in Rats. Second International Conference - Carbon Black World 94, Houston, TX, February 23-24, 1994.

Mauderly, J. L.: Current View of the Carcinogenic Hazard of Diesel Exhaust. International Conference on Towards Clean Transport: Clean and Fuel-Efficient Motor Vehicles, Mexico City, DF, March 29-30, 1994.

Mauderly, J. L.: Current View of the Carcinogenic Hazard and Lung Cancer Risk from Diesel Exhaust. American Mining Congress, Albuquerque, NM, April 6, 1994.

Mauderly, J. L.: Implications of the Pulmonary Carcinogenicity of Carbon Black in Rats. Cabot Corporation, Boston, MA, May 12, 1994.

Mauderly, J. L.: Current Issues Concerning the Toxicology of Inhaled Particles. American Lung Association/American Thoracic Society International Conference, Boston, MA, May 21-25, 1994.

Mauderly, J. L. and J. R. Harkema: Respiratory Function Alterations in F344 Rats Following Chronic Ozone Inhalation. American Lung Association/American Thoracic Society International Conference, Boston, MA, May 22-25, 1994.

Mauderly, J. L.: Current View of the Carcinogenic Hazard and Lung Cancer Risk of Diesel Exhaust. Indian Lakes Seminar on Occupational Claims, Indian Lakes Resort, Chicago, IL, June 10, 1994.

Mauderly, J. L.: Particle Research at the Inhalation Toxicology Research Institute, U.S. Environmental Protection Agency Meeting on Particulate Matter, Research Triangle Park, NC, June 27, 1994.

Mauderly, J. L.: Health Effects of Diesel Emissions. Reformulated Diesel Symposium, Toronto, Ontario, Canada, September 14-15, 1994.

Melo, D. R., J. L. Lipsztein, C. A. N. Oliveira, D. L. Lundgren, B. A. Muggenburg, and R. A. Guilmette: A $^{137}Cs$ Age-Dependent Biokinetic Study. Health Physics Society Annual Meeting, San Francisco, CA, June 26-30, 1994.

Mitchell, C. E., S. A. Belinsky, and J. F. Lechner: Rapid Detection and Quantitation of Mutant K-ras Codon 12 Restriction Fragments by Capillary Electrophoresis. American Association for Cancer Research, San Francisco, CA, April 10-13, 1994.

Muggenburg, B. A., F. F. Hahn, W. C. Griffith, R. D. Lloyd, and B. B. Boecker: The Biological Effects of $^{224}Ra$ Injected Into Dogs. Health Effects of Internally Deposited Radionuclides, Heidelberg, Germany, April 18-22, 1994.

Nikula, K. J., G. L. Finch, E. B. Barr, W. E. Bechtold, B. T. Chen, W. C. Griffith, M. D. Hoover, and J. L. Mauderly: Interaction of Cigarette Smoke and $^{239}PuO_2$ in the Induction of Lung Cancer in Rats. 85 American Association of Cancer Research, San Francisco, CA, April 10-13, 1994.

Nikula, K. J., L. A. Sachetti, G. L. Finch, B. T. Chen, and J. L. Lewis: Tobacco Smoke-Induced Alterations Rhodanese and Carboxylesterase in the Olfactory Mucosa of F344 Rats. Association of Chemoreception Senses, Sarasota, FL, April 13-17, 1994.

Palmisano, W. A., C. H. Kennedy, and J. F. Lechner: A Scaffold-Attachment-Like Region on Chromosome 9 is Frequently Amplified in Human Lung Tumors. American Association for Cancer Research, San Francisco, CA, April 10-13, 1994.

Palmisano, W. A., C. H. Kennedy, and J. F. Lechner: Amplification of a Scaffold-Attachment-Like Region on Chromosome 9 is a Common Event in Human Lung Tumors. Detection by Arbitrarily Primed Chain Reaction Amplification. 7th World Conference on Lung Cancer, Colorado Springs, CO, June 26 - July 1, 1994.

Rohrbacher, K. D.: Immunohistochemical Localization of CYP2A in Rat Nasal Cavity. Mountain West Chapter Society of Toxicology 12th Annual Meeting, Albuquerque, NM, September 29-30, 1994.

Sanders, C. L.: Radiation Dose Threshold for Lung Cancer in Irradiated Nonsmokers. Radiation Research Society - 42nd Annual Meeting and North American Hyperthermia Society - 14th Annual Meeting, Nashville, TN, April 29 - May 4, 1994.

Snipes, M. B., K. J. Nikula, W. C. Griffith, and R. A. Guilmette: Spatial and Temporal Distribution Patterns of Inhaled Fluorescent Microspheres in Lungs of Rats, Guinea Pigs, and Dogs. American Lung Association/American Thoracic Society International Conference, Boston, MA, May 22-25, 1994.

Strunk, M. R.: A Novel Interface for Multidimensional Gas Chromatography/Mass Spectroscopy with Applications to Complex Biological Samples. Mountain West Chapter Society of Toxicology 12th Annual Meeting, Albuquerque, NM, September 29-30, 1994.

Swafford, D. S., K. J. Nikula, and S. A. Belinsky: Genetic Alterations in Rat Lung Tumors Induced by Diesel Exhaust or Carbon Black. American Association for Cancer Research, San Francisco, CA, April 10-13, 1994.

Swafford, D. S., K. J. Nikula, and S. A. Belinsky: Genetic Alterations in Rat Lung Tumors Induced by Diesel Exhaust or Carbon Black. Mountain West Chapter Society of Toxicology 12th Annual Meeting, Albuquerque, NM, September 29-30, 1994.

Thornton-Manning, J. R., W. E. Bechtold, A. R. Dahl, and R. F. Henderson: Analysis of Butadiene Monoepoxide and Butadiene Diepoxide in Rats and Mice Following 4-Hour Exposures to Low Levels of 1,3-Butadiene. Chemical Manufacturers Association Butadiene Research Review Meeting, Santa Fe, NM, June 6-7, 1994.

Yeh, H. C., B. A. Muggenburg, and J. R. Harkema: *In Vivo* Deposition of Inhaled Ultrafine Particles in Airways of Rhesus Monkeys. American Association for Aerosol Research Annual Meeting, Oak Brook, IL, October 11-15, 1993.

Yeh, H. C.: Deposition of Radon and Radon Progeny in the Respiratory Tract. Annual DOE Radon Contractors Meeting, New York, NY, October 17-19, 1994.

Yeh H. C., R. S. Turner, R. K. Jones, and B. A. Muggenburg: Characterization of Blood-Associated Aerosols Produced During Surgical Procedures. College of Public Health, National Taiwan University, Taipei, Taiwan, April 25, 1994.

Yeh H. C. and Y. S. Cheng: Method of Lung Deposition Research. College of Public Health, National Taiwan University, Taipei, Taiwan, April 25, 1994.

Yeh, H. C., B. A. Muggenburg, R. A. Guilmette, M. B. Snipes, R. K. Jones, R. S. Turner, and J. P. Smith: Characterization of Aerosols Produced During Total Hip Replacement Surgery in Beagle Dogs with $^{51}$Cr-Labeled Blood. Fourth International Aerosol Conference, Los Angeles, CA, August 28 - September 2, 1994.

## APPENDIX G

## SEMINARS PRESENTED BY VISITING SCIENTISTS

## OCTOBER 1, 1993 - SEPTEMBER 30, 1994

Dr. Thomas W. Hesterberg, Schueller International, Inc., Littleton, CO: *Chronic Inhalation Toxicity of Manmade Vitreous Fibers*, October 7, 1993.

Dr. Terry Gordon, Institute of Environmental Medicine, Tuxedo, NY: *Stress Proteins in the Lung: Induction by Environmental and Occupational Agents*, October 18, 1993.

Dr. Gary D. Stoner, Ohio State University, Columbus, OH: *Isothio Cyanates as Inhibitors of Nitrosamine Carcinogenesis*, October 21, 1993.

Dr. Guadalupe Ponciano, Programa Universitario de Medio Ambiente, Mexico City, Mexico: *Research on Environmental Health at the National Institute of Cancerology of Mexico,* November 1, 1993.

Dr. Martin J. Ronis, University of Arkansas Medical Sciences, Little Rock, AR: *Regulation of Cytochrome P450 CYP2E1 by Alcohol and Its Role in Alcohol Metabolism and Alcohol-Induced Liver Damage*, December 21, 1993.

Dr. Lilian Calderon, Universidad Nacional Autonoma de Mexico, Mexico City, Mexico: The *Nasal Mucosa in Southwest Metropolitan Mexico City Inhabitants. What Now?*, January 10, 1994.

Dr. William K. Kaufmann, University of North Carolina, Chapel Hill, NC: *Cell Cycle Checkpoints, DNA Repair and Initiation of Carcinogenesis*, January 13, 1994.

Dr. Michael Galvin, National Institute of Environmental Health Sciences, Washington, DC: *How to Write Successful NIH Grants*, February 8, 1994.

Dr. Frank Margolis, Roche Institute of Molecular Biology, Nutley, NJ: *Regulation of Gene Expression in Olfactory Neurons*, March 9, 1994.

Dr. Michael McClelland, California Institute of Biological Research, La Jolla, CA: *RNA Fingerprinting by Arbitrarily Primed PCR*, April 29, 1994.

Dr. Stewart Camero, Sandia National Laboratories, Albuquerque, NM: *Prospects for Optical Biomedical Imaging*, May 10, 1994.

Dr. Louise H. Lutze-Mann, University of California, San Francisco, CA: *From In Vitro to In Vivo: Spectrum of Ionizing Radiation-Induced Mutations*, May 11, 1994.

Dr. Lanny J. Rosenwasser, National Jewish Center for Immunology and Respiratory Medicine, Denver, CO: *Immune Responses in the Pathogenesis of Asthma*, May 17, 1994.

Dr. Oscar Ward, University of Arizona, Tucson, AZ: *Overview and Evolution of the Dog Karyotype*, June 2, 1994.

Dr. Colin Dunlop and Dr. Kathy Magnusson, College of Veterinary Medicine, Colorado State University, Fort Collins, CO: *Age-Related Responses in Animals*, June 10, 1994.

Dr. Monica Dahlqvist, Royal Institute of Technology, Stockholm, Sweden: *Detecting Acute, Temporary Health Effects - Is It Useful to Improve the Environment?*, June 17, 1994.

Dr. Rong Z. Gan, The Lovelace Institutes, Albuquerque, NM: *Pulmonary Circulation: Correlation of Theory and Experiment*, June 23, 1994.

Dr. Rick A. Rogers, Harvard School of Public Health, Boston, MA: *From Airways to Alveoli: A Walk Through the Lungs Using Confocal Microscopy*, July 15, 1994.

Dr. Aron B. Fisher, University of Pennsylvania School of Medicine, Philadelphia, PA: *Oxidative Lung Damage in Ischemia and Reperfusion*, July 21, 1994.

Dr. John P. H. Th'Ng, University of California School of Medicine, Davis, CA: *Histone Phosphorylation and Chromosome Condensation in the Mammalian Cell Cycle*, July 21, 1994.

Dr. Kvetoslav R. Spurny, Fraunhofer-Institut (Retired), Schmallenberg, Germany: *Atmospheric Anthropogenic Aerosols and Their Carcinogenicity*, September 8, 1994.

Dr. Aage Haugen, National Institute of Occupational Health, Oslo, Norway: *Mutagenesis in the p53 Gene and Genetic Susceptibility Markers in Human Lung Cancer*, September 28, 1994.

Dr. Thomas W. Hesterberg, Schuller International, Inc., Littleton, CO: *Subchronic Inhalation Studies of Fibrous Glass in Rats and Hamsters*, September 29, 1994.

## APPENDIX H

## ADJUNCT SCIENTISTS

## AS OF NOVEMBER 30, 1994

Dr. Carol Basbaum
Department of Anatomy
University of California School of Medicine
San Francisco, CA 94143

Dr. Rick Crowell
Pulmonary Department
University of New Mexico
Albuquerque, NM 87131

Dr. William W. Carlton
Department of Veterinary Microbiology,
Pathology and Public Health
School of Veterinary Medicine
Purdue University
West Lafayette, IN 47907

Dr. Frank D. Gilliland
Cancer Center
New Mexico Tumor Registry and Department
of Medicine
University of New Mexico
Albuquerque, NM 87131

Dr. Terry Gordon
Institute of Environmental Medicine
Long Meadow Road
Tuxedo, NY 10987

Dr. William M. Hadley
Dean, College of Pharmacy
University of New Mexico
Albuquerque, NM 87131

Dr. Steve Kleeberger
Division of Physiology
Department of Environmental Health
Johns Hopkins University
615 N. Wolfe Street
Baltimore, MD 21205

Dr. David L. Swift
Johns Hopkins University
School of Hygiene and Public Health
615 N. Wolfe Street
Baltimore, MD 21205

Dr. Donna Kusewitt
The Lovelace Institutes
2425 Ridgecrest S.E.
Albuquerque, NM 87108

Dr. Douglas Mapel
Pulmonary Division
Department of Medicine
University of New Mexico
Albuquerque, NM 87131-5271

Dr. Raymond F. Novak
Wayne State University
Institute of Chemical Toxicology
Detroit, MI 48201

Dr. Judy Raucy
College of Pharmacy
University of New Mexico
Albuquerque, NM 87131

Dr. Alan H. Rebar
School of Veterinary Medicine
Purdue University
West Lafayette, IN 47907

Dr. Jonathan M. Samet
Department of Epidemiology
School of Hygiene and Public Health
The Johns Hopkins University
615 N. Wolfe Street, Suite 6039
Baltimore, MD 21205-2179

Dr. Thomas Sandström
Department of Lung Medicine
University Hospital
S-901 85
Umea, Sweden

Dr. Steven Q. Simpson
Albuquerque VA Medical Center
2100 Ridgecrest S.E.
Albuquerque, NM 87108

Dr. Mark Schuyler
Albuquerque VA Medical Center
2100 Ridgecrest S.E.
Albuquerque, NM 87108

Dr. Jonathan B. Ward
University of Texas Medical Branch
2.102 Ewing Hall, S-10
Galveston, TX 77555-1010

Dr. Ross Zumwalt
Office of Medical Investigation
Assistant Chief Medical Investigator
University of New Mexico
School of Medicine
Albuquerque, NM 87131

# APPENDIX I

# EDUCATION ACTIVITIES AT THE INHALATION TOXICOLOGY RESEARCH INSTITUTE

During the last 30 years, ITRI education programs have reached over 600 individuals. These programs provide environmental health science research opportunities to precollege, undergraduate, and graduate students; teachers of these students; postdoctoral fellows; and visiting scientists. The goal of these programs is to encourage students to pursue careers in environmental health science so that the need for specialists in this field will continue to be met.

## Precollege Students

To stimulate precollege student interest in science, tours and demonstrations are provided, and students who participate in science fairs are supported. High school students also have the opportunity to work in research laboratories. This program has worked well during the last four summers, and high school students will work in ITRI laboratories in FY-1995.

Teachers are a key to promoting environmental health science awareness in the precollege classroom. These educators need background and experience in environmental health science in order to instill their students with relevant and accurate information. Each summer, eight middle school and high school teachers are invited to participate in research. One program, the Summer Teacher Enrichment Program (STEP), is specifically for New Mexico teachers. A second program is the Teacher Research Associates Program (TRAC) for teachers throughout the United States. Teachers in these programs are involved in all steps of a scientific study, including the design of experiments, the conduct of experimental assays, evaluation of data, and the presentation of scientific results. The direct involvement of teachers in all phases of a research project provides them with information valuable to students interested in careers in science. The STEP and TRAC participants have been enthusiastic about their work at ITRI and have found various ways to incorporate their experiences into the classroom. Eight high school teachers will participate in these two programs during the summer of FY-1995. Since its beginning in 1984, 36 New Mexico middle school and high school science teachers have participated in research at ITRI through STEP. TRAC started in 1989, and 19 high school teachers have been supported at ITRI by this program. There were three STEP and three TRAC teachers in these programs at ITRI during the summer of FY-1994.

In FY-1994, a Field Task Proposal was funded by the U. S. Department of Energy for a program in "Environmental Health Science - Educational Awareness." This funding facilitated the hiring of an Education Specialist to coordinate and expand these programs into grades K-12.

Scientific staff members continued their involvement in precollege education as science fair judges and as tutors and mentors.

## Undergraduate Students

There are two programs at ITRI for undergraduate students. The first is for undergraduate students who are science majors and plan to continue their education with postgraduate training. Students in this program are given the opportunity to initiate and complete a scientific investigation under the direction of an ITRI staff member. By being involved in the design of the study, the conduct of the experiments, analysis of the data, and the presentation of results, the students gain an understanding of research and

experience the excitement of new discovery. Nine students carried out research at ITRI during the past summer.

The second educational program for undergraduate students provides work opportunities for engineering students. Nine students worked in various areas of engineering at ITRI during the summer of FY-1994.

A total of 603 undergraduate students have received educational opportunities at ITRI since 1966.

Graduate Students

The ITRI/University of New Mexico (UNM) Graduate Program provides the opportunity for students to obtain a Ph.D. degree. Course work is completed at UNM, and the research portion of the doctoral degree is carried out at ITRI, with a scientist serving as the research advisor. One new student was accepted into this graduate program in FY-1994. At least one more student will begin in FY-1995. Support from industry continues for the graduate program. Both Lilly Laboratories and E. I. duPont de Nemours & Company contributed funds that support the attendance of students at scientific meetings as well as stipend support.

In addition to the ITRI-UNM program, graduate students attending other universities can also carry out the research necessary for their graduate degrees at ITRI. All course work for the advanced degree is completed at the university before the student starts research at ITRI. The advanced degree is awarded by the participating university upon completion of all degree requirements. Since 1968, 33 graduate students have conducted all or part of their research at ITRI.

The graduate programs take advantage of the complementary academic resources available at universities and the research resources available at ITRI. For example, joint graduate programs were established in pathology and medicine with the School of Veterinary Medicine at Purdue University. Graduate veterinary students complete the research portion of a Ph.D. degree at ITRI as part of their residency program in pathology.

Postgraduate Training

Research appointments are available to recent doctoral graduates to continue their research training. One program, which was funded by the National Institutes of Health during FY-1994, is the Pulmonary Epidemiology and Toxicology Training Program. This program is conducted jointly with UNM. Participants choose to specialize in either epidemiology or toxicology and receive cross-training in the other discipline. One postdoctoral fellow is participating in the program and recruitment for a second position is ongoing.

The second program provides research opportunities at ITRI for students in life science, chemistry, veterinary medicine, or engineering. This program is designed to develop research capabilities both in inhalation toxicology and one or more of the areas of basic pulmonary biology. During FY-1995, four postdoctoral fellows will participate in research at ITRI.

University Faculty and Industrial Scientists

Opportunities are available for scientists from universities or industry to visit the Institute or collaborate in research at ITRI. The length of these visits ranges from a few days, to obtain information or learn techniques, to up to a full year, to conduct research. During FY-1994, participants included scientists from UNM, the Albuquerque Veterans Medical Center, Purdue University, Johns Hopkins University, and New York University.

Other Educational Activities

Several staff members hold academic appointments and present lectures to university students. ITRI also holds periodic workshops in inhalation toxicology that have received international recognition. The book, "Concepts in Inhalation Toxicology," published in 1989 from the workshop held in 1987, has become a key text in the field. The last workshop was held in October 1992, and approximately 90 attendees benefitted from the lectures and laboratory demonstrations.

Marcy Wood
Education Specialist

## APPENDIX J

## AUTHOR INDEX